Study on Consolidating Requirements and Error Budget for CO_2 Monitoring Mission (CO2M-REB):

Requirements Justification Report

for anthropogenic CO_2 Monitoring Mission (CO2M)

Technical Note (TN-1000)

ESA Study
"Study on Consolidating Requirements and Error Budget for CO_2 Monitoring Mission"
ESA Contract N^o 4000125122/18/NL/FF/gp

Authors:
Michael.Buchwitz@iup.physik.uni-bremen.de,
Stefan Noël, Maximilian Reuter, Heinrich Bovensmann, Andreas Richter
Institute of Environmental Physics (IUP) / Institute of Remote Sensing (IFE), University of Bremen (UB), Bremen, Germany

Jochen Landgraf, Hein van Heck
SRON, Utrecht, The Netherlands

Pepijn Veefkind, Johan de Haan
KNMI, De Bilt, The Netherlands

Hartmut Boesch
University of Leicester, Leicester, UK

Change log

Version	Date	Status	Authors	Reason for change
1.0	22-Jan-2019	Submitted	CO2M-REB team	New document
1.1	25-Apr-2019	Submitted	-"-	To consider comments from ESA
1.2	4-Oct-2019	Intermediate version generated only for project internal use	-"-	To consider remaining open aspects and to document post-MTR results
2.0	25-Feb-2020	Submitted	-"-	Update for MRDv2.0
2.1	8-May-2020	Submitted	-"-	To consider comments from ESA

Table of Contents

1. Abstract 4
2. Executive Summary 5
3. Mission Objectives 8
4. Justification of Mission Requirements 8
   - 4.1. Mission requirements at System Level 10
     - 4.1.1. Geophysical product requirements of the space component 10
     - 4.1.2. Lifetime 18
     - 4.1.3. Time and geolocation requirements 19
     - 4.1.4. Coverage requirements 22
     - 4.1.5. Glint mode observations 24
     - 4.1.6. Summary and Conclusions 27
   - 4.2. Mission Requirements of the CO_2 Observations 28
     - 4.2.1. Geometric Requirements 28
     - 4.2.2. Spectral Requirements 31
     - 4.2.3. Radiometric Requirements 34
     - 4.2.4. Summary and Conclusions 40
   - 4.3. Mission Requirements of Aerosol and Cloud Observations 41
     - 4.3.1. Geometric Requirements 41
     - 4.3.2. Modulation concept, Spectral and Radiometric Requirements 43
     - 4.3.3. Bandpass concept, Spectral and Radiometric Requirements 47
     - 4.3.4. Summary and Conclusions 49
   - 4.4. Mission Requirements of NO_2 Observations 50
     - 4.4.1. Geometric requirements 50
     - 4.4.2. Spectral and Radiometric Requirements 52
     - 4.4.3. Summary and Conclusions 57
   - 4.5. Mission Requirements on Cloud Coverage 58
     - 4.5.1. Geometric requirements 58
     - 4.5.2. Spectral and Radiometric Requirements 59
     - 4.5.1. Summary and Conclusions 60
   - 4.6. Mission Performance and Error Budget 61
5. Acronyms and abbrevations 62
6. References 65

1. Abstract

This document is a deliverable of ESA Study “Study on Consolidating Requirements and Error Budget for CO_2 Monitoring Mission”. The anthropogenic CO_2 Monitoring satellite mission is referred to as CO2M mission in this document.

This document (technical note 1000, i.e., TN-1000), the “Requirements Justification Report for CO2M”, is one document of three closely related documents. The other two are: the “Requirements Sensitivity Analysis for CO2M” (TN-2000) and “Error Budgets and Performance for CO2M” (TN-3000).

The objective of this document is to provide justification for all Level 1 requirements as given in the CO2M Mission Requirements Document (MRD) version 2.0 including recommendations for modifications of requirements, if required. This implies that each Level 1 performance requirement is consistent with the corresponding Error Budget (EB) as presented in TN-3000 for the following parameters: XCO_2 (dry-air column-average mole fraction of carbon dioxide (CO_2)), XCH_4 (dry-air column-average mole fraction of methane (CH_4)), SIF (solar-induced fluorescence), tropospheric NO_2 column and aerosol and cloud parameters from the Multi-Angle-Polarization (MAP) instrument.

This document is an update of the previous version of this documents (version 1.1) which provided justification of MRDv1.0 requirements.

This updated document provides justification of all Level 1 requirements as listed in MRDv2.0. It also presents for some requirements recommendations for improvements.

2. Executive Summary

This document is a deliverable of ESA Study "Study on Consolidating Requirements and Error Budget for CO_2 Monitoring Mission". The anthropogenic CO_2 Monitoring satellite mission is referred to as CO2M mission in this document.

This document (technical note 1000, i.e., TN-1000), the "Requirements Justification Report for CO2M", is one document of three closely related documents. The other two are: the "Requirements Sensitivity Analysis for CO2M" (TN-2000) **/CO2M-REB TN-2000 v2.1, 2020/** and "Error Budgets and Performance for CO2M" (TN-3000) **/CO2M-REB TN-3000 v2.1, 2020/**.

The objective of this document is to provide justification for all Level 1 requirements as given in the CO2M Mission Requirements Document (MRD) version 2.0 **/CO2M MRD v2.0, 2019/** including recommendations for modifications of requirements, if required. This implies that each Level 1 performance requirement is consistent with the corresponding Error Budget (EB). EBs are presented in TN-3000 "Error Budget and Performance of CO2M" **/CO2M-REB TN-2000 v2.1, 2020/** for the following parameters: XCO_2 (dry-air column-average mole fraction of carbon dioxide (CO_2)), XCH_4 (dry-air column-average mole fraction of methane (CH_4)), SIF (solar-induced fluorescence), tropospheric NO_2 column and aerosol and cloud parameters from the Multi-Angle-Polarization (MAP) instrument.

Previous versions of these three documents, i.e., of TN-1000 **/CO2M-REB TN-1000 v1.1, 2019/**, TN-2000 **/CO2M-REB TN-2000 v1.2, 2019/** and TN-3000 **/CO2M-REB TN-3000 v1.1, 2019/**, have been used to provide feedback on version 1 of the CO2M MRD **/CO2M MRD v1.0, 2018/**. These feedbacks have been used by ESA to generate version 2.0 of the MRD **/CO2M MRD v2.0, 2019/**. In the previous version of this document, i.e., in **/CO2M-REB TN-1000 v1.1, 2019/**, all relevant MRDv1.0 requirements are listed and for each requirement its "justification status" is given. The justification status can have one of several "values": "JNA": Justification not applicable (e.g., requirement is a higher level MRD input (user) requirement); "No": requirement is applicable but no agreed justification is yet available (this classification is needed primarily for initial drafts of this document); "Yes": requirement is applicable and agreed justification available and reported in this document; "Partially": requirement is applicable but justification needs refinement; "Modify": requirement is applicable but needs refinement. Concerning "Mission Requirements at System Level" and "Mission Requirements of the CO_2 Observations" all requirements as listed in the MRD are presented and for each requirement information on its justification status is given based on existing peer-reviewed publications, relevant results from ESA or other studies and specific new simulation results carried out in the framework of this study. Documents **/CO2M-REB TN-1000 v1.1, 2019/**, **/CO2M-REB TN-2000 v1.2, 2019/** and **/CO2M-REB TN-3000 v1.1, 2019/** have been used for the generation of the updated version of the MRD, i.e., for the generation of MRDv2.0 **/CO2M MRD v2.0, 2019/.**

This (updated) document provides justification of all Level 1 requirements as listed in MRDv2.0.

The findings concerning “Mission requirements at System Level” (MRDv2.0, Sect. 3.1) can be summarized as follows:

This section differs significantly from the corresponding section as given in MRDv1.0. For example, this section now also contains numbered requirements for precision and systematic error of XCO_2 and several other parameters (especially for XCH_4, NO_2 tropospheric columns and Solar Induced Fluorescence (SIF)). Detailed justification of these higher level user requirements is out of the scope of the present study, which focusses on L1 requirements. Nevertheless, each MRDv2.0 requirement is listed in this document and information on its justification is given in this document. This section also contains a number of other input user requirements such as on timeliness and lifetime. Also these requirements are listed in this document but it is explained that justification of these requirements is out of the scope of this study. Justification is provided for requirements related to temporal co-registration of the CO_2, MAP (Multi-Angle-Polarimeter), NO_2 and CLIM (Cloud Imager) observations based on the overarching requirement to observe essentially the same air mass at the same time. Related to this are also the corresponding geolocation knowledge requirements. Furthermore, justification is given for the coverage requirements and the MRD requirements related the glint mode observations. Earlier recommendations related to refinement of requirements have been considered for MRDv2.0. For example, it has been added to characterise the radiometric performance for solar zenith angles up to 80^o and the temporal co-registration requirement is better and clearer now. Some recommendations are given on how to further improve the MRD. For example, some requirements (e.g., S7MR-DAT-010) refer to a “reference SNR”, which is not specified in the MRD, and requirement S7MR-DAT-020 refers to a cloud coverage of 5%, which is likely not demanding enough.

The findings concerning the “Mission Requirements of the CO_2 Observations” (MRDv2.0, Sect. 3.2) can be summarized as follows:

In this section, all requirements as listed in MRDv2.0 are presented and for each requirement justification is provided based on existing peer-reviewed publications, relevant results from ESA or other studies and specific new simulation results carried out in the framework of this study. As shown in this document, essentially all requirements are considered justified. This is an improvement compared to MRDv1.0. Several earlier recommendations related to refinement of MRDv1.0 requirements have been considered for MRDv2.0. For example, the minimum across-track swath width is wider now, the requirement on the overlap of spatial samples is more demanding, recommendations on improvements related to the required signal-to-noise-ratio (SNR) have been considered and a requirement on spectral stability has been added.

The findings concerning the “Mission Requirements of Aerosol and Cloud Observations” (MRDv2.0, Sect. 3.3) can be summarized as follows:

An assessment of the MRDv2.0 requirements for the Multi Angle Polarimeter (MAP; for additional information on aerosols and clouds) modulation and band concepts of CO2M has been carried out. Several requirements have been modified compared to the earlier MRD version v1.0 following previous recommendations. All requirements as formulated in MRD v2.0 are considered justified.

The findings concerning the “Mission Requirements of NO_2 Observations” (MRDv2.0, Sect. 3.4) can be summarized as follows:

The corresponding section provides an assessment of the MRDv2.0 requirements for the NO_2 observations of CO2M. This has strong heritage to other missions, including S5P/TROPOMI, S4/UVN and S5/UVNS. However, the primary use of the NO_2 data is different than for these heritage missions because for CO2M the primary use is plume detection. For some requirements minor modifications are proposed. This includes the formulation of the requirements on the ISRF, where the current formulation is harmonized with the other CO2M bands, but could be an over-specification. Furthermore, highlight the goal requirement of 1000 for the SNR, to stress the importance of high SNR.

The findings concerning the “Mission Requirements on Cloud Coverage” (MRDv2.0, Sect. 3.5) can be summarized as follows:

In contrast to MRDv1.0, the new MRDv2.0 contains requirements on cloud coverage to be derived from a dedicated cloud imager (CLIM). Each of these requirements are listed in this document together with its justification. This comprises geometric (e.g., swath width and spatial sampling distance (SSD), spectral (e.g., spectral bands) and radiometric (e.g., SNR and accuracy) requirements.

3. Mission Objectives

MRDv2.0 **/CO2M MRD v2.0, 2019/** contains a section 3 on “Mission Objectives”.

The content of that section is not explicitly addressed in this document because this document focusses on Mission Requirements, see **Sect. 4** of this document.

4. Justification of Mission Requirements

In this section, all CO2M Level-1 (L1) requirements as listed in the MRDv2.0 **/CO2M MRD v2.0, 2019/** are shown together with comments related to their justification.

For easy comparison with the MRD, the sub-section titles and numbers in this section are the same as in MRDv2.0 Section 4 (“Mission Requirements”).

Note that this document focusses on the justification of the MRD L1 requirements. Specifically, it refers to the link between Level-2 (L2) and L1. A L1 requirement is considered justified if it is demonstrated - via the information provided in this document – that meeting it is consistent with the required L2 performance.

L2 requirements – which originate from the link between the Level-4 (L4) and L2 products – are (given) input for this document.

Figure 1 illustrates the link between the various levels of data products: Requirements on the L4 products (primarily CO_2 emissions) result in requirements on the L2 products (primarily atmospheric XCO_2) (for L4 and L2 requirements see, for example, **/Pinty et al. 2017/ /CO2M MRD v2.0, 2019/**) which result in requirements on the L1 products (primarily radiances spectra) and, therefore, on the MRD L1 requirements.

As already mentioned, L2 requirements are considered input for the assessments carried out in this study and they will therefore not be justified in this document. Specifically, this implies that those requirements whose justification requires “inverse modelling” (i.e., L2 to L4 processing) will not be justified in this document. Nevertheless, some information on justification of L2 requirements is also given in this document for the convenience of the reader.

As shown in **Figure 1**, the L2 performance does not only depend on the satellite and its L1 product / performance but also on other aspects, most notably on the retrieval algorithm(s) and the investigated scenarios. Therefore, it is important to assess at least the most critical L1 requirements with more than one algorithm and to select appropriate scenarios.

Furthermore, the L1 assessment requires an Error Budget (EB), as it needs to be known how large the XCO_2 random and systematic errors, i.e., the L2 errors, for a given L1 error source are / can be (e.g., for an additive radiance error).

On the other hand, the EB also depends on the L1 requirements / performance and the final EB needs to be consistent with the MRD L1 requirements.

This “hen and egg” problem is solved iteratively.

The corresponding EB is presented and discussed in a separate document **/CO2M-REB TN-3000 v2.1, 2020/**.

The presented justification assessment is based on available literature, if considered appropriate. New assessments are reported in a separate document **/CO2M-REB TN-2000 v2.1, 2020/**.

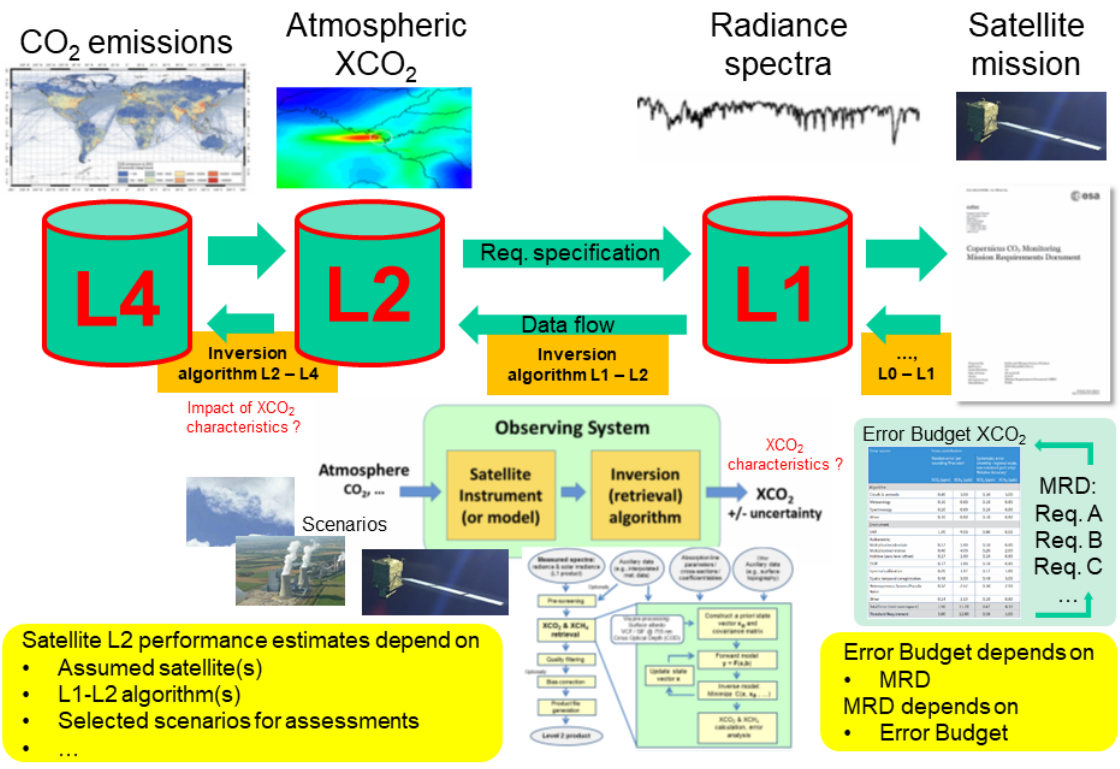

Figure 1: Schematic representation of the process for establishing MRD requirements, which iteratively flows from the Level-4 user requirements to Level-2, and from Level-2 to Level-1 into the MRD.

4.1. Mission requirements at System Level

The numbering of the sub-sections of this document is identical with the corresponding sub-sections numbering of MRDv2.0 **/CO2M MRD v2.0, 2019/** with the exception of the "Summary and Conclusions" sub-sections, which have been added for this document to summarize the justification status.

In this document, all MRDv2.0 requirements (at least all "numbered requirements") are also listed (repeated). They are shown in **blue**.

4.1.1. Geophysical product requirements of the space component

The corresponding section 4.1.1 of MRDv2.0 provides a table of (mostly) Level-2 (L2) requirements (see MRDv2.0 Tab. 4.1: "Characteristics of the geophysical product as required from the space component of the anthropogenic CO_2 monitoring system").

The purpose of this document is to provide justification of the MRD L1 requirements. The L2 requirements as given in Tab. 4.1 of MRDv2.0 are not required to be justified in this document. They originate primarily from the MRD input user requirements as formulated in **/Pinty et al., 2017/** and related documents.

Nevertheless, each L2 requirement listed in Tab. 4.1 of MRDv2.0 is shown in the following together with a short comment related to its justification:

Parameter	**Level 2 requirement**
XCO_2 precision	0.7 ppm for vegetation scenario at SZA of 50 degrees

A numbered requirement is given in MRDv2.0 to cover this requirement, see comments below on requirement S7MR-DAT-010.

Parameter	**Level 2 requirement**
XCO_2 systematic error	<0.5 ppm

A numbered requirement is given in MRDv2.0 to cover this requirement, see comments below on requirement S7MR-DAT-050.

Parameter	**Level 2 requirement**
XCO_2 spatial resolution	4 km^2, aspect ratio ≤2

A numbered requirement is given in MRDv2.0 to cover this requirement, see comments below on requirement S7MR-OBS-020.

Parameter	Level 2 requirement
XCO_2 plume image	Imaging capability of 250 x 250 km^2 spatial scale

A numbered requirement is given in MRDv2.0 to cover this requirement, see comments below on requirement S7MR-OBS-010.

Parameter	Level 2 requirement
XCO_2 emission area temporal coverage	Global coverage and on average once per week effective coverage over land for latitudes above 40 degrees, where the strongest emitting areas are located

A numbered requirement is given in MRDv2.0 to cover this requirement, see comments below on requirement S7MR-SYS-110.

Parameter	Level 2 requirement
Aerosol and cloud information for accurate XCO_2 retrieval	High accuracy XCO_2 retrieval requires spatially and temporally collocated 1) aerosol & cloud information (e.g., vertical profile, optical depth, size distribution and composition) needed to calculate their effect on optical path length in CO2 spectral bands, 2) detection of low fraction of cloud fractions (5%) of optically thick clouds, 3) measuring CH_4 spectral bands (allowing proxy retrieval of XCO_2), 4) measuring solar induced fluorescence (SIF) for correction in O_2-A band

Numbered requirements are given in MRDv2.0 to cover this requirement, see comments below on requirements related to aerosols and clouds (Sect. 4.3) and detection of low cloud fractions (Sect. 4.5). Therefore, we here provide only some remarks related to justification. Additional details are given below in Sect. 4.3 and Sect. 4.5 of this document:

General remarks:

In order to obtain high accuracy and precision the observations not only have to be sensitive to CO_2 but also have to allow for corrections to a number of other interfering parameters (e.g., **/Bovensmann et al., 2010/ /Butz et al., 2011/ /Cogan et al., 2012/ /Buchwitz et al., 2013a, 2013b, 2017d/ /CS L1L2-II study FR, 2015/ /CS L1L2-II TN nadir, 2015/ /GHG-TCPS E2ES, 2018/ /CO2M AEROCARB FR, 2019/**) and this requirement considers this important aspect.

Aerosols and clouds:

Scattering by aerosols and clouds modifies the light path and light path errors needed to be minimized for accurate XCO_2 retrievals. Therefore, all XCO_2 retrieval algorithms carefully take this into account by identification and removal (flagging) of cloud contaminated scenes and by considering scattering by aerosols and (thin) clouds (e.g., thin cirrus) in the retrieval and its underlying radiative transfer model (e.g., **/Reuter et al., 2010, 2017a, 2017b, 2018/ /Heymann et al., 2012/ /O'Dell et al., 2012/ /Guerlet et al., 2013/ /Yoshida et al. 2013/ /Galli et al., 2014/ /Eldering et al., 2017/**).

Information on scattering parameters is provided, for example, by the NIR and SWIR-2 bands containing strong absorption bands of O_2, CO_2 and H_2O (e.g., **/Crisp et al., 2004/ /Aben et al., 2007/ /Heymann et al., 2012/ /O'Dell et al., 2012/ /Reuter et al., 2017b/**). The retrieval algorithms typically need *a priori* and first guess information on scattering parameters for example from models (see, e.g., **/O'Dell et al., 2012/**).

Where is the cloud fraction requirement for the detection of optically thick clouds coming from? Let us assume a thick cloud at 1 km altitude which covers 1% of a ground pixel. If the XCO_2 in this ground pixel is enhanced by 1 ppm than this would correspond to a 10 ppm enhancement in the lowest 1 km corresponding to approximately 10% of the air column. This 10 ppm enhancement would not be observed in that part of the ground pixel where the (shielding) cloud is present. 1% of 10 ppm is 0.1 ppm, i.e., the XCO_2 would be underestimated by 0.1 ppm in this case. An error of 0.1 ppm would be a significant fraction of the total error budget for the XCO_2 systematic error, which is 0.5 ppm. Therefore, 1% is required as a goal and 5% as a threshold as a 5% error would result already in a very significant XCO_2 error (0.5 ppm in this case). This simple example shows that a more demanding (threshold) requirement of about 3% would be more appropriate to avoid / minimize potentially significant XCO_2 errors.

Recommendation:

- We recommend to remove the reference to 5% cloud fraction in this requirement. It is clear that even small cloud fractions may be an issue if not considered by the retrieval algorithm. Because of this is a known potential issue, CO2M contains several means (coverage of strong and weak O_2, CO_2 and H_2O lines/bands, cloud imager, MAP instrument), which need to be used/exploited by the XCO_2 retrieval algorithm.

Remarks related to methane:

Covering also CH_4 bands is important primarily for two reasons:

(i) Methane is an important GHG and measuring XCH_4 in addition to XCO_2 would dramatically increase the benefit of the CO2M mission.

(ii) Methane helps to improve the accuracy of the estimated CO_2 emissions for CO_2 emission targets such as coal fired power plants which emit large amounts of CO_2 but only little or no CH_4. The reason is that systematic error cancel to a large extent when the CO_2 to CH_4 column ratio is computed as done in the "CH_4 proxy method", which is used for aircraft data (e.g., **/Kring et al., 2011, 2018/**) and has also been studied for CarbonSat (**/Bovensmann et al., 2010/ /Buchwitz et al., 2013a/**).

Remarks related to SIF:

Measuring SIF in the NIR band is also very important as neglecting it would result in significant XCO_2 errors **/Frankenberg et al., 2011a, 2012/**. Furthermore, SIF is related to carbon uptake by plants and therefore highly relevant for increasing our knowledge of the carbon cycle (e.g., **/Frankenberg et al., 2011b/**).

Parameter	**Level 2 requirement**
NO_2 plume images for locating CO_2 plumes	Tropospheric NO_2 shall be measured spatially and temporally collocated with XCO_2 at the same spatial resolution and with a NO_2 precision of $1.5 \cdot 10^{15}$ molec/cm^2. This anthropogenic proxy supports the emission estimates by identifying the XCO_2 source, plume direction and local wind speed

It has been shown that it is highly beneficial to also measure NO_2 as this permits to obtain much better CO_2 emission information for many localized anthropogenic emission sources (e.g., **/CO2M SMARTCARB FR, 2019/**). The benefit of co-located (simultaneous) NO_2 observations is also clearly shown in **/Reuter et al., 2014b/** and in **/Reuter et al., 2019/**.

A numbered requirement is given in MRDv2.0 to cover this requirement, see comments below on requirement S7MR-DAT-020.

MRDv2.0 contains in section 4.1.1 also several “numbered requirements”. These requirements are essentially L2 requirements. Below we provide some high level justification of these requirements (as already explained, the justification of L2 requirements is not the purpose of this document):

Requirements on overall precision:

S7MR-DAT-010	The precision of the XCO_2 product shall be better than 0.7 ppm for retrievals based on measurements with the reference SNR and fulfilling the observational requirements.

The XCO_2 precision refers to the random error or “noise” of the retrieved XCO_2. It originates primarily from the noise of the radiance observations as characterized by the instrument’s signal-to-noise ratio (SNR) but also depends on the retrieval algorithm and its state vector elements (including smoothing and interference errors) and other contributions such as instrument related “pseudo noise” originating from inhomogeneous scenes, residual XCO_2 retrieval errors due to the variability of aerosols and clouds, etc. Even constant instrument errors (e.g., residual radiometric calibration errors) will result in some pseudo noise.

Achieving high precision is important for all satellite missions aiming at improved information on CO_2 sources and sinks such as SCIAMACHY **/Bovensmann et al., 1999/ /Reuter et al., 2010/ /Reuter et al., 2011/ /Buchwitz et al., 2017a/**, GOSAT **/Yoshida et al. 2013/** and OCO-2 **/Miller et al., 2007/ /Eldering et al., 2017/** because the source / sink information is typically contained in small (few ppm to sub ppm) XCO_2 spatio-temporal gradients (e.g., **/Reuter et al., 2014/**).

High precision is specifically important if XCO_2 images shall be used to obtain information on the CO_2 emissions of localized CO_2 emission sources such as power plants or cities as the amplitude of the emission signal / plume is typically only on the order of 1 ppm (and often even less) (e.g., **/Bovensmann et al., 2010/ /Pillai et al. 2016/ /Nassar et al., 2017/ /Broquet et al., 2018/ /Reuter et al., 2019/**).

The noise of the XCO_2 image must be less than 1 ppm (and often even significantly better than 1 ppm) to "see" the CO_2 emission plume in the image for many (less strong) emission sources. Otherwise it will be very difficult if not impossible to use an image to quantify the CO_2 emission with useful precision and accuracy. Therefore, the considered driving scale for this requirement is a typical image size of approximately 100 x 100 km^2. This requirement is not meant to be a worst case requirement in the sense that it has to be met for all single ground-pixels ("spatial samples") individually but relates to the average precision for a given scene corresponding to the described scenario.

The required precision of 0.7 ppm is the minimum to be achieved (on average) for an appropriate reference scene (e.g., for a "vegetation albedo scene" or for the "Berlin reference scene" and for a solar zenith angle (SZA) of 50°). Note that the instrument noise contribution to precision is primarily determined by surface reflectivity and SZA.

Recommendation:

- "Reference SNR" is not defined in the MRDv2.0. We recommend to remove the undefined reference to the "reference SNR" and replace it by a reference to a reference scene (e.g., to the vegetation albedo scene with solar zenith angle 50°, defined as VEG50 scenario in MRDv2.0 Appendix B).

S7MR-DAT-020	The precision of the tropospheric column NO2 product shall be better than $1.5 \cdot 10^{15}$ molec/cm^2 for retrievals based on measurements with the reference SNR and fulfilling the observational requirements.

This requirement originates from CO2M specific studies and investigations related to co-located CO_2 and NO_2 plumes from localized fossil fuel burning emission targets **/CO2M SMARTCARB FR, 2019/ /CO2M-REB TN-2000 v2.1, 2020/.**

Recommendation:

- "Reference SNR" is not defined in the MRDv2.0. We recommend to remove the undefined reference to the "reference SNR" and replace it by a reference to a reference scene.

S7MR-DAT-030	The precision of the XCH4 product shall target a value better than 10 ppb for retrievals based on measurements with the reference SNR and fulfilling the observational requirements.

This requirement originates from user requirements documents such as **/Chevalier et al., 2016/**, specifying a breakthrough requirement for the XCH_4 precision of better than 17 ppb and a goal requirement of better than 9 ppb for regional scale CH_4 source/sink determination. For CO2M highest precision is required especially for the "CH_4-proxy method" XCO_2 imaging application (e.g., **/Bovensmann et al., 2010/**) because here the ratio of CO_2 and CH_4 columns are computed and, therefore, the noise of the CH_4 retrievals add (quadratically) to the XCO_2 precision.

Recommendation:

- Same as for S7MR-DAT-010.

S7MR-DAT-040	The precision of the Solar-induced Fluorescence (SIF) of Vegetation product (at 750 nm) shall target a value better than 0.7 $mW/m^2/sr/nm$ for retrievals based on measurements with the reference SNR, fulfilling the observational requirements and a SIF signal of 1.0 $mW/m^2/sr/nm$.

Achieving a good precision for SIF is important to create a reliable a priori for the CO_2 retrieval and for the use of the SIF data to investigate vegetation productivity. A precision of less than 100% will avoid significant spatial and temporal averaging which reduces the usefulness of the SIF data.

The single sounding precision for GOSAT is typically 100% or larger (i.e. 1.0 $mW/m^2/sr/nm$). The precision for SIF from OCO-2 has been estimated to be around 0.3 - 0.5 $mW/m^2/sr^1/nm$ (/**Frankenberg et al., 2014/**). A single sounding precision requirement for SIF of 0.7 $mW/m^2/sr^1/nm$ will ensure a precision comparable to OCO-2.

Requirements on overall maximum systematic error:

S7MR-DAT-050	The systematic error in the XCO2 product shall not exceed 0.5 ppm for retrievals based on measurements with the reference SNR, fulfilling the observational requirements, with a maximum AOD of 0.5 and maximum cloud coverage of 5%.

Achieving high accuracy is important for all satellite missions aiming at providing improved information on CO_2 sources and sinks such as SCIAMACHY **/Bovensmann et al., 1999/ /Reuter et al., 2010/ /Reuter et al., 2011/ /Buchwitz et al., 2017a/**, GOSAT **/Yoshida et al. 2013/** and OCO-2 **/Miller et al., 2007/ /Eldering et al., 2017/** because the source / sink information is contained in only small XCO_2 spatio-temporal gradients (e.g., **/Reuter et al., 2014/ /Reuter et al., 2019/**).

Requirements on XCO_2 biases have been formulated by **/Chevalier et al., 2016/** (and used for related documents such as **/Buchwitz et al., 2017b/**). According to these documents a threshold requirement of 0.5 ppm or better has been formulated. The analysis of the latest version of the SCIAMACHY and GOSAT XCO_2 retrievals shows that a relative accuracy close to 0.5 ppm can be achieved (after bias correction) **/Buchwitz et al., 2017c/ /Reuter et al., 2019c/**. In **/Buchwitz et al., 2017c/** it has also been estimated what the probability is that the satellite-derived products are better than 0.5 ppm taking into account that the uncertainty of the TCCON reference data **/Wunch et al., 2010, 2011, 2016/**) is about 0.4 ppm (1-sigma). These findings indicate that achieving 0.5 ppm is very demanding but not impossible. But of course also the considered spatial scale for meeting a requirement is important.

High accuracy is also important if XCO_2 images shall be used to obtain information on the CO_2 emissions of localized CO_2 emission sources such as power plants or cities as the amplitude of the emission signal / plume is typically only on the order of 1 ppm (and often even less) (e.g., **/Bovensmann et al., 2010/ /Pillai et al. 2016/ /Nassar et al., 2017/ /Broquet et al., 2018/ /Reuter et al., 2019/**). For this application biases are especially critical if they correlate with the signal of interest such as a CO_2 emission plume. If the errors do not correlate with the emission plume they may even be not critical at all but to what extent this is true or not depends on the (spatial) structure of this error and on the inversion algorithm.

Recommendations:

- "Reference SNR" is not defined in the MRDv2.0. We recommend to remove the undefined reference to the "reference SNR". This is not relevant for systematic errors.
- A cloud cover of 5% will likely result in systematic errors larger than 0.5 ppm if not corrected for. The satellite must provide enough (spectral, radiometric, spatial) information to be used by appropriate algorithms to deal with some cloud cover. It is recommended to remove the reference to 5% cloud cover.
- "Shall not exceed" suggests that 0.5 ppm is the maximum error under all conditions. This would be too demanding. The specified value is meant to be the maximum value of the standard deviation of the systematic error component relative to accurate reference measurements and therefore corresponds to a 1-sigma value rather than a maximum value.

S7MR-DAT-060	The systematic error in the NO2 product shall not exceed $3.5 \cdot 10^{15}$ molec/cm^2 for retrievals based on measurements with the reference SNR and fulfilling the observational requirements.

This requirement originates from CO2M specific studies and investigations related to co-located CO_2 and NO_2 plumes from localized fossil fuel burning emission targets **/CO2M SMARTCARB FR, 2019/ /CO2M-REB TN-2000 v2.1, 2020/.**

Recommendation:

- "Reference SNR" is not defined in the MRDv2.0. We recommend to remove the undefined reference to the "reference SNR". Note that SNR is also not directly relevant for systematic errors.

S7MR-DAT-070	The systematic error in the XCH4 product shall target not to exceed a value of 5 ppb for retrievals based on measurements with the reference SNR and fulfilling the observational requirements.

This requirement originates from relevant user requirements documents such as **/Chevalier et al., 2016/**, specifying a breakthrough requirement for XCH_4 systematic errors of better than 5 ppb.

Recommendation:

- Same as for S7MR-DAT-050

Requirements on timeliness:

S7MR-DAT-080	The Level-1 products associated with the Level-2 products shall be made available within 24 hours from sensing

This is a user input requirement and its justification is out of scope of this study.

S7MR-DAT-090	From the moment of sensing, Level-2 products shall be available within 24 hours timeliness for CO2, SIF and CH4, and as target (if feasible) faster for NO2 and aerosol parameters. Note that the product accuracy is considered more important and shall prevail over meeting the timeliness requirement for the MVS capacity

This is a user input requirement and its justification is out of scope of this study.

4.1.2. Lifetime

The corresponding MRD requirement(s) is/are:

S7MR-SYS-010	The CO2M space component shall be operational in early 2026 in order to have a complete year of CO_2 data inventory available for the stock take of 2028.

S7MR-SYS-020	The CO_2 Monitoring mission shall deliver continuous measurements over a minimum of two global stock takes, each of 5 years interval.

These requirements originate from the MRD input requirements as formulated in **/Pinty et al. 2017/**, i.e., these are user input requirements and their justification is out of scope of this study.

4.1.3. Time and geolocation requirements

In the following, the MRDv2.0 requirements are shown in **blue** and for each requirement comments are given concerning justification, proposed modification, etc.

S7MR-SYS-030	The temporal co-registration between the supporting observations (aerosol, NO_2 and cloud) and the CO_2 observations shall be better than			
	Observation	**MAP nadir**	**NO_2**	**CLIM**
	CO_2	±30 sec	±30 sec	±10 sec

This is a requirement needed to make sure that the CO_2, the MAP and the NO_2 instruments (or bands) observe "the same air mass" at "the same time". The time needed to perform all relevant MAP observations may require 180 seconds or 360 seconds but this is not relevant here but needs to be covered by a separate MAP requirement. What is relevant here is the "centre of the time interval" (which should be "the same" as the time when the CO_2 is observed) and not the length of the time interval.

30 seconds corresponds to 300 m assuming a wind speed of 10 m/s, which corresponds to 3/20-th of the ground pixel size. This is acceptable for co-located MAP aerosol and NO_2 observations.

10 seconds corresponds to 100 m assuming a wind speed of 10 m/s, which corresponds to 1/20-th of the ground pixel size. This is acceptable for CLIM cloud observations.

S7MR-SYS-040	The absolute geo-location knowledge of the Level-1b for the CO_2/NO_2/cloud products and of the Level-1c for the Aerosol products shall be better than 300 m. The requirement is applicable at sub-satellite point in nadir view assuming limited degradation toward the edge of the swath.

S7MR-SYS-045	The relative geo-location knowledge shall be better than 300 m between the Level-1b CO_2 products and the Level-1c aerosols / Level-1b NO_2 products, and 100 m with the Level-1b cloud products. The requirement is applicable at sub-satellite point in nadir view assuming limited degradation toward the edge of the swath.

Very good relative and absolute geolocation knowledge is required for a number of reasons, which are related to the XCO_2 retrieval algorithm (e.g., proper use of high spatial resolution auxiliary data such as a Digital Elevation Model (DEM) used to, for example, surface pressure computation) and to the interpretation of the XCO_2 observations / images via inverse modelling (e.g., use of XCO_2 images to obtain emission estimates).

For example it has been shown in **/CS L1L2-II TN nadir, 2015/** using a high resolution DEM for a scene covering large parts of China that the mean surface elevation (Δz) may change by 50 m at 2x2 km^2 resolution for a horizontal shift (geolocation error Δx) of 200 m, i.e., for a slope (= Δz/Δx) 25% (of course, the slope depends on spatial position and may be much less elsewhere but also higher in regions with mountains). The lowest 50 m of the atmosphere contain typically approximately 0.5% of the air mass corresponding to a 0.5% error of the

surface pressure if not corrected for. This relative error may propagate directly into a relative error of XCO_2 **/Kiel et al., 2018/**, i.e., 0.5% surface pressure error may result in a 0.5% (2 ppm) XCO_2 error. In order to reduce the XCO_2 error to below 0.5 ppm (see error budget) the surface pressure error must be less than 0.1%, which corresponds to 1 hPa or 8 m at sea level. For a geolocation error of 200 m this implies a maximum slope of 4% (=8/200) or, for 300 m, a slope of 2.7% (=8/300). The findings of **/Kiel et al., 2018/** have been confirmed using FOCAL XCO_2 retrievals **/CO2M-REB TN-2000 v2.1, 2020/.** This indicates that the 200 m geo-location knowledge requirement is well justified. If his requirement would be relaxed to 300 m than this would not be a show stopper but this probably would imply that more problematic scenes corresponding to “rough terrain” would suffer from some additional error (or requires the need to treat such scenes with more care; in the worst case such scenes need to identifies and removed from further analysis in terms of emission assessments; note that inverse modelling for regions with rough terrain / mountains will typically always be a challenge).

It may also be possible to significantly reduce the XCO_2 error by implementing corrections schemes based on appropriate analysis of (real, i.e., in-orbit) Level 1 and/or Level 2 products. Note that it has been shown for OCO-2 that very good geolocation knowledge can be critical if a bias correction is applied to reduce systematic errors **/Kiel et al., 2018/**. Currently, all missions use such a bias correction to achieve sufficiently accurate XCO_2 retrievals. These bias corrections use, among other parameters, the surface pressure difference between the retrieval and the meteorological reanalysis. Erroneous surface pressure estimates from uncertainties in the geo-location knowledge, however, may propagate nearly 1:1 into bias-corrected XCO_2, thus leading to XCO_2 biases for areas with rough terrain. This implies the development of better bias correction schemes, which do not suffer from these shortcomings.

Note:

- Good geolocation knowledge is needed even if the bands would be perfectly co-registered (imperfect co-registration may result in larger errors but could also have no significant overall effect).
- Depending on the geolocation error and on the topography the overall effect is an overestimation of the XCO_2 for certain ground pixels and an underestimation for others and therefore may be a (less critical) pseudo-noise effect.
- The impact cannot be simulated in a reliable way but needs to be studied using real data such as OCO-2 retrievals using scenes with significant changes in topography an a well characterized CO2 emission source such as a coal-fired power plant with reliable frequent (e.g., hourly in stack) emission monitoring.

S7MR-SYS-050	The Level-1 Aerosol instrument products and Level-2 NO_2 products shall be sampled on the CO_2 grid.

Maps of the CO_2, the MAP and the NO_2 products for the same scenes observed at the same time are needed in order to reduce aerosol and cloud related errors (MAP) and to obtain better CO_2 emissions using additional information on NO_2.

In order to use the MAP radiances and the radiances of the CO_2 instrument together via an appropriate XCO_2 retrieval algorithm ("joint retrieval") **/CO2M SSS FR, 2019/** it is important to resample the MAP radiances to the Level-1 (L1b) grid of the CO_2 radiances. However, other alternative approaches are also possible such as the use of the MAP aerosol information (on the MAP grid or on the CO_2 grid) for XCO_2 retrieval using Level 2 aerosol information as *a priori* information or via *a posteriori* bias correction schemes. Assuming that no significant (additional) errors are introduced by resampling to the Level-1 (L1b) CO_2 grid, then the Level-1 sampling approach is more general as it is appropriate for both methods, i.e., joint retrieval and using an alternative method.

The MAP data always need to be resampled at Level-1, as otherwise the different views (corresponding to different angles) cannot be combined for the retrieval.

In any case it is required to generate the MAP Level-2 products on the CO_2 Level-2 grid. This is important for a number of reasons such as aerosol related error assessments ("To what extent could the XCO_2 signal I am interested in be affected by aerosols contamination?") and potentially improved bias correction (overall and/or only for specific scenes).

For NO_2 the application is different as it is based on Level-2 for using the NO_2 plumes in order to be able to obtain additional information on the (noisy) CO_2 plumes **/CO2M SMARTCARB FR/, 2019/**. Note that the NO_2 retrieval should be done with the original (not resampled) radiances as any modification (such as resampling) bears the risk of resulting in a lower quality NO_2 product. It is therefore important for the envisaged application to resample the NO_2 L2 product to the XCO_2 L2 product grid, i.e., to require resampling at Level-2.

4.1.4. Coverage requirements

In the following, the MRDv2.0 requirements are shown in **blue** and for each requirement comments are given concerning justification, proposed modification, etc.

S7MR-SYS-070	Spatial coverage shall be optimised for daylight hours over the northern hemisphere with an equator crossing-time in the morning close to noon (e.g., 11:30 hrs).

Note: Time 11:30 originates from the need to have good illumination conditions (maximum around local noon), typically less clouds before noon and to have glint in the orbit even without the need to perform a pitch manoeuvre. Note also that the purpose of the pitch manoeuvre is to have a larger latitudinal coverage extending further North and South for this local time.

S7MR-SYS-080	Observations shall be made whenever the solar zenith angle (SZA) at the observed ground sample is smaller than 80° degrees.

The XCO_2 is retrieved from radiance spectra of reflected and backscattered sunlight. This requires solar zenith angles less than approximately 90°. Simulated XCO_2 retrievals but also analysis of real data shows that retrieval errors typically increase with increasing SZA and that observations at a SZA of 80° or larger often suffer from large biases due to large sensitivity to atmospheric scattering parameters (e.g., **/Buchwitz et al., 2013a/ /Eldering et al., 2017/ /Reuter et al., 2017b/**).

S7MR-SYS-090	All radiometric requirements shall be met up to a SZA of 70° degrees, with radiometric performance characterised up to 80° degrees.

Analysis of real data shows that high-quality (low bias) XCO_2 retrievals are possible if the SZA is 70° or less (e.g., **/Buchwitz et al., 2013a/ /Eldering et al., 2017/ /Reuter et al., 2017b/**). The radiometric requirements should therefore be met for all SZAs up to at least 70° and radiometric performance should be characterised up to approximately 80° degrees.

S7MR-SYS-100	Solar reference spectra shall be measured regularly allowing to compute the top-of-atmosphere reflectance and to track possible variations of the instrument response.

Satellite instruments such as SCIAMACHY/ENVISAT also performed regular observations of solar spectra and these observations have been used for the purposes listed in the requirement and they were very important to identify issues/changes of the instrument and to significantly improve the quality of the Level 1 data product (e.g., **/Hilbig et al., 2018/**). Some retrieval algorithms are based on reflectance and use the observed solar spectrum for retrieval (e.g., **/Schneising et al., 2011/**).

Recommendation:

- It is recommended to perform solar observations once per day.

S7MR-SYS-110	Global coverage and on average once per week effective coverage over land surfaces for latitudes above 40°. Note that gaps at the poles are an inherent exception of LEO missions.

It is also important to observe the emission plumes as frequently as possible and this requirement considers this important aspect (see also **/CO2M PMIF FR, 2018/**).

4.1.5. Glint mode observations

In the following, the MRDv2.0 requirements are shown in **blue** and for each requirement comments are given concerning justification, proposed modification, etc.

S7MR-SYS-120	The viewing geometry shall be optimised targeting sun glitter over large water bodies and snow-covered surfaces, which from now on will be called glint mode observation. Note that this optimisation shall be made in areas when large parts of the swath are predominantly viewing a dark water surface, assuming an average surface wind speed of 7 m/s, or dark snow-covered surfaces.

The reflectance from ocean and snow-surfaces in the SWIR in nadir geometry is too low for reliable XCO_2 and XCH_4 retrievals **/Boesch et al, 2011/.** In an orbit close to noon (as targeted) and in the Tropical region around the sub-solar point, there will be zones in the swath where the solar light is reflected at the water surface as (so- called) sun glitter which then allows XCO_2 and XCH_4 retrievals with sufficient precision. These zones can be increased to higher latitudes (i.e., poleward) by adapting the observation viewing geometry **/Boesch et al., 2014/**. It is expected that the coverage in regions with predominantly water in the field of view will be optimised to target zones with sun glitter, which will be referred to as glint mode. Unlike the observations over land, the albedo over water will strongly depend on the surface wind speed and roughness (i.e., waves). In the optimisation of the viewing geometry in glint mode, the assumed average wind speed shall be 7 m/s **/Lekouara et al., 2008/**. Care shall be taken that the radiance levels in glint mode can exceed the dynamic range maximum of the nadir mode for low wind speed conditions.

S7MR-SYS-125	Glint mode observations shall be considered valid for the coverage only if their signal is within the dynamic range of nadir mode assuming for water surfaces 7 m/s wind speed and the same viewing optimisation for snow-covered areas as for water.

Due to the nature of the sun-glitter, only part of the swath during glint mode (typically ~30km) is likely to have a signal within the instrument's dynamic range (and thus allow CO_2 retrieval within the requirements) and data in a significant part of the swath would fall outside this range. Only the fraction of the observations of a swath within the dynamic range will contribute to the coverage.

S7MR-SYS-130	Glint observations shall target coverage of all large water and snow-covered surfaces typically at monthly regional scale. Any data related to observations in glint mode over land surfaces shall be downlinked and processed.

To obtain global coverage, it is necessary to target all large water and snow-covered surfaces in glint mode. Such glint mode observations will provide a clear background level assisting the estimates of CO_2 emissions and help to constrain data assimilation models. Larger-scale flux inversion models will benefit of ocean coverage for estimating land-sea fluxes. Less frequent (monthly) coverage is sufficient over water and snow surfaces away from anthropogenic emission sources.

Note: To what extent glint more observations over land are useful in general compared to nadir observations needs to be assessed but (depending on angles) differences may be small.

S7MR-SYS-135	Glint mode observation shall target coverage of coastal areas as frequent as possible.

The primary target of the mission requires a good coverage over and near anthropogenic emission areas, which includes islands and coastal outflow regions. The objective of measuring over large water bodies is to enable observing coastal zones and the potential outflow of anthropogenic CO_2 from cities or other sources near the coast which need to be captured as often as possible.

S7MR-SYS-140	The degradation in performance of observations in glint mode shall remain limited as compared to the performance in nadir mode. Note that aerosol information would still be useful even if the observations would rely on less useful observation angles

To obtain XCO_2 retrievals within the retrieval performance requirements will require glint mode observations with similar observational performance as nadir mode observations.

S7MR-SYS-145	Land areas can be covered in glint mode if they are not part of the mask depicted in red in Figure 4.1 and/or if the area can be observed with a pitch angle up to $\pm 15^o$ degrees and/or it is snow-covered.

Land areas are best covered while in nadir mode, however there are many small land areas (e.g., islands) that could prevent the mission to switch mode. In order to increase coverage over water, a mask has been generated excluding small land areas, excluding land areas covered with ice (i.e., Greenland and Antarctic) and excluding larger islands with low population densities (i.e., no hot spot sources). Land areas and water bodies are equally covered in nadir and glint mode close to the sub solar point within 15^o degrees pitch angle, as the geometrical degradation is considered limited.

4.1.6. Summary and Conclusions

This section differs significantly from the corresponding section as given in MRDv1.0. For example, this section now also contains numbered requirements for precision and systematic error of XCO_2 and several other parameters (especially for XCH_4, NO_2 tropospheric columns and Solar Induced Fluorescence (SIF)). Detailed justification of these higher level user requirements is out of the scope of the present study, which focusses on L1 requirements. Nevertheless, each MRDv2.0 requirement is listed in this document and information on its justification is given in this document.

This section also contains a number of other input user requirements such as on timeliness and lifetime. Also these requirements are listed in this document but it is explained that justification of these requirements is out of the scope of this study. Justification is provided for requirements related to temporal co-registration of the CO_2, MAP (Multi-Angle-Polarimeter), NO_2 and CLIM (Cloud Imager) observations based on the overarching requirement to observe essentially the same air mass at the same time. Related to this are also the corresponding geolocation knowledge requirements. Furthermore, justification is given for the coverage requirements and the MRD requirements related the glint mode observations.

Earlier recommendations related to refinement of requirements have been considered for MRDv2.0. For example, it has been added to characterise the radiometric performance for solar zenith angles up to 80^o and the temporal co-registration requirement is better and clearer now.

Some recommendations are given on how to further improve the MRD. For example, some requirements (e.g., S7MR-DAT-010) refer to a “reference SNR”, which is not specified in the MRD, and requirement S7MR-DAT-020 refers to a cloud coverage of 5%, which is likely not demanding enough.

4.2. Mission Requirements of the CO_2 Observations

4.2.1. Geometric Requirements

In the following, the MRDv2.0 requirements are shown in **blue** and for each requirement comments are given concerning their justification, proposed modification, etc.

S7MR-OBS-010	The minimum across-track swath width shall be 250 km contiguously sampled

The wider the (swath of the) XCO_2 images are, the more frequently the CO_2 emission signals of the localized emission sources are observed and the larger the area of the observed emission plume (e.g., **/Bovensmann et al., 2010/ /Pillai et al. 2016/ /Nassar et al., 2017/ /Broquet et al., 2018/ /Reuter et al., 2019/**).

The swath width shall therefore be as wide as possible but not much narrower than about 200 km in order to properly include the plumes and their background **/CO2M SMARTCARB FR, 2019/ /CO2M PMIF FR, 2018/**.

S7MR-OBS-020	The area covered by the product of SR_{ALT} x SR_{ACT} shall be ≤ 4 km^2. Note that this requirement is applicable at the sub satellite point assuming limited degradation toward the edge of the swath.

The spatial resolution of the XCO_2 image needs to be high enough to resolve emission plumes and, therefore, should ideally be smaller than the smallest dimension of an emission plume, which is (typically) the direction perpendicular to the wind direction. The magnitude (amplitude) of the observed emission plume decreases with increasing spatial resolution as shown in, for example, **/Bovensmann et al., 2010/** (see their Fig. 1 and Tab. 1). High spatial resolution is therefore important (along with other parameters such as SNR) to detect emission plumes and to accurately quantify the corresponding emission source.

As shown in **/Bovensmann et al., 2010/**, the ground pixels should not be significantly larger than about 2 km.

The exact shape of the ground pixel is not very critical but it is important that the shape is well enough known. Shapes which deviate strongly from a square or a circle, especially too elongated shapes, need to be avoided (depending on orientation this may result in bad sampling of emission plumes). This is considered by the aspect ratio requirement.

Comment on aspect ratio:

The geometric extent of the satellite footprints should be “similar” in all directions (but not necessarily a circle or a square). This ensures that the sampling of emission plumes is similar for all orientations (directions) of an emission plume. An approximately square

footprint shape has been assumed in several previous CO2M related studies (e.g., **/Bovensmann et al., 2010, 2015/ /CS L1L2-II TN nadir, 2015/ /Pillai et al. 2016/ /Broquet et al., 2018/ /GHG-TCPS E2ES, 2018/ /CO2M PMIF FR, 2018/**).

Note: The MRD contains the following textual requirement: "The spatial sampling distance (SSD) in across-track and along-track direction, resp. SSD_{ACT} and SSD_{ALT}, should be such that its product is smaller than 1.2 times the product of the SR_{ACT} and SR_{ALT} as required in S7MR-OBS-020."

Strictly speaking, the footprint is characterized by its System Energy Distribution Function (SEDF). As shown in **/CS L1L2-II TN nadir, 2015/** it is important to know the shape of the SEDF for accurate plume inversions. It is therefore important to have a requirement on the SEDF shape knowledge (see below).

Even if the SEDF error would be zero, the emission error would typically not be zero due to other error sources present for plume inversions (e.g., wind speed errors, errors in the *a priori* assumptions on the emissions, residual background XCO_2 errors, etc.) and one may expect errors on the order of 10% (e.g., **/Bovensmann et al., 2010, 2015/ /CS L1L2-II TN nadir, 2015/ /Pillai et al. 2016/ /Broquet et al., 2018/ /GHG-TCPS E2ES, 2018/ /CO2M PMIF FR, 2019/**). If the overarching requirement is that the additional SEDF-related error should be significantly small compared to other errors (so that the additional error contribution is insignificant) than a reasonable requirement is that the SEDF-related error should be << 10%, i.e., approximately 3% or less. Depending on the "shape" of this error one may expect that a 3% error in the width (no shape error) or a 3% error in the shape (no width error) results in an approximately 3% error of the estimated emission. The reason is that, for example, a 3% width error implies a 3% amplitude (height) error (if the area remains the same) which implies a 3% emission error due to a 3% error of the scaling factor applied to the plume model when fitting the modelled plume to the observed plume (which suffers from an SEDF error). Detailed assessments related to the impact of SEDF errors on emissions are presented in **/CS L1L2-II TN nadir, 2015/** (their Sect. 11), where it is shown (see their Tab. 25) that emission errors can be 2% for SEDF errors of 5% (= 0.1 km / 2.0 km). Also this confirms that SEDF width and shape errors of less than 3% would ensure acceptable emission errors.

This is consider by MRDv2.0 where the following is written:

The spatial resolution along-track and across-track should be known to an accuracy better than 3.0%. The SEDF shape should be known to an accuracy better than 3.0% of the peak value of the SEDF in the spatial range Λ where the SEDF is at least 3% of the peak value.

Comment:

CO_2 imaging requires (per definition) approximately consecutive footprints across track and along track. This feature has been assumed in several previous CO2M related studies (e.g., **/Bovensmann et al., 2010, 2015/ /CS L1L2-II TN nadir, 2015/ /Pillai et al. 2016/ /Broquet et al., 2018/ /CO2M PMIF FR, 2018/**).

S7MR-OBS-050	The spatial samples observed by any two channels shall overlap ≥ 95%

XCO_2 errors resulting from intra-/inter-band spatial co-registration related errors of the CO_2 imager need to be minimized. XCO_2 errors originating from spatio-temporal co-registration related errors have been assessed in **/CS L1L2-II TN nadir, 2015/** (their Sect. 12). It has been found that XCO_2 errors typically do not exceed 0.48 ppm for spatial co-location errors in the range 100-400 m. 100 m corresponds to 5% of 2 km, i.e., to 95% overlap (= goal (G)). 300 m corresponds to 15% of 2 km, i.e., to 85% overlap (= threshold (T)).

According to the Error Budget (EB) **/CO2M-REB TN-3000 v2.1, 2020/** a Total Uncertainty of 0.5 ppm has been allocated for error source “Spatio-temporal co-registration”.

How large the XCO_2 error is for a given overlap error depends on the scene. For scenes with little variations of surface topography and reflectivity and little variation of aerosols, even a large overlap error will result only in a negligible XCO_2 error but for scenes where this is not the case, the XCO_2 error will be larger. How large the resulting emission errors is depends in addition on the error pattern in the image and the location of the emission plume in the image. A larger overlap error will not be a show stopper but will likely result in a larger number of too problematic scenes, where the emission error will be larger than the average error or – in the worst case – more scenes need to be exclude for reliable emission assessment. This shows that it is difficult if not imposible to define a clear value different from zero which is acceptable for all cases.

The past study (**/CS L1L2-II TN nadir, 2015/**) has shown that XCO_2 errors are likely less than 0.5 ppm for co-location errors less than approximately 300 m, which corresponds to the 85% (T) MRDv1.0 requirement but of course smaller errors are preferred. MRDv2.0 considers this by this 95% requirement.

It is obviously important that the same air mass needs to be observed at all wavelength (as good as possible) as this is the fundamental concept of a spectrometer, which shall measure spectra for well-defined scenes / footprints. This requirement takes this into account. But note that “same air mass” is not well defined as the observation light path depends on the (variable scattering and absorption) optical depth and surface properties. “Same air mass” therefore means same geometric (light) path in this context. This requirement is therefore important and appropriate.

4.2.2. Spectral Requirements

In the following, the MRDv2.0 requirements are shown in **blue** and for each requirement comments are given concerning justification, proposed modification, etc.

S7MR-OBS-080	**Band ID**	**Spectral range [nm]**	**Spectral resolution [nm]**	**Spectral sampling ratio ***
	NIR	747–773	0.12	3
	SWIR-1	1590–1675	0.3	3
	SWIR-2	1990–2095	0.35	3
	* This value shall be the average achieved value for the spectral oversampling across the band with a minimum value of 2.8 required anywhere in the band			

The required spectral coverage, spectral resolution and spectral sampling ratios originate from several retrieval studies, where it has been shown that such an instrument provides sufficient information on CO_2 and other important parameters to permit XCO_2 retrievals of the required quality (of course this depends also on other parameters such as SNR) **/CS L1L2-II TN nadir, 2015/ /Buchwitz, 2018/ /Reuter et al., 2018/ /GHG-TCPS E2ES, 2018/ /CO2M SSS FR, 2019/**.

The following is written in MRDv2.0 w.r.t. spectral knowledge:

The position of the spectral channel centres should be known at Level-1b with an accuracy better than 1/20 of the spectral sampling interval (SSI) for spatially uniform and nonuniform scenes. Note that this should be fulfilled by combined analysis of on-ground calibration & characterisation and in-flight data.

This requirement originates from retrieval simulations performed in order to quantify XCO_2 biases originating from spectral calibration errors **/CS L1L2-I study FR, 2014/** (Sect. 7.8).

The following is written in MRDv2.0 w.r.t. spectral stability:

The spectral stability of all spectral channels should be better than 5/20 SSI between two consecutive solar calibrations.

It is assumed that this is sufficient to meet the spectral knowledge requirement, which his stricter, namely 1/20 SSI.

Ideally, the spectral stability should be better (smaller required value) compared to the required spectral knowledge to keep the spectral knowledge from one calibration to the next.

The following is written in MRDv2.0 w.r.t. the Instrument Spectral Response Function (ISRF) shape:

> The ISRF should be of the form that its integrated area satisfies
>
> $$\int_{\text{FWHM}} \text{ISRF}(\lambda)\,d\lambda \;\geq\; 0.7 \int_{\Lambda} \text{ISRF}(\lambda)\,d\lambda$$
>
> Here Λ covers the spectral range where the ISRF is at least 1.0% of its maximum value.

This requirement ensures that the ISRF shape is "useful" as it ensures that within one spectral resolution interval at least 70% of the signal is contained and that less than 30% is mixed in from neighbouring intervals.

The following is written in MRDv2.0 w.r.t. ISRF shape knowledge:

> The ISRF shape should be known to an accuracy better than 2.0% of the peak value of the ISRF in the spectral range Λ where the ISRF is at least 2% of the peak value.

ISRF related XCO_2 errors have been quantified in **/CS L1L2-II TN nadir, 2015/** (their Sect. 10 referring mainly to **/CS L1L2-I study FR, 2014/**). They report worst case errors as large as 1 ppm but argue that this may correspond to approx. 0.2 ppm (1-sigma), which is the Total Uncertainty value for ISRF in the EB (see **/CO2M-REB TN-3000 v2.1, 2020/**). However, here the assumption was that the ISRF shape is known to 1%, which is a factor of two stricter than the 2% requirement in the MRD (S7MR-OBS-110).

ISRF related errors have also been assessed in the framework of an ESA study focussing on "spectral sizing" using three independent analyses. **/Buchwitz, 2018/** obtained errors in the range 0.15 to 0.46 ppm (their Figs. 43 and 44 top) depending on the assume wavelength dependence of the error. **/Landgraf et al., 2017c/** report mean biases less than 0.35 ppm for a global ensemble and using a different retrieval algorithm. Using another algorithm and other scenarios, **/Boesch, 2018/** reports errors exceeding 1 ppm.

New simulation for CO2M have been carried out and are reported in **/CO2M-REB TN-2000 v2.1, 2020/**. The results obtained with FOCAL indicate that XCO_2 errors are less than the 0.2 ppm as permitted according to the EB but may exceed 2 ppb as permitted for XCH_4 as a 2% shape error in the SWIR-1 band may result in errors of 4.5 ppb.

The following is written in MRDv2.0 w.r.t. ISRF shape variations:

> The difference between the ISRF shape over non-uniform scenes and the ISRF over a uniform scene should be smaller than 1.5% of the peak value of the ISRF in the spectral range Λ where the ISRF is at least 2% of the peak value. Note that a spectral shift effect is covered separately.

Heterogeneous scenes may result in XCO_2 errors due to (unknown) ISRF variations caused by inhomogeneous slit illumination. Corresponding XCO_2 errors have been investigated in **/CS L1L2-II TN nadir, 2015/** (their Sect. 9.6). It has been found that a 2% ISRF shape error corresponds to an XCO_2 error of approximately 0.3 ppm. However, for very challenging scenes the error may be somewhat larger. According to the Error Budget (EB) **/CO2M-REB TN-3000 v2.1, 2020/** a Total Uncertainty of 0.35 ppm has been allocated for this error source.

The following is written in MRDv2.0 w.r.t. ISRF FWHM knowledge:

> The FWHM of the ISRF should be known to an accuracy of 1%.

Simulation for CO2M have been carried out and are reported in **/CO2M-REB TN-2000 v2.1, 2020/**. The results obtained with FOCAL indicate that XCO_2 errors are less than the 0.2 ppm as permitted according to the EB and that XCH_4 errors are less than 2 ppb.

4.2.3. Radiometric Requirements

In the following, the MRDv2.0 requirements are shown in **blue** and for each requirement comments are given concerning their justification, proposed modification, etc.

Dynamic range:

S7MR-OBS-140	The requirements shall be met for radiance levels in the dynamic range as specified in Table 4.7 between DR-max-0 and DR-min-70 corresponding to scenarios with a SZA of 0 and 70 degrees, respectively. The continuum signal levels for other SZAs can be derived by scaling the DR-max-0 signal levels with the cosine(SZA).

Note that Tab. 4.7 is not repeated here. Note also that the following is written in MRDv2.0:

In some regions, such as the Sahara desert, the radiance levels will exceed the nominal ranges specified in requirement S7MR-OBS-140 and Table 4.7. In these specific regions, where the radiance levels do not exceed these values by more than a factor of 2, the observation should not saturate. As such it should be possible, by scaling the dynamic range up to a factor 2, without altering the along-track or cross-track sampling, to quantify radiance levels twice as high as in S7MR-OBS-140 for specific (to be specified) regions. Note that in these regions, the minimum of the dynamic range can be increased proportionally to preserve the amplitude of the dynamic range specified in S7MR-OBS-140.

Dynamic range maximum value:

The corresponding MRDv1.0 dynamic range maximum “DR-max-0” radiances were:

- NIR: 9.4×10^{13} photons/s/nm/cm^2/sr corresponding to the continuum radiance of this scenario: Solar Zenith Angle (SZA) 0^o and albedo 0.6
- SWIR-1: 2.6×10^{13} photons/s/nm/cm^2/sr, corresponding to SZA 0^o and albedo 0.4
- SWIR-2: 1.4×10^{13} photons/s/nm/cm^2/sr, corresponding to SZA 0^o and albedo 0.4

Simulation for CO2M have been carried out and are reported in **/CO2M-REB TN-2000 v2.1, 2020/** using surface albedos from MODIS and analysis of OCO-2 radiances.

The recommendation as given in **/CO2M-REB TN-2000 v2.1, 2020/** with respect to the upper limit of the dynamic range are:
The DR-max-0 values as listed in the MRDv1.0 need to be enlarged to (at least):
For cloud-free nadir observations over land:

- NIR: 14.7×10^{13} photons/s/nm/cm^2/sr
- SWIR-1: 5.1×10^{13} photons/s/nm/cm^2/sr
- SWIR-2: 2.8×10^{13} photons/s/nm/cm^2/sr

For observations with clouds to (at least):

- NIR: 20×10^{13} photons/s/nm/cm^2/sr
- SWIR-1: 6.0×10^{13} photons/s/nm/cm^2/sr
- SWIR-2: 2.8×10^{13} photons/s/nm/cm^2/sr

It is therefore very good that MRDv2.0 considers the fact that radiances may exceed the listed "DR-max-0" values. This ensures that the radiance spectra will not "saturate" under certain conditions (e.g., over deserts combined with low SZA), i.e., remain potentially very useful.

Dynamic range minimum value:

Concerning the dynamic range minimum, DR-min-70, ESA pointed out the DR-min-70 values as specified in the MRDv1.0 are very demanding (for a number of requirements). However, as shown in **/CO2M-REB TN-2000 v2.1, 2020/** the currently specified values are very reasonable and even lower may values occur in spectral regions with very strong absorptions. A relaxation is therefore not recommended.

Signal-to-Noise Ratio (SNR):

	Band ID	**SNRmin @ Lmin**	**SNRref @ Lref**	**SNRmax @ Lmax**
S7MR-OBS-150	NIR	75 @ 7.0 x 10^{11}	330 @ 6.4 x 10^{12}	1350 @ 9.4 x 10^{13}
	SWIR-1	240 @ 1.1 x 10^{12}	400 @ 2.1 x 10^{12}	1600 @ 2.6 x 10^{13}
	SWIR-2	150 @ 5.6 x 10^{11}	400 @ 1.8 x 10^{12}	1300 @ 1.4 x 10^{13}
The total XCO_2 random error budget has a large contribution from SNR, which in this requirement has a component of 0.6 ppm coming from SNR.				

An update of the corresponding requirement as given in MRDv1.0 is proposed in **/CO2M-REB TN-2000 v2.1, 2020/** Sect. 4.2.1 including formulas and corresponding parameters but also alternatively in terms of SNRmin@Lin and SNRref@Lref. This recommendation has been considered for MRDv2.0.

Note: The SNR requirement has been specified to achieve a total XCO_2 random error of 0.7 ppm with 0.5 ppm allocated to SNR based on the VEG50 and REF50 scenarios (two relevant "typical" scenarios in terms of surface albedo and for a solar zenith angle of 50^o).

The following table is given in MRDv2.0 w.r.t. the SNR of solar irradiance signals:

Band ID	L_{sun} [photons/s/nm/cm^2]	SNRref *
NIR	4.9 x 10^{14}	10000
SWIR-1	2.1 x 10^{14}	5000
SWIR-2	1.15 x 10^{14}	5000

Justification:

The required SNR for the solar irradiance is much higher compared to the required SNR of the radiance spectra and therefore the SNR of the sun-normalized radiance or of the reflectance is essentially determined by the SNR of the radiance. Therefore the required performance is very good which justifies this requirement.

Note: The solar irradiance values correspond to typical background irradiances in the three CO2M bands. The required SNR originates from the need to have an SNR much higher than the SNR of the nadir and glint mode scenes such that the (relative) noise of the reflectance spectra is essentially identical with the (relative) noise of the radiance spectra, i.e., the (relative) noise of the irradiance spectra is negligible in comparison to the radiance spectra. The required SNR as listed in the table above is not to be interpreted as a threshold requirement, i.e., if the performance would be somewhat worse than this would still be acceptable.

Radiometric requirements for TOA radiance and reflectance:

S7MR-OBS-180	The absolute radiometric accuracy (ARA) of the radiance measurement at the TOA shall be better than 3% in NIR, SWIR-1, and SWIR-2 for the dynamic range of the continuum levels in Table 4.7 (DR-cont-min-70 to DR-max-0).

Justification:

Continuum radiances are typically used in retrieval algorithms to obtain estimates of the surface albedo for each spectral band. Corresponding retrieval simulations are reported in **/CS L1L2-II TN nadir, 2015/** (their Sect. 9.7), where it has been estimated how large the XCO_2 error (and the XCH_4 error) is for various surface albedo errors. Based on these results it has been concluded that a 3% requirement for ARA is appropriate.

This has been confirmed by additional assessments results as shown in **/CO2M-REB TN-2000 v2.1, 2020/**.

The following is written in MRDv2.0 w.r.t. relative spectral radiometric accuracy (RSRA):

The Relative Spectral Radiometric Accuracy (RSRA) of the ratio between the radiance and irradiance within each band (intra-band) should be better than 0.5%.

Note: This requirement is a backstop for the limitations of the ESRA requirement.

Performance assessments for RSRA are reported in **/CS L1L2-II TN nadir, 2015/** (their Sect. 9.3). As shown in that document, the resulting XCO_2 errors are typically less than about 0.2 ppm. According to the Error Budget (EB) **/CO2M-REB TN-3000 v2.1, 2020/** a Total Uncertainty of 0.2 ppm has been allocated for this error source. From this it is concluded that the requirement is justified.

The following is written in MRDv2.0 w.r.t. relative spatial radiometric accuracy (RXRA):

> The relative spatial radiometric accuracy (RXRA) of the ratio between the radiance and irradiance measurements within the swath should be better than 0.5%.

XCO_2 error analysis results for this error source are shown in **/CS L1L2-II TN nadir, 2015/** (their Sect. 9.7). As shown in that document, XCO_2 errors are about 0.03 ppm. When (quadratically) adding this to the ARA-related error one obtains a total uncertainty of about 0.1 ppm. This is somewhat less than the value listed in the EB (see **/CO2M-REB TN-3000 v2.1, 2020/**) but it is recommended to have some margin, as the final L1-L2 retrieval algorithm still needs to be defined and it is therefore at present unknown if it will have a somewhat stronger sensitivity to this type of error or not. Overall, this indicates that the requirement is justified.

The following is written in MRDv2.0 w.r.t. relative spatial radiometric accuracy (RXRA):

> The relative spatial radiometric accuracy (RXRA) of the ratio between the radiance and irradiance measurements within the swath should be better than 0.5%.

Note: This requirement is needed to avoid striping (like in OMI).

Performance assessments for RXRA are reported in **/CS L1L2-II TN nadir, 2015/** (their Sect. 9.3). As shown in that document, the resulting XCO_2 errors are typically less than about 0.1 ppm. According to the Error Budget (EB) **/CO2M-REB TN-3000 v2.1, 2020/** a Total Uncertainty of 0.2 ppm has been allocated for radiometric error source "Multiplicative/relative" which comprises ESRA and RSRA in addition to RXRA. From this it is concluded that the requirement is justified.

Effective Spectral Radiometric Accuracy (ESRA):

S7MR-OBS-220	The effective spectral radiometric accuracy (ESRA) correlating with atmospheric spectral structures shall be constrained using the Gain Matrix Method. The systematic XCO_2 error due to ESRA shall be lower than 0.4 ppm. Efforts shall be made to limit the systematic XCH_4 error due to ESRA with a target value of 5 ppb. This shall assume incident light with maximum DoLP of 60% in NIR and 30% in SWIR. Note that this requirement accounts for the largest fraction in the systematic error budget of Table 4.1.

The purpose of this requirement is to minimize erroneous “spectral features”, especially those which interfere with spectral variations of interest such as those due to CO_2, O_2, and CH_4 absoption lines.

According to the Error Budget (EB) **/CO2M-REB TN-3000 v1.1, 2019/ /CO2M-REB TN-3000 v2.1, 2020/** Tab. 1 a Total Uncertainty of 0.4 ppm has been allocated for this error source for XCO_2 (0.45 ppm for ESRA, RSRA, RXRA).

The EB **/CO2M-REB TN-3000 v1.1, 2019/ /CO2M-REB TN-3000 v2.1, 2020/** lists in Tab. 2 a Total Uncertainty of 5 ppb for this error source for XCO_2 (5 ppb for ESRA, RSRA, RXRA).

This shows that this requirement is consistent with the EB.

The following is written in MRDv2.0 w.r.t. Zero-Level-Offset (ZLO):

As unknown small additive offsets on the radiance have a severe impact on XCO_2 retrievals, there is a need to define the offset correction accuracy.

The offset (zero-level baseline) correction accuracy (in photons/s/nm/cm^2/sr) of the radiance should be known to

- 6.0×10^9 in NIR,
- 3.0×10^9 in SWIR-1,
- 1.5×10^9 in SWIR-2.

According to the Error Budget (EB) **/CO2M-REB TN-3000 v2.1, 2020/** a Total Uncertainty of 0.2 ppm has been allocated for this error source.

Simulation for CO2M have been carried out and are reported in **/CO2M-REB TN-2000 v2.1, 2020/**. These simulations have been done using ZLO errors as specified in MRDv1.0. The results obtained with FOCAL indicate that XCO_2 errors may exceed the 0.2 ppm as permitted according to the EB if ZLO is not added as state vector elements but are less than 0.2 ppm if ZLO is added as state vector element. This shows that the justification status depends critically on the retrieval algorithm. When FOCAL is applied to real OCO-2 data **/Reuter et al., 2017b/** then ZLO is not added as state vector elements but a ZLO correction is used instead. This indicates that the values specified in MRDv1.0 are appropriate but to be on the

save side it was recommended to specify somewhat lower values compared to the values specified in MRDv1.0. This recommendation has been considered for MRDv2.0.

4.2.4. Summary and Conclusions

In this section, all requirements as listed in MRDv2.0 are presented and for each requirement justification is provided based on existing peer-reviewed publications, relevant results from ESA or other studies and specific new simulation results carried out in the framework of this study.

As shown in this document, essentially all requirements are considered justified.

This is an improvement compared to MRDv1.0. Several earlier recommendations related to refinement of MRDv1.0 requirements have been considered for MRDv2.0. For example, the minimum across-track swath width is wider now, the requirement on the overlap of spatial samples is more demanding, recommendations on improvements related to the required signal-to-noise-ratio (SNR) have been considered and a requirement on spectral stability has been added.

4.3. Mission Requirements of Aerosol and Cloud Observations

The section gives justifications and recommendations to MRDv2.0 requirements, which are related to the Multi-Angle Polarimeter (MAP) instrument.

The corresponding MRDv2.0 requirements are shown in **blue** and for each requirement comments are given concerning their justification, proposed modification, etc.

4.3.1. Geometric Requirements

S7MR-OBS-300	The across-track swath width shall be equal or larger than for the CO2 instrument (i.e., S7MR-OBS-010) and contiguously sampled

MAP measurements will be resampled on the CO_2 pixel, so contiguous sampling and overlap is needed for the swaths of polarimeter and the CO_2 spectrometer.

S7MR-OBS-305	The spatial resolution of aerosol observations, after resampling, shall be such that the area covered by SR_{ALT} x SR_{ACT} is $\leq$ 16 km^2. Note that this requirement is applicable at the sub satellite point assuming limited degradation toward the edge of the swath.

Using Aeronet data at several ground stations **/Dubowik et al., 2020/** studied the variation of aerosol properties in wind direction with the following main conclusions:

- The changes of aerosol type (indicated by changes of the Angstrom exponent, and the single scattering albedo) are negligible at scales of 4 km;
- Mean changes of aerosol loading (specified by the aerosol optical depth (AOD) at 440 nm) are acceptable on both a 2 and 4 km horizontal scale. Here, the maximum variability for all observations are:
    - AOD(440nm) for 4 km: mean = ~ 0.04(0.024), max = ~ 0.25(0.1)
    - AOD(440nm) for 2 km: mean = ~ 0.02(0.012) , max = ~ 0.125(0.05)

  where numbers in parentheses exclude high AOD events. The mean variability changes insignificantly with a mean = ~0.004 when enhancing the horizontal scale from 2 km to 4 km with highest values over urban sites (e.g. Beijing 0.019 (2.8%); GSFC; Kanpur; Xianghe; Mexico_City > 0.01).
- Based on observation geometry consideration, acquisition of high accuracy multi-angular observations at 2 km spatial resolution can be challenging, whereas the 4 km sampling strategy is less affected.

Therefore, a relaxation in the spatial resolution from 2x2 km^2 to 4x4 km^2 is justified, where the polarimeter spatial pixel shall be centred around the spectrometer pixel.

The following is written in MRDv2.0:

The aerosol measurements need to be acquired at a sampling high enough to allow its resampling to the CO2 measurements. Therefore, the spatial sampling distance is expected to be at least twice as small in both the ALT and the ACT direction. This means that the aerosol observation's spatial resolution is oversampled.

Resampling errors can be reduced significantly for spatially oversampled MAP measurements. It is shown that for a common spatial resolution a spatial oversampling of 2 in both spatial dimension is sufficient to be compliant with the radiometric requirements both on radiance and DoLP **/CO2M SSS FR, 2019/**. See also **/CO2M-REB TN-2000 v2.1, 2020/** (Sect. 7.6).

S7MR-OBS-330	The relative geo-location knowledge shall be better than 400 m between spatial position of the different viewing angles

For a spatial resolution of 4 km in both directions, a geo-location knowledge of better than 400 m is sufficient. See **/CO2M-REB TN-2000 v2.1, 2020/** (Sect. 7.6).

4.3.2. Modulation concept, Spectral and Radiometric Requirements

In the following, the MRDv2.0 requirements are shown in **blue** and for each requirement comments are given concerning their justification, proposed modification, etc.

S7MR-OBS-340M	The number of OZAs along track (ALT) shall be 5

Sensitivity studies on the numbers of MAP viewing angles showed a very significant change in the induced XCO_2 error when enhancing the number of observation zenith angles from 3 to 4. Five angles allow nadir view with symmetric angle distribution in forward and backward direction and introduces some redundancy. Having more than 5 viewing angles leads only to a marginal increase of XCO_2 accuracy. An odd number of viewing angles is preferred to an even number because of the inclusion of the nadir view. The setup with 5 viewing angles meets the target XCO_2 error (<=0.15%), whereas that with 3 viewing angles does not. A corresponding analysis is shown in **/CO2M SSS FR, 2019/** and **/CO2M-REB TN-2000 v2.1, 2020/** (Sect. 7.5.2.3).

S7MR-OBS-350M	The observation zenith angle angular sampling interval, for targets on the sub-satellite track, shall be regular within a total angular sampling range of +/-60 degrees including 0 degree (nadir) as one of the OZAs

Multiangle observations are needed to cover different scattering angle (single scattering geometry) for all relevant pixels and solar position. An optimisation of OZAs other than a regular sampling is not possible because the corresponding scattering angles depend also on solar geometry, which changes over an orbit. The nadir mode is needed for cross calibration with the CO_2 spectrometer in the NIR **/CO2M SSS FR, 2019/**. For outer angles larger than +/- 60 degrees coregistration and the sphericity of the Earth atmosphere causes problems in the data interpretation. The maximum angle of +/-60 degrees is chosen based on experience with POLDER and MISR, where a limit of 60 degrees is used.

S7MR-OBS-360M	**Band ID**	**Spectral range [nm]**	**Spectral resolution [nm]**	**Spectral sampling ratio**
	UVN	385–770	5	3 *
* This value shall be the average achieved value for the spectral oversampling across the band with a minimum value of 2.8 required anywhere in the band				

Both, the UV and the NIR edge of the spectral range is validated **/CO2M SSS FR, 2019/** and the spectral range of 385-770nm with spectral resolution of 5 nm is justified for 5 OZAs. Expanding the spectral range to include more UV wavelengths down to 350 nm or to include 2 SWIR channels (at 1640 and 2250 nm) leads to no to little gain in XCO_2 accuracy (see also **/CO2M-REB TN-2000 v2.1, 2020/**). The spectral modulation concept requires resampling of radiances. Here, we follow the common requirement of spectrometers for a spectral sampling ratio ≥ 3 to limit any errors on spectral resampling.

S7MR-OBS-370M	**Band ID**	**Spectral range [nm]**	**DoLP spectral resolution [nm]**	**Spectral sampling ratio**
	UVN	385–770	15 @ 385 nm 40 @ 755 nm	1

The spectral range, resolution and sampling is justified in **/CO2M SSS FR, 2019/.** DOLP measurements below 385 nm (till 350 nm) did not provide additional error reduction in XCO_2. Neither do extra SWIR measurements due to the SWIR measurements of the spectrometer. Note: It is not required to measure a larger spectral range in order to have this resolution covered at 385 nm as long as at 385 nm all requirements are met.

S7MR-OBS-375M	The requirements shall be met for radiance levels in the dynamic range of the spectra depicted in Figure 4.2 between L_{max} and L_{min}

Figure 4.2 of MRDv2.0 shows the reference spectra:

- L_{max} for an elevated aerosol layer at 4 km (coarse mode) with for total AOT = 0.3, SZA = 1°, VZA = -20°, with the maximum spectral radiance of a vegetation and sand spectrum including 20 % margin
- Lmin for a boundary layer with total AOT=0.12, SZA=70°, VZA = 30°, soil BDRF
- Lref for an elevated aerosol layer at 4 km (coarse mode) with total AOT=0.3, SZA=50°, VZA = 50°, vegetation BDRF

where L_{max} and L_{min} covers the radiometric range of the majority of cloud free observations.

S7MR-OBS-380M	The ARA of the (TOA) radiance shall be better than 3%

This requirement is verified as a total uncertainty of 3 % on the radiances **/CO2M SSS FR, 2019/.** In order to keep the XCO2 error below 0.15% the total uncertainty of the (TOA) radiance shall be better than 3%.

S7MR-OBS-390M	The DoLP absolute accuracy shall be ≤ 0.0035 over the range 0–0.70 in DoLP

This requirement is verified as a total uncertainty on the DoLP **/CO2M SSS FR, 2019/**
In order to keep the XCO_2 error below 0.1%, the DoLP absolute accuracy shall be ≤ 0.0035.

The following is written in MRDv2.0:

> The DoLP absolute accuracy will consist of a random noise, a pseudo noise (including resampling errors and albedo effects) and a systematic error. There has been an equal partition (RSS) assumed for each component leading to an allocation of the random component of 0.0025.
>
> The DoLP precision (at the required DoLP spectral resolution) should be ≤ 0.0025 over the range 0–0.70 in DoLP.

The error derived for DoLP (0.0035) is the total uncertainty. We assume that both bias and precision adds up quadratically and are of the same size, thus $0.0025^2 + 0.0025^2 = 0.0035^2$

The following is written in MRDv2.0:

> The knowledge and characterization of the instrument spectral response function (ISRF) shall fulfil certain requirements.
>
> The instrument spectral response function (ISRF) should be of the form that its integrated area satisfies
>
> $$\int_{FWHM} \mathrm{ISRF}(\lambda)\,d\lambda \;\geq\; 0.7 \int_{\Lambda} \mathrm{ISRF}(\lambda)\,d\lambda$$
>
> Here Λ covers the spectral range where the ISRF is at least 1.0% of its maximum value. The FWHM of the ISRF needs to be known especially in the O2A-band and less relevant in the continuum levels.
>
> The FWHM of the ISRF should be known to an accuracy better than 2%for spectral channels in the spectral range 747–760 nm and 4% for all other spectral channels.

The statement about the integrated area is hard to verify but based on experience with other spectrometers. Justification is the same as for the CO_2 spectrometer (S7MR-OBS-100). This requirement ensures that the ISRF shape is “reasonable” and it ensures that within one spectral resolution interval at least 70% of the signal is contained. The remaining of this text is justified in TN-2000 Sec. 7.7. Here, for radiometric cross-calibration, the ISRF of the nadir port and at the spectral range around the O_2 A band shall be known with an accuracy of 2 % for the MAP-mod concept.

Overall, ISRF errors over non-uniformed scenes are considered to be of little relevance due to the overall relaxed requirement on the ISRF knowledge. For cross-calibration, homogenous scenes can be selected.

Note: The ISRF requirement is also important to allow resampling of radiances.

4.3.3. Bandpass concept, Spectral and Radiometric Requirements

In the following, the MRDv2.0 requirements are shown in **blue** and for each requirement comments are given concerning their justification, proposed modification, etc.

S7MR-OBS-340B	The number of OZAs along track (ALT) shall be 40

This requirement is coupled to the number of spectral bands, which are listed in the table below. For less bands, more viewing angles are needed (see **/CO2M SSS FR, 2019/).** Current baseline is 7 bands (band 1-6 and 753 nm for cross calibration) and 40 viewing angles.

S7MR-OBS-350B	The observation zenith angle angular sampling interval, for targets on the sub-satellite track, shall be regular within a total angular sampling range of +/-60 degrees including 0 degree (nadir) as one of the OZAs

Same as for S7MR-OBS-350M.

MRDv2.0 requirement S7MR-OBS-370B:

	Channel ID	Central Wavelength (nm)	Channel Spectral Width (nm)	DoLP
S7MR-OBS-370B	VNIR-1	410	20	Y
	VNIR-2	443	20	Y
	VNIR-3	490	20	Y
	VNIR-4	555	20	Y
	VNIR-5	670	20	Y
	VNIR-6*	753	9	N
	VNIR-7	865	40	Y
	* VNIR-6 is spectrally overlapping the NIR band of the primary observation, as such offers the possibility to co-register both observations by image correlation methods and to perform inter-instrument radiometric calibration.			

Different band selections were considered adjusting the number of viewing angles such that the total number of measurements are similar. Omitting the SWIR bands, which is preferred because in this case detectors cooling is not needed, but enhancing the number of viewing angles to 40 provides similar results as the MAP modulation concept **/CO2M SSS FR, 2019/**.

S7MR-OBS-375B	The requirements shall be met for radiance levels in the dynamic range of the spectra depicted in Figure 4.2 between L_{max} and L_{min}

See justification of S7MR-OBS-375M.

S7MR-OBS-380B	The ARA of the (TOA) radiance shall be better than 3%

See error budget discussion **/CO2M-REB TN-3000 v2.1, 2020/** (Sect. 6.2).

S7MR-OBS-390B	The DoLP absolute accuracy shall be ≤ 0.0035 over the range 0–0.70 in DoLP

Justification: See S7MR-OBS-390M.

The following is written in MRDv2.0:

> The DoLP absolute accuracy will consist of a random noise, a pseudo noise (including resampling errors and albedo effects) and a systematic error. There has been an equal partition (RSS) assumed for each component leading to an allocation of the random component of 0.0025.
>
> The DoLP precision (at the required DoLP spectral resolution) should be ≤ 0.0025 over the range 0–0.70 in DoLP. The DoLP systematic error should be ≤ 0.0025 over the range 0–0.70 in DoLP.

See corresponding justification for modulation concept.

4.3.4. Summary and Conclusions

This section provides an assessment of the MRDv2.0 requirements for the MAP concepts of CO2M. All requirements as formulated in MRDv2.0 are considered justified. Several requirements have been modified compared to the earlier MRDv1.0 following previous recommendations.

4.4. Mission Requirements of NO_2 Observations

This sub-section lists and comments on the mission requirements for the NO_2 observations.

In the following, the MRDv2.0 requirements are shown in **blue** and for each requirement comments are given concerning their justification, proposed modification, etc.

4.4.1. Geometric requirements

S7MR-OBS-500	The across-track swath width shall be equal or larger than the swath of the CO_2 instrument (i.e., S7MR-OBS-010) and contiguously sampled

The requirement ensures that the NO_2 swath entirely covers the CO_2 swath, as defined in S7MR-OBS-010 as at least 250 km. A NO_2 swath that is a few tens of kilometres wider than the CO_2 swath, will provide additional context to the CO_2 observations near the edge of the swath.

S7MR-OBS-510	The spatial sampling shall be equal to the CO2 sampling grid or allow resampling to the same grid. In the latter case, the spatial sampling distance is expected to be twice as high in both the ALT and the ACT direction. In case higher sampling is provided, then the level-2 performance (i.e. SNR) can be reached at the CO2 sampling grid.

The requirements on the co-registration depend on the use of the CO_2 and NO_2 observations. The first purpose of the NO_2 band is to use them as an indicator or flag. For this purpose, co-registration requirements may be more relaxed and no demanding hardware solutions may be needed. However, if the CO_2 and NO_2 data will also be used for quantitative analyses of the NO_2/CO_2 ratio, a better co-location, as described in the requirement, is needed. This can either be achieved by co-location in hardware, or by interpolation in Level 1B or 2. If this is done by interpolation, spatial oversampling as described in S7MR-OBS-510 is required to limit interpolation errors.

Note: Requirement S7MR-OBS-510 is also needed for plume flagging.

S7MR-OBS-520	The spatial samples observed by any two channels shall overlap ≥ 85% Note that if the VIS band is not spatially oversampled compared to the CO_2 observations, then this spatial co-registration is also applicable between the VIS & NIR bands

This requirement states that:

- The intra band co-registration in the VIS band shall be better than 85%, i.e. intra-band co-registration errors should be less than 15%.
- If the VIS band is not spatially oversampled w.r.t. the NIR band, then the inter-band co-registration errors between the VIS and NIR bands should be less than 15%.

Intra-band co-registration is defined as the degree to which all spectral channels of a ground pixel observe the same scene. In two-dimensional imaging spectrometers the intra-band co-registration error usually increases towards the end of the swath. Also, intra-band co-registration errors will in first order scale with the fit window length.

Inter-band co-registration is defined as the degree to which two or more spectral bands of a ground pixel observe the same scene. Like intra-band co-registration, the errors usually increase towards the end of the swath.

Intra-band errors have been extensively studied for Sentinel 5 **/S5UVN_Req, 2016/**, although for different values of the co-registration error. For Sentinel 5 requirement studied was 10% (Threshold) / 5% (Goal) of an SSD, versus 15% for this study. Different effects were studied for Sentinel 5, including the effect of clouds and the effect of spatial inhomogeneous NO_2 amounts. These errors were found to be less than 0.5%. Also, the effect was studied using OMI zoom-in orbits, which have a spatial sampling of 13x12 km^2, by mixing the spectra of neighbouring pixels. The study using OMI data showed that the error is (quasi) random in nature and for an introduced co-registration error of 20%, a 1-sigma error in the NO2 slant column of 2.8% was found. Assuming that the error varies linearly with the co-registration error, gives an error of 2.1% for co-registration error according to S7MR-OBS-520.

The higher spatial resolution may give larger effects on NO_2, due to the higher spatial variability. This could be tested on the TROPOMI zoom data but this is currently not in the scope of this study.

For the NO_2 retrieval, cloud pressure information may come for the NIR band, or -if available from the O_2-O_2 absorption in the VIS. If the cloud pressure is taken from the NIR, inter-band errors may occur. We note that the effective cloud fraction will be derived in the VIS, so no inter-band errors apply to the cloud-fraction. Inter-band cloud fraction errors have been studied for Sentinel 5 in **/S5UVN_Req, 2016/**. Based on an analysis using OMI and GOME-2 data, it was concluded that 20% co-registration is acceptable. Because of the smaller ground pixel used for CO2M, the errors are expected to be less than for Sentinel 5, because cloud pressure variations are less over shorter distances. Therefore, we expect that the inter-band co-registration requirement is sufficient. Also, we note that VIS-NIR inter-band errors are significantly larger for TROPOMI, and no apparent problems are reported.

4.4.2. Spectral and Radiometric Requirements

In the following, the MRDv2.0 requirements are shown in **blue** and for each requirement comments are given concerning their justification, proposed modification, etc.

S7MR-OBS-540	**Band ID**	**Spectral range [nm]**	**Spectral resolution [nm]**	**Spectral sampling ratio**
	VIS	405–490	0.6	3

The spectral range from 405 – 490 nm covers the NO_2 fitting window used for OMI/TROPOMI (405 – 465 nm), as well as the O_2-O_2 fitting window used in OMI from 460 – 490 nm. Inclusion of the O_2-O_2 fitting window allows for the retrieval of effective cloud fraction and pressure. Alternatively, cloud height information can be derived from the O_2 A band in the NIR, but this needs co-registration between these bands in the Level L1-2 processing.

The following is written in MRDv2.0 w.r.t. spectral knowledge:

> The position of the spectral channel centres should be known at Level-1b with an accuracy better than 1/20 of the spectral sampling interval (SSI) for spatially uniform scenes. Note that this should be fulfilled by combined analysis of on-ground calibration & characterisation and in-flight data.

Errors in the retrieved tropospheric NO_2 column due to imperfect wavelength calibration have been investigated by applying artificial wavelength shifts, see ***/CO2M-REB TN-2000 v2.1, 2020/***, where it is shown that large errors can occur when there is little NO_2 in the atmosphere. It is noted that no shift still gives a (small) bias because the retrieval method, DOMINO, is not perfect. For instance, a wavelength has to be selected where the air mass factor is calculated. Based on these results, it seems that the value of 0.002 nm mentioned in requirement S7MR-OBS-550 is reasonable. It is noted that prior to or in the DOAS fit a spectral shift can also be fitted, to further mitigate this error.

In practice, the spectral calibration is performed in the L1-2 retrieval algorithms, by fitting a shift and if needed also a stretch. An important boundary condition for this is that the instrument is spectrally stable.

The following is written in MRDv2.0 w.r.t. spectral stability:

> For spatially uniform scenes, the position of the spectral channels in the radiance measurements should not vary by more than 0.1 SSI for Level-0 samples acquired between two consecutive solar measurements.

The spectral stability requirement ensures that the instrument is sufficiently stable. This requirement is based heritage missions (OMI/GOME-2) and on expert judgement and cannot be assessed using retrieval simulations.

The following is written in MRDv2.0 w.r.t. ISRF shape knowledge:

> The knowledge and characterisation of the instrument spectral response function (ISRF) is important. The ISRF shape should be known to an accuracy better than 2.0% of the peak value of the ISRF in the spectral range Λ where the ISRF is at least 2% of the peak value.

An ISRF shape knowledge requirement analysis is provided in **/CO2M-REB TN-2000 v2.1, 2020/**.

As described in **/CO2M-REB TN-2000 v2.1, 2020/,** the proposed requirement is formulated assuming that the ISRF is normalized as follows

$$\int s(\lambda) d\lambda = 1$$

By requiring that the standard deviation of the ISRF is known with an accuracy of 0.01, the bias in NO_2 is expected to be within 2%. The following alternative requirement is proposed: "The standard deviation of the normalized ISRF shall be known to an accuracy better than 0.01". It is expected that this potential alternative requirement will avoid a possible over specification. Furthermore, as shown in that document / section, specifying in terms of the standard deviation has a better physical basis.

S7MR-OBS-590	The requirements shall be met for radiance levels in the dynamic range as specified in Table 4.14 between DR-VIS-max-0 and DR-VIS-min-70 corresponding to scenarios with a SZA of 0 and 70 degrees, respectively. The continuum signal levels for other SZAs can be derived by scaling the DR-max-0 signal levels with the cosine(SZA).

We drive the maximum radiance requirement such that the instrument will only saturate under exceptional conditions, e.g. very bright clouds in the tropics. An analysis performed on OMI data of the visible band, reported in **/NO2CS, 2017/**, showed that the sun-normalized radiance seldomly exceeds 0.25. Based on this number a maximum radiance of 1.3 10^{14} ph cm^{-2} nm^{-1} s^{-1} sr^{-1} is found. This maximum radiance will give some saturation. Therefore, a Sun normalized radiance of 0.30 is a more conservative choice to avoid this. This gives a maximum radiance of 1.6 10^{14} ph cm^{-2} nm^{-1} s^{-1} sr^{-1}. For reference: Sentinel 5 uses a value of 1.6 10^{14} ph cm^{-2} nm^{-1} s^{-1} sr^{-1}, which is also the value in the current version of the MRD (Table 4.14).

The maximum radiance is valid for a SZA of 0°. Depending on latitude, season and satellite orbit, the maximum radiance should be multiplied by the cosine of the minimum SZA at that latitude.

The minimum radiance is driven by the maximum SZA and the surface albedo for which the Level 2 requirements should be met. For the maximum SZA we use 70°, which is defined by the coverage requirements (S7MR-SYS-090). The minimum surface albedo over land in the wavelength range around 440 nm is 0.02, whereas the mean value over the midlatitudes is 0.05. In general, surface reflectance for urban areas are larger than over vegetation.

For the Minimum radiance, the SZA of 70°, in combination with a surface albedo of 0.02 is justified.

S7MR-OBS-600	The SNR shall be better than 750 at a reference radiance of $1.35 \cdot 10^{13}$ photons/s/nm/sr/cm^2. Note that this requirement is applicable at the CO2 sampling grid

In **/CO2M-REB TN-2000 v2.1, 2020/** plots are provided on the SNR and the corresponding reference radiance spectrum. From the analyses of the SNR results it follows that the resulting random errors in tropospheric NO2 do not vary significantly with SZA. In order to reach the MRD requirement of 1.5×10^{15} molec.cm^{-2} an SNR of 750 is needed for a reference radiance of $1.35 \cdot 10^{13}$ photons/s/nm/sr/cm^2. An SNR of 1000 is needed for a NO2 random error of 1×10^{15} molec. cm^{-2}. Because the SNR requirement is considered as one of the most important performance requirements, we recommend adding a goal requirement of 1000.

Recommendation:

- We recommend adding a goal requirement of 1000.

S7MR-OBS-610	The ARA of the (TOA) radiance shall be better than 5% in VIS including polarization sensitivity with maximum 70% degree of linear polarization (DoLP) Note that the relative spectral variation of DoLP across the VIS bandwidth is lower than 20%.

Multiplicative errors in the reflectance do not affect the DOAS slant column amounts, because of the polynomial used in DOAS. However, if the cloud parameters (effective cloud fraction and cloud pressure) are derived from the reflectance spectrum, multiplicative errors will have an impact through the air mass factor. This error is simulated by using a different cloud fraction in the simulation and retrieval and the results are shown in **/CO2M-REB TN-2000 v2.1, 2020/**. The findings indicate that the requirement is appropriate.

The following is written in MRDv2.0 w.r.t. additive radiance errors:

> The additive error of the radiance measurement at the TOA should be better than $2.0 \cdot 10^{11}$ photons/s/nm/sr/cm^2. Note that this offset is 1.5% of the radiance at 405 nm.

It is shown in **/CO2M-REB TN-2000 v2.1, 2020/** that a significant bias can occur for a moderately polluted atmosphere when the additive offset is 1% at 405 nm. Further investigation into these errors show that the magnitude depends on the polynomial used in the retrieval algorithm.

The requirement S7MR-OBS-620 states: The additive error of the radiance measurement at the TOA shall be better than $2.0 \cdot 10^{11}$ photons/s/nm/sr/cm^2. Note that this offset is 1.5% of the radiance at 405 nm. It is also shown in **/CO2M-REB TN-2000 v2.1, 2020/** that this may lead to errors in the tropospheric NO_2 column of about 7% - 10% for a polluted atmosphere with a tropospheric column of 1.0E16 molecules/cm^2 and significantly larger at lower concentrations. For a realistic case of TROPOMI zoom data, we find mean errors of 5% for a radiance offset of $2.0 \cdot 10^{11}$ photons/s/nm/sr/cm^2, for the pixels with an NO_2 column > 0.9E16 molecules/cm^2. This error is somewhat smaller for the TROPOMI test, which maybe caused by some absorption of the error by fitting for the Ring effect and other additional fitting terms. However, this is not a large effect. Furthermore, no spatial correlation was found between the NO_2 error and the original NO_2 field. Therefore, it is not expected that such errors will have a significant effect on the plume detection.

Recommendation:

- It is recommended to assess this requirement by using the gain matrices.

The following is written in MRDv2.0 w.r.t. RSRA:

> The RSRA of the ratio between the radiance and irradiance measurements within the VIS band should be better than 0.5% including polarization sensitivity with maximum 70% DoLP. Note that the relative spectral variation of DoLP across the VIS bandwidth is lower than 20%.

For spectral features the primary requirement should be defined using the gain vectors. The intention of this requirement is a safety net, because of the variation of the gain vectors with amongst others the surface albedo and the column amount. Assuming that this RSRA error doesn't interfere significantly with the NO_2 spectral features, the number is appropriate.

The following is written in MRDv2.0 w.r.t. RXRA:

> The RXRA of the radiance measurements within the swath should be better than 0.5%.

The purpose of this requirement is to limit a systematic left to right error in NO_2 over the swath or "striping errors". This requirement is driven by additive errors. According to the results shown in **/CO2M-REB TN-2000 v2.1, 2020/**, a 0.5% additive error leads to errors of the order 3% in tropospheric NO_2, which is considered acceptable.

S7MR-OBS-650	The ESRA correlating with atmospheric spectral structures shall be constrained using the Gain Matrix Method. The systematic error in the tropospheric NO_2 column due to ESRA shall be lower than 10% of the background NO_2 value assuming incident light with maximum 70% DoLP. Note that the relative spectral variation of DoLP across the VIS bandwidth is lower than 20%.

The ESRA requirement is used to limit the effects of spectral features. Spectral features are errors that vary strongly over the spectral fit window. Spectral features may be caused by optical elements, such as polarisation scramblers or coatings, but can also be caused by the detector or electronics. In defining requirements, different approaches have been used. Sometimes the requirements are given as the maximum amplitude of errors with a spectral frequency. However, this approach is not very practical as it leads to very stringent requirements, whereas spectral features with one specific frequency are also not very realistic. Requirements can also be formulated using the gain vector, which can be used to compute the Level 2 impact from a L1B error spectrum. The gain vector and its dependencies are discussed in **/CO2M-REB TN-2000 v2.1, 2020/**.

Depending on the root-cause, spectral features maybe constant in time, vary randomly, or vary quasi- randomly. We assume that constant spectral features can be included as additional fit parameters or removed after in-flight calibration. We therefore set the requirements assuming that the spectral features lead to (quasi) random errors. The effect of the spectral features should preferable be smaller than the errors related to SNR. This leads to an upper boundary of 10% on the tropospheric column, as formulated in the requirement. The requirement states that the error shall be < 10% of the background NO_2 column. We recommend using an absolute number of $<1 \times 10^{15}$ molec cm^{-2}.

Recommendation:

- We recommend using an absolute number of $< 1 \times 10^{15}$ molec cm^{-2}.

4.4.3. Summary and Conclusions

This section provides an assessment of the MRDv2.0 requirements for the NO_2 observations of CO2M. This has strong heritage to other missions, including S5P/TROPOMI, S4/UVN and S5/UVNS. However, the primary use of the NO_2 data is different than for these heritage missions; for CO2M the primary use is plume detection. For some requirements we suggest minor modifications. This includes the formulation of the requirements on the ISRF, where the current formulation is harmonized with the other CO2M bands, but could be an overspecification. Furthermore, we want to highlight the goal requirement of 1000 for the SNR, to stress the importance of high SNR. For ESRA it is recommend using an absolute number of $< 1 \times 10^{15}$ molec cm^{-2}.

4.5. Mission Requirements on Cloud Coverage

4.5.1. Geometric requirements

S7MR-OBS-700	The across-track swath width shall be 10 km larger on either side than the swath of the CO_2 instrument (i.e., S7MR-OBS-010) and contiguously sampled

One of the main objectives of the cloud image is to estimate the cloud coverage of the observed and surrounding pixels. Cloud coverage of surrounding pixels may affect the XCO_2 data quality due to spectrometer stray light. This is constrained for the range of 5 spatial sampling distances (~10 km) or larger and so an extended swath of the cloud imager with respect to the main spectrometer of 10 km at both sides is justified.

S7MR-OBS-710	The SSD of the Cloud Imager, in ALT and ACT directions, shall be smaller than 400 m

Baseline of the sizing of the cloud imager is a lower detection limit of 5 % cloud coverage of the CO_2 instrument ground pixels. The required CLIM SSD means that a single pixel of the imager covers 5 % of the CO_2 instrument pixel size, which we consider as a justified baseline for the cloud imager sizing. It is essential, that this requirement is harmonized with the SNR requirement of the imager to meet the required detection limit.

4.5.2. Spectral and Radiometric Requirements

S7MR-OBS-730	**Band ID**	**Spectral band center (nm)**	**Spectral band width (nm)**
	CLIM-1	670	20
	CLIM-2*	753	9
	CLIM-3*	1370	15
* Spectral band CLIM-2 is spectrally overlapping the NIR band of the primary observation, offering thereby the possibility to co-register both observations by image correlation methods and to perform inter-instrument radiometric calibration.			

The CLIM-1 and CLIM-3 band definition is adapted from MODIS and VIIRS:

	CLIM-1	CLIM-3
MODIS	662-683 nm (band 13 and 14)	1360-1390 nm (band 26)
VIIRS	673 nm (M5 band with 21 nm band width)	1.378 nm (M9 band with 20 nm band width)

Similar band definitions are used also for other cloud imagers. Here, the CLIM-3 band width of 15 nm is chosen to enhance the cirrus sensitivity of the band. CLIM-2 band overlaps with spectral radiance measurements of CO2I (CO_2 Instrument) and so can be used for cross calibration. The narrow band width of 9 nm is needed to avoid interference with the absorption features of the O_2 A band.

Dynamic range:

Band ID	Minimum radiance Lmin-clim (phot/s/nm/cm^2/sr)	**Reference radiance** $L_{ref\text{-}clim}$ (phot/s/nm/cm^2/sr)	**Maximum radiance** $L_{max\text{-}clim}$ (phot/s/nm/cm^2/sr)
CLIM-1	2.06×10^{12}	1.88×10^{13}	1.94×10^{14}
CLIM-2*	2.91×10^{12}	1.77×10^{13}	1.83×10^{14}
CLIM-3*	5.03×10^{12}	9.24×10^{12}	4.39×10^{13}

Radiance level are justified in **/CO2M-REB TN-2000 v2.1, 2020/**.

S7MR-OBS-760	The requirements shall be met for radiance levels in the dynamic range as specified in Table 4.16 between Lmin-clim and Lmax-clim.

Lmin and Lmax cover the dynamical range of the cloud imager, which justifies this requirement.

S7MR-OBS-770	The SNR shall be better than 200 at the reference radiance Lref-clim indicated in Table 4.16. Note that the SNR applies per SSDCLIM

The SNR is required to detect the required radiometric contract for cirrus and cloud detection. The numbers are derived in **/CO2M-REB TN-2000 v2.1, 2020/**.

S7MR-OBS-780	The ARA of the (TOA) radiance shall be better than 10%.

Compared to MODIS, the radiometric accuracy requirement is relaxed by a factor of 2. This relaxation is justified by the use of the CLIM data for cloud filtering only. The application relies on radiometric contracts between cloudy and non-cloudy scenes and so for CLIM data, the required absolute radiometric accuracy is not driven by the objective to derive cloud and aerosol properties from the observations.

4.5.1. Summary and Conclusions

In contrast to MRDv1.0, the new MRDv2.0 contains requirements on cloud coverage to be derived from a dedicated cloud imager (CLIM). Each of these requirements are listed in this document together with its justification. This comprises geometric (e.g., swath width and spatial sampling distance (SSD), spectral (e.g., spectral bands) and radiometric (e.g., SNR and accuracy) requirements.

4.6. Mission Performance and Error Budget

Detailed results related to mission performance are provided in various documents cited in this document including the dedicated reports prepared in the framework of this study **/CO2M-REB TN-2000 v1.2, 2019/ /CO2M-REB TN-2000 v2.1, 2020/**.

Error Budgets for CO2M XCO_2, XCH_4, tropospheric NO_2 columns, aerosol parameters and SIF taking into account MRD Level 1 requirements are compiled in **/CO2M-REB TN-3000 v1.1, 2019/ /CO2M-REB TN-3000 v2.1, 2020/.**

The “Error Budget of Level-1 Observational Parameters” listed in Tab. 4.17 of MRDv2.0 are consistent with these assessments.

5. Acronyms and abbrevations

Acronym	Meaning
ABL	Algorithm Baseline
ACT	Across Track
Aeronet	Aerosol Robotic Network
ALT	Along Track
AOD	Aerosol Optical Depth
AOT	Aerosol Optical Thickness
ARA	Absolute Radiometric Accuracy
ATBD	Algorithm Theoretical Basis Document
BESD	Bremen optimal EStimation DOAS
BESD/C	BESD algorithm used for CarbonSat assessments
BL	Boundary Layer
CA	Continental Average (aerosol scenario)
CarbonSat	Carbon Monitoring Satellite
CC	Continental Clean (aerosol scenario)
CCI	Climate Change Initiative (of ESA)
CI	Cloud Imager
CL	Close Loop
CLIM	Cloud Imager
CNES	Centre national d'études spatiales
CO2I	CO_2 Instrument
CO2M	Anthropogenic CO_2 Monitoring Mission
CO2M-REB	Anthropogenic CO_2 Monitoring Mission Requirements Consolidation and Error Budget study
COD	Cloud Optical Depth
COT	Cloud Optical Thickness
CP	Continental Polluted (aerosol scenario)
CS	CarbonSat
CS-L1L2-II	CarbonSat Earth Explorer 8 Candidate Mission Level-1 Level-2 (L1L2) Performance Assessment Study No. 2
CTH	Cloud Top Height
DE	Desert (aerosol scenario)
DEM	Digital Elevation Model
DES	Desert (surface albedo)
DOAS	Differential Optical Absorption Spectroscopy
DOF	Degrees of Freedom
DoLP	Degree of Linear Polarization
EB	Error Budget
EE8	Earth Explorer No. 8 (satellite)
ENVISAT	Environmental Satellite
ESA	European Space Agency
ESRA	Effective Spectral Radiometric Accuracy
FR	Final Report

FWHM	Full Width at Half Maximum
G	Goal requirement
GHG	Greenhouse Gas
GHG-CCI	Greenhouse Gas project of ESA's Climate Change Initiative (CCI)
GM	Gain Matrix
GMM	Gain Matrix Method
GOSAT	Greenhouse Gases Observing Satellite
ISRF	Instrument Spectral Response Function
IUP-UB	Institute of Environmental Physics (Institut für Umweltphysik), University of Bremen, Germany
JNA	Justification not applicable
L1	Level 1
L2	Level 2
LoTBRR	List of to be refined requirements
MAP	Multi Angle Polarimeter
MLS	Mid-latitude summer (profiles)
MODIS	Moderate resolution Imaging Spectrometer
MRD	Mission Requirements Document
NA	Not applicable
NIR	Near Infra Red (band)
OCO	Orbiting Carbon Observatory
OE	Optimal Estimation
OMI	Ozone Monitoring Instrument
OPAC	Optical Properties of Aerosol and Clouds
RfMS	Report for Mission Selection
RMS	Root Mean Square
RMSE	Root Mean Square Error
RSRA	Relative Spectral Radiometric Accuracy
RSS	Root Sum Square
RTM	Radiative Transfer Model
RXRA	Relative Spatial Radiometric Accuracy
SCIAMACHY	Scanning Imaging Absorption Spectrometers for Atmospheric Chartography
SCIATRAN	Radiative Transfer Model under development at IUP
SEDF	System Energy Distribution Function
SIF	Sun-Induced Fluorescence
SNR	Signal to Noise Ratio
SSI	Spectral Sampling Interval
SSP	Spectral Sizing Point
SSR	Spectral Sampling Ratio
SW1 or SWIR-1	SWIR 1 band
SW2 or SWIR-2	SWIR 2 band
SWIR	Short Wave Infrared
SZA	Solar Zenith Angle
T	Threshold requirement
TCCON	Total Carbon Column Observing Network

TOA	Top of atmosphere
VCF	Vegetation Chlorophyll Fluorescence
VEG	Vegetation (surface albedo)
VIIRS	Visible Infrared Imaging Radiometer Suite
VMR	Volume Mixing Ratio

6. References

/Aben et al., 2007/ Aben, I., Hasekamp, O., Hartmann, W., Uncertainties in the space-based measurements of CO_2 columns due to scattering in the Earth's atmosphere, Journal of Quantitative Spectroscopy & Radiative Transfer, 104, 450–459, 2007.

/Boesch et al., 2011/ Boesch, H., D. Baker, B. Connor, D. Crisp and C. Miller, Global Characterization of CO_2 Column Retrievals from Shortwave-Infrared Satellite Observations of the Orbiting Carbon Observatory-2 Mission, *Remote Sens*., 3(2), 270-304, 2011.

/Boesch et al., 2014/ Boesch, H. and L. Vogel, Mission Requirements Analysis and Level 2 Error Characterization for CarbonSat Glint Observations over Water, WP 1200, 3000 & 4200 Report, CarbonSat Earth Explorer 8 Candidate L1L2 Performance Assessment Study CSL1L2-II, 2014.

/Bovensmann et al., 1999/ Bovensmann, H., J. P. Burrows, M. Buchwitz, J. Frerick, S. Noël, V. V. Rozanov, K. V. Chance, and A. H. P. Goede, SCIAMACHY - Mission objectives and measurement modes, J. Atmos. Sci., 56, (2), 127-150, 1999.

/Bovensmann et al., 2010/ Bovensmann, H., Buchwitz, M., Burrows, J. P., Reuter, M., Krings, T., Gerilowski, K., Schneising, O., Heymann, J., Tretner, A., and Erzinger, J., A remote sensing technique for global monitoring of power plant CO_2 emissions from space and related applications, Atmos. Meas. Tech., 3, 781-811, 2010.

/Bovensmann et al., 2014/ Bovensmann, H., M. Buchwitz, M. Reuter, T. Krings, J. Heymann, H. Boesch, J. Landgraf, CarbonSat Earth Explorer 8 Candidate Mission "Level-2 and Level-1B Requirements Consolidation Study", Final Report ESA Study CarbonSat Earth Explorer 8 Candidate Mission "Level-2 and Level-1B Requirements Consolidation Study ", ESA Contract No 4000105676/12/NL/AF, Version 2.2, Date: 18. July 2014, Doc.ID: IUP-CS-L1L2-FR-01, 2014.

/Bovensmann et al., 2015/ Bovensmann, H., M. Buchwitz, M. Reuter, T. Krings, J. Heymann, H. Boesch, J. Landgraf, CarbonSat Earth Explorer 8 Candidate Mission "Level-1 Level-2 (L1L2) Performance Assessment Study ", Final Report ESA Study, ESA Contract No 4000109814/13/NL/FF/lf, Version 1.0, Date: 11. December 2015, Doc.ID: IUP-CS-L1L2-II-FR-01, 2015.

/Broquet et al., 2018/ Broquet, G., F.-M. Bréon, E. Renault, M. Buchwitz, M. Reuter, H. Bovensmann, F. Chevallier, L. Wu, and P. Ciais, The potential of satellite spectro-imagery for monitoring CO2 emissions from large cities, Atmos. Meas. Tech., 11, 681-708, https://doi.org/10.5194/amt-11-681-2018, 2018.

/Buchwitz et al., 2013a/ Buchwitz, M., M. Reuter, H. Bovensmann, D. Pillai, J. Heymann, O. Schneising, V. Rozanov, T. Krings, J. P. Burrows, H. Boesch, C. Gerbig, Y. Meijer, and A. Loescher, Carbon Monitoring Satellite (CarbonSat): assessment of atmospheric CO_2 and CH_4 retrieval errors by error parameterization, Atmos. Meas. Tech., 6, 3477-3500, 2013.

/Buchwitz et al., 2013b/ Buchwitz, M., H. Bovensmann, M. Reuter, J. Heymann, O. Schneising, et al., CARBONSAT: ERROR ANALYSIS FOR PRIMARY LEVEL 2 PRODUCTS XCO_2 AND XCH_4 AND SECONDARY PRODUCT VEGETATION CHLOROPHYLL

FLUORESCENCE FOR NADIR OBSERVATIONS OVER LAND, ESA Living Planet Symposium, Sept 9-13, 2013, Edinburgh, UK, conference proceedings ESA Special Publication SP-722 (on CD-ROM), link: http://www.iup.uni-bremen.de/sciamachy/NIR_NADIR_WFM_DOAS/2846996buchwitz.pdf, 2013.

/Buchwitz et al., 2017a/ ESA Climate Change Initiative (CCI) Product Validation and Intercomparison Report (PVIR) for the Essential Climate Variable (ECV) Greenhouse Gases (GHG) for data set Climate Research Data Package No. 4 (CRDP#4), Version 5.0, 9. Feb. 2017, link: http://www.esa-ghg-cci.org/?q=webfm_send/352, 2017.

/Buchwitz et al., 2017b/ Buchwitz, M., Aben, I., Anand, J., Armante, R., Boesch, H., Crevoisier, C., Detmers, R. G., Hasekamp, O. P., Reuter, M., Schneising-Weigel, O., Target Requirement Document, Copernicus Climate Change Service (C3S) project on satellite-derived Essential Climate Variable (ECV) Greenhouse Gases (CO_2 and CH_4) data products (project C3S_312a_Lot6), Version 1.3, 20-October-2017, pp. 53, 2017.

/Buchwitz et al., 2017c/ Buchwitz, M., Aben, I., Anand, J., Armante, R., Boesch, H., Crevoisier, C., Detmers, R. G., Hasekamp, O. P., Reuter, M., Schneising-Weigel, O., Product Quality Assessment Report (PQAR) – Main document, C3S project C3S_312a_Lot6_IUP-UB – Greenhouse Gases, v1.1, 2017.

/Buchwitz et al., 2017d/ Buchwitz, M., Aben, I., Anand, J., Armante, R., Boesch, H., Crevoisier, C., Detmers, R. G., Hasekamp, O. P., Reuter, M., Schneising-Weigel, O., Algorithm Theoretical Basis Document (ATBD) – Main document, C3S project C3S_312a_Lot6_IUP-UB – Greenhouse Gases, v1.1, 2017.

/Buchwitz, 2018/ Buchwitz, M., Error analysis for CarbonSat scenarios and different spectral sizing, Technical Report ESA „Study on Spectral Sizing for CO_2 Observations“, Version 4.0, 30-Apr-2018, Doc ID: IUP-CO2SS-TN-5, pp. 93, 2018.

/Buchwitz and Reuter, 2018/ Buchwitz, M., and M. Reuter, Level 2 error files, Technical Report ESA Study of Assessing thresholds for a space borne observation system to monitor fossil CO_2 emissions (PMIF study), Version 2.1, 30-Jan-2018, Doc ID IUP-PMIF_L2e_S7-c, pp. 100, 2018.

/Butz et al., 2011/ Butz, A., Guerlet, S., Hasekamp, O., Schepers, D., Galli, A., Aben, I., Frankenberg, C., Hartmann, J. M., Tran, H., Kuze, A., Keppel-Aleks, G., Toon, G., Wunch, D., Wennberg, P., Deutscher, N., Griffith, D., Macatangay, R., Messerschmidt, J., Notholt, J., and Warneke, T.: Toward accurate CO_2 and CH_4 observations from GOSAT, Geophys. Res. Lett., 38, L14 812, doi:10.1029/2011GL047888, http://www.agu.org/pubs/crossref/2011/2011GL047888.shtml, 2011.

/Ciais et al., 2015/ Ciais, P., et al.: Towards a European Operational Observing System to Monitor Fossil CO_2 emissions - Final Report from the expert group, http://www.copernicus.eu/main/towards-european-operational-observing-system-monitor-fossil-co2-emissions, pp. 68, October 2015, 2015.

/Chevalier et al., 2016/ Chevallier, F., et al., User Requirements Document (URD), ESA Climate Change Initiative (CCI) GHG-CCI project, Version 2.1, 19 Oct 2016, link: http://www.esa-ghg-cci.org/?q=webfm_send/344, 2016.

/Cogan et al., 2012/ Cogan, A. J., et al., Atmospheric carbon dioxide retrieved from the Greenhouse gases Observing SATellite (GOSAT): Comparison with ground-based

TCCON observations and GEOS-Chem model calculations, J. Geophys. Res., 117, D21301, doi:10.1029/2012JD018087, 2012.

/CO2M-REB TN-1000 v1.1, 2019/ Buchwitz, M., M. Reuter, S. Noël, H. Bovensmann, A. Richter, J. Landgraf, P. Vefking, J. de Haan, H. Boesch, Requirements Justification Report for anthropogenic CO2 Monitoring Mission (CO2M), Technical Report ESA Study on Consolidating Requirements and Error Budget for CO_2 Monitoring Mission (CO2M-REB), version 1.1, 25-April-2019, 74 pages, Doc ID: IUP-CO2M-REB-TN-1000, 2019.

/CO2M-REB TN-2000 v1.2, 2019/ Buchwitz, M., M. Reuter, S. Noël, H. Bovensmann, A. Richter, J. Landgraf, P. Vefking, J. de Haan, H. Boesch, Requirements Sensitivity Analysis for anthropogenic CO2 Monitoring Mission (CO2M), Technical Report ESA Study on Consolidating Requirements and Error Budget for CO_2 Monitoring Mission (CO2M-REB), version 1.1, 26-April-2019, 133 pages, Doc ID: IUP-CO2M-REB-TN-2000, 2019.

/CO2M-REB TN-3000 v1.1, 2019/ Buchwitz, M., M. Reuter, S. Noël, H. Bovensmann, A. Richter, J. Landgraf, P. Vefking, J. de Haan, H. Boesch, Error Budgets and Performance for anthropogenic CO2 Monitoring Mission (CO2M), Technical Report ESA Study on Consolidating Requirements and Error Budget for CO_2 Monitoring Mission (CO2M-REB), version 1.1, 25-April-2019, 46 pages, Doc ID: IUP-CO2M-REB-TN-3000, 2019.

/CO2M-REB TN-2000 v2, 2020/ Buchwitz, M., M. Reuter, S. Noël, H. Bovensmann, A. Richter, J. Landgraf, P. Vefking, J. de Haan, H. Boesch, Requirements Sensitivity Analysis for anthropogenic CO2 Monitoring Mission (CO2M), Technical Report ESA Study on Consolidating Requirements and Error Budget for CO_2 Monitoring Mission (CO2M-REB), version 2.0, Doc ID: IUP-CO2M-REB-TN-2000, 2020.

/CO2M-REB TN-3000 v2, 2020/ Buchwitz, M., M. Reuter, S. Noël, H. Bovensmann, A. Richter, J. Landgraf, P. Vefking, J. de Haan, H. Boesch, Error Budgets and Performance for anthropogenic CO2 Monitoring Mission (CO2M), Technical Report ESA Study on Consolidating Requirements and Error Budget for CO_2 Monitoring Mission (CO2M-REB), version 2.0, Doc ID: IUP-CO2M-REB-TN-3000, 2020.

/CO2M-REB TN-2000 v2.1, 2020/ Buchwitz, M., M. Reuter, S. Noël, H. Bovensmann, A. Richter, J. Landgraf, P. Vefking, J. de Haan, H. Boesch, Requirements Sensitivity Analysis for anthropogenic CO2 Monitoring Mission (CO2M), Technical Report ESA Study on Consolidating Requirements and Error Budget for CO_2 Monitoring Mission (CO2M-REB), version 2.1, Doc ID: IUP-CO2M-REB-TN-2000, 2020.

/CO2M-REB TN-3000 v2.1, 2020/ Buchwitz, M., M. Reuter, S. Noël, H. Bovensmann, A. Richter, J. Landgraf, P. Vefking, J. de Haan, H. Boesch, Error Budgets and Performance for anthropogenic CO2 Monitoring Mission (CO2M), Technical Report ESA Study on Consolidating Requirements and Error Budget for CO_2 Monitoring Mission (CO2M-REB), version 2.1, Doc ID: IUP-CO2M-REB-TN-3000, 2020.

/CO2M MRD v1.0, 2018/ Copernicus CO_2 Monitoring Mission Requirements Document, ESA, v1.0, date of issue: 18/04/2018, EOP-SM/3088/YM-ym, 2018.

/CO2M MRD v2.0, 2019/ Copernicus CO_2 Monitoring Mission Requirements Document, ESA, v2.0, date of issue: 27/09/2019, EOP-SM/3088/YM-ym, 2019.

/CO2M AEROCARB FR, 2019/ Houweling, S., J. Landgraf, H. van Heck, T. Vlemmix, W. Tao, Final report: Synthesis and Recommendation, Technical Report ESA AEROCARB

Study, AEROCARB – Study on use of aerosol information for estimating fossil CO_2 emissions, ESA study RFP/3-14860/17/NL/FF/gp, Version: 2.0, 18 November 2019, pp. 12, 2019.

/CO2M PMIF FR, 2018/ Final report of Study on Assessing thresholds for a space borne observation system to monitor fossil CO_2 emissions ("PMIF Study"), Technical Report, ESA study contract n° No. 4000120184/17/NL/FF/mg, Lead: P. Ciais LSCE), December 2018, pp. 38, 2018.

/CO2M SMARTCARB FR, 2019/ Kuhlmann, G., V. Clément, J. Marshall, O. Fuhrer, G. Broquet, C. Schnadt-Poberaj, A. Löscher, Y. Meijer, and D. Brunner, SMARTCARB – Use of Satellite Measurements of Auxiliary Reactive Trace Gases for Fossil Fuel Carbon Dioxide Emission Estimation, Final report of ESA study contract n°4000119599/16/NL/FF/mg, project led by Empa (Switzerland), pp. 107, 2019.

/CO2M SSS FR, 2019/ ESA Spectral Sizing Study Final Report, in preparation, 2019.

/Crisp et al., 2004/ Crisp, D., Atlas, R. M., Breon, F.-M., Brown, L. R., Burrows, J. P., Ciais, P., Connor, B. J., Doney, S. C., Fung, I. Y., Jacob, D. J., Miller, C. E., O'Brien, D., Pawson, S., Randerson, J. T., Rayner, P., Salawitch, R. S., Sander, S. P., Sen, B., Stephens, G. L., Tans, P. P., Toon, G. C., Wennberg, P. O., Wofsy, S. C., Yung, Y. L., Kuang, Z., Chudasama, B., Sprague, G., Weiss, P., Pollock, R., Kenyon, D., and Schroll, S.: The Orbiting Carbon Observatory (OCO) mission, Adv. Space Res., 34, 700-709, 2004.

/CS L1L2-I study FR, 2014/ Bovensmann, H., M. Buchwitz, M. Reuter, T, Krings, J. Heymann, H. Boesch, J. Landgraf, Final Report ESA study "CarbonSat Earth Explorer 8 Candidate Mission "Level-2 and Level-1B Requirements Consolidation Study", Technical Report, ESA Contract No. 4000105676/13/NL/AF, Version 2.2, 18-July-2014, Doc ID: IUP-CS-L1L2-FR-01, pp. 188, 2014.

/CS L1L2-II TN nadir, 2015/ Buchwitz, M., Bovensmann, T. Krings, M. Reuter, V. V. Rozanov, P. Liebing, J. Landgraf, F. Alkemade, Mission Requirements Analysis and Level 2 Error Characterization for CarbonSat Nadir Observations over Land - WP 1100, 2000 & 4100 Report, ESA Study CarbonSat Earth Explorer 8 Candidate Mission "Level-1 Level-2 (L1L2) Performance Assessment Study" ESA Contract No 4000109814/13/NL/FF/lf, Version 1.2, 3 Dec 2015, Doc ID: IUP-CS-L1L2-II-TNnadir, 2015.

/CS L1L2-II study FR, 2015/ Bovensmann, H., M. Buchwitz, M. Reuter, T, Krings, H. Boesch, J. Landgraf, Final Report ESA study "CarbonSat Earth Explorer 8 Candidate Mission "Level-1 Level-2 (L1L2) Performance Assessment Study", Technical Report, ESA Contract No. 4000109814/13/NL/FF/lf, Version 1.0, 11-Dec-2015, Doc ID: IUP-CS-L1L2-II-FR-01, pp. 43, 2015.

/CS MRD v1.0, 2011/ ESA, CarbonSat – Candidate Earth Explorer Opportunity Mission – Mission Requirements Document, Issue 1, Revision 0, 8 July 2011, ESA Mission Science Division, Reference EOP-SMA/2232/PI-pi, 2011.

/CS MRD v1.2, 2013/ ESA, CarbonSat – Candidate Earth Explorer Opportunity Mission – Mission Requirements Document, Issue 1, Revision 2, 23 May 2013, ESA Mission Science Division, Reference EOP-SMA/2232/PI-pi, 2011.

/CS RfMS, 2015/ ESA, Report for Mission Selection: CarbonSat, ESA SP-1330/1 (2 volume series), European Space Agency, Noordwijk, The Netherlands. link: http://esamultimedia.esa.int/docs/EarthObservation/SP1330-1_CarbonSat.pdf, 2015.

/Dubovik et al., 2006/ Dubovik, O., Sinyuk, A., Lapyonok, T., Holben, B. N., Mishchenko, M., Yang, P., Eck, T. F., Volten, H., Munoz, O., Veihelmann, B., Zande, v. d. W. J., Leon, J.-F., Sorokin, M., and Slutsker, I.: Application of spheroid models to account for aerosol particle non-sphericity in remote sensing of desert dust, J. Geophys. Res. Atmos., 111, D11208, doi:10.1029/2005JD006619, 2006.

/Eldering et al., 2017/ Eldering, A., O'Dell, C. W., Wennberg, P. O., Crisp, D., Gunson, M. R., Viatte, C., Avis, C., Braverman, A., Castano, R., Chang, A., Chapsky, L., Cheng, C., Connor, B., Dang, L., Doran, G., Fisher, B., Frankenberg, C., Fu, D., Granat, R., Hobbs, J., Lee, R. A. M., Mandrake, L., McDuffie, J., Miller, C. E., Myers, V., Natraj, V., O'Brien, D., Osterman, G. B., Oyafuso, F., Payne, V. H., Pollock, H. R., Polonsky, I., Roehl, C. M., Rosenberg, R., Schwandner, F., Smyth, M., Tang, V., Taylor, T. E., To, C., Wunch, D., and Yoshimizu, J.: The Orbiting Carbon Observatory-2: first 18 months of science data products, Atmos. Meas. Tech., 10, 549-563, https://doi.org/10.5194/amt-10-549-2017, 2017.

/Frankenberg et al., 2011a/ Frankenberg, C., Butz, A., and Toon, G. C.: Disentangling chlorophyll fluorescence from atmospheric scattering effects in O_2 A-band spectra of reflected sun-light, Geophys. Res. Lett., 755 38, L03 801, doi:10.1029/2010GL045896, http://www.agu.org/pubs/crossref/2011/2010GL045896.shtml , 2011.

/Frankenberg et al., 2011b/ Frankenberg, C., Fisher, J., Worden, J., Badgley, G., Saatchi, S., Lee, J.-E., Toon, G., Butz, A., Jung, M., Kuze, A., and Yokota, T.: New global observations of the terrestrial carbon cycle from GOSAT: Patterns of plant fluorescence with gross primary productivity, Geophys. Res. Lett., 38, L17 706, http://dx.doi.org/10.1029/2011GL048738 , 2011.

/Frankenberg et al., 2012/ Frankenberg, O'Dell, C, Guanter, L., and McDuffie,J., Chlorophyll fluorescence remote sensing from space in scattering atmospheres: Implications for its retrieval and interferences with atmospheric CO_2 retrievals, submitted to Atmos. Meas. Tech., 2012.

/Frankenberg et al., 2014/ C. Frankenberg, C. O'Dell, J. Berry, L. Guanter, J. Joiner, P. Köhler, R. Pollock, T. E. Taylor, Prospects for chlorophyll fluorescence remote sensing from the Orbiting Carbon Observatory-2, Remote Sensing of Environment, 2014.

/Galli et al., 2014/ Galli, A., Guerlet, S., Butz, A., Aben, I., Suto, H., Kuze, A., Deutscher, N. M., Notholt, J., Wunch, D., Wennberg, P. O., Griffith, D. W. T., Hasekamp, O., Landgraf, J., The impact of spectral resolution on satellite retrieval accuracy of CO_2 and CH_4, Atmos. Meas. Tech., Volume 7, Issue 4, pp.1105-1119, 2014.

/GHG-TCPS E2ES, 2018/ Reuter, M., H. Bovensmann, S. Noël, K. Bramstedt, Validation and Performance Simulations, Technical Report, ESA Study Greenhouse Gas Total Column Performance Simulations (GHG-TCPS), Doc: IUP-GHG-TCPS-VPSR-01, Version 1.0, 18 June 2018, 2018.

/Guerlet et al., 2013/ Guerlet, S., Butz, A., Schepers, D., et al., Impact of aerosol and thin cirrus on retrieving and validating XCO_2 from GOSAT shortwave infrared measurements, J. Geophys. Res., VOL. 118, 4887–4905, doi:10.1002/jgrd.50332, 2013.

/Hess et al., 1998/ Hess, M., P. Koepke, and I. Schult, Optical Properties of Aerosols and Clouds: The software package OPAC, Bull. Am. Met. Soc., 79, 831-844, 1998.

/Heymann et al., 2012/ Heymann, J., H. Bovensmann, M. Buchwitz, J. P. Burrows, N. M. Deutscher, J. Notholt, M. Rettinger, M. Reuter, O. Schneising, R. Sussmann, and T. Warneke SCIAMACHY WFM-DOAS XCO_2: reduction of scattering related errors, Atmos. Meas. Tech., 5, 2375-2390, 2012.

/Heymann et al., 2015/ Heymann, J., M. Reuter, M. Hilker, M. Buchwitz, O. Schneising, H. Bovensmann, J. P. Burrows, A. Kuze, H. Suto, N. M. Deutscher, M. K. Dubey, D. W. T. Griffith, F. Hase, S. Kawakami, R. Kivi, I. Morino, C. Petri, C. Roehl, M. Schneider, V. Sherlock, R. Sussmann, V. A. Velazco, T. Warneke, and D. Wunch, Consistent satellite XCO_2 retrievals from SCIAMACHY and GOSAT using the BESD algorithm, Atmos. Meas. Tech., 8, 2961-2980, 2015.

/Hilbig et al., 2018/ Hilbig, T., Weber, M., Bramstedt, K. et al., The New SCIAMACHY Reference Solar Spectral Irradiance and Its Validation, Sol Phys, 293: 121. https://doi.org/10.1007/s11207-018-1339-9, 2018.

/Kiel et al., 2018/ Kiel, M., O'Dell, C. W., Fisher, B., Eldering, A., Nassar, R., MacDonald, C. G., and Wennberg, P. O.: How bias correction goes wrong: Measurement of X_{CO2} affected by erroneous surface pressure estimates, Atmos. Meas. Tech. Discuss., https://doi.org/10.5194/amt-2018-353, in review, 2018.

/Kring et al., 2018/ Krings, T., B. Neininger, K. Gerilowski, S. Krautwurst, M. Buchwitz, J. P. Burrows, C. Lindemann, T. Ruhtz, D. Schuettemeyer, and H. Bovensmann, Airborne remote sensing and in situ measurements of atmospheric CO_2 to quantify point source emissions, Atmos. Meas. Tech., 11, 721-739, https://doi.org/10.5194/amt-11-721-2018, 2018.

/Kring et al., 2011/ Krings, T., Gerilowski, K., Buchwitz, M., Reuter, M., Tretner, A., Erzinger, J., Heinze, D., Pflüger, U., Burrows, J. P., and Bovensmann, H., MAMAP - a new spectrometer system for column-averaged methane and carbon dioxide observations from aircraft: retrieval algorithm and first inversions for point source emission rates, Atmos. Meas. Tech., 4, 1735-1758, 2011.

/Landgraf et al., 2017/ Landgraf, J., J. aan de Brugh, A. Butz, K. Graf, Specification of Instrument Spectral Sizing Concepts, Spectral Errors and Geo-Physical Scenarios, Technical Note, SRON-CSS-TN-2016-002, 21-Feb-2017, version 3, pp. 20, 2017.

/Landgraf et al., 2017b/ Landgraf, J., J. aan de Brugh, A. Butz, K. Graf, Specification of Instrument Spectral Sizing Concepts, Spectral Errors and Geo-Physical Scenarios, Technical Note, SRON-CSS-TN-2016-002, 20-May-2017, version 4, pp. 21, 2017.

/Lekouara et al., 2018/ Lekouara, M., B. Carnicero Dominguez, M. Aguirre, and M. A. Rubio, A New Climatology of Sea Surface Wind Speed under Cloud-free Conditions for the Estimation of the Impact of sunglint in GMES Sentinel-3, Proc. of the '2nd MERIS / (A)ATSR User Workshop', Frascati, Italy, 22–26 September 2008, ESA SP-666, November 2008, 2008.

/Miller et al., 2007/ Miller, C. E., Crisp, D., DeCola, P. L., et al.: Precision requirements for space-based XCO_2 data, J. Geophys. Res., 112, D10314, doi:10.1029/2006JD007659, 2007.

/Nassar et al., 2017/ Nassar, R., T. G. Hill, C. A. McLinden, D. Wunch, D. B. A. Jones, and D. Crisp, Quantifying CO_2 emissions from individual power plants from space. Geophysical Research Letters, 44, doi:10.1002/2017GL074702, 2017.

/NO2CS, 2017/ NO_2 Compact Spectrometer Technical Note 2: Level 1 requirements; source: KNMI; ref: KNMI-NO2CS-002-TN; issue: 2.0.0; date: 2017-11-02.

/O'Dell et al., 2012/ O'Dell, C. W., B. Connor, H. Boesch, D. O'Brien, C. Frankenberg, R. Castano, M. Christi, D. Crisp, A. Eldering, B. Fisher, M. Gunson, J. McDuffie, C. E. Miller, V. Natraj, F. Oyafuso, I. Polonsky, M. Smyth, T. Taylor, G. C. Toon, P. O. Wennberg, and D.Wunch, The ACOS CO_2 retrieval algorithm – Part 1: Description and validation against synthetic observations, Atmos. Meas. Tech., 5, 99–121, 2012.

/Pillai et al. 2016/ Pillai, D., M. Buchwitz, C. Gerbig, T. Koch, M. Reuter, H. Bovensmann, J. Marshall, J. P. Burrows, Tracking city CO_2 emissions from space using a high resolution inverse modeling approach: A case study for Berlin, Germany, Atmos. Chem. Phys., 16, 9591-9610, doi:10.5194/acp-16-9591-2016, 2016.

/Pinty et al. 2017/ Pinty B., G. Janssens-Maenhout, M. Dowell, H. Zunker, T. Brunhes, P. Ciais, D. Dee, H. Denier van der Gon, H. Dolman, M. Drinkwater, R. Engelen, M. Heimann, K. Holmlund, R. Husband, A. Kentarchos, Y. Meijer, P. Palmer and M. Scholze, An Operational Anthropogenic CO_2 Emissions Monitoring & Verification Support capacity - Baseline Requirements, Model Components and Functional Architecture, doi: 10.2760/39384, European Commission Joint Research Centre, EUR 28736 EN.

/Rascher et al., 2009/ Rascher, U., Agati, G., Alonso, L., Cecchi, G., Champagne, S., Colombo, R., Damm, A., Daumard, F., de Miguel, E., Fernandez, G., Franch, B., Franke, J., Gerbig, C., Gioli, B., Gomez, J. A., Goulas, Y., Guanter, L., Gutierrez-de-la-Camara, O´ ., Hamdi, K., Hostert, P., Jimenez, M., Kosvancova, M., Lognoli, D., Meroni, M., Miglietta, F., Moersch, A., Moreno, J., Moya, I., Neininger, B., Okujeni, A., Ounis, A., Palombi, L., Raimondi, V., Schickling, A., Sobrino, J. A., Stellmes, M., Toci, G., Toscano, P., Udelhoven, T., van der Linden, S., and Zaldei, A.: CEFLES2: the remote sensing component to quantify photosynthetic efficiency from the leaf to the region by measuring sun-induced fluorescence in the oxygen absorption bands, Biogeosciences, 6, 1181–1198, doi:10.5194/bg-6-1181-2009, 2009.

/Reuter et al., 2010/ Reuter, M., Buchwitz, M., Schneising, O., Heymann, J., Bovensmann, H., and Burrows, J. P., A method for improved SCIAMACHY CO_2 retrieval in the presence of optically thin clouds, Atmos. Meas. Tech., 3, 209-232, 2010.

/Reuter et al., 2011/ Reuter, M., Bovensmann, H., Buchwitz, M., et al. (2011), Retrieval of atmospheric CO_2 with enhanced accuracy and precision from SCIAMACHY: Validation with FTS measurements and comparison with model results, J. Geophys. Res., 116, D04301, doi:10.1029/2010JD015047.

/Reuter et al., 2014/ Reuter, M., M. Buchwitz, M. Hilker, J. Heymann, O. Schneising, D. Pillai, H. Bovensmann, J. P. Burrows, H. Bösch, R. Parker, A. Butz, O. Hasekamp, C. W. O'Dell, Y. Yoshida, C. Gerbig, T. Nehrkorn, N. M. Deutscher, T. Warneke, J. Notholt, F. Hase, R. Kivi, R. Sussmann, T. Machida, H. Matsueda, and Y. Sawa, Satellite-inferred European carbon sink larger than expected, Atmos. Chem. Phys., 14, 13739-13753, 2014.

/Reuter et al., 2014b/ Reuter, M., M. Buchwitz, A. Hilboll, A. Richter, O. Schneising, M. Hilker, J. Heymann, H. Bovensmann and J. P. Burrows, Decreasing emissions of NOx

relative to CO_2 in East Asia inferred from satellite observations, Nature Geoscience, 28 Sept. 2014, doi:10.1038/ngeo2257, pp.4, 2014.

/Reuter et al., 2017a/ Reuter, M., M. Buchwitz, O. Schneising, S. Noel, V. Rozanov, H. Bovensmann, J. P. Burrows, A Fast Atmospheric Trace Gas Retrieval for Hyperspectral Instruments Approximating Multiple Scattering - Part 1: Radiative Transfer and a Potential OCO-2 XCO_2 Retrieval Setup, Remote Sens., 9, 1159, doi:10.3390/rs9111159, 2017.

/Reuter et al., 2017b/ Reuter, M., M. Buchwitz, O. Schneising, S. Noel, H. Bovensmann, J. P. Burrows, A Fast Atmospheric Trace Gas Retrieval for Hyperspectral Instruments Approximating Multiple Scattering - Part 2: Application to XCO_2 Retrievals from OCO-2, Remote Sens., 9, 1102, doi:10.3390/rs9111102, 2017.

/Reuter et al., 2018/ Reuter, M., H. Bovensmann, S. Noël, K. Bramstedt, H. Bovensmann, Green-House-Gas Total Column Performance Simulations (GHG-TCPS) Validation and Performance Simulation Report, Technical Report Univ. Bremen, version 1.0, 18-June-2018, Doc. ID: IUP-GHG-TCPS-VPSR-01, 2018.

/Reuter et al., 2019/ Reuter, M., Buchwitz, M., Schneising, O., Krautwurst, S., O'Dell, C. W., Richter, A., Bovensmann, H., and Burrows, J. P.: Towards monitoring localized CO2 emissions from space: co-located regional CO2 and NO2 enhancements observed by the OCO-2 and S5P satellites, Atmos. Chem. Phys., https://www.atmos-chem-phys.net/19/9371/2019/, 19, 9371-9383, 2019.

/Reuter et al., 2019b/ Reuter, M., Buchwitz, M., Schneising, O., Noel, S., Bovensmann, H., Burrows, J. P., Boesch, H., Di Noia, A., Anand, J., Parker, R. J., Somkuti, P., Wu, L., Hasekamp, O. P., Aben, I., Kuze, A., Suto, H., Shiomi, K., Yoshida, Y., Morino, I., Crisp, D., O'Dell, C., Notholt, J., Petri, C., Warneke, T., Velazco, V., Deutscher, N. M., Griffith, D. W. T., Kivi, R., Pollard, D., Hase, F., Sussmann, R., Te, Y. V., Strong, K., Roche, S., Sha, M. K., De Maziere, M., Feist, D. G., Iraci, L. T., Roehl, C., Retscher, C., and Schepers, D., Ensemble-based satellite-derived carbon dioxide and methane column-averaged dry-air mole fraction data sets (2003-2018) for carbon and climate applications, Atmos. Meas. Tech. Discuss., https://doi.org/10.5194/amt-2019-398, in review, 2019.

/Rodgers 2000/ Rodgers, C. D.: “Inverse Methods for Atmospheric Sounding: Theory and Practice”, World Scientific, Singapore, 2000.

/Rodgers and Connor, 2003/ Rodgers, C. D. and B. J. Connor, Intercomparison of remote sounding instruments, J. Geophys. Res., Vol. 108, No. D3, 4116, pp. 1-13, 2003.

/Rozanov et al. 2014/ Rozanov, V.V., A.V. Rozanov, A.A. Kokhanovsky, J.P. Burrows: Radiative transfer through terrestrial atmosphere and ocean: Software package SCIATRAN. Journal of Quantitative Spectroscopy and Radiative Transfer, http://dx.doi.org/10.1016/j.jqsrt.2013.07.004, Vol. 133, p. 13–71, 2014.

/S5UVN_Req, 2016/ Sentinel-5 Requirement Consolidation for the UV-VIS Bands Final Report; source: KNMI; ref: S5-KNMI-RQ-0003-RP; issue: 2.1.0; date: 2016-05-03.

/Schneising et al., 2011/ Schneising, O., Buchwitz, M., Reuter, M., Heymann, J., Bovensmann, H., Burrows, J. P., Long-term analysis of carbon dioxide and methane column-averaged mole fractions retrieved from SCIAMACHY, Atmos. Chem. Phys., 11, 2881-2892, 2011.

/VIIRS Cloud Mask ATBD, 2014/ GSFC JPSS CMO, Joint Polar Satellite System (JPSS) VIIRS Cloud Mask (VCM) Algorithm Theoretical Basis Document (ATBD), Aug. 5, 2014, Revision E, Goddard Space Flight Center, Greenbelt, Maryland, 2014.

/Wunch et al. 2010/ Wunch, D., Toon, G. C., Wennberg, P. O., Wofsy, S. C., Stephens, B. B., Fischer, M. L., Uchino, O., Abshire, J. B., Bernath, P., Biraud, S. C., Blavier, J.-F. L., Boone, C., Bowman, K. P., Browell, E. V., Campos, T., Connor, B. J., Daube, B. C., Deutscher, N. M., Diao, M., Elkins, J. W., Gerbig, C., Gottlieb, E., Griffith, D. W. T., Hurst, D. F., Jiménez, R., Keppel-Aleks, G., Kort, E. A., Macatangay, R., Machida, T., Matsueda, H., Moore, F., Morino, I., Park, S., Robinson, J., Roehl, C. M., Sawa, Y., Sherlock, V., Sweeney, C., Tanaka, T., and Zondlo, M. A.: Calibration of the Total Carbon Column Observing Network using aircraft profile data, Atmospheric Measurement Techniques, 3, 1351–1362, doi:10.5194/amt-3-1351-2010, URL http://www.atmos-meas-tech.net/3/1351/2010/, 2010.

/Wunch et al. 2011/ Wunch, D., Toon, G. C., Blavier, J.-F. L., Washenfelder, R. A., Notholt, J., Connor, B. J., Griffith, D. W. T., Sherlock, V., and Wennberg, P. O.: The Total Carbon Column Observing Network (TCCON), Philosophical Transactions of the Royal Society of London, Series A: Mathematical, Physical and Engineering Sciences, 369, 2087–2112, doi:10.1098/rsta.2010.0240, 2011.

/Wunch et al. 2015/ Wunch, D., Toon, G.C., Sherlock, V., Deutscher, N.M., Liu, X., Feist, D.G., Wennberg, P.O., The Total Carbon Column Observing Network's GGG2014 Data Version. Carbon Dioxide Information Analysis Center, Oak Ridge National Laboratory, Oak Ridge, Tennessee, USA (available at: doi:10.14291/tccon.ggg2014.documentation.R0/1221662), 2015.

/Yoshida et al. 2013/ Yoshida, Y., Kikuchi, N., Morino, I., Uchino, O., Oshchepkov, S., Bril, A., Saeki, T., Schutgens, N., Toon, G. C., Wunch, D., Roehl, C. M., Wennberg, P. O., Griffith, D. W. T, Deutscher, N. M., Warneke, T., Notholt, J., Robinson, J., Sherlock, V., Connor, B., Rettinger, M., Sussmann, R., Ahonen, P., Heikkinen, P., Kyrö, E., Mendonca, J., Strong, K., Hase, F., Dohe, S., and Yokota, T.: Improvement of the retrieval algorithm for GOSAT SWIR XCO_2 and XCH_4 and their validation using TCCON data, Atmos. Meas. Tech., 6, 1533–1547, doi:10.5194/amt-6-1533-2013, 2013.

***** End of Document *****

Study on Consolidating Requirements and Error Budget for CO_2 Monitoring Mission (CO2M-REB):

Requirements Sensitivity Analysis for anthropogenic CO_2 Monitoring Mission (CO2M)

Technical Note (TN-2000)

ESA Study
"Study on Consolidating Requirements and Error Budget for CO_2 Monitoring Mission"
ESA Contract N^o 4000125122/18/NL/FF/gp

Authors:
Michael.Buchwitz@iup.physik.uni-bremen.de,
Stefan Noël, Maximilian Reuter, Heinrich Bovensmann, Andreas Richter
Institute of Environmental Physics (IUP) / Institute of Remote Sensing (IFE), University of Bremen (UB), Bremen, Germany

Jochen Landgraf, Hein van Heck
SRON, Utrecht, The Netherlands

Pepijn Veefkind, Johan de Haan
KNMI, De Bilt, The Netherlands

Hartmut Boesch
University of Leicester, Leicester, UK

Change log

Version	Date	Status	Authors	Reason for change
1.0	22-Jan-2019	Submitted	CO2M-REB team	New document
1.1	25-Apr-2019	Submitted	-"-	To consider comments from ESA on v1.0
1.2	26-Apr-2019	Submitted	-"-	Section 7 added
2.0	25-Feb-2020	Submitted	-"-	Update for MRDv2
2.1	8-May-2020	Submitted	-"-	To consider comments from ESA

Table of Contents

1. Abstract 6
2. Executive summary 7
3. Analysis Tools 11
   3.1. Tools used by University of Bremen 11
   3.2. Tools used by SRON 16
      3.2.1. RemoTeC 16
      3.2.2. AeroMAP 17
   3.3. Tools used by University of Leicester (UoL) 17
   3.4. Tools used by KNMI 18
4. Analysis results for XCO_2 and XCH_4 19
   4.1. Dynamic range maximum 19
      4.1.1. University of Bremen analysis 19
      4.1.2. Summary and conclusions 36
   4.2. Dynamic range minimum 38
      4.2.1. University of Bremen analysis 38
      4.2.2. Summary and conclusions 39
   4.3. Signal-to-noise ratio (SNR) 40
      4.3.1. University of Bremen assessments: SNR-related XCO_2 error 41
      4.3.2. Comparison with SRON and Univ. Leicester results 47
      4.3.3. Sensitivity of SNR-related XCO_2 error w.r.t. SNR 49
      4.3.4. Summary and conclusions 50
   4.4. Zero Level Offset (ZLO) 51
      4.4.1. University of Bremen error analysis results for ZLO 51
      4.4.2. Analysis of Jänschwalde power plant scene 54
      4.4.3. Comparison of ZLO related errors via three different algorithms 59
      4.4.1. Summary and conclusions 61
   4.5. Non-linearity (NL) 62
      4.5.1. Comparison of NL related errors via three different algorithms 62
      4.5.2. Summary and conclusions 64
   4.6. Instrument Spectral Response Function (ISRF) 65
      4.6.1. University of Bremen error analysis results for ISRF 65
      4.6.2. Summary and conclusions 69
   4.7. Multiplicative radiance errors 70

4.7.1. University of Bremen error analysis results 70
4.7.2. Comparison of MULT errors via three different algorithms 71
4.7.3. Summary and conclusions 73
4.8. Spectral calibration errors....74
4.8.1. University of Bremen error analysis results 74
4.8.2. Summary and conclusions 76
4.9. Geolocation knowledge related XCO_2 errors....77
5. Analysis results for Tropospheric NO_2 80
5.1. Analysis results for SNR....80
5.2. Analysis results for spectral calibration....82
5.3. Analysis results for ISRF 83
5.4. Analysis results for multiplicative radiometric errors 88
5.5. Analysis results for additive radiometric errors 90
5.6. Summary and conclusions 94
6. Analysis results for SIF 95
6.1. Signal-to-noise ratio (SNR)....95
6.2. Radiometric: Multiplicative....98
6.3. Radiometric: Additive (ZLO) 100
6.4. Instrument Spectral Response Function (ISRF) 100
6.5. Spectral calibration....102
6.6. Summary and conclusions 103
7. Reference cases for Aerosols from the MAP instrument....104
8. Analysis results for Aerosols from the MAP instrument....106
8.1. Measurement setups....107
8.2. State vector definition....108
8.3. Linear error analysis....109
8.4. Requirements....110
8.4.1. Modulation concept (MAP-mod) 111
8.4.2. Bandpass concept (MAP-band)....119
8.4.3. Alternative setups to MAP-band 125
8.4.4. Inclusion of 753-nm wavelength 126
8.5. Spatial oversampling 130
8.5.1. Chess-board scenario 130
8.5.2. Sentinel 2 scenario....134
8.6. ISRF knowledge requirement 139

8.7. Summary and conclusions 142
9. Reference spectra incl. gain vectors: XCO_2 and XCH_4 143
9.1. Scenarios and instrument configurations 143
9.2. Univ. Bremen reference spectra for XCO_2 and XCH_4 145
10. Reference spectra incl. gain vectors: Tropospheric NO_2 150
10.1. Scenarios and instrument configurations 150
10.2. KNMI data: ESRA and Gain: S7MR-OBS-650 151
10.3. Summary and conclusions 154
11. Reference spectra incl. gain vectors: RemoTeC XCO_2 and MAP aerosols 155
11.1. Gain vector and reference spectra using RemoTeC 155
11.1.1. Scenarios and instrument configurations 155
11.1.2. SRON data 157
11.2. MAP reference spectra 159
11.2.1. Atmospheric Scenarios 159
11.2.2. Reference Spectra 162
12. Reference spectra incl. XCO_2 gain vectors from Univ. Leicester 165
13. Acronyms and abbrevations 167
14. References 169

1. Abstract

This document is a deliverable of ESA Study "Study on Consolidating Requirements and Error Budget for CO_2 Monitoring Mission". The anthropogenic CO_2 Monitoring satellite mission is referred to as CO2M mission in this document.

This document, the "Requirements Sensitivity Analysis for CO2M" (technical note 2000, i.e., TN-2000), is one document of three closely related documents. The other two are: the "Requirements Justification Report for CO2M" (TN-1000) and "Error Budgets and Performance for CO2M" (TN-3000).

Previous versions of these three documents have been used to provide feedback on version 1.0 of the CO2M Mission Requirements Document (MRD), referred to as MRDv1.0 in this document. These feedbacks have been used by ESA to generate version 2.0 of the MRD, referred to as MRDv2.0 in this document. Updates of these three reports, including this document, are based on using MRDv2.0 as the key input document.

The objective of this report is to document requirements sensitivity analysis methods and corresponding error analysis results for CO2M and to describe specific data sets (reference spectra) relevant for this purpose. The results and data sets described in this document (TN-2000) are used as input for two other documents, namely for TN-1000 and for TN-3000.

For the CO2M CO_2 (and CH_4) main instrument simulated retrieval have been carried out using the FOCAL retrieval algorithm in order to quantify the impact of several potentially critical error sources on the quality of the retrieved XCO_2 (and XCH_4). In particular it has been investigated if errors as allocated by the Error Budget (EB, see TN-3000) for various error sources can be significantly exceeded or not given the required instrument performance as specified in the CO2M Mission Requirements Document (MRD) version 2.0.

Among the error sources investigated are additive and multiplicative radiometric errors, errors of the Instrument Spectral Response Function (ISRF) and spectral calibration related errors. For the Signal-to-Noise-Ratio (SNR) requirement detailed recommendations are given on how to improve the MRD SNR requirement. Also for additive radiance errors recommendations are given on how the requirement can be improved.

The assessments also show that the dynamic range needs to be optimized. Solar Induced Fluorescence (SIF) can also be retrieved from these spectra and error analysis results for SIF are also presented in this document. Furthermore, error analysis results are presented for the instrument (or from a band added to the CO_2 instrument) which will deliver information on tropospheric NO_2 and for the Multi-Angle-Polarimeter (MAP) instrument which will deliver additional information on aerosols and cirrus clouds in order to improve the accuracy of the retrieved XCO_2.

2. Executive summary

This document is a deliverable of ESA Study "Study on Consolidating Requirements and Error Budget for CO_2 Monitoring Mission". The anthropogenic CO_2 Monitoring satellite mission is referred to as CO2M mission in this document.

This document, the "Requirements Sensitivity Analysis for CO2M" (technical note 2000, i.e., TN-2000) is one document of three closely related documents. The other two are: the "Requirements Justification Report for CO2M" (TN-1000) **/CO2M-REB TN-1000 v2.1, 2020/** and "Error Budgets and Performance for CO2M" (TN-3000) **/CO2M-REB TN-3000 v2.1, 2020/**.

Previous versions of these three documents have been used to provide feedback on version 1.0 of the CO2M Mission Requirements Document (MRD), referred to as MRDv1.0 in this document **/CO2M MRD v1.0, 2018/**. These feedbacks have been used by ESA to generate version 2.0 of the MRD, referred to as MRDv2.0 in this document **/CO2M MRD v2.0, 2019/**. Updates of these three reports, including this document, are based on using MRDv2.0 as the key input document.

The objective of this report is to document requirements sensitivity analysis methods and corresponding error analysis results for CO2M and to describe specific data sets relevant for this purpose ("reference spectra", "gain vectors"). The new results and data sets described in this document (i.e., in TN-2000) are used as input for two other documents, mentioned above, namely the "Requirements Justification Report" (TN-1000) and "Error Budgets and Performance" (TN-3000).

<u>The XCO_2 and XCH_4 related analysis results can be summarized as follows:</u>

CO_2 instrument: Overview:
For the CO_2 (and CH_4) main instrument simulated retrievals have been carried out using the FOCAL retrieval algorithm in order to quantify the impact of several potentially critical error sources on the quality of the retrieved XCO_2 (and XCH_4). In particular it has been investigated if errors as allocated by the Error Budget (EB) can be significantly exceeded or not - given the required performance as specified in the CO2M Mission Requirements Document (MRD) version 2.0. Among the error sources investigated are additive and multiplicative radiometric errors, errors of the Instrument Spectral Response Function (ISRF) and spectral calibration related errors. For the Signal-to-Noise-Ratio (SNR) requirement detailed recommendations are given on how to improve the MRD SNR requirement. Also for additive radiance errors recommendations are given on how the requirement can be improved. The assessments also show that the maximum value of the dynamic range needs to be redefined to avoid saturation or non-useful spectra for other reasons. Also the dynamic range minimum needs to be adjusted. Furthermore, a set of reference spectra (high resolution radiance and irradiance, XCO_2 and XCH_4 gain vectors, etc.) have been generated and made available for ESA.

CO_2 instrument: Dynamic range:

Full performance is according to the MRD only guaranteed if the radiances (in the different spectral bands) of the CO2M instrument do not exceed the dynamic range maximum values as specified in the MRD ("DR-max-0"). If the radiances exceed these thresholds than the spectra may saturate or suffer from low quality for other reasons. It has been shown using MODIS data (surface albedo) and OCO-2 radiances that the current thresholds as given in the MRD are too low and recommendations are given to what extent these values need to be enlarged to ensure good performance over land. The results indicated that DR-max-0 needs to be significantly enlarged. It is also shown that the minimum value of the dynamic range ("DR-min-70") needs to be optimized, esp. for the NIR and SWIR-2 bands.

CO_2 instrument: Signal-to-Noise-Ratio:
A very important requirement is the Signal-to-Noise-Ratio (SNR) requirement as it essentially determines (along with some other error sources resulting in "pseudo-noise") the XCO_2 and XCH_4 random error ("precision"). According to the Error Budget (EB) 0.5 ppm (1-sigma) is allocated for the XCO_2 random error due to SNR-related errors. Recommendations have been given to improve the SNR requirement based on retrieval simulations using the FOCAL retrieval method. Specifically, a formula is given which permits to compute the SNR for any radiance given two parameters *A* and *B* and values for *A* and *B* are specified (for each spectral band) such that an SNR-related XCO_2 random error of 0.5 ppm can be achieved for a relevant typical scenario ("REF50", SZA=50^o, and surface albedos corresponding to the "Berlin reference scene", 0.25 in the NIR, 0.2 in SWIR-1 and 0.1 in SWIR-2). For the VEG50 scenario (vegetation albedo assumed having a factor of 2 lower albedos in the SWIR) the SNR-related XCO_2 random error would be in the range 0.57 – 0.68 ppm, depending on the selected *A*-*B* pair. A single *A*-*B* pair (per band) has been defined and used to improve the SNR requirement and it is shown that the 0.5 ppm requirement for SNR-related XCO_2 random errors is met for this pair by all 3 retrieval algorithms (i.e., the ones from Univ. Bremen, Univ. Leicester and SRON) for REF50 (but not for VEG50).

CO_2 instrument: Additive radiance errors:
Additive radiance errors, denoted here as Zero-Level-Offsets (ZLO), need to be minimized to avoid systematic XCO_2 retrieval errors. Using simulated retrievals using the FOCAL retrieval algorithm it has been investigated how large these systematic errors can be given the (maximum) ZLO values specified in the MRD. According to the Error Budget (EB) an XCO_2 error of 0.2 ppm has been allocated for this error source. If ZLO is added as a state vector element to FOCAL then the resulting systematic error is zero suggesting that this error source is negligible. However, it is not entirely clear if robust retrievals are possible when ZLO is added as a state vector element. Furthermore, the retrieval simulations assume that the error is constant in each band, which is a very optimistic assumption. If ZLO is not a state vector element, than this error source can result in errors significantly larger than 0.2 ppm. One may expect that at the end (i.e., for the final algorithm including bias correction and/or ZLO correction) the ZLO-related error is in between the two extremes discussed here. It is therefore concluded that the ZLO requirement as given in the MRD is appropriate. This is also corroborated by simulation of scenes using the End-to-End-Simulator (E2ES) software.

CO_2 instrument: Multiplicative radiance errors:
Multiplicative radiance errors may result in XCO_2 retrieval errors but this error source is expected to be much less critical than additive radiance errors. According to the Error Budget (EB) 0.2 ppm is allocated for this error source. Retrieval simulations with FOCAL confirm that this error source is less critical compared to additive errors and that the MRD requirement is appropriate. However, the sensitivity to this error source also depends on the retrieval algorithm. It is shown that the algorithms of SRON and UoL are more sensitive to this error source compared to the IUP FOCAL algorithm. It therefore cannot be recommended to relax the MRDv1 absolute radiometric requirement of 3%

CO_2 instrument: Instrument Spectral Response Function:
Residual errors of the Instrument Spectral Response Function (ISRF) result in errors of the XCO_2 retrievals. According to the Error Budget (EB) 0.2 ppm has been allocated for this error source. Simulated XCO_2 retrievals have been carried out with FOCAL for several types of ISRF errors. The results indicate that the MRD requirement is appropriate.

CO_2 instrument: Spectral calibration errors:
Spectral calibration errors will result in errors of the retrieved XCO_2. According to the Error Budget (EB) 0.2 ppm has been allocated for this error source. Simulated retrievals have been carried out with FOCAL and the results indicate that the MRD requirement is appropriate.

CO_2 instrument: Solar Induced Fluorescence:
The CO2M requirements have been analyzed for the retrieval of Solar Induced Fluorescence (SIF) based on available literature, first-order considerations and on linear error analysis using the UoL retrieval algorithm. The results are assessed against the requirements given in MRDv2.0 for the precision of the SIF retrieval of better than 0.7 mW m^{-2} sr^{-1} nm^{-1} and for systematic errors of less than 0.2 mW m^{-2} sr^{-1} nm^{-1}. The considered CO2M requirements include SNR, multiplicative radiometric gain, additive zero level offset, relative radiometric gain, ISRF, spectral calibration errors. The analysis show that it can be expected that the random errors from measurement noise are much lower than the requirements. The most significant other error sources are ISRF uncertainties and straylight contributions. If we assume that both error sources can be well corrected using SIF-free retrieval over bare and snow areas then systematic errors will reduce to below the bias requirement. However, this assumes that IRSF errors and straylight characteristics does only slowly change (or in a well predicable manner) with time. Also, clouds within the field of view can contribute additional, more random straylight, which cannot be easily corrected.

<u>The Tropospheric NO_2 related analysis results can be summarized as follows:</u>

Assessments of the MRD requirements for the NO_2 observations of CO2M are presented. This has strong heritage from other missions, including S5P/TROPOMI, S4/UVN and S5/UVNS. However, the primary use of the NO_2 data is different than for these heritage missions; for CO2M the primary use is plume detection. For this application observation requirements have to be formulated, especially regarding the systematic errors. For several of the requirements we propose modifications, which often is an update of the values. For the ISRF we propose a new approach, which we consider a relaxation compared to the original requirement. Furthermore, we want to highlight the importance of the SNR requirement. The

requirement for SNR is currently set at 750 for the provided reference scenario. This results in errors in the tropospheric NO_2 column of approximately 1.5 x 10^{15} molec. cm^{-2}. A further improvement of the SNR towards 1000 would enable the detection of even smaller plumes, which is judged to be very important for the envisaged application of obtaining CO_2 emission from observed XCO_2 plumes.

The Aerosols and Clouds related analysis results can be summarized as follows:

The CO2M requirements for the MAP instrument have been analyzed with respect to the XCO_2 performance. The analysis accounts for two different instrument concepts using the spectral modulation technique and bandpass polarimetry. For the modulation concept, we conclude that the radiance uncertainty must be < 3 % and the DLP uncertainty < 0.0035. We have broken down this requirement to a radiance precision and bias requirement to be 0.2 % and 3 %, respectively, and a DLP precision and bias requirement to be < 0.0025. Here, the radiance precision is driven by the DLP precision of 0.0025, which allows to allocate nearly the entire error contribution to radiometric biases. The instrument must measure radiance and DLP in at least 5 viewing angles in the spectral range 385-765nm. For the bandpass concept, the same radiometric requirements hold, i.e. the radiance uncertainty must be < 3 % and the DLP uncertainty < 0.0035 with the same breakdown to precision and bias requirement. This instrument concept must measure radiance and DLP in a least 21 viewing angles at 11 wavelengths (410, 440, 465, 490, 520, 550, 610, 669, 735, 800, 863 nm) (note: other settings are also possible, e.g., more angles (e.g., 40) but a reduced number of bands). For instrument cross calibration, it is desirable to have one particular measurement at 753 nm. In case an already existing band must be omitted for this implementation, replacing the 550 nm has the smallest impact on the CO2M performance. Independent on the MAP concept, the radiance and polarization measurements must the spatially resampled, both for a consistent interpretation of the different viewing angles and for a co-alignment with the CO_2 measurements. For this purpose, a spatial oversampling of a factor 2 is required.

3. Analysis Tools

3.1. Tools used by University of Bremen

For the assessment results presented in this document, University of Bremen is using the FOCAL radiative transfer and retrieval system described in detail in **/Reuter et al., 2017a, 2017b/**.

FOCAL has also been used for CO2M relevant performance assessments as shown in **/Reuter et al., 2018/**. These performance assessments have been carried out using the so-called Greenhouse Gas (GHG) End-to-End-Simulator (E2ES) system.

The version of FOCAL used for the results presented in this document is similar to the version used for the assessments shown in **/Reuter et al., 2018/**. However, the focus of **/Reuter et al., 2018/** was to study the performance of "real instruments" (using simulation software provided by industry). In this new study the purpose is to perform simulations and to generate data "Reference spectra") in order to assess the performance as specified in the CO2M Mission Requirements Document version 2.0 (MRDv2.0) **/CO2M MRD v2.0, 2019/**. Therefore, the industry instrument modules are not used in this study. Instead, they are replaced by simplified versions of instrument models consistent with the MRD (in terms of spectral range, resolution, sampling, signal-to-noise ratio (SNR), etc.).

The FOCAL retrieval method is based on "Optimal Estimation" (OE) **/Rodgers 2000/ /Rodgers and Connor, 2003/**. The FOCAL state vector elements (fit parameters) are listed in **Table 1** (see **/Reuter et al., 2017a/** for details). As can be seen, surface pressure is not fitted. Retrieval studies based on FOCAL have shown that the chosen 5 vertical elements are appropriate for CO_2, CH_4 and H_2O.

Parameter	Description	Number of elements
CO_2	CO_2 mixing ratio in 5 vertical layers	5
CH_4	CH_4 mixing ratio in 5 vertical layers	5
H_2O	H_2O mixing ratio in 5 vertical layers	5
Scattering parameters	Altitude (pressure), thickness (optical depth) and wavelength dependence (Angstrom parameter) of scattering layer	3
SIF	Solar induced fluorescence	1
Polynom coefficients	Coefficients of low order polynomial (SIF band: 2; NIR: 3, SWIR-1: 3, SWIR-2: 3)	11
Shift & squeeze parameters	Spectral shift and squeeze parameters per band	8
FWHM scaling factors	Instrument Spectral Response Function (ISRF) Full Width at Half Maximum (FWHM) scaling factors in NIR, SWIR-1 and SWIR-2 bands	3

Table 1: FOCAL state vector elements. See **/Reuter et al., 2017a/** for details.

Note that XCO_2 errors computed (with FOCAL or other OE-type algorithms) not only depend on the satellite instrument and its characteristics but also on the retrieval algorithm and assumptions with respect to *a priori* errors. This is illustrated in **Figure 1**, where the *a posteriori* total XCO_2 uncertainty (red curve), the noise or SNR-related random error (green) and the smoothing (and interference) error (blue) is shown as a function of the assumed XCO_2 *a priori* error. As can be seen, the SNR-related XCO_2 error is approx. 0.7 ppm if the *a priori* error is 10 ppm (for the investigated REF50 scenario) but only 0.5 ppm if the assumed *a priori* error is 5 ppm. The latter is the baseline for FOCAL XCO_2 *a priori* errors assumed for this study.

This aspect has been further studied using a scene with a power plant in the center of the XCO_2 image: **Figure 2** shows the corresponding results assuming 10 ppm *a priori* uncertainty and **Figure 3** assuming 5 ppm. The simulated XCO_2 is the same and "perfect" in both cases, i.e., without any systematic error. Only instrument noise is considered and this is error source is the same for both cases. As can be seen from **Figure 2**, the XCO_2 retrieval precision is 0.65 ppm, the averaging kernel (AK) at the surface is 0.99, the power plant emission error is -0.9% without AK correction and -0.3% with AK correction. The AK correction is based on using the retrieval algorithm AK to correct the modelled XCO_2 (here the true XCO_2).

As can be seen from **Figure 3**, the XCO_2 retrieval precision is 0.5 ppm (i.e., better), the averaging kernel (AK) at the surface is 1.06 (i.e., "worse"), the power plant emission error is 6.3% without AK correction (worse) and -0.1% (similar) with AK correction. This confirms that assuming 5 ppm instead of 10 ppm *a priori* uncertainty results in better retrieval precision but somewhat larger systematic error but also that the resulting systematic emission error can be significantly reduced by applying the averaging kernels.

The underlying "Jänschwalde power plant scene" has also been used for other error analysis related assessments as presented in this document.

FOCAL version 2 is used for this study.

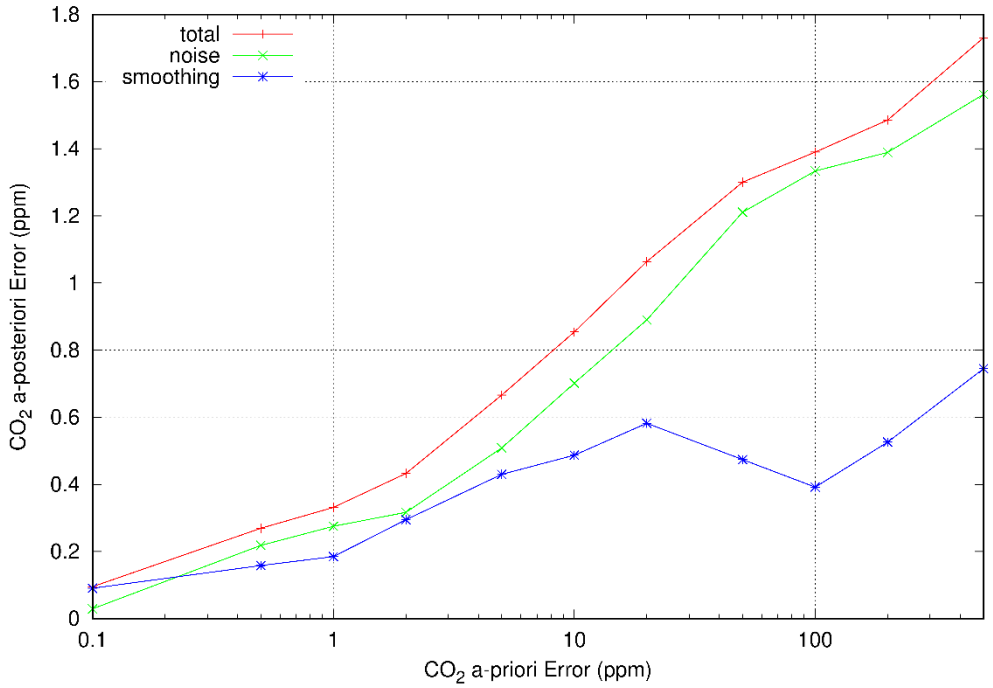

Figure 1: XCO_2 *a posteriori* errors computed with FOCAL as a function of XCO_2 *a priori* errors (for scenario REF50 and instrument CO2M_002).

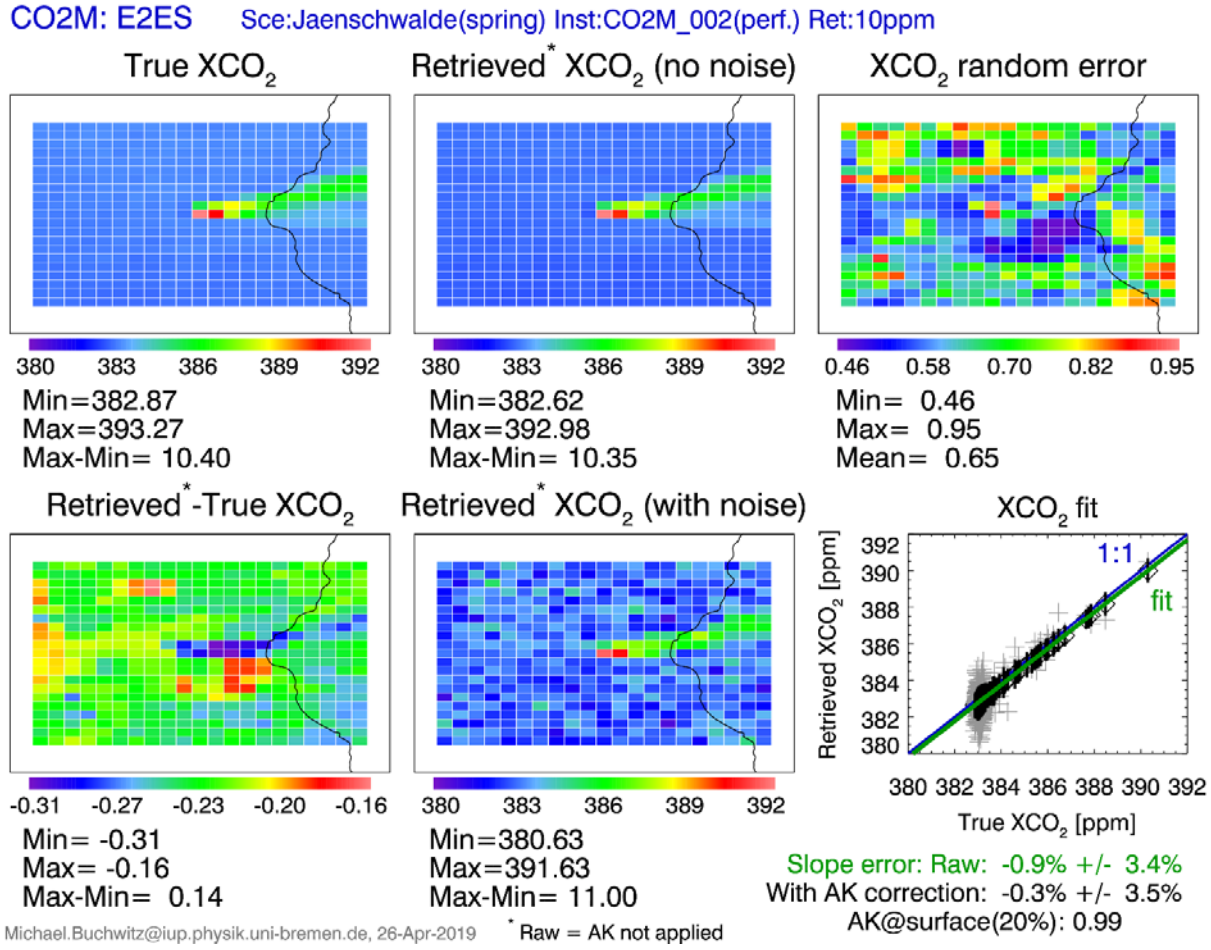

Figure 2: Analysis of Jänschwalde power plant scene with FOCAL retrievals assuming an *a priori* XCO_2 uncertainty of 10 ppm. Top: Left: True XCO_2 at CO2M resolution. The Jaenschwalde power plant is located in the center of the figure. Middle: Retrieved XCO_2 but without noise. Right: XCO_2 noise, i.e., the random error (1-sigma uncertainty). Listed is the mean random error, which is 0.65 ppm. Bottom: Left: Difference retrieved – true XCO_2. Middle: Retrieved XCO_2 with noise. Right: Scatter plot retrieved versus true XCO_2. The linear fit is shown as green line. The deviation of the slope of the fit from 1.0 (or the 1:1 line) has been used to estimate the emission error, which his -0.9% without averaging kernel (AK) correction and -0.3% with correction. The value of the averaging kernel at the surface is 0.99.

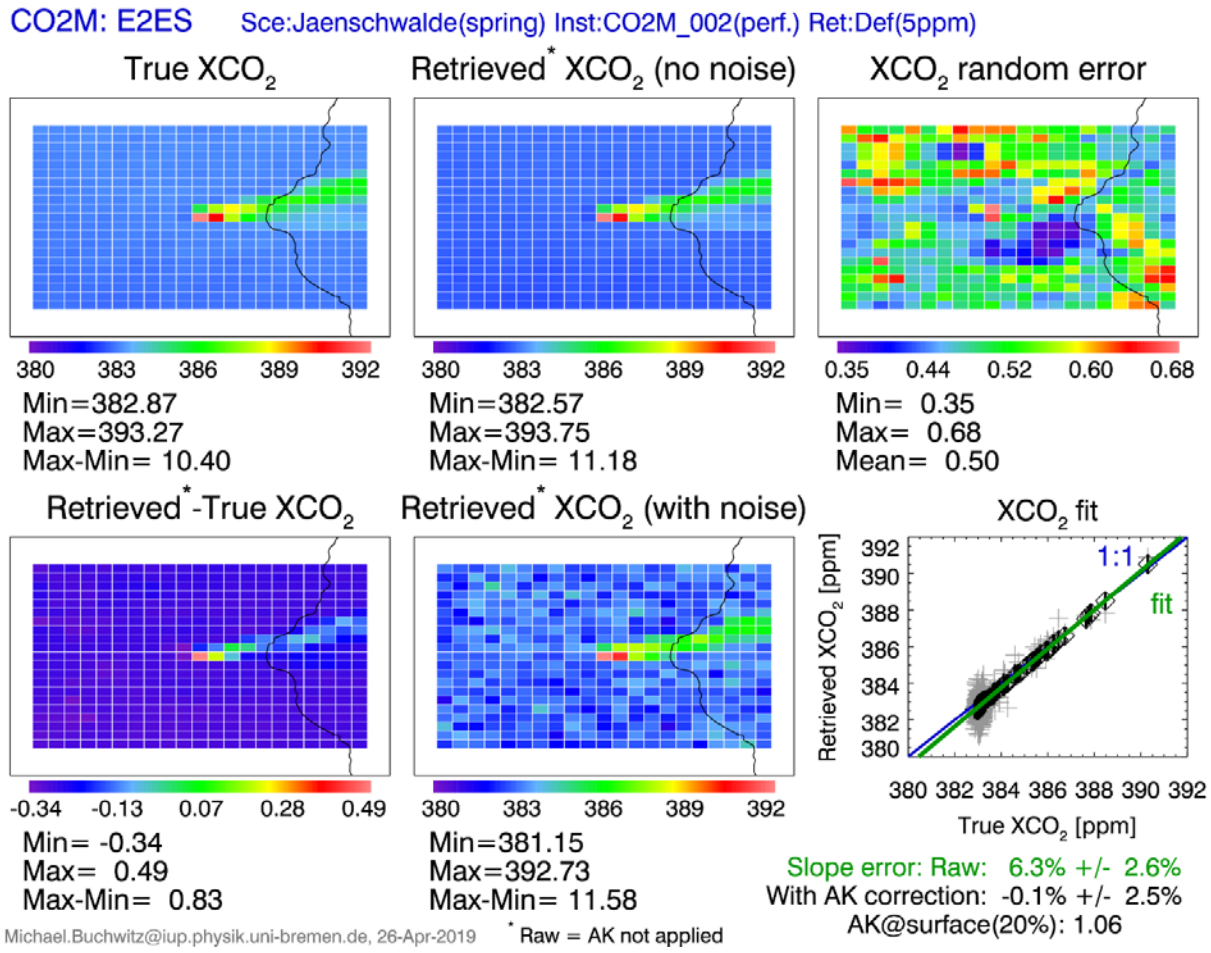

Figure 3: As **Figure 2** but using a FOCAL XCO_2 *a priori* uncertainty of 5 ppm.

3.2. Tools used by SRON

3.2.1. RemoTeC

RemoTeC has been successfully applied to GOSAT, OCO-2 and S5P data, and is the baseline algorithm for CO and CH4 operational data processing of the S5P and Sentinel-5 mission. The algorithm is described in detail in the literature (e.g. **/Butz et al., 2009/**, **/Butz et al,2011a/**, **/Butz et al. 20011b/**, /**Guerlet et al. 2013/**, **/Schepers et al, 2016/**, **/Hu et al. 2016/**) and so, only a short summary will be given here.

Estimating the CO_2, CH_4 and/or H_2O total column concentrations from shortwave infrared measurements faces the challenge that the light-path from the sun to the satellite observer via backscattering at the Earth's surface is not known with sufficient accuracy. In practice, light scattering by atmospheric particles causes unknown light path modification. As a consequence, state-of-the-art retrieval algorithms must retrieve particle properties simultaneously with the CO_2, CH_4, and H_2O concentration. Therefore, RemoTeC aims at retrieving the trace gas vertical profile (with slightly more than 1 degree of freedom) and 3 scattering parameters characterizing the particle amount, size and height. Particle amount is represented through the total column number density of particles. For the particle number density size distribution, RemoTeC assumes a power-law $n(r) \sim r^{\alpha}$, with *r* the particle radius and α the retrieved size distribution parameter. The particle height distribution is a Gaussian function of center height z_c and a fixed width of 2 km. Particle refractive index is assumed fixed-value at m_r=1.400 and m_i=-0.003. Note that surface pressure is not fitted in the standard setup but could be included if ever desired.

The retrieval method infers the partial column concentration (sub-column) profile, the three aforementioned particle parameters, interfering absorber column concentrations as well as some auxiliary parameters such as surface albedo by iteratively minimizing the Phillips-Tikhonov cost function.

The software is used as baseline for the prototype software of operational CH_4 processing from S5-P and S5 shortwave infrared measurements. The software is thread safe, which means that the software parallelizes well assuming appropriate hardware configuration. RemoTeC is managed under version control and so well suited for the purpose of this project. This project uses RemoTeC version 2.5.1.

3.2.2. AeroMAP

The algorithm AeroMAP is developed at the SRON for aerosol retrieval from multiangle measurements of intensity and polarization (/**Hasekamp et al., 2011/; /Stap et al., 2015/; /Wu et al., 2015/**). The retrieval approach is based on iteratively fitting the multiangle photopolarimetric measurements with simulations calculated using the linearized vector radiative transfer model developed at SRON **(/Hasekamp et al. ,2002/, /Hasekamp et al. 2005/; /Schepers et al., 2014/**). For this study we use version 7.42.

Recently, as part of the CO_2 Spectral Sizing Study (ESA-IPL-PEO-FF-gp-LE-2016-456) this algorithm is coupled to the RemoTeC CO2 retrieval algorithm using linear error propagation. The software package includes the option to simulate multiangle intensity and polarization measurements with moderate spectral resolution.

3.3. Tools used by University of Leicester (UoL)

The University of Leicester (UoL) retrieval algorithm is an Optimal Estimation (OE) algorithm that estimates a number of state vector elements from spectrally-resolved radiance spectra in the near-infrared and shortwave-infrared region **/Boesch et al 2006/,** /**Boesch et al., 2011/**.

The forward model employs the LIDORT radiative transfer model combined with a fast 2-orders-of-scattering vector radiative transfer code to approximate polarization /**Natraj et al., 2008/**. In addition, the code can use the low-streams interpolation functionality **/O'Dell , 2010/** or the principal component analysis (PCA) **/Somkuti et al., 2017/** method to accelerate the radiative transfer component of the retrieval algorithm.

The algorithm includes an instrument model to convolve the monochromatic radiance spectrum with the Instrument Spectral Response Function (ISRF) which can either be given analytically or tabulated. The code can also simulate continuum intensity scaling, zero-level offsets and channeling effects.

For the XCO_2 retrievals used to assess the Signal-to-Noise-Ratio (SNR), we have used a retrieval setup that includes a CO_2 profile, scaling values for the H_2O and temperature profile, surface albedo and slope, AOD, height and width of a Gaussian-shaped aerosol profile, dispersion and zero level offset in the NIR band. The forward model uses the PCA method and a Gaussian shaped IRSF function.

3.4. Tools used by KNMI

The main tool used is DISAMAR, which stands for "Determining Instrument Specifications and Analysing Methods for Atmospheric Retrieval". DISAMAR is a software package that enables one to specify an instrument / atmosphere / surface model, simulate a sun-normalized spectrum in the UVN and shortwave infrared region[1], and perform retrieval on that simulated spectrum. It can also ingest measured spectra and perform retrieval for such spectra. When running in the simulation mode one can use different settings for the instrument / atmosphere / surface model for simulation and retrieval, yielding information of the bias in the retrieved parameters due to the difference in settings. For example, one can add stray light to the simulated spectrum and calculate the bias in the retrieved NO_2 column.

DISAMAR can use different retrieval algorithms, such as Optimal Estimation **/Rodgers, 2000/** and various variants of DOAS (Differential Optical Absorption Spectroscopy). One variant of DOAS which is implemented in DISAMAR, called DOMINO, is used here. In DOMINO the total slant NO_2 column is fitted using DOAS. The stratospheric vertical column NO_2 is derived from data assimilation using a Chemical Transport Model. Using the air mass factor for the stratospheric NO_2, this vertical column is transformed into a stratospheric slant column. By subtracting the stratospheric slant column from the total slant column the tropospheric slant column is obtained. Next the vertical column of tropospheric NO_2 is calculated using the air mass factor for the tropospheric NO_2. When calculating the air mass factors for the tropospheric and stratospheric NO_2 a temperature correction is applied. More detailed information can be obtained from **/Boersma et al., 2004/**.

Version 4.1.1 of DISAMAR was used in this study.

[1] Note that DISAMAR was used in this study for NO_2 analyses and not for SWIR CO_2/CH_4 analyses.

4. Analysis results for XCO_2 and XCH_4

4.1. Dynamic range maximum

According to Table 4.7 of MRDv1.0 the maximum radiances of the **Dynamic Range** are (DR-max-0):

- NIR: $9.4x10^{13}$ photons/s/nm/cm^2/sr corresponding to the continuum radiance of this scenario: Solar Zenith Angle (SZA) 0^o and albedo 0.6
- SWIR-1: $2.6x10^{13}$ photons/s/nm/cm^2/sr, corresponding to SZA 0^o and albedo 0.4
- SWIR-2: $1.4x10^{13}$ photons/s/nm/cm^2/sr, corresponding to SZA 0^o and albedo 0.4

The purpose of the dynamic range is to define the range (including the lowest radiance levels) where all requirements have to be met.

Also listed in the MRDv1.0 are radiances defining the **Measurement Range**. The corresponding upper limit (MR-BC-0) is:

- NIR: $9.4x10^{13}$ photons/s/nm/cm^2/sr corresponding to SZA 0^o and albedo 0.8
- SWIR-1: $2.6x10^{13}$ photons/s/nm/cm^2/sr, corresponding to SZA 0^o and albedo 0.7
- SWIR-2: $1.4x10^{13}$ photons/s/nm/cm^2/sr, corresponding to SZA 0^o and albedo 0.6

These values originate from CarbonSat studies **/CS L1L2-II TN nadir, 2015/**. The purpose of the measurement range was, for example (i.e., in addition to other aspects such as straylight, etc.), to define radiance levels, where the spectra are not saturated, i.e., potentially still very useful, although without guarantee.

While this was assumed to be acceptable for a demonstration mission, this may not be acceptable for an operational mission as this likely results in (too) many non-useful observations.

Additional corresponding assessments have been carried out and are presented in the following. The corresponding recommendations have been considered for MRDv2.0.

4.1.1. University of Bremen analysis

The following assessments have been carried out assuming that at least all cloud-free observations over land shall be of good quality.

Analysis using MODIS albedo

To determine where a given radiance level may be exceeded, an albedo climatology from MODIS has been used (the same data based as also used and described in **/Reuter et al., 2018/**). Note that snow coverage is not considered in this climatology. It is assumed that the radiance is proportional to the product of albedo and cos(SZA), where the SZA has been computed for local noon using an analytic formula. Note that snow coverage is not considered in the albedo climatology but this is not considered as a significant limitation

(although the snow albedo can be high in the NIR) because snow coverage is typically not present for small SZAs.

The results are shown in **Figure 4** - **Figure 6**.

As can be seen from **Figure 4** it can be expected that the MRDv1.0 dynamic range maximum can be exceeded.

As can be seen from **Figure 5** this is also expected for the upper limit of the (currently defined) measurement range.

Figure 6 suggests that the risk of saturation is essentially eliminated (for snow free and cloud free scenes outside of sun-glint conditions) if the upper limit of the radiance corresponds to this scene:

- SZA 0^o, albedo: NIR: 0.9, SWIR-1; 0.75, SWIR-2: 0.7

The corresponding radiances (as obtained by scaling the MRDv1.0 MR-BC-0 radiances) are:

- NIR: 14.7 x 10^{13} photons/s/nm/cm^2/sr
- SWIR-1: 4.9 x 10^{13} photons/s/nm/cm^2/sr
- SWIR-2: 2.5 x 10^{13} photons/s/nm/cm^2/sr

Conclusions based on the analysis of MODIS albedos:

To have some margin it is recommended to use somewhat larger albedos (or corresponding radiances) for the upper limit of the dynamic range, e.g.:

- SZA 0^o, albedo: NIR: 0.95, SWIR-1; 0.80, SWIR-2: 0.77

To further investigate the important aspect, additional results are shown in the following sub-sections.

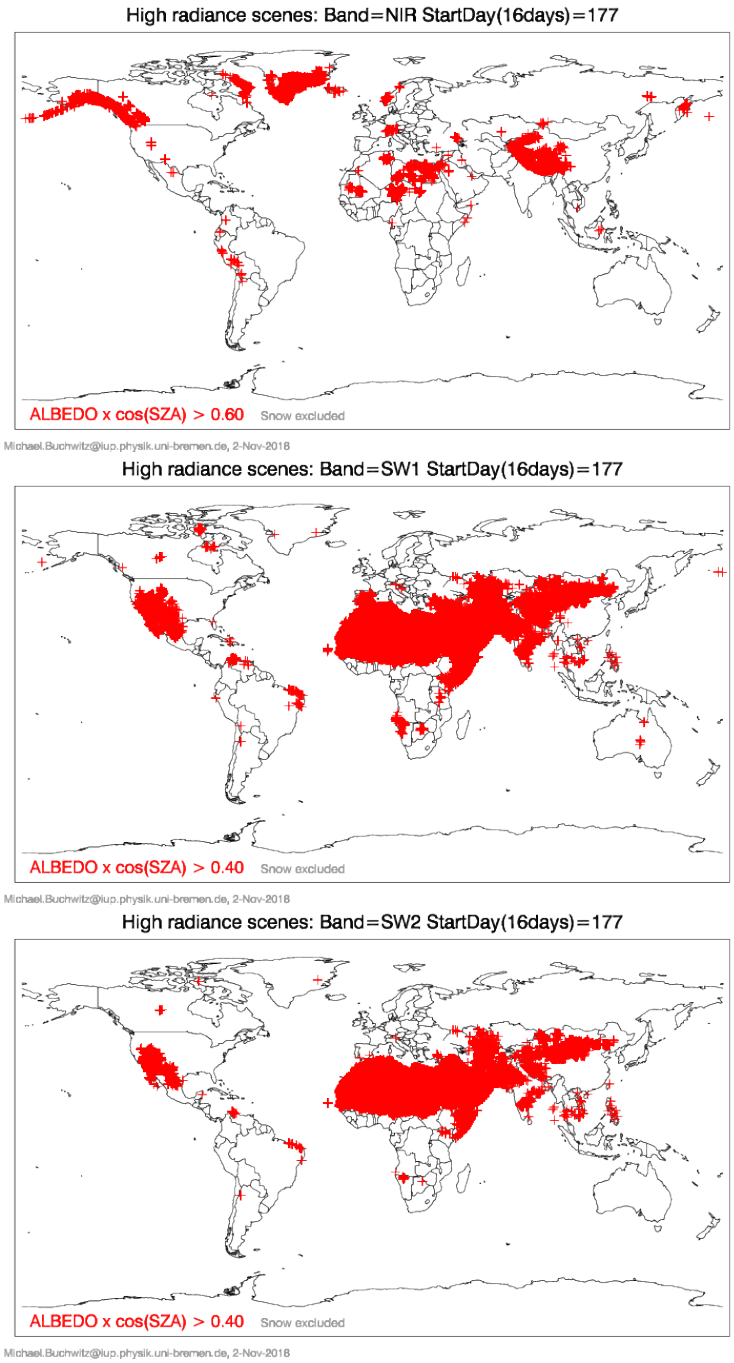

Figure 4: High radiance scenes in NIR band (top), SWIR-1 (middle) and SWIR-2 (bottom) during a 16 day period around summer solstice, where albedo times cos(SZA) > 0.6 (NIR), > 0.4 (SWIR-1) and > 0.4 (SWIR-2), which corresponds to DR-max-0.

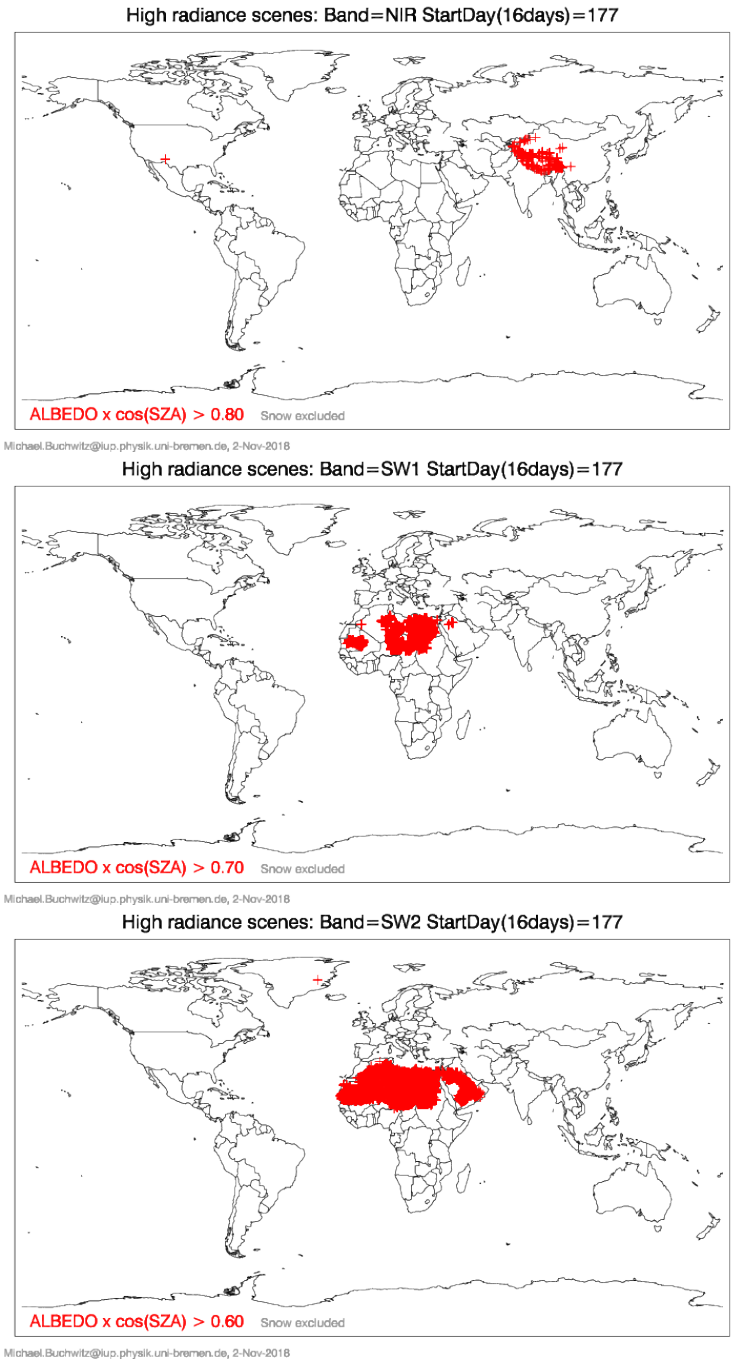

Figure 5: High radiance scenes in NIR band (top), SWIR-1 (middle) and SWIR-2 (bottom) during a 16 day period around summer solstice, where albedo times cos(SZA) > 0.8 (NIR), > 0.7 (SWIR-1) and > 0.6 (SWIR-2), which corresponds to MR-BC-0.

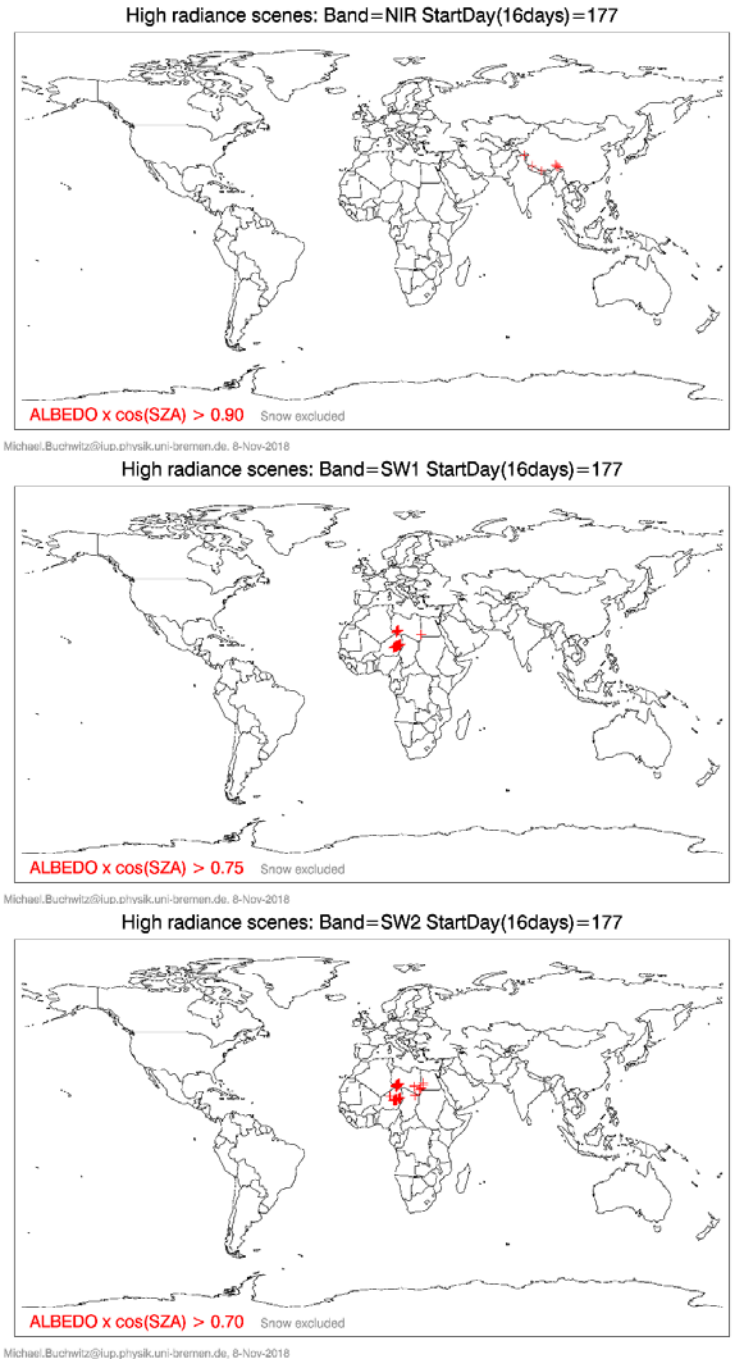

Figure 6: High radiance scenes in NIR band (top), SWIR-1 (middle) and SWIR-2 (bottom) during a 16 day period around summer solstice, where albedo times cos(SZA) > 0.9 (NIR), > 0.75 (SWIR-1) and > 0.7 (SWIR-2).

Analysis using OCO-2 radiances

In order to confirm and/or refine the analysis presented in the previous sub-section, OCO-2 measured radiances have been analysed.

For this purpose one month (June 2018) of L1B files has been analysed (approx. 30 million ground pixels). In order to obtain the continuum radiance in each of the three OCO-2 bands the corresponding continuum radiances, which are reported in the L1B files have been used (rad_continuum_o2, rad_continuum_wco2, rad_continuum_sco2), which correspond to "good samples" and radiances located in between the 98 and 99 percentile (e.g., to avoid possible erroneous radiance spikes). To approximately consider polarizations the OCO-2 radiances have been multiplied with a factor of 2 as OCO-2 measures only one of the two linear polarization directions.

To identify cloud free cases the corresponding Level 2 files have been used ("Lite files") and only those observations are used which are classified "good".

Initial results for nadir mode observations are shown in **Figure 7** for cloud free (a) and all (b) observations. The radiance unit is the OCO-2 radiance unit (photons/s/m^2/µm/sr), which results in radiances a factor of 10^7 larger than the default radiance unit used in this study (photons/s/cm^2/nm/sr). Furthermore, it is important to note that OCO-2 measures only one polarization direction (note that in this figure the original radiances are shown, which correspond only to one polarization direction).

To generate similar figures as those shown in the previous sub-section, the OCO-2 radiances have been converted to the default radiance unit and multiplied with a factor of two to (approximately) correct for polarization (note that this is assumed to be appropriate as only scenes with low SZA (i.e., high radiance) are relevant here).

The results for the NIR band are show in **Figure 8**. As can be seen from panel (a) only very few ground pixels for cloud free scenes have radiances larger than 9.4×10^{13} photons/s/cm^2/nm/sr corresponding to DR-max-0 (as defined in the MRD). Assuming that OCO-2 covers all relevant scenes and does not suffer from major calibration errors this suggest that the DR-max-0 values as listed in the MRD is approximately appropriate for cloud free observations over land. This is in contrast to the findings based on the simplified analysis of MODIS albedos, which suggest that radiances may be 50% larger (albedo ratio 0.9/0.6). Panel (b) shows that DR-max-0 is often exceeded for cloudy pixels and that this can only be avoided if DR-max-0 is enhanced by approx. 80%, i.e., with margin by a factor of 2.

The corresponding results for the SWIR-1 band (using OCO-2's wco2 band) are shown in **Figure 9**. Panel (a) shows that radiances often exceed DR-max-0 for cloud free observations over land and that this can only be avoided if DR-max-0 is enhanced by 70% (Panel (b)). For cloud pixels at least a factor of 2 is required (Panel (c)).

The corresponding results for the SWIR-2 band (using OCO-2's sco2 band) are shown in **Figure 10**. Panel (a) shows that radiances often exceed DR-max-0 for cloud free observations over land and that this can only be avoided if DR-max-0 is enhanced by 40% (Panel (b)). For cloud pixels a factor of 2 is required (Panel (c)).

(a)

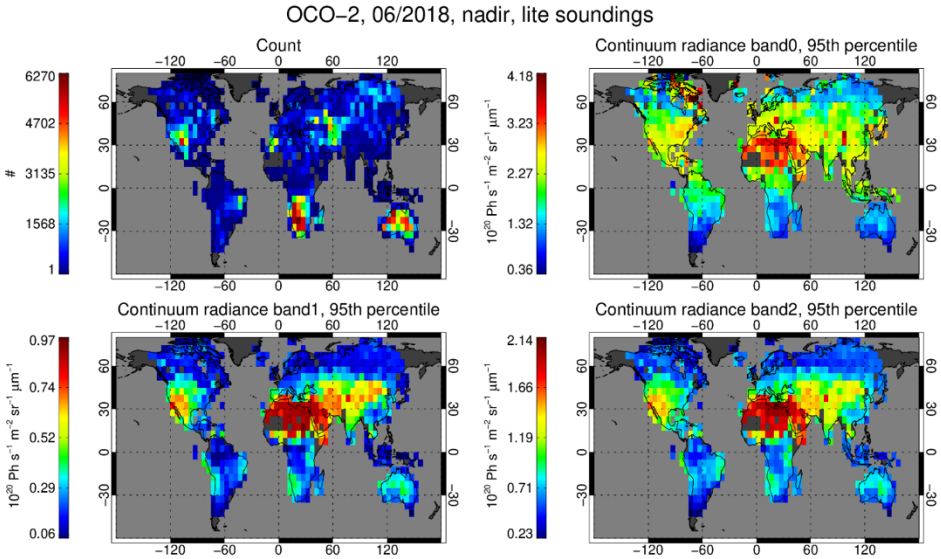

(b)

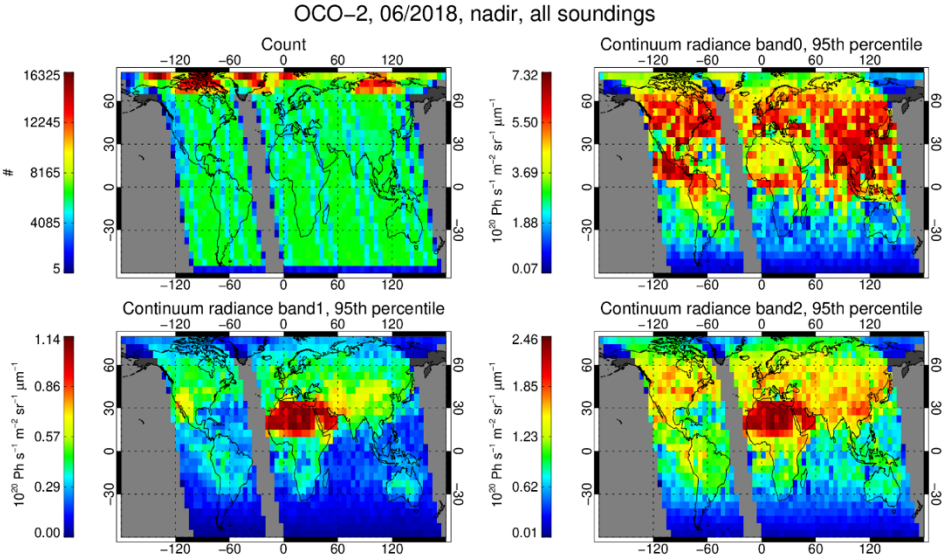

Figure 7: Analysis of OCO-2 radiances measured in June 2018. (a) Top left: Number of quality filtered nadir mode ground pixels (via XCO_2 "Lite files") at 5ºx5º resolution. Top right: maximum radiance (95 percentile) in NIR band (here: band0), bottom right: max. radiance in weak CO_2 band (SW1, here: "band2"), bottom left: max. radiance in strong CO_2 band (SW2, here: "band1"). (b) As (a) but for all nadir soundings (i.e., including clouds).

(a) OCO-2 – NIR – CloudFree Land – Radiance > DR-max-0

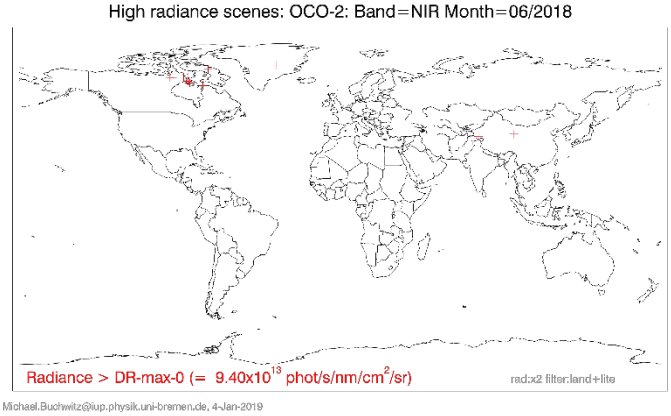

(b) OCO-2 – NIR – All Land – Radiance > DR-max-0

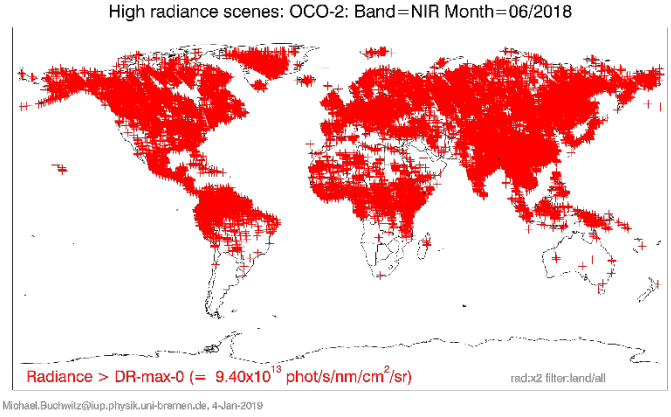

(c) OCO-2 – NIR – All Land – Radiance > DR-max-0 x 1.8

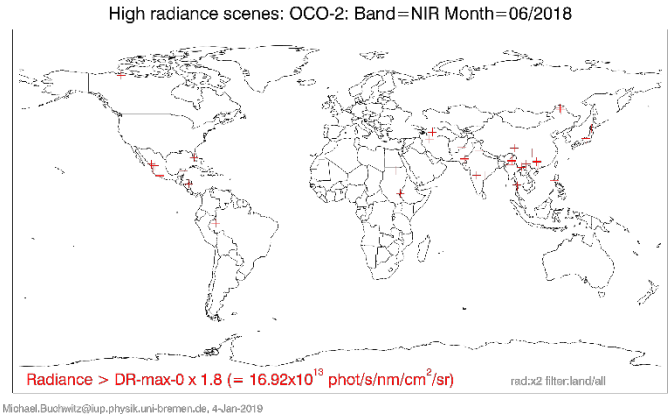

Figure 8: OCO-2 high radiance scenes: NIR band.

(a) OCO-2 – wco2 (SWIR-1) – CloudFree Land – Radiance > DR-max-0

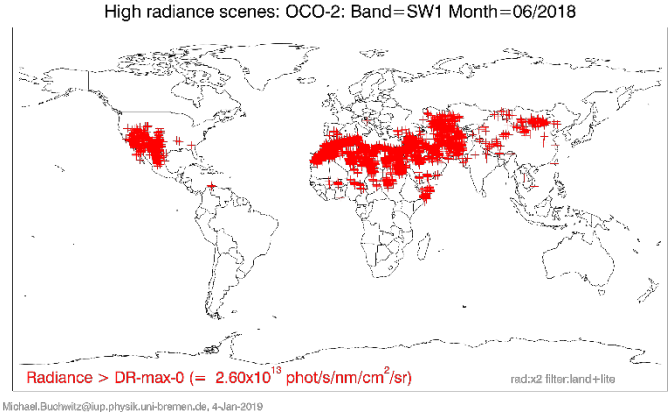

(b) OCO-2 – wco2 (SWIR-1) – CloudFree Land – Radiance > DR-max-0 x 1.7

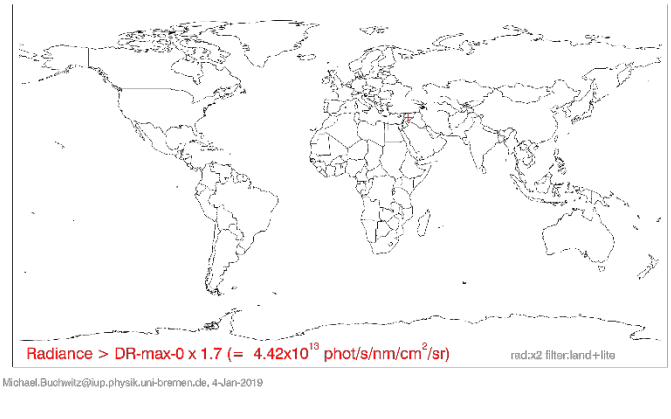

(c) OCO-2 – wco2 (SWIR-1) – All Land – Radiance > DR-max-0 x 2.0

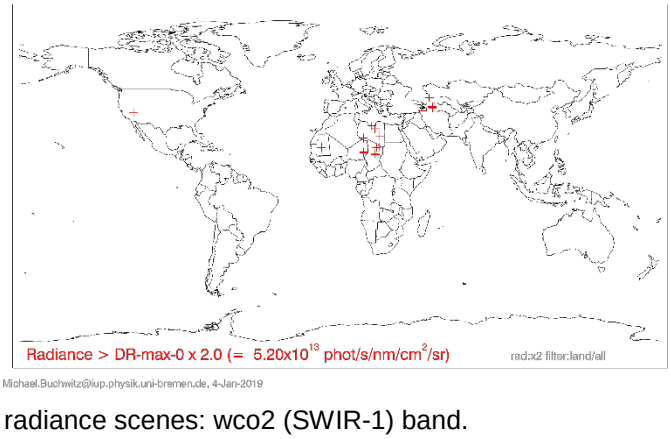

Figure 9: OCO-2 high radiance scenes: wco2 (SWIR-1) band.

(a) OCO-2 – sco2 (SWIR-2) – CloudFree Land – Radiance > DR-max-0

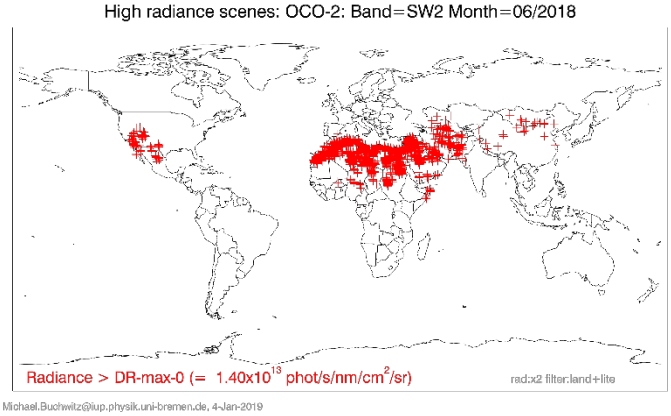

(b) OCO-2 – sco2 (SWIR-2) – CloudFree Land – Radiance > DR-max-0 x 1.4

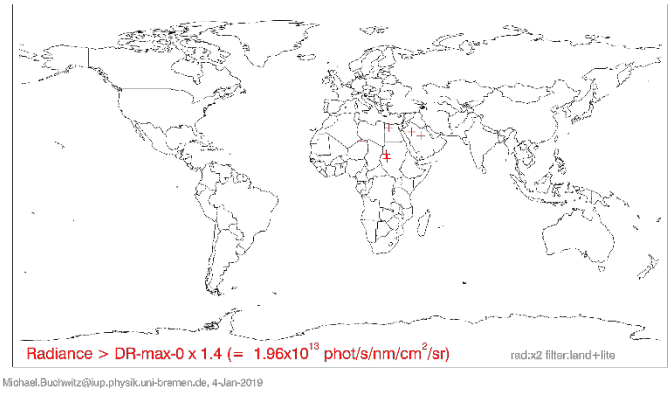

(c) OCO-2 – sco2 (SWIR-2) – All Land – Radiance > DR-max-0 x 2.0

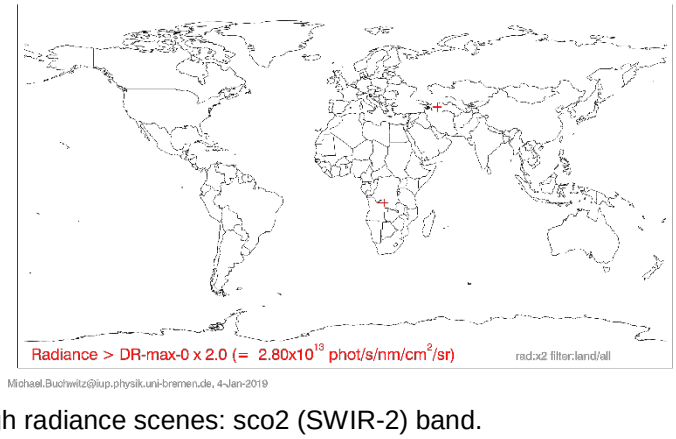

Figure 10: OCO-2 high radiance scenes: sco2 (SWIR-2) band.

Analysis using CO2M L2e orbit files from PMIF study

In this section we present additional analysis results carried out to estimate the spatially and temporally resolved fraction of the observations above a given radiance threshold. The analysis as presented in this sub-section is restricted to cloud-free scenes over land.

Input data for the analysis CO2M Level 2 error (L2e) files, which have been generated in the framework of the ESA PMIF study **/Buchwitz and Reuter, 2018/**. This data set contains for each cloud-free CO2M ground-pixel in a one year time period (among many other parameters) the following parameters, which have been used for this study: latitude, longitude and time of the observation, solar zenith angle (SZA), surface albedo in the NIR band and surface albedo in the SWIR-1 band.

Based on these parameters the continuum radiance (for cloud-free conditions) has been computed using this formula:

$$Rad = Albedo * SolarIrradiance * \cos(SZA) / \pi \qquad \text{(Eq. 1)}$$

In order to consider at least approximately atmospheric scattering (Eq. 1 neglects scattering by aerosols, which may enhance the radiance), 10% has been added to the radiance computed according to Eq. 1.

These radiances have then been used to compute for each months and each 10^o x 10^o grid cell the percentage of the observations exceeding a given radiance threshold. Because the L2e files contain only albedos for the NIR and SWIR-1 band, this approach could not be used for the SWIR-2 band. In order to obtain radiances also for the SWIR-2 band, the SWIR-1 radiances have been multiplied with a scaling factor. The used scaling factor is 0.54. This is the ratio of the SWIR-2/SWIR-1 DR-max-0 values and this conversion factor is also confirmed using independent assessments, e.g., the analysis of OCO-2 data shown in **Table 2.**

Table 2 shows results of assessments carried out by SRON and NASA based on OCO-2 radiances. Both groups determined maximum radiance values in the three OCO-2 bands, which correspond to a good approximation to the three CO2M bands. The listed maximum radiance values correspond to cloud free and cloudy cases, in contrast to the other results presented in this section, which are restricted to cloud free scenes.

The cloud-free scene results obtained using the PMIF L2e files are shown in **Figure 11** - **Figure 15**. As can be concluded from these figures, the following radiance values are not (or only very rarely) exceeded for cloud free observations over land:

- NIR band: 11.3×10^{13} photons/s/nm/cm^2/sr (**Figure 13**)
- SWIR-1 band: 5.1×10^{13} photons/s/nm/cm^2/sr (**Figure 15**)
- SWIR-2 band: 2.8×10^{13} photons/s/nm/cm^2/sr (= 0.54 x 5.1×10^{13})

These values are higher than the current DR-max-0 radiance by these factors:

- NIR: 1.2 (= 11.3 / 9.4)
- SWIR-1: 2.0 (= 5.1 / 2.6)
- SWIR-2: 2.0 (= 2.8 / 1.4)

Band	MRD DR-max-0	Maximum radiance OCO-2 – SRON analysis	Maximum radiance OCO-2 – NASA analysis	Radiance ratio SRON/MRD	Radiance ratio NASA/MRD
	Radiance [10^{13} photons/s/nm/cm^2/sr]			[-]	[-]
O2-A (NIR)	9.4	16	20	1.7	2.1
WeakCO2 (SWIR-1)	2.6	5.6	6	2.2	2.3
StrongCO2 (SWIR-2)	1.4	2.6	2.4	1.9	1.7

Table 2: Maximum radiances as determined from OCO-2 (for cloud-free and cloudy conditions) using two assessment methods, the one from SRON (J. Landgraf) and the one from NASA (kindly provided by D. Crisp).

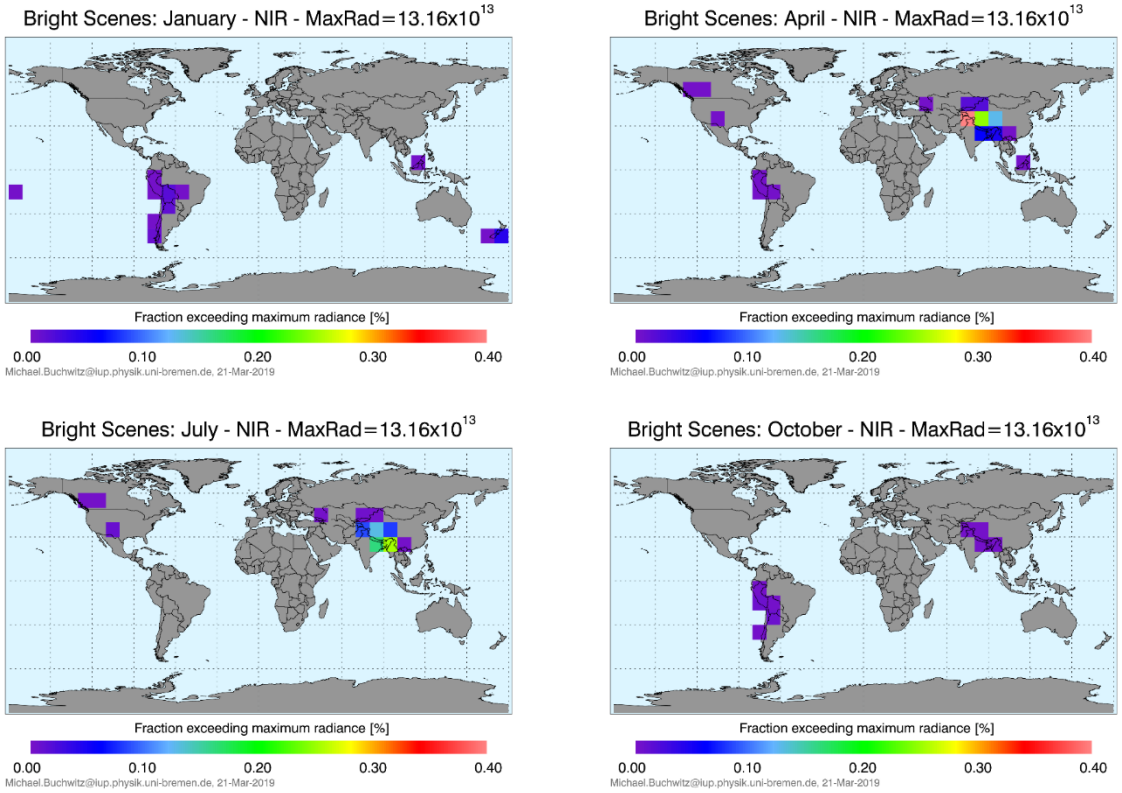

Figure 11: Fraction of observations exceeding a given radiance threshold in the NIR band. The radiance threshold is: 13.2x10^{13} photons/s/nm/cm^2/sr (= 1.4 x 9.4x10^{13} photons/s/nm/cm^2/sr). The four panels show the results for January (top left), April (top right), July (bottom left) and October (bottom right).

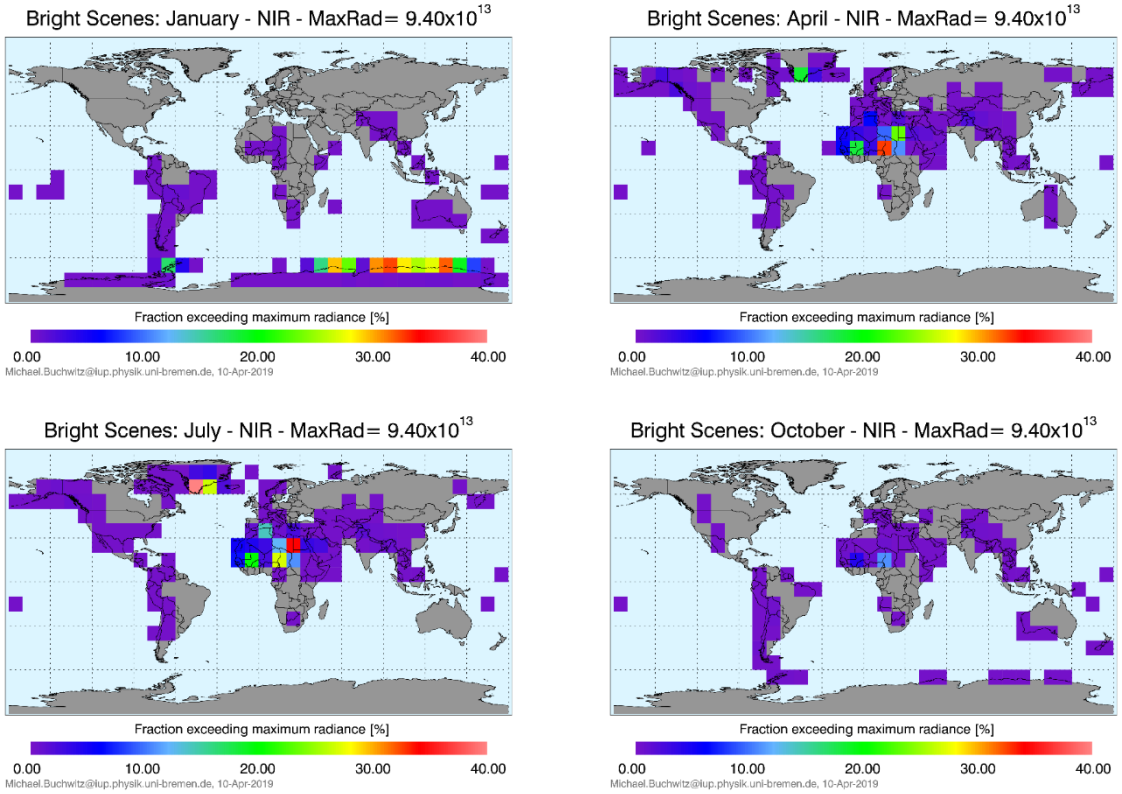

Figure 12: As **Figure 11** but for this radiance threshold in the NIR band: 9.4×10^{13} photons/s/nm/cm^2/sr (= $1.0 \times 9.4 \times 10^{13}$ photons/s/nm/cm^2/sr).

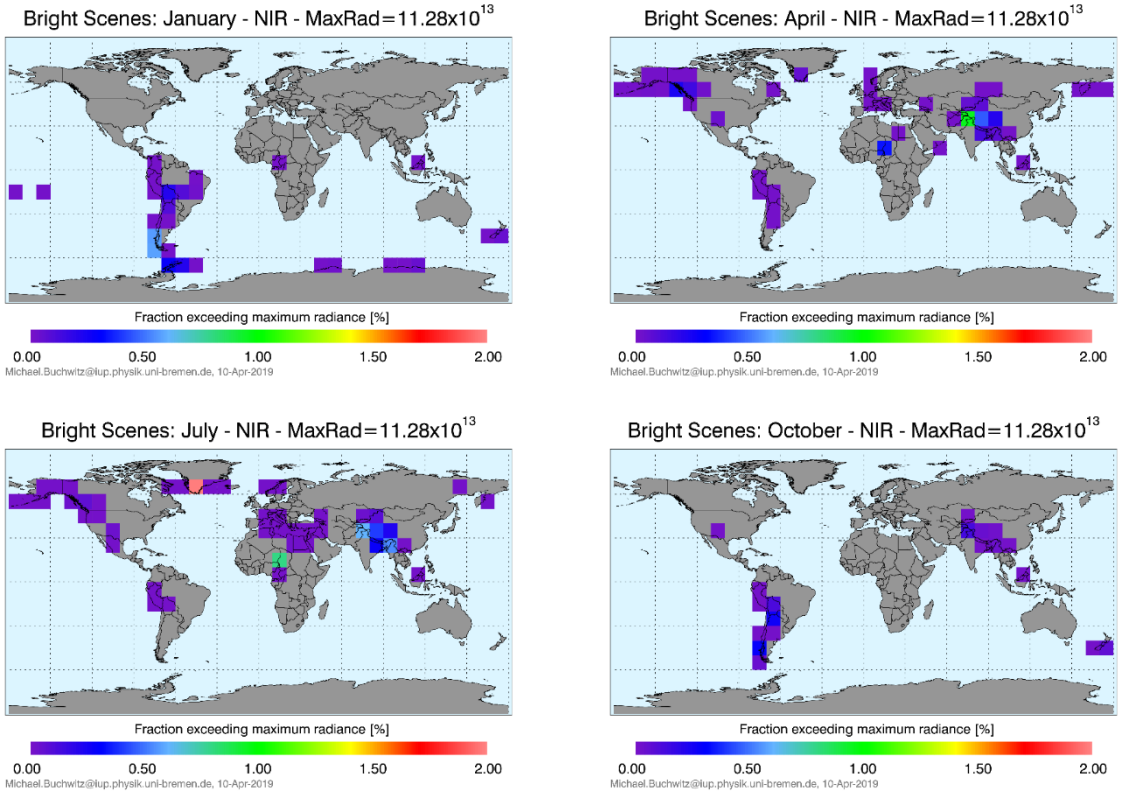

Figure 13: As **Figure 11** but for this radiance threshold in the NIR band: 11.3×10^{13} photons/s/nm/cm^2/sr (= 1.2 x 9.4×10^{13} photons/s/nm/cm^2/sr).

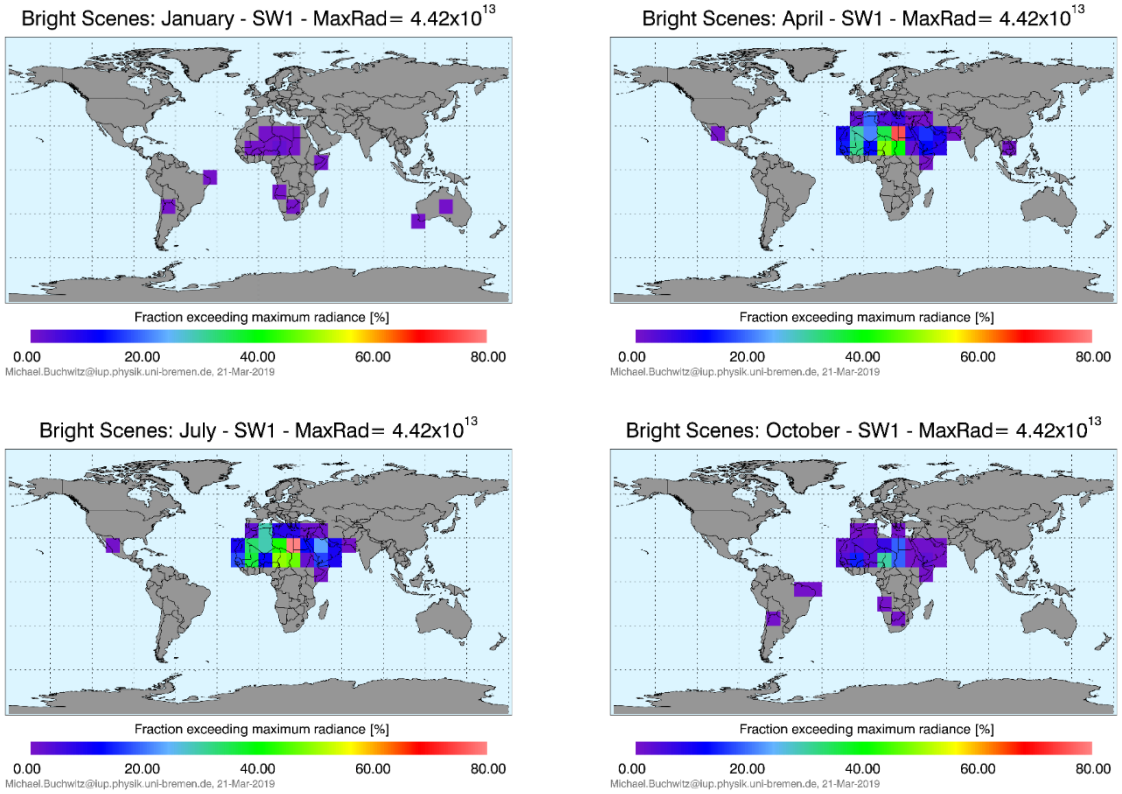

Figure 14: As **Figure 11** but for this radiance threshold in the SWIR-1 band: 4.2×10^{13} photons/s/nm/cm^2/sr (= 1.7 x 2.6×10^{13} photons/s/nm/cm^2/sr).

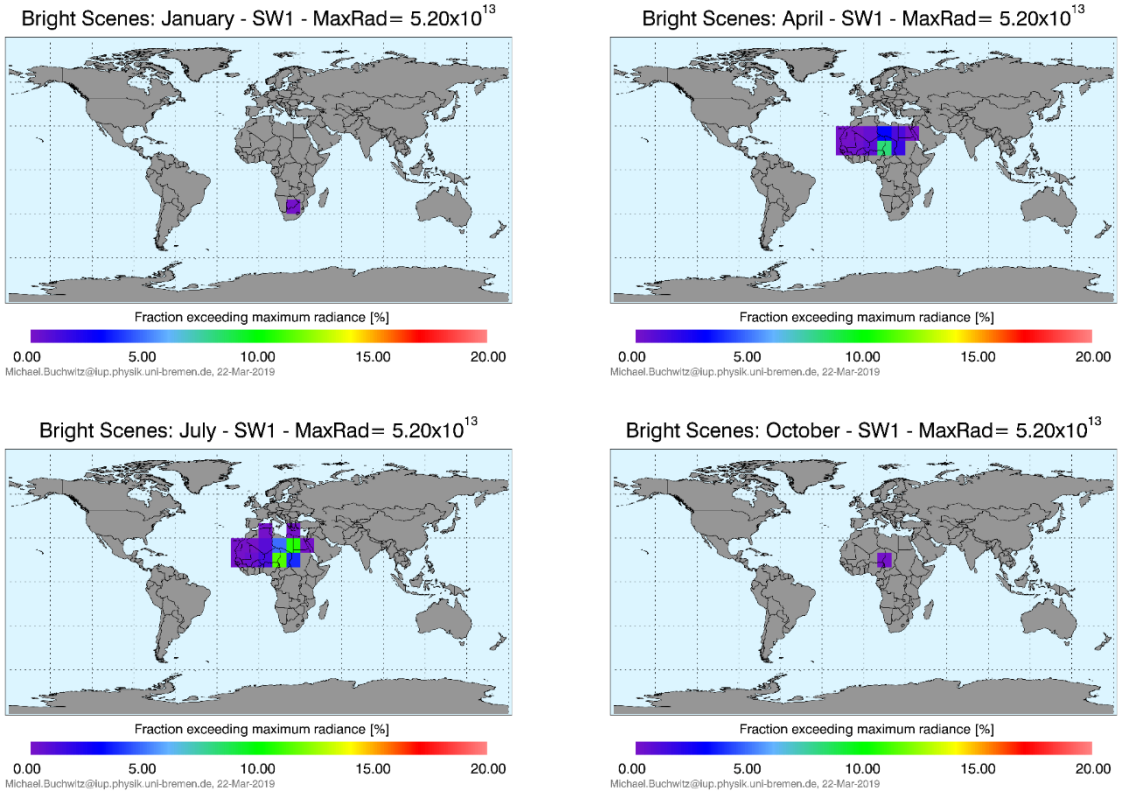

Figure 15: As **Figure 11** but for this radiance threshold in the SWIR-1 band: 5.2×10^{13} photons/s/nm/cm^2/sr (= 2.0 x 2.6×10^{13} photons/s/nm/cm^2/sr).

Maximum radiance for ocean glint around sub-solar latitudes

To estimate maximum radiance values over the ocean, radiance simulations are used, which have been carried out using the radiative transfer model SCIATRAN **/Buchwitz, 2011/**. The results are shown in **Table 3**.

As can be seen, for SZA less than 30°, corresponding to sub-solar latitudes, the maximum radiances are (in brackets to ratio with the MRDv1 DR-max-0 value is shown):

- NIR band: 6.6×10^{13} photons/s/nm/cm^2/sr (0.7 = 6.6/9.4)
- SWIR-1 band: 3.3×10^{13} photons/s/nm/cm^2/sr (1.3 = 3.3/2.6)
- SWIR-2 band: 1.8×10^{13} photons/s/nm/cm^2/sr (1.3 = 1.8/1.4)

These radiances are less than the expected maximum radiances as presented in the previous section for cloud-free observations over land. Appropriate DR-max-0 radiance for land are therefore also acceptable for cloud-free ocean observations around sub-solar latitudes. For SZA significantly larger than 30°, radiances can be larger but it also depends on how close one is to the (geometric) glint spot, wind speed, etc. Note that the assumption of a wind speed of 1 m/s as used for **Table 3** is rather extreme, i.e., reflects conditions close to a worst case scenario.

Michael Buchwitz, 17-Apr-2019

Maximum radiances via SCIATRAN with ocean BRDF

Source: Buchwitz et al., CarbonSat Reference Spectra, Technical Report CSL1L2-I Study, Doc ID: IUP-CS-RS-TN-001, 25 Nov 2011, 2011 (Sect.4 Sun-glint Radiance)

SZA [deg]	Wind speed [m/s]	Band	Max. radiance [1e13 phot/s/nm/cm2/sr]	Reference Radiance DR-max-0 MRDv1 [1e13 phot/s/nm/cm2/sr]	Ratio Max.rad./Ref.rad. [-]
10	1	NIR	6,0	9,4	0,6
10	1	SW1	2,9	2,6	1,1
10	1	SW2	1,6	1,4	1,1
10	2	NIR	4,1	9,4	0,4
10	2	SW1	2,0	2,6	0,8
10	2	SW2	1,1	1,4	0,8
20	1	NIR	6,1	9,4	0,6
20	1	SW1	3,0	2,6	1,2
20	1	SW2	1,7	1,4	1,2
30	1	NIR	6,6	9,4	0,7
30	1	SW1	3,3	2,6	1,3
30	1	SW2	1,8	1,4	1,3
40	1	NIR	8,5	9,4	0,9
40	1	SW1	4,3	2,6	1,7
40	1	SW2	2,4	1,4	1,7
50	1	NIR	13,1	9,4	1,4
50	1	SW1	6,8	2,6	2,6
50	1	SW2	3,8	1,4	2,7

Table 3: SCIATRAN radiances with ocean BRDF (from **/Buchwitz, 2011/**).

4.1.2. Summary and conclusions

Full performance is according to the MRD only guaranteed if the radiances (in the different spectral bands) of the CO2M instrument do not exceed the dynamic range maximum values as specified in the MRD ("DR-max-0"). If the radiances exceed these thresholds than the spectra may saturate or suffer from low quality for other reasons.

The following table summarizes the results presented in this section:

Method	**Cloudfree ?**	**Maximum radiance [10^{13} photons/s/nm/cm^2/sr]**		
		NIR	**SWIR-1**	**SWIR-2**
MRD DR-max-0	n.a. *Note: The MRD assumes cloud free conditions to be identified via a dedicated cloud imager.*	9.4	2.6	1.4
MODIS albedo	Yes	14.7	4.9	2.5
PMIF L2e files	Yes	11.3	5.1	2.8
OCO-2 IUP	Yes	9.4	4.4	2.0
OCO-2 IUP	No, with clouds	16.9	5.2	2.8
OCO-2 SRON	No, with clouds	16	5.6	2.6
OCO-2 NASA	No, with clouds	20	6	2.4
Maximum radiance cloud free		**14.7**	**5.1**	**2.8**
Maximum radiance with clouds		**20**	**6.0**	**2.8**

Table 4: Overview maximum radiances determined to obtain reliable values for DR-max-0 radiance values.

As can be seen, the maximum radiances are significantly higher that the MRD DR-max-0 values. It is therefore recommended to enhance the DR-max-0 values to (at least) the maximum values listed in **Table 4**.

As can be seen, the radiances are higher for cloudy scenes compared to cloud-free scenes (except for the SWIR-2 band). As can also be seen, for SWIR-2 the cloud-free and cloudy radiances are identical, for SWIR-1 the difference is quite small (+18%) and also for the NIR the difference is only marginal (+36%).

The lower the DR-max-0 values (as specified in the MRD), the better the optimization for scenes with low radiance values (i.e., low albedos, large SZA) and the lower the resulting XCO_2 errors for these scenes. This is because a narrower dynamic range is in general highly beneficial as a large dynamic range is much more difficult to deal with. This suggests to obtain the required DR-max-0 values from cloud-free scenes, where the radiance is typically lower than for cloudy scenes. For CO2M this is the current baseline.

According to ESA, CO2M will be designed for cloud-free conditions. This has important advantages (e.g., better performance for the highly relevant more typical scenes with lower radiance levels) but also disadvantages (e.g., possible saturation in case of high radiance levels under cloudy conditions).

It is currently assumed that only cloud-free observations are relevant to meet the CO2M mission goals and for current retrieval algorithms this seems to be true. However, it cannot be entirely ruled out at present that future algorithm will also be able to extract very useful information considering also the cloudy observations in addition to the cloud-free ones. Being able to only measure in case of no clouds implies to “throw away” many potentially useful observations.

The question is: Is it justified to take this risk? Taking into account the relatively small difference between the radiances without and with clouds as shown in **Table 4** it is not clear how much worse the performance for (the important) low radiance scenes will be if the dynamic range would be large enough to perform useful measurements also for cloudy scenes. It is at present not clear if it is really mandatory to limit the observations to cloud free scenes (as otherwise the performance for the highly relevant and frequent low radiance scenes would be “too bad”).

To avoid saturation for conditions where radiances may exceed the DR-max-0 values it has been recommended to modify the MRDv1.0 such that useful spectra are generated even for these conditions. For MRDv2.0 this recommendation has been considered.

4.2. Dynamic range minimum

According to MRDv1.0 the dynamic range minimum DR-min-70 corresponds to a scenario with SZA 70^o and albedos 0.1 / 0.05 / 0.05 (in the NIR, SWIR-1 and SWIR-2 bands). The corresponding radiances are:

- NIR: $7x10^{11}$ photons/s/nm/cm^2/sr
- SW1: $9x10^{11}$ photons/s/nm/cm^2/sr
- SW2: $1.5x10^{11}$ photons/s/nm/cm^2/sr

According to ESA these (low) DR-min-70 radiances are very challenging for many (other) requirements as the dynamic range defines the full performance range of the instrument.

In the following some assessments related to DR-min-70 are presented.

4.2.1. University of Bremen analysis

Table 5 lists minimum radiances for several scenarios. The HL (high latitude) scenarios correspond to SZA 70^o and the TR (tropical) scenarios to SZA 0^o. The D (dark) scenarios correspond to albedos 0.1 / 0.05 / 0.05 (as DR-min-70) and the B (bright) scenarios to albedo 0.6 / 0.4 /0.4.

Discussion:

- NIR: At high latitudes the minimum radiances are even less than DR-min-70. A relaxation is therefore not recommended.
- SWIR-1: Only the high latitude dark scenario has a radiance less than DR-min-70. As SWIR-1 does not contain very strong absorptions (in contrast to the other two bands) a relaxation is also not recommended.
- SWIR-2: Here the situation is similar as for the NIR band. A relaxation is therefore not recommended.

Scenario	Band		
	NIR	SWIR-1	SWIR-2
HLD	4	6	0.03
REF70	5	24	0.04
HLB	6	47	0.09
MLD	7	13	0.1
REF50	11	51	0.2
MLB	19	100	0.7
TRD	12	21	0.3
REF00	22	85	0.6
TRB	46	170	2.3
MRD: DR-min-70	7	9	1.5
Comment			Strong CO_2 absorption at 2003 nm

Table 5: Minimum radiances in 10^{11} photons/s/nm/cm^2/sr for several scenarios. Radiances less than DR-min-70 are shown in red (note that these very low radiance levels only occur at certain wavelengths and that excluding these wavelength from the spectral fitting windows may not results in a significant performance degradation).

4.2.2. Summary and conclusions

It has been investigated if radiance DR-min-70 can be relaxed but the results suggest that DR-min-70 should not be relaxed. It is even recommended to specify lower values, at least in the NIR and SWIR-2 bands.

4.3. Signal-to-noise ratio (SNR)

An important requirement is the SNR requirement (MRDv1.0, S7MR-OBS-150).

In the following simulated retrieval results are shown using different retrieval methods but using instrument simulations consistent with MRDv1.0. The most relevant instrument parameters are shown in **Table 6**.

Band	Spectral range [nm]	Spectral resolution (FMHM) [nm]	Spectral sampling ratio [1/FWHM]	Comment
NIR	747- 773	0.12	3	
SWIR-1	1590 – 1675	0.3	3	
SWIR-2 (B&C)	1990 – 2095	0.35	3	Note: New baseline resolution

Table 6: Instrument parameters.

In this section results are reported for scenarios VEG50, REF50 and TRB (see **Table 36**).

According to the Error Budget (EB), which is shown in TN-3000 **/CO2M-REB TN-3000, 2019/**, the maximum errors for SNR-related random errors are:

- XCO_2: 0.5 ppm
- XCH_4: 8 ppb

As the main parameter for CO2M is XCO_2 and because this parameter drives the SNR specification, the following discussion focusses on XCO_2.

4.3.1. University of Bremen assessments: SNR-related XCO_2 error

The performance assessments have been carried out using FOCAL.

The main results are shown in **Figure 16 - Figure 19**.

For all three bands, i.e., NIR, SWIR-1 and SWIR-2, the following SNR formula is used (see also **/Landgraf et al., 2017a/**):

$$SNR\ (L) = \frac{L \cdot A}{\sqrt{L \cdot A + B^2}} \qquad \text{Eq. (1)}$$

Here *L* is the radiance in photons/s/nm/cm^2/sr and *A* and *B* are instrument parameters.

In this document the dimension of *A* is 1/(photons/s/nm/cm^2/sr) (i.e., inverse radiance units) and *B* is dimensionless. Roughly speaking, *A* corresponds to instrument throughput and *B* corresponds to (radiance independent) detector noise.

The SNR – esp. the SNR in the SWIR bands – determines the XCO_2 random error (which is also influenced by other parameters such as a priori XCO_2 uncertainty). The mapping from the *A*-*B* pairs to XCO_2 errors is however not unambiguous as, for example, a larger *B* value can be compensated by a larger *A* value. How we deal with this is described below.

High enough SNR performance in the NIR band is important to obtain "enough" information on scattering parameters, SIF, etc., i.e., the impact on XCO_2 errors is more indirectly compared to the SWIR bands.

To have a realistic starting point, we use the *A*-*B* values (provided by ESA) shown in **Table 7**. Note that these specific *A*-*B* values are listed here primarily for illustration. These are not required values. As shown below, many different *A*-*B* pairs (i.e., combinations of *A* and *B* values) may lead to an equivalent performance as a "worse A" can be compensated by a "better B".

Band	SNR parameter A [10^{-7}/(phot./s/nm/cm^2/sr)]	SNR parameter B [-]	Comments
NIR	0.2	140	
SWIR-1	1.32	450	
SWIR-2	1.54	450	

Table 7: Initial SNR-formula (Eq. 1) with default *A*-*B* values.

Note that for the SWIR bands parameter *A* is proportional to spectral resolution:

$$A_{SWIR-1} = A_{SWIR-2} \cdot \frac{0.3}{0.35} \qquad \text{Eq. (2)}$$

XCO_2 errors have been computed for several SWIR *A*-*B* pairs (using the NIR *A*-*B* values listed in **Table 7** and also considering Eq. 2) and from these *A*-*B* pairs those have been "selected" which correspond to a XCO_2 SNR-related error of 0.5 ppm. These "equivalent" *A*-*B* pairs have been obtained for the two scenarios VEG50 (**Figure 16** and **Figure 17**) and REF50 (**Figure 18** and **Figure 19**).

As can be seen from **Figure 18** the 0.5 ppm requirement is met using the *A*-*B* values listed in **Table 7**.

As can be seen from **Figure 16** the 0.5 ppm requirement cannot be met using the *A*-*B* values listed in **Table 7**. Here a factor of 2 larger *A* values are needed for the same values of B, corresponding to an instrument with a factor of 2 higher throughput (assuming the same detector). Meeting the 0.5 ppm requirement for the VEG50 scenario is more demanding compared to the REF50 scenario (because of the different albedos, which are approx. a factor of 2 higher for REF50).

As a minimum, 0.5 ppm needs to be achieved for REF50 and it is proposed to use this scenario to define the SNR requirement (VEG50 may be used to formulate a goal requirement).

<u>Baseline recommendation to formulate the SNR requirement:</u>

The SNR in each band shall be equal or larger than the SNR given by Eq. 1 using the *A*-*B* values listed in **Table 7**.

<u>Alternative 1 to formulate the SNR requirement:</u>

Because different SWIR *A*-*B* pairs are essentially equivalent (a larger *B* can be compensated with a larger *A* and vice versa) one may formulate the SNR requirement as follows:

NIR: See baseline recommendation.

SWIR-1 & SWIR-2:
The SNR for a given radiance *L* (in photons/s/nm/cm^2/sr) shall be equal or larger than SNR = SNR(*L*, *A*, *B*) (Eq. 1) with – for a given *B* – *A* larger or equal than

- *Amin* = 0.54 + 0.00177 x *B* [10^{-7} / (photons/s/nm/cm^2/sr)] for SWIR-1
- *Amin* = 0.63 + 0.00206 x *B* [10^{-7} / (photons/s/nm/cm^2/sr)] for SWIR-2

Alternative 2 to formulate the SNR requirement:

One may also specify the SNR at specific values of the radiance, e.g., *Lmin* and *Lref* (but note that this would result in an "incomplete requirement" as SNR is not specified for every relevant *L*). This would result in the following requirement:

Band	SNRmin @ Lmin	SNRref @ Lref	Lmax	Comments
NIR	75 @ 0.7	260 @ 4.2	93	
SWIR-1	240 @ 0.9	420 @ 2.1	26	
SWIR-2	100 @ 0.15	320 @ 1.15	14	

Table 8: SNR requirement in terms of *SNR@L*, i.e., in terms of minimum SNR for a given radiance. Here the unit of the radiances *L* is 10^{12} photons/s/nm/cm^2/sr.

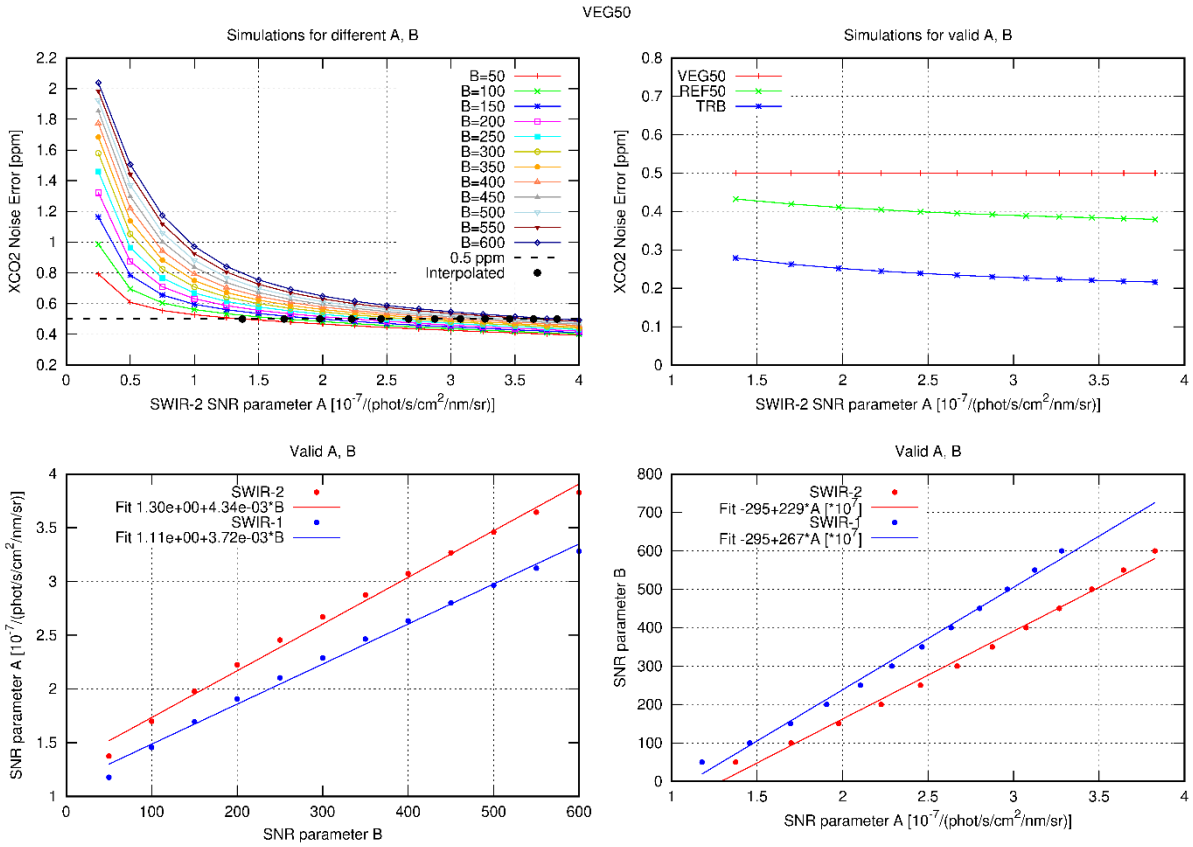

Figure 16: Top left: SNR-related XCO_2 random error as a function of SWIR-2 SNR parameter A for scenario VEG50. Bottom left: SNR parameter A (for SWIR-1 (blue) and SWIR-2 (red)) as a function of SNR parameter B for those A-B pairs, for which the SNR-related XCO_2 error is 0.5 ppm. The dots correspond to the (thick black) dots shown in the top left panel. The solid lines correspond to a linear fit (see annotation). Bottom right: As bottom left but for B versus A. Top right: SNR-related XCO_2 errors for the selected A-B pairs for the scenarios VEG50 (red), REF50 (green) and TRB (blue).

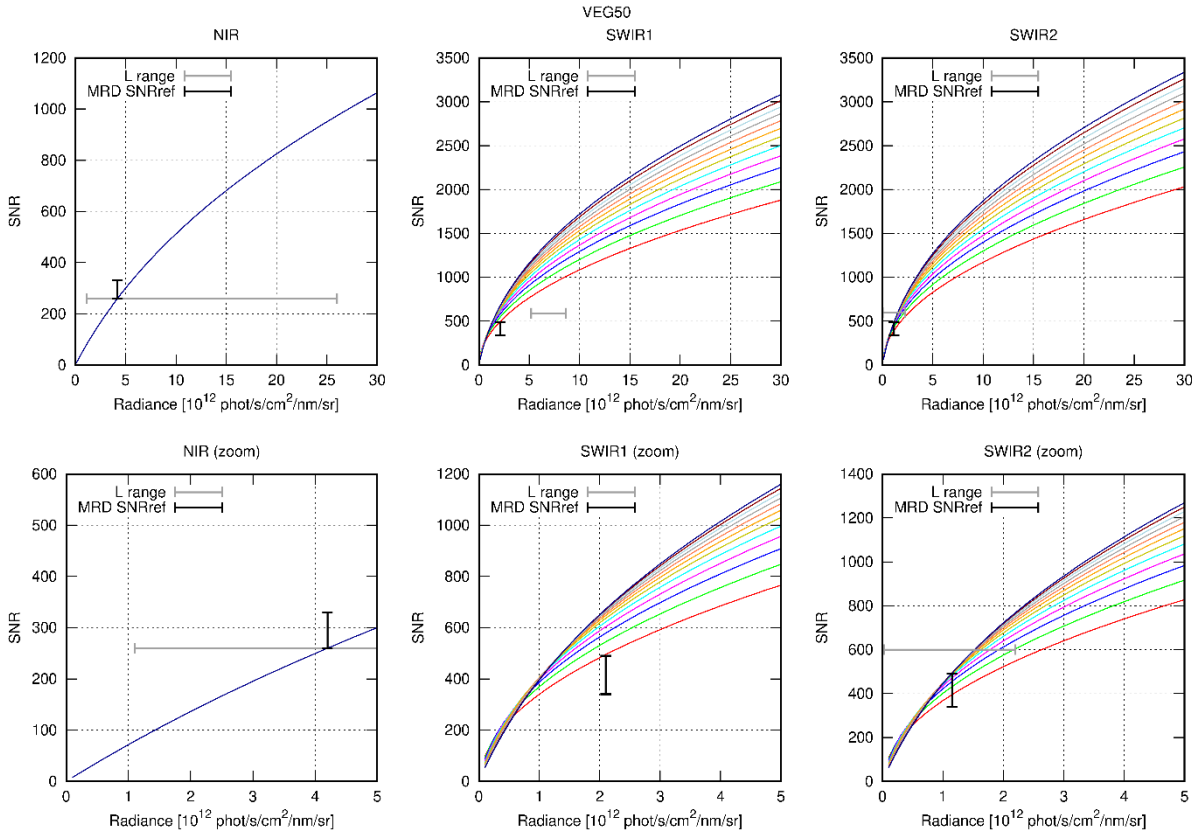

Figure 17: Top: SNR as a function of the radiance in the NIR (left), SWIR-1 (middle) and SWIR-2 (right) for those SNR-formula A-B pairs which result in a SNR-related XCO_2 error of 0.5 ppm for VEG50. Bottom: As top but zoomed.

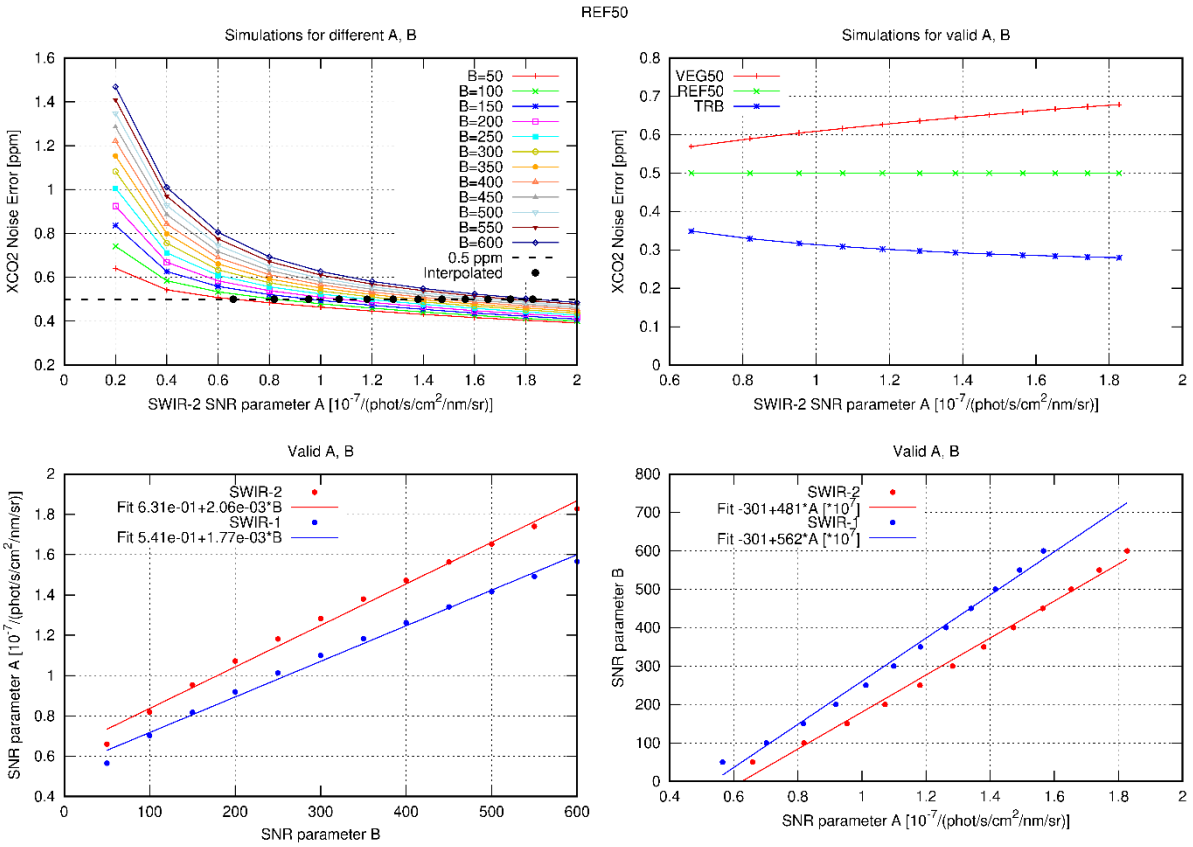

Figure 18: Top left: SNR-related XCO_2 random error as a function of SWIR-2 SNR parameter A for scenario REF50. Bottom left: SNR parameter A (for SWIR-1 (blue) and SWIR-2 (red)) as a function of SNR parameter B for those A-B pairs, for which the SNR-related XCO_2 error is 0.5 ppm. The dots correspond to the (thick black) dots shown in the top left panel. The solid lines correspond to a linear fit (see annotation). Bottom right: As bottom left but for B versus A. Top right: SNR-related XCO_2 errors for the selected A-B pairs for the scenarios VEG50 (red), REF50 (green) and TRB (blue).

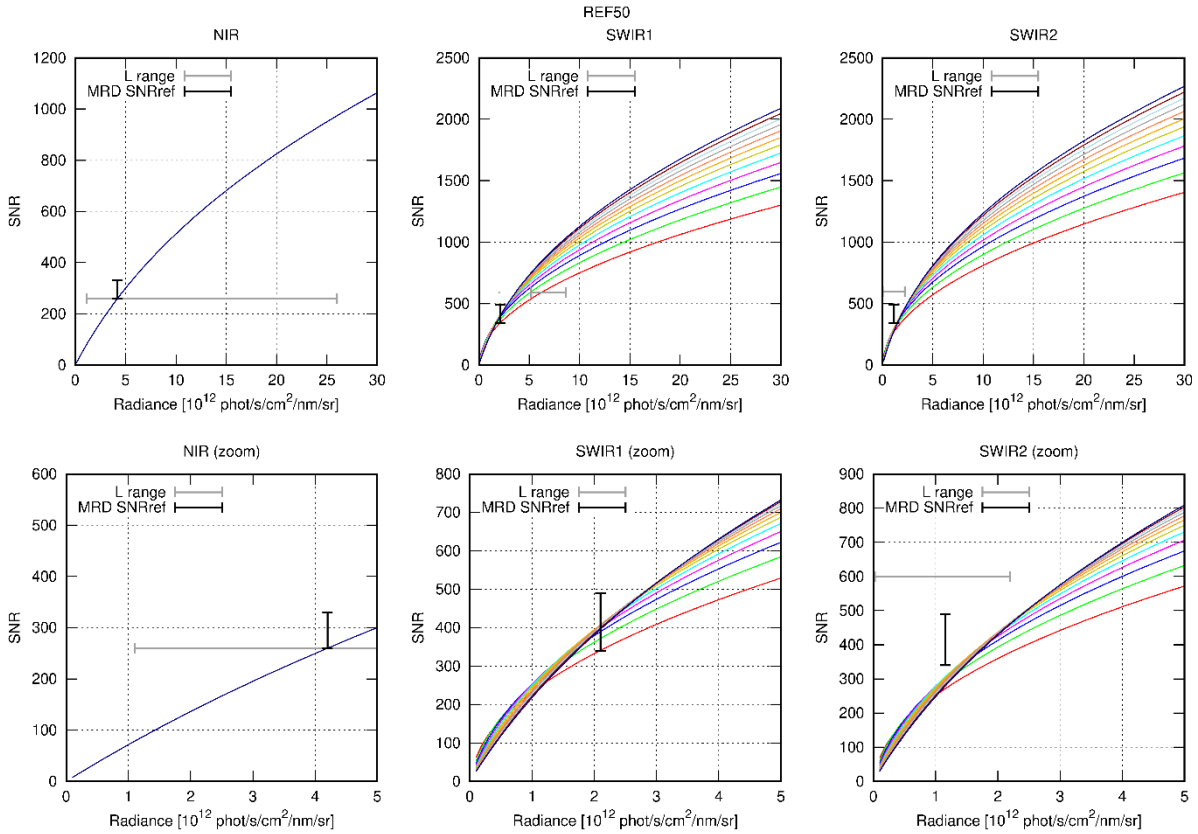

Figure 19: Top: SNR as a function of the radiance in the NIR (left), SWIR-1 (middle) and SWIR-2 (right) for those SNR-formula A-B pairs which result in a SNR-related XCO_2 error of 0.5 ppm for REF50. Bottom: As top but zoomed.

4.3.2. Comparison with SRON and Univ. Leicester results

For instrument CO2M_002 (see **Table 6**, **Table 7** and **Table 37**) XCO_2 random errors have also been computed using the algorithms of SRON and Univ. Leicester. The results are shown in **Table 9**.

The table below shows the total random error and its two components "SNR-related random error" and "Smoothing & interference" (S&I) error. The total error is the root-sum-square value of its two components. The SNR-related error is primarily determined by instrument noise (but also depends on the retrieval algorithm and its parameter settings) whereas the S&I error depends primarily on the assumptions on the assumed *a priori* variability of the state vector elements (vertical profiles of CO_2, H_2O, temperature, etc.). Depending on the scene and how well averaging kernels and other information is used / can be to obtain emissions from XCO_2 images, the effective real S&I errors can be much smaller. Therefore and for other reasons the two components are listed separately in **Table 9**. The most important reason to report the SNR-related random error separately is that this error is closely related to the instrument (SNR, spectra coverage and sampling, etc.).

As can be seen, the 0.5 ppm requirement for SNR-related XCO_2 random errors is met by all three algorithms for scenario REF50 (but not for VEG50).

Institute (Algorithm)	Scenario	Total XCO_2 random error [ppm]	SNR-related XCO_2 error [ppm]	Smoothing and interference [ppm]
IUP-UB (FOCAL)	VEG50 REF50	0.86 0.64	0.66 0.50	0.54 0.39
SRON (RemoTeC)	VEG50 REF50	(*) (*)	0.51 0.33	(*) (*)
UoL (OCFP)	VEG50 REF50	0.68 0.40	0.60 0.36	0.32 0.17

Table 9: Comparison of XCO_2 random errors as computed using the 3 XCO_2 retrieval algorithms used in this study. (*) Not computed as not a standard output.

SNR-related errors have also been computed using the provided gain vectors, see **Table 10**. The corresponding continuum radiance and SNR values are shown in **Table 11**.

Scenario ID	SNR-related XCO_2 error [ppm]			SNR-related XCH_4 error [ppb]		
	IUP-UB (FOCAL)	SRON (RemoTeC)	UoL (OCFP)	IUP-UB (FOCAL)	SRON (RemoTeC)	UoL (OCFP)
REF00	0.36	-	0.30	3.71	-	-
TRD	0.41	0.38	0.43	5.36	4.56	-
TRB	0.25	0.19	0.19	2.92	2.24	-
VEG50	0.48	0.33	0.51	5.45	3.76	-
REF50	0.40	0.25	0.34	4.59	2.95	-
MLD	0.42	0.36	0.50	5.96	5.14	-
MLB	0.28	0.20	0.20	3.62	2.54	-
REF70	0.44	-	0.38	5.79	-	-
HLD	0.47	0.49	0.54	6.39	5.87	-
HLB	0.33	0.21	0.26	4.58	2.80	-

Table 10: SNR-related XCO_2 and XCH_4 errors computed via linear error analysis using the gain vectors as computed for several scenarios ("-" means no gain vector available). Note that the values listed here may differ somewhat from the values listed in **Table 9** because the values in that table are based on full iterative retrievals and not on linear error analysis.

Scenario ID	Continuum radiance [10^{13} phot/s/nm/cm^2/sr]			Continuum SNR [-]		
	NIR	SWIR-1	SWIR-2	NIR	SWIR-1	SWIR-2
REF00	4.0	1.3	0.4	897	1332	735
TRD	1.7	0.3	0.2	576	667	520
TRB	9.6	2.7	1.4	1384	1884	1470
VEG50	2.1	0.4	0.1	649	756	412
REF50	2.6	0.9	0.2	722	1068	582
MLD	1.1	0.2	0.1	467	535	412
MLB	6.2	1.7	0.9	1111	1510	1165
REF70	1.4	0.5	0.1	533	779	413
HLD	0.6	0.1	0.1	351	391	292
HLB	3.3	0.9	0.4	812	1101	825

Table 11: Continuum radiances and SNR values for the gain vector scenarios.

4.3.3. Sensitivity of SNR-related XCO_2 error w.r.t. SNR

For instrument CO2M_002 (defined by **Table 6** and **Table 7**) the sensitivity of the SNR-related XCO_2 random error on SNR has been computed and the results are shown in **Figure 20**. As expected, the XCO_2 error depends almost linearly on SNR (see bottom panel), i.e., an enhancement of the SNR by, for example, 30%, improves the XCO_2 precision by 30%.

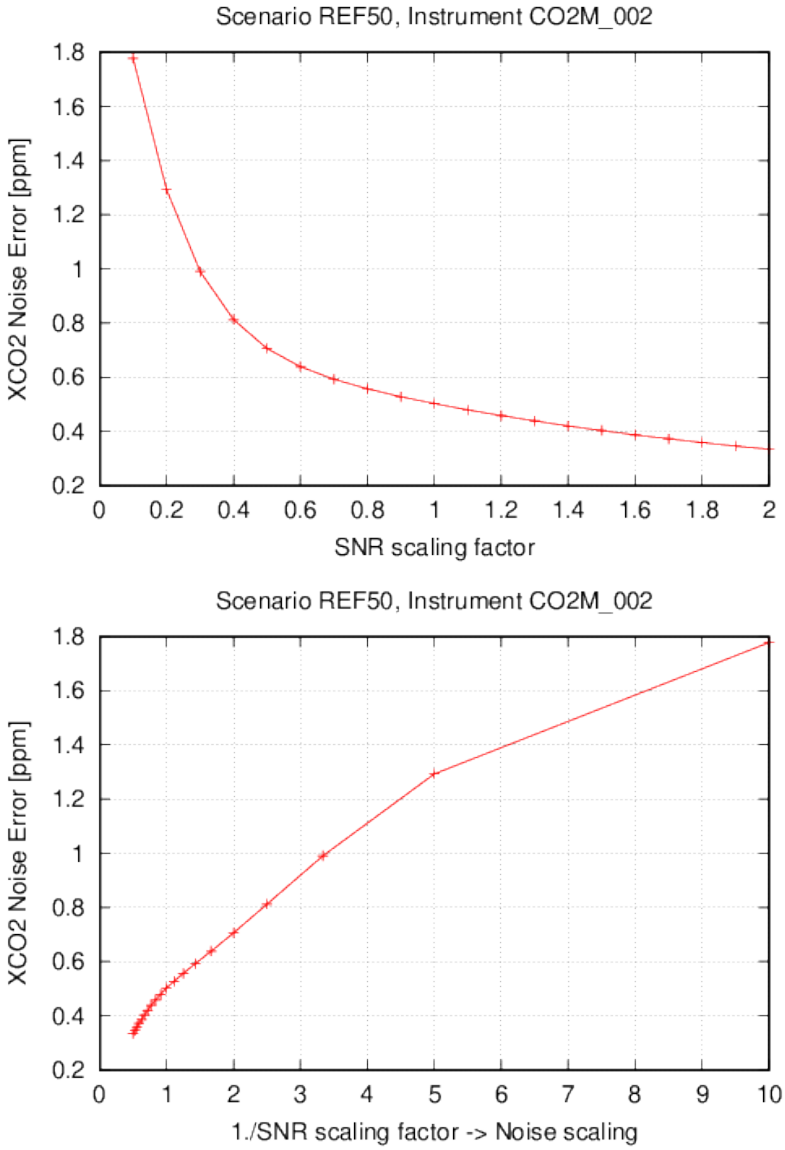

Figure 20: SNR-related XCO_2 error versus SNR (top) and versus 1/SNR (bottom). A SNR scaling factor of 1 corresponds to SNR(L) computed with the default *A-B* parameters (**Table 7**). A SNR scaling factor of X corresponds to a scaling of SNR(L) with a factor of X. Scenario: REF50. Instrument: CO2M_002. Algorithm: FOCAL.

4.3.4. Summary and conclusions

A very important requirement is the Signal-to-Noise-Ratio (SNR) requirement as it essentially determines (along with some other error sources resulting in "pseudo-noise") the XCO_2 and XCH_4 random error ("precision"). According to the Error Budget (EB) 0.5 ppm (1-sigma) is allocated for the XCO_2 random error due to SNR-related errors. Recommendations have been given to improve the SNR requirement based on retrieval simulations using the FOCAL retrieval method. Specifically, a formula is given which permits to compute the SNR for any radiance given two parameters *A* and *B* and values for *A* and *B* are specified (for each spectral band) such that an SNR-related XCO_2 random error of 0.5 ppm can be achieved for a relevant typical scenario ("REF50", SZA=50^o, and surface albedos corresponding to the "Berlin reference scene", 0.25 in the NIR, 0.2 in SWIR-1 and 0.1 in SWIR-2). For the VEG50 scenario (vegetation albedo assumed having a factor of 2 lower albedos in the SWIR) the SNR-related XCO_2 random error would be in the range 0.57 – 0.68 ppm, depending on the selected *A*-*B* pair. A single *A*-*B* pair (per band) has been defined and used to improve the SNR requirement and it is shown that the 0.5 ppm requirement for SNR-related XCO_2 random errors is met for this pair by all 3 retrieval algorithms (i.e., the ones from Univ. Bremen, Univ. Leicester and SRON) for REF50 (but not for VEG50).

4.4. Zero Level Offset (ZLO)

4.4.1. University of Bremen error analysis results for ZLO

Zero Level Offset (ZLO) related XCO_2 and XCH_4 errors have been computed with FOCAL.

The ZLO values used for the error analysis are those from MRDv1.0 requirement S7MR-OBS-230 (note that MRDv2.0 specifies different values but the linear error analysis results presented here permit to scale errors to different ZLO values):

- NIR: 8.4×10^9 phot/s/nm/cm^2/sr
- SWIR-1: 8.6×10^9 phot/s/nm/cm^2/sr
- SWIR.2: 2.0×10^9 phot/s/nm/cm^2/sr

Results for several scenarios (see **Table 36**) are shown in the tables below for XCO_2 and XCH_4 for an instrument configuration consistent with MRDv1.0 (see **Table 6** and instrument CO2M_002 in **Table 37**). Errors exceeding the Total Uncertainty values as listed in the Error Budget (EB) **/CO2M-REB TN-3000, 2019/** (i.e., 0.2 ppm for XCO_2 and 2 ppb for XCH_4) are shown in red.

Table 12 (for XCO_2) and **Table 13** (for XCH_4) show the results computed via the full iterative FOCAL method. Note that here ZLO is not a state vector element, i.e., the baseline configuration of FOCAL has been used. These results indicated that the ZLO error is about a factor of 2 too large in the SWIR-1 and SWIR-2 bands.

If ZLO would be added as a state vector element than the systematic error is expected to be (much) smaller but the random error should be somewhat larger. **Table 14** (for XCO_2) and **Table 15** (for XCH_4) show that this is in fact the case. As can be seen, the systematic errors are zero and the random errors are a bit larger. This suggests that ZLO is not necessarily an important issue. However, one has to be very careful because (i) here the very optimistic assumption has been used that ZLO is (exactly) constant in each band and (ii) in reality one has to deal with a larger number of errors simultaneously.

Nevertheless, the results presented here seem to indicate that the ZLO values as specified in the MRDv1.0 are acceptable. For this study we keep the FOCAL baseline configuration (except if noted otherwise), which is not using ZLO as state vector element, as this is also the configuration we are using for real satellite (OCO-2) data (see **/Reuter et al., 2017b/,** where ZLO related errors are minimized using a correction method).

To further investigate this important aspect, we have carried out additional investigations, which are presented in the following sub-sections.

XCO_2 errors in ppm Algorithm: FOCAL (ZLO in state vector: no) Error source: ZLO *(in brackets: SNR-related random error)*						
Scenario		**Bands**				**Comment**
	No ZLO error	**All 3 bands**	**NIR**	**SWIR-1**	**SWIR-2**	
HLD	0.00 *(1.07)*	-0.15 *(1.06)*	0.00 *(1.07)*	-1.52 *(1.07)*	1.53 *(1.07)*	
HLB	0.00 *(0.43)*	-0.13 *(0.43)*	0.00 *(0.43)*	-0.43 *(0.43)*	0.30 *(0.43)*	
VEG50	0.00 *(0.66)*	-0.22 *(0.66)*	0.00 *(0.66)*	-0.84 *(0.66)*	0.63 *(0.66)*	
REF50	0.00 *(0.50)*	-0.20 *(0.50)*	0.00 *(0.50)*	-0.49 *(0.50)*	0.29 *(0.50)*	
TRD	0.00 *(0.65)*	-0.15 *(0.65)*	0.00 *(0.65)*	-0.50 *(0.65)*	0.38 *(0.65)*	
TRB	0.00 *(0.29)*	-0.14 *(0.29)*	0.00 *(0.29)*	-0.11 *(0.29)*	-0.03 *(0.29)*	

Table 12: ZLO related XCO_2 errors as computed with full iterative FOCAL. The SNR-related XCO_2 random error is shown in brackets. The EB requires a Total Uncertainty of 0.2 ppm or less. Here the baseline configuration of FOCAL has been used, i.e., ZLO is not a state vector element. Instrument: CO2M_002.

XCH_4 errors in ppb Algorithm: FOCAL (ZLO in state vector: no) Error source: ZLO *(in brackets: SNR-related random error)*						
Scenario		**Bands**				**Comment**
	No ZLO error	**All 3 bands**	**NIR**	**SWIR-1**	**SWIR-2**	
HLD	0.0 *(12.7)*	-4.7 *(12.5)*	0.0 *(12.7)*	-19.1 *(12.6)*	14.4 *(12.6)*	
HLB	0.0 *(5.9)*	-0.4 *(5.9)*	0.0 *(5.9)*	-1.2 *(5.9)*	0.9 *(5.9)*	
VEG50	0.0 *(7.6)*	-1.7 *(7.5)*	0.0 *(7.6)*	-5.0 *(7.5)*	3.3 *(7.5)*	
REF50	0.0 *(5.8)*	-1.0 *(5.8)*	0.0 *(5.8)*	-2.2 *(5.8)*	1.2 *(5.8)*	
TRD	0.0 *(7.5)*	-2.2 *(7.5)*	0.0 *(7.5)*	-6.3 *(7.5)*	4.2 *(7.5)*	
TRB	0.0 *(3.4)*	-0.8 *(3.4)*	0.0 *(3.4)*	-0.6 *(3.4)*	-0.2 *(3.4)*	

Table 13: ZLO related XCH_4 errors as computed with full iterative FOCAL. The SNR-related XCH_4 random error is shown in brackets. The EB requires a Total Uncertainty of 2 ppb or less. Here the baseline configuration of FOCAL has been used, i.e., ZLO is not a state vector element. Instrument: CO2M_002.

XCO_2 errors in ppm Algorithm: FOCAL (ZLO in state vector: yes) Error source: ZLO *(in brackets: SNR-related random error)*						
Scenario		**Bands**				**Comment**
	No ZLO error	**All 3 bands**	**NIR**	**SWIR-1**	**SWIR-2**	
HLD	0.00 *(1.11)*	0.00 *(1.11)*	0.00 *(1.11)*	0.00 *(1.11)*	0.00 *(1.11)*	
HLB	0.00 *(0.47)*	0.00 *(0.47)*	0.00 *(0.47)*	0.00 *(0.47)*	0.00 *(0.47)*	
VEG50	0.00 *(0.75)*	0.00 *(0.75)*	0.00 *(0.75)*	0.00 *(0.75)*	0.00 *(0.75)*	
REF50	0.00 *(0.56)*	0.00 *(0.56)*	0.00 *(0.56)*	0.00 *(0.56)*	0.00 *(0.56)*	
TRD	0.00 *(0.65)*	0.00 *(0.65)*	0.00 *(0.65)*	0.00 *(0.65)*	0.00 *(0.65)*	
TRB	0.00 *(0.32)*	0.00 *(0.32)*	0.00 *(0.32)*	0.00 *(0.32)*	0.00 *(0.32)*	

Table 14: ZLO related XCO_2 errors as computed with full iterative FOCAL. The SNR-related XCO_2 random error is shown in brackets. The EB requires a Total Uncertainty of 0.2 ppm or less. Here ZLO has been added as a state vector element in each band. Instrument: CO2M_002.

XCH_4 errors in ppb Algorithm: FOCAL (ZLO in state vector: yes) Error source: ZLO *(in brackets: SNR-related random error)*						
Scenario		**Bands**				**Comment**
	No ZLO error	**All 3 bands**	**NIR**	**SWIR-1**	**SWIR-2**	
HLD	0.0 *(14.2)*	0.0 *(14.2)*	0.0 *(14.2)*	0.0 *(14.2)*	0.0 *(14.2)*	
HLB	0.0 *(6.0)*	0.0 *(6.0)*	0.0 *(6.0)*	0.0 *(6.0)*	0.0 *(6.0)*	
VEG50	0.0 *(8.3)*	0.0 *(8.3)*	0.0 *(8.3)*	0.0 *(8.3)*	0.0 *(8.3)*	
REF50	0.0 *(6.1)*	0.0 *(6.1)*	0.0 *(6.1)*	0.0 *(6.1)*	0.0 *(6.1)*	
TRD	0.0 *(8.4)*	0.0 *(8.4)*	0.0 *(8.4)*	0.0 *(8.4)*	0.0 *(8.4)*	
TRB	0.0 *(3.6)*	0.0 *(3.6)*	0.0 *(3.6)*	0.0 *(3.6)*	0.0 *(3.6)*	

Table 15: ZLO related XCH_4 errors as computed with full iterative FOCAL. The SNR-related XCH_4 random error is shown in brackets. The EB requires a Total Uncertainty of 2 ppb or less. Here ZLO has been added as a state vector element in each band. Instrument: CO2M_002.

4.4.2. Analysis of Jänschwalde power plant scene

ZLO related errors have also been computed using University of Bremen's E2ES system applied to the Jänschwalde power plant scene.

Figure 21 shows XCO_2 related errors and corresponding power plant emission errors, when an additive offset (ZLO) is added as systematic error to the radiance spectrum of each band using the MRDv1.0 S7MR-OBS-230 ZLO values for all three bands. Here FOCAL's baseline configuration has been used, i.e., ZLO is not a state vector element and the XCO2 a priori uncertainty is 5 ppm (see **Figure 3** showing the corresponding analysis without ZLO error).

The ZLO related error can be obtained from the difference of the retrieve - true XCO_2 values shown in the bottom left panel when compared with the corresponding differences for the error-free case show in **Figure 3**. These ZLO related errors are:

- Minimum XCO_2: -0.19 ppm (= -0.53 – (-0.34))
- Maximum XCO_2: -0.18 ppm (= 0.31 – 0.49)
- Maximum – minimum XCO_2: 0.0 ppm (= 0.83 – 0.83)

This shows that the main effect of an ZLO on the retrieved XCO_2 is an offset (which is not critical for the plume inversion because the emission signal is the difference of the XCO_2 values in the plume and in the background).

Figure 22 show results for the same analysis but here ZLO has been added as state vector elements to the FOCAL algorithm (= 3 additional parameters, i.e., one ZLO value per band). The corresponding ZLO related errors are:

- Minimum XCO_2: 0.03 ppm (= -0.31 – (-0.34))
- Maximum XCO_2: 0.42 ppm (= 0.91 – 0.49)
- Maximum – minimum XCO_2: 0.39 ppm (= 1.22 – 0.83)

This suggests that adding ZLO as state vector elements is not recommended.

The analysis shown in **Figure 21 - Figure 22** has been repeated but with ZLO (error) only added to the SWIR-1 band. The results are shown in **Figure 23** - **Figure 24**.
If ZLO is not added as a state vector element then the corresponding ZLO related errors are:

- Minimum XCO_2: -0.80 ppm (= -1.14 – (-0.34))
- Maximum XCO_2: -0.50 ppm (= -0.01 – 0.49)
- Maximum – minimum XCO_2: 0.29 ppm (= 1.12 – 0.83)

If ZLO is added as a state vector element then the corresponding ZLO related errors are:

- Minimum XCO_2: 0.03 ppm (= -0.31 – (-0.34))
- Maximum XCO_2: 0.42 ppm (= 0.91 – 0.49)
- Maximum – minimum XCO_2: 0.39 ppm (= 1.22 – 0.83)

This also suggests that adding ZLO as state vector elements is not recommended.

The results shown in this sub-section indicate that ZLO does not have to be / should not be added as a state vector element to FOCAL; this differs from the results shown in the previous section, where it is indicated that adding ZLO reduces ZLO related XCO_2 errors but obviously this is not always the case.

The results also indicate that the MRDv1.0 ZLO values should be reduced by approximately a factor of 2 because according to the error budget "only" 0.2 ppm are "available" for this error source but the results above indicate that 0.2 ppm can be easily exceeded using MRDv1.0 ZLO values.

These findings may also depend on the used retrieval algorithm. Therefore, the next sub-section show comparisons using all three XCO_2 algorithms.

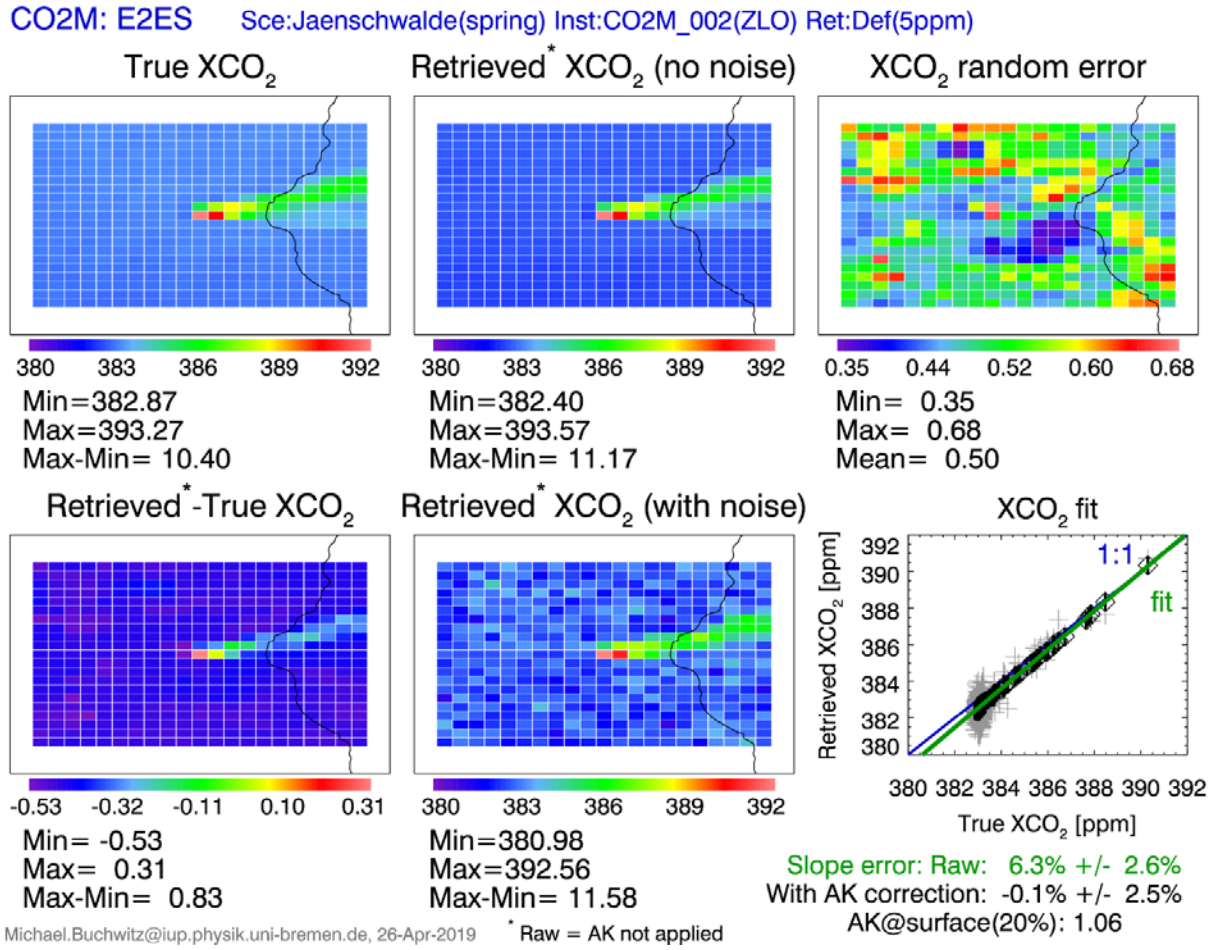

Figure 21: As **Figure 3** but with an additive offset (ZLO) added as systematic error to the radiance spectrum of each band using the MRDv1.0 S7MR-OBS-230 ZLO values for all three bands. FOCAL's baseline configuration has been used, i.e., ZLO is not a state vector element.

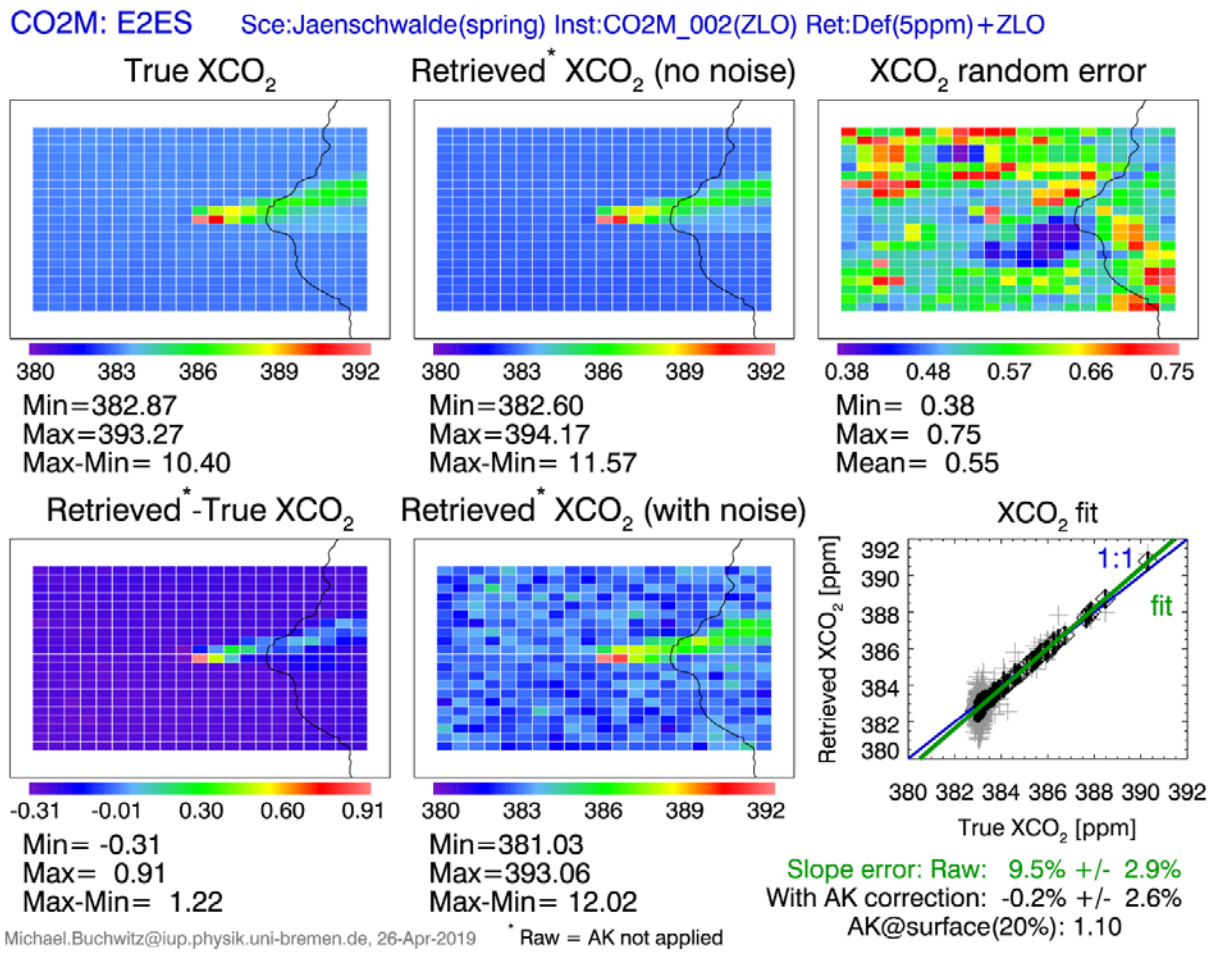

Figure 22: As **Figure 21** but adding ZLO as a state vector element to the FOCAL retrieval.

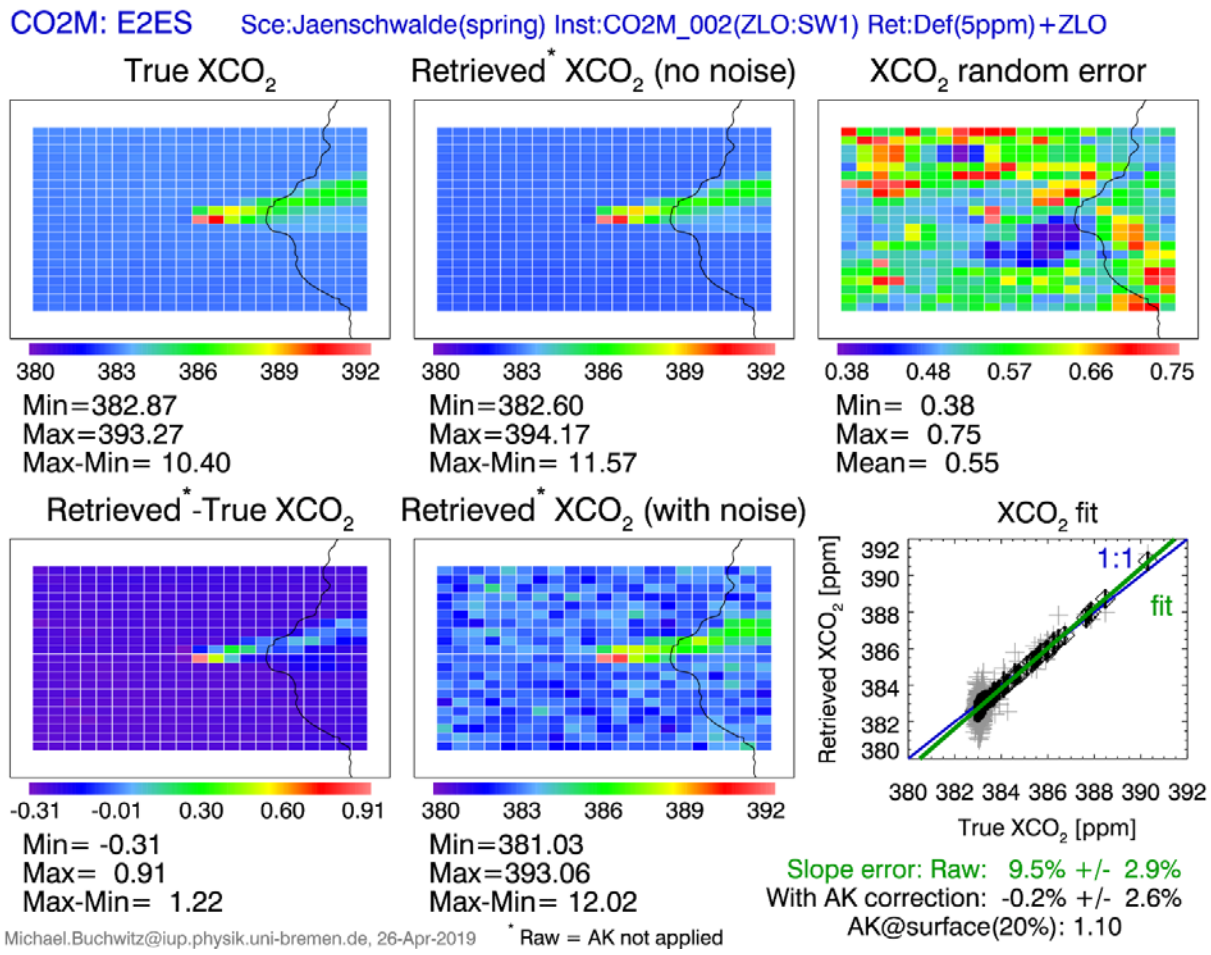

Figure 23: As **Figure 21** but adding a ZLO error only to the SWIR-1 band.

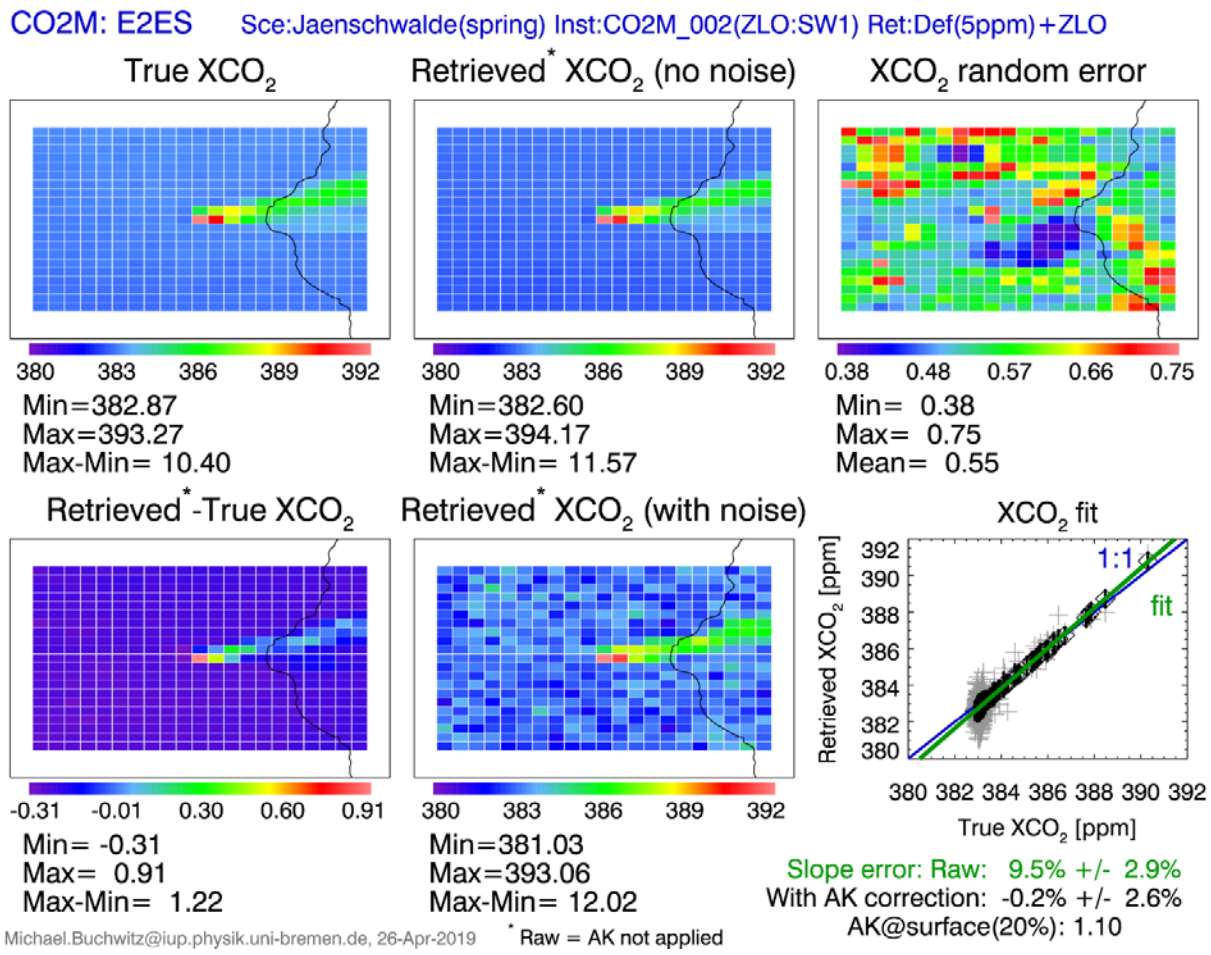

Figure 24: As **Figure 23** but adding ZLO as a state vector element to the FOCAL retrieval.

4.4.3. Comparison of ZLO related errors via three different algorithms

The retrieval algorithms of Univ. Bremen (IUP), SRON and Univ. Leicester (UoL) have been used to quantify ZLO related XCO_2 errors for several scenarios.

The results have been obtained using the gain vector approach applied to the scenarios VEG50, MLD and MLB (see **Table 36**) and to instrument CO2M_002 (see **Table 37**) and are shown in **Table 16**.

The following (MRDv1) ZLO values have been used for this assessment:

- NIR: 8.4×10^9 photons/s/nm/cm^2/sr
- SW1: 8.6×10^9 photons/s/nm/cm^2/sr
- SW2: 2.0×10^9 photons/s/nm/cm^2/sr

The “IUP errors” have been computed using the reference spectra / gain files described in **Sect. 9**.

The “SRON errors” have been computed using the reference spectra / gain files described in **Sect. 11.1**.

The “UoL errors” have been computed using the reference spectra / gain files described in **Sect. 12**.

As can be seen from **Table 16**, the resulting XCO_2 errors of SRON and UoL are typically larger compared to the errors computed using the IUP FOCAL algorithm. The largest errors correspond to the UoL algorithm if ZLO is not included as state vector element and surface pressure is included. If ZLO is added then the UoL errors are in between the errors of IUP and SRON.

This shows that the magnitude of ZLO-related XCO_2 errors depends on the retrieval algorithm and its settings (e.g., adding ZLO as state vector element or not).

The results in this section shown that ZLO related errors may significantly exceed the 0.2 ppm as specified in the error budget for this error source. Based on the results presented in this section it is recommended to reduce the ZLO values as specified in the MRDv1.0 by approximately a factor of 2.

Scenario	ZLO added to band:	XCO2 error [ppm] IUP	SRON	UoL(§)		Difference (absolute): IUP-SRON	UoL-SRON
VEG50	All 3	-0,191	-1,287	-2,129		1,10	0,84
VEG50	NIR	0,002	0,502	0,647		0,50	0,15
VEG50	SW1	-0,839	-0,736	-0,554		0,10	0,18
VEG50	SW2	0,646	-1,038	-2,221		1,68	1,18
MLD	All 3	-0,152	-1,446	-2,055		1,29	0,61
MLD	NIR	0,001	0,518	1,049		0,52	0,53
MLD	SW1	-0,746	-1,027	-0,509		0,28	0,52
MLD	SW2	0,593	-0,937	-2,595		1,53	1,66
MLB	All 3	-0,138	-0,643	-0,505		0,51	0,14
MLB	NIR	0,001	0,048	0,107		0,05	0,06
MLB	SW1	-0,192	-0,056	-0,133		0,14	0,08
MLB	SW2	0,052	-0,635	-0,480		0,69	0,16
Root Mean Square (RMS):		0,42	0,85	1,39	Mean:	0,70	0,51

Scenario	ZLO added to band:	XCO2 error [ppm] IUP	SRON	UoL(*)		Difference (absolute): IUP-SRON	UoL-SRON
VEG50	All 3	-0,191	-1,287	-1,384		1,10	0,10
VEG50	NIR	0,002	0,502	0,000		0,50	0,50
VEG50	SW1	-0,839	-0,736	-0,622		0,10	0,11
VEG50	SW2	0,646	-1,038	-0,762		1,68	0,28
MLD	All 3	-0,152	-1,446	-1,056		1,29	0,39
MLD	NIR	0,001	0,518	0,000		0,52	0,52
MLD	SW1	-0,746	-1,027	-0,329		0,28	0,70
MLD	SW2	0,593	-0,937	-0,727		1,53	0,21
MLB	All 3	-0,138	-0,643	-0,197		0,51	0,45
MLB	NIR	0,001	0,048	0,000		0,05	0,05
MLB	SW1	-0,192	-0,056	-0,079		0,14	0,02
MLB	SW2	0,052	-0,635	-0,117		0,69	0,52
Root Mean Square (RMS):		0,42	0,85	0,63	Mean:	0,70	0,32

Table 16: Comparison of ZLO related XCO_2 errors using the retrieval algorithms of IUP, SRON and UoL. Top: Results obtained with the default algorithms / default settings of IUP and SRON. The UoL algorithm settings were: ZLO not included as state vector element and surface pressure included as state vector element. The different colours highlight the magnitude of the error: the largest error is shown in red and the smallest error in green. Bottom: as top but using these UoL settings: ZLO included for NIR band and surface pressure not included.

4.4.1. Summary and conclusions

Additive radiance errors, denoted here as Zero-Level-Offsets (ZLO), need to be minimized to avoid systematic XCO_2 retrieval errors. Using simulated retrievals using the FOCAL retrieval algorithm it has been investigated how large these systematic errors can be given the (maximum) ZLO values specified in the MRD. According to the Error Budget (EB) an XCO_2 error of 0.2 ppm has been allocated for this error source. If ZLO is added as a state vector element to FOCAL then the resulting systematic error is zero suggesting that this error source is negligible. However, it is not entirely clear if robust retrievals are possible when ZLO is added as a state vector element. Furthermore, the retrieval simulations assume that the error is constant in each band, which is a very optimistic assumption. If ZLO is not a state vector element, than this error source can result in errors significantly larger than 0.2 ppm. One may expect that at the end (i.e., for the final algorithm including bias correction and/or ZLO correction, see **/Reuter et al., 2017b/**, where a ZLO correction is used when applying FOCAL to real OCO-2 data) the ZLO-related error may be in between the two extremes discussed here. It is therefore concluded that the ZLO requirement as given in the MRD is appropriate. This is also corroborated by simulation of scenes using the End-to-End-Simulator (E2ES) software (results will be shown in the next update of this document). However, in order to be on the save side, it is recommended to add as a goal requirement ZLO values for the SWIR bands, which are a factor of two smaller than the values currently listed in the MRD.

4.5. Non-linearity (NL)

4.5.1. Comparison of NL related errors via three different algorithms

The retrieval algorithms of Univ. Bremen (IUP), SRON and Univ. Leicester (UoL) have been used to quantify radiance non-linearity (NL) related XCO_2 errors for several scenarios.

The results have been obtained using the gain vector approach applied to the scenarios VEG50, MLD and MLB (see **Table 36**) and to instrument CO2M_002 (see **Table 37**) and are shown in **Table 17**.

The used approach to simulated NL is described in **/Landgraf et al., 2017a/.** Here use we "their" instrument B, which is essentially CO2M.

The "IUP errors" have been computed using the reference spectra / gain files described in **Sect. 9**.

The "SRON errors" have been computed using the reference spectra / gain files described in **Sect. 11.1**.

The "UoL errors" have been computed using the reference spectra / gain files described in **Sect. 12**.

As can be seen, the resulting XCO_2 errors of SRON and UoL are significantly higher compared to the errors computed using the IUP FOCAL algorithm. The largest errors correspond to the UoL algorithm if ZLO is not included as state vector element and surface pressure is included.

Scenario	NL error to band:	XCO2 error [ppm] IUP	SRON	UoL(§)		Difference (absolute): IUP-SRON	UoL-SRON
VEG50	All 2	2,863	-5,018	-10,705		7,88	5,69
VEG50	SW1	-0,358	-0,349	-0,232		0,01	0,12
VEG50	SW2	3,221	-4,673	-10,472		7,89	5,80
MLD	All 2	2,480	-5,010	-12,622		7,49	7,61
MLD	SW1	-0,715	-0,991	-0,476		0,28	0,52
MLD	SW2	3,195	-4,018	-12,146		7,21	8,13
MLB	All 2	-1,668	-2,010	-3,657		0,34	1,65
MLB	SW1	-2,385	-0,574	-1,361		1,81	0,79
MLB	SW2	0,717	-1,436	-2,296		2,15	0,86
Root Mean Square (RMS):		2,22	3,26	7,83	Mean:	3,90	3,46
Mean:		0,82	-2,68	-6,00			

Scenario	NL error to band:	XCO2 error [ppm] IUP	SRON	UoL(*)		Difference (absolute): IUP-SRON	UoL-SRON
VEG50	All 2	2,863	-5,018	-3,764		7,88	1,25
VEG50	SW1	-0,358	-0,349	-0,260		0,01	0,09
VEG50	SW2	3,221	-4,673	-3,503		7,89	1,17
MLD	All 2	2,480	-5,010	-3,416		7,49	1,59
MLD	SW1	-0,715	-0,991	-0,307		0,28	0,68
MLD	SW2	3,195	-4,018	-3,109		7,21	0,91
MLB	All 2	-1,668	-2,010	-0,418		0,34	1,59
MLB	SW1	-2,385	-0,574	-0,854		1,81	0,28
MLB	SW2	0,717	-1,436	0,436		2,15	1,87
Root Mean Square (RMS):		2,22	3,26	2,33	Mean:	3,90	1,05
Mean:		0,82	-2,68	-1,69			

Table 17: Comparison of NL related XCO_2 errors using the retrieval algorithms of IUP, SRON and UoL. Top: Results obtained with the default algorithms / default settings of IUP and SRON. The UoL algorithm settings were: ZLO not included as state vector element and surface pressure included as state vector element. The different colours highlight the magnitude of the error: the largest error is shown in red and the smallest error in green. Bottom: as top but using these UoL settings: ZLO included for NIR band and surface pressure not included.

4.5.2. Summary and conclusions

XCO_2 errors resulting from non-linearity (NL) have been computed via linear errors analysis by applying the gain vectors of the algorithms of Univ. Bremen, SRON and Univ. Leicester to several scenarios and assuming a certain dependence of the NL error on the radiance (NL = NL(radiance)).

The resulting XCO_2 errors are on the order of 3 ppm for the assumed NL(radiance).

This shows that NL is potentially an important error source. The magnitude of the resulting XCO_2 error depends on NL(radiance) and how relevant / realistic the assumed function investigated here is, is currently unclear.

4.6. Instrument Spectral Response Function (ISRF)

4.6.1. University of Bremen error analysis results for ISRF

ISRF related XCO_2 and XCH_4 errors have been computed with FOCAL using the gain vector (GV) approach (see **Sect. 9.2**) and instrument CO2M_002.

Two "perturbed ISRF" have been defined and used. They are shown in **Figure 25** (PERT_01: +1% FWHM error; see MRDv1 S7MR-OBS-130) and **Figure 26** (PERT_02: approx. 2% shape error; see MRDv1 S7MR-OBS-110).

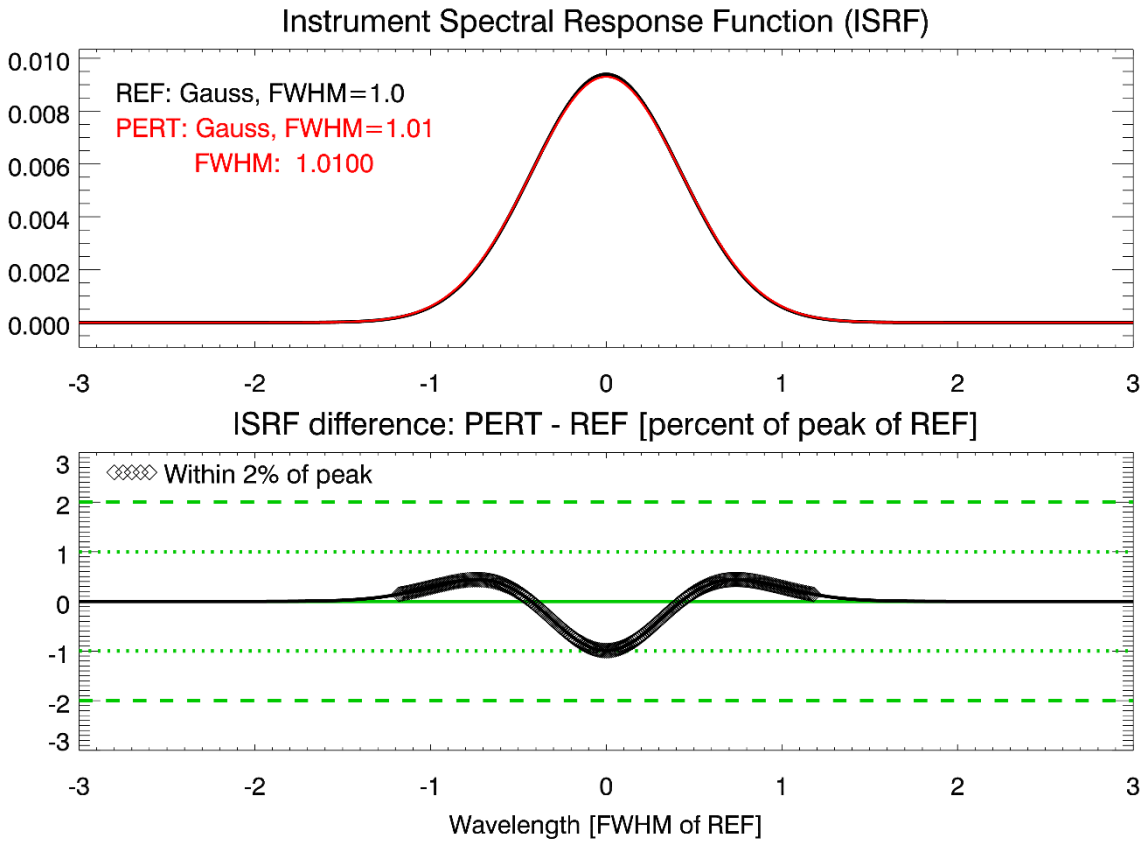

Figure 25: Top: Gaussian reference ISRF (black) with FWHM=1.0 and perturbed Gaussian ISRF (red) with FWHM=1.01 (+1%). The perturbed ISRF has a +1% larger FWHM (PERT_01 ISRF). Bottom: Difference of the two ISRFs. The black symbols indicate the range where the perturbed ISRF is within 2% of the peak value of the reference ISRF.

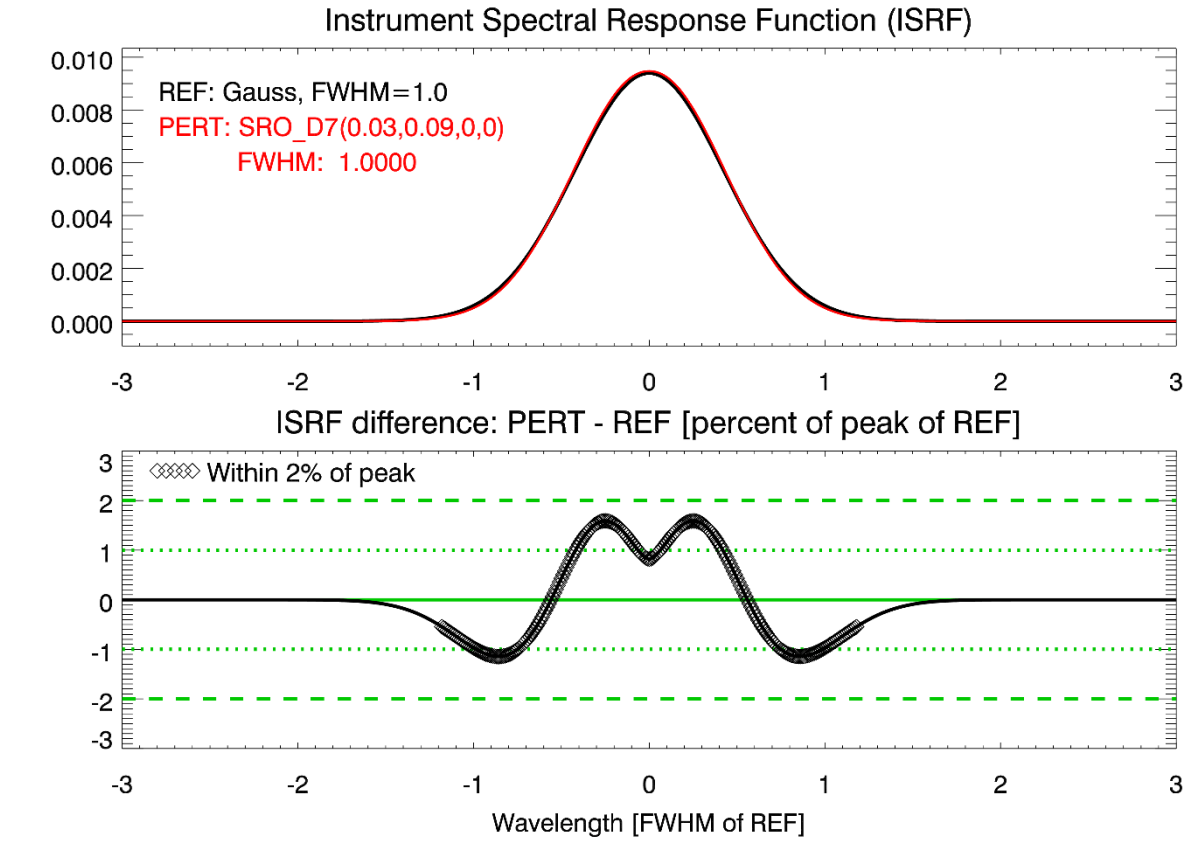

Figure 26: As **Figure 25** but using perturbed ISRF "PERT_02", which has the same FWHM as the reference ISRF but a different shape. The shape error is close to 2% of the peak value of the reference ISRF (see dashed green horizontal line). The perturbed ISRF has been computed using Eq. (6) of **/Landgraf et al., 2017a/** (page 3) using parameters k0=2, a1=0.03, k1=0.09, a2=k2=0.

Error analysis results for ISRF errors for scenario VEG50 are shown in **Table 18** for XCO_2 PERT_01 and in **Table 20** for PERT_02 4 instrument configurations consistent with MRDv1.0. The corresponding XCH_4 results are shown in **Table 19** and **Table 21**.

Errors exceeding the Total Uncertainty values as listed in the Error Budget (EB) **/CO2M-REB TN-3000, 2019/** (EB: 0.2 ppm for XCO_2 and 2 ppb for XCH_4) are shown in red.

As can be seen, the resulting errors for XCO_2 are smaller than the EB value for the FOCAL algorithm (where FWHM are state vector elements), not however for the other two algorithms. For XCH_4 retrieved with FOCAL errors are less than the EB value with the exception of the 2% shape error in the SWIR-1 band, where the error is significantly larger than the EB value.

XCO_2 errors in ppm Error source: ISRF: FWHM +X% (PERT_01)						
Scenario	**Bands**				**Error**	**Algorithm (gains)**
	All 3 bands	**NIR**	**SWIR-1**	**SWIR-2**		
REF50	0.008	0.001	-0.006	0.013	+1%	FOCAL
REF50	0.520	0.517	0.542	0.545	+1%	RemoTeC
REF50	-1.780	-0.185	-0.481	-1.113	+1%	UoL-FP (#)
VEG50	0.026	0.001	-0.011	0.036	+1%	FOCAL
VEG50	0.716	0.591	-0.735	0.861	+1%	RemoTeC
VEG50	-2.182	-0.392	-0.567	-1.223	+1%	UoL-FP (#)
VEG50	0.044	0.008	-0.021	0.057	+2%	FOCAL
VEG50	0.069	0.037	-0.035	0.067	+4%	FOCAL

Table 18: ISRF related XCO_2 errors. ISRF error: FWHM +X% (PERT_01), with X listed in column "Error". (#) The UoL-FP gains include ZLO in the NIR (and surface pressure is not included) as state vector element.

XCH_4 errors in ppb Error source: ISRF: FWHM +X% (PERT_01)						
Scenario	**Bands**				**Error**	**Algorithm (gains)**
	All 3 bands	**NIR**	**SWIR-1**	**SWIR-2**		
REF50	0.18	0.00	-0.09	0.28	+1%	FOCAL
VEG50	-0.01	0.00	-0.21	0.20	+1%	FOCAL
VEG50	-0.21	0.02	-0.53	0.30	+2%	FOCAL
VEG50	-1.08	0.09	-1.52	0.34	+4%	FOCAL

Table 19: ISRF related XCH_4 errors. ISRF error: FWHM +X% (PERT_01), with X listed in column "Error"

XCO_2 errors in ppm Algorithm: FOCAL/GV Error source: ISRF: 2% shape error (PERT_02)					
Scenario	**Bands**				**Comment**
	All 3 bands	**NIR**	**SWIR-1**	**SWIR-2**	
VEG50	-0.119	0.171	-0.017	0.070	
REF50	-0.079	-0.124	-0.041	0.085	

Table 20: ISRF related XCO_2 errors as computed with FOCAL. ISRF error: 2% shape error (PERT_02).

XCH_4 errors in ppb Algorithm: FOCAL/GV Error source: ISRF: 2% shape error (PERT_02)					
Scenario	**Bands**				**Comment**
	All 3 bands	**NIR**	**SWIR-1**	**SWIR-2**	
VEG50	4.46	-0.37	4.75	0.08	
REF50	4.30	-0.22	4.36	0.16	

Table 21: ISRF related XCH_4 errors as computed with FOCAL. ISRF error: 2% shape error (PERT_02).

4.6.2. Summary and conclusions

Residual errors of the Instrument Spectral Response Function (ISRF) result in errors of the XCO_2 retrievals. According to the Error Budget (EB) 0.2 ppm has been allocated for this error source. Simulated XCO_2 retrievals have been carried out with FOCAL for several types of ISRF errors. The results indicate that the MRD requirement is appropriate.

4.7. Multiplicative radiance errors

4.7.1. University of Bremen error analysis results

Multiplicative radiance error related XCO_2 and XCH_4 errors have been computed with FOCAL using the gain vector (GV) approach (see **Sect. 9.2**).

Results for several scenarios (see **Table 36**) are shown in the tables below for XCO_2 and XCH_4 for an instrument configuration consistent with MRDv1.0 (see **Table 6** and instrument CO2M_001, which is identical with CO2M_002 except for SNR, in **Table 37**).

Errors exceeding the Total Uncertainty values as listed in the Error Budget (EB) **/CO2M-REB TN-3000, 2019/** (i.e., 0.2 ppm for XCO_2 and 2 ppb for XCH_4) are shown in red. As can be seen, the errors are less than permitted according to the EB.

XCO_2 errors in ppm Algorithm: FOCAL/GV Error source: Multiplicative radiance error (+3%)					
Scenario	**Bands**				**Comment**
	All 3 bands	**NIR**	**SWIR-1**	**SWIR-2**	
HLD	0.000	0.014	-0.057	0.043	
HLB	0.000	0.006	-0.016	0.009	
VEG50	0.003	0.013	-0.029	0.019	
REF50	-0.001	0.007	-0.020	0.009	
TRD	0.003	0.011	-0.018	0.010	
TRB	0.000	0.007	-0.006	-0.002	

Table 22: XCO_2 errors as computed with FOCAL for a 3% radiometric error. The EB requires a Total Uncertainty of 0.2 ppm or less.

XCH_4 errors in ppb Algorithm: FOCAL/GV Error source: Multiplicative radiance error (+3%)					
Scenario	**Bands**				**Comment**
	All 3 bands	**NIR**	**SWIR-1**	**SWIR-2**	
HLD	0.00	0.12	-0.62	0.49	
HLB	-0.01	0.01	-0.05	0.03	
VEG50	0.00	0.05	-0.18	0.12	
REF50	-0.02	0.02	-0.08	0.05	
TRD	0.00	0.07	-0.23	0.16	
TRB	-0.03	0.01	-0.03	-0.01	

Table 23: XCH_4 errors as computed with FOCAL for a 3% radiometric error. The EB requires a Total Uncertainty of 2 ppb or less.

4.7.2. Comparison of MULT errors via three different algorithms

The retrieval algorithms of Univ. Bremen (IUP), SRON and Univ. Leicester (UoL) have been used to quantify multiplicative radiance related XCO_2 errors for several scenarios.

The results have been obtained using the gain vector approach applied to the scenarios VEG50, MLD and MLB (see **Table 36**) and to instrument CO2M_002 (see **Table 37**) and are shown in **Table 16**.

The following (MRDv1) radiance error values have been used for this assessment:

- NIR: 3%
- SW1: 3%
- SW2: 3%

The “IUP errors” have been computed using the reference spectra / gain files described in **Sect. 9**.

The “SRON errors” have been computed using the reference spectra / gain files described in **Sect. 11.1**.

The “UoL errors” have been computed using the reference spectra / gain files described in **Sect. 12**.

As can be seen, the resulting XCO_2 errors of SRON and UoL are significantly larger compared to the errors computed using the IUP FOCAL algorithm. The largest errors correspond to the UoL algorithm if ZLO is not included as state vector element and surface pressure is included.

As can also be seen, for many situations the SRON and UoL error exceeds the value of 0.2 ppm as listed for this error source in the error budget. Based on this a relaxation of the MRDv1 requirement is not recommended.

Scenario	MULT error to band:	XCO2 error [ppm] IUP	SRON	UoL(§)		Difference (absolute): IUP-SRON	UoL-SRON
VEG50	All 3	0,001	0,295	0,772		0,29	0,48
VEG50	NIR	0,015	0,693	0,873		0,68	0,18
VEG50	SW1	-0,038	0,003	-0,038		0,04	0,04
VEG50	SW2	0,025	-0,402	-0,062		0,43	0,34
MLD	All 3	0,003	0,377	1,278		0,37	0,90
MLD	NIR	0,015	0,733	1,515		0,72	0,78
MLD	SW1	-0,034	-0,045	-0,044		0,01	0,00
MLD	SW2	0,022	-0,311	-0,192		0,33	0,12
MLB	All 3	-0,004	-0,194	0,192		0,19	0,39
MLB	NIR	0,004	0,049	0,180		0,05	0,13
MLB	SW1	-0,011	-0,052	0,017		0,04	0,07
MLB	SW2	0,002	-0,191	-0,006		0,19	0,19
Root Mean Square (RMS):		0,02	0,36	0,67	Mean:	0,28	0,30

Scenario	MULT error to band:	XCO2 error [ppm] IUP	SRON	UoL(*)		Difference (absolute): IUP-SRON	UoL-SRON
VEG50	All 3	0,001	0,295	0,120		0,29	0,18
VEG50	NIR	0,015	0,693	0,128		0,68	0,57
VEG50	SW1	-0,038	0,003	-0,043		0,04	0,05
VEG50	SW2	0,025	-0,402	0,035		0,43	0,44
MLD	All 3	0,003	0,377	0,209		0,37	0,17
MLD	NIR	0,015	0,733	0,291		0,72	0,44
MLD	SW1	-0,034	-0,045	-0,023		0,01	0,02
MLD	SW2	0,022	-0,311	-0,059		0,33	0,25
MLB	All 3	-0,004	-0,194	0,052		0,19	0,25
MLB	NIR	0,004	0,049	0,038		0,05	0,01
MLB	SW1	-0,011	-0,052	0,013		0,04	0,07
MLB	SW2	0,002	-0,191	0,001		0,19	0,19
Root Mean Square (RMS):		0,02	0,36	0,12	Mean:	0,28	0,22

Table 24: Comparison of multiplicative radiance related XCO_2 errors using the retrieval algorithms of IUP, SRON and UoL. Top: Results obtained with the default algorithms / default settings of IUP and SRON. The UoL algorithm settings were: ZLO not included as state vector element and surface pressure included as state vector element. The different colours highlight the magnitude of the error: the largest error is shown in red and the smallest error in green. Bottom: as top but using these UoL settings: ZLO included for NIR band and surface pressure not included.

4.7.3. Summary and conclusions

Multiplicative radiance errors may result in XCO_2 retrieval errors but this error source is expected to be much less critical than additive radiance errors. According to the Error Budget (EB) 0.2 ppm is allocated for this error source. Retrieval simulations with FOCAL confirm that this error source is less critical compared to additive errors and that the MRD requirement is appropriate. However, results obtained with other algorithms typically show somewhat larger errors than the errors obtained with FOCAL. It can therefore not be recommended to relax the requirement.

4.8. Spectral calibration errors

4.8.1. University of Bremen error analysis results

According to the EB the Total Uncertainty for spectral calibration related errors is 0.2 ppm for XCO_2 and 2 ppb for XCH_4.

Spectral shift related XCO_2 errors have been computed with FOCAL using the gain vector (GV) approach (see **Sect. 9.2**). The XCO_2 and XCH_4 errors have been computed assuming instrument CO2M_001, which is identical with CO2M_002 except for SNR, and using two approaches:

- Approach 1 (A1): The interpolation of the radiance from the perturbed spectral grid to the measurement spectral grid has been done based on high spectral sampling radiances
- Approach 2 (A2): As A1 but using the measurement spectral grid, which has a much lower spectral sampling than the grid used for A1 and therefore typically results in a larger – and likely more realistic – error as interpolation errors are not neglected.

Depending on how spectral errors are dealt with in the operational algorithm, one may expect that errors are in between the errors listed in the tables shown in this sub-section.

The results are shown in **Table 25** for XCO_2. As can be seen, the errors are less than permitted according to the EB. But note that spectral errors might be more complex than a simple spectral shift per band.

XCO_2 errors in ppm Algorithm: FOCAL/GV Error source: Spectral shift					
Scenario	**Spectral shift [fraction of FWHM]**			**Error [ppm]**	**Comment**
	NIR	**SWIR-1**	**SWIR-2**		
REF50	0.05	0	0	-0.002 0.003	
REF50	0	0.05	0	-0.010 -0.049	
REF50	0	0	0.05	-0.100 0.065	
REF50	0.05	0.05	0.05	-0.112 0.020	
VEG50	0.05	0	0	0.000 0.007	
VEG50	0	0.05	0	-0.015 -0.064	
VEG50	0	0	0.05	-0.088 0.058	
VEG50	0.05	0.05	0.05	-0.103 0.001	

Table 25: XCO_2 errors as computed with FOCAL/GV for spectral shift errors. The EB requires a Total Uncertainty of 0.2 ppm. Error are compute using approach A1 (top) and A2 (bottom).

The corresponding results for XCH_4 are shown in **Table 26**. Here errors exceeds 2 ppb if a spectral shift of 5% of the FWHM is present the SWIR-1 band.

XCH_4 errors in ppb Algorithm: FOCAL/GV Error source: Spectral shift					
Scenario	**Spectral shift [fraction of FWHM]**			**Error [ppb]**	**Comment**
	NIR	**SWIR-1**	**SWIR-2**		
REF50	0.05	0	0	0.00 0.02	
REF50	0	0.05	0	-0.15 -4.48	
REF50	0	0	0.05	-0.38 -0.20	
REF50	0.05	0.05	0.05	-0.54 -4.67	
VEG50	0.05	0	0	0.00 0.03	
VEG50	0	0.05	0	-0.32 -4.74	
VEG50	0	0	0.05	-0.33 -0.03	
VEG50	0.05	0.05	0.05	-0.65 -4.73	

Table 26: XCH_4 errors as computed with FOCAL/GV for spectral shift errors. The EB requires a Total Uncertainty of 2 ppb.

4.8.2. Summary and conclusions

Spectral calibration errors will result in errors of the retrieved XCO_2. According to the Error Budget (EB) 0.2 ppm has been allocated for this error source. Simulated retrievals have been carried out with FOCAL and the results indicate that the MRD requirement is appropriate.

4.9. Geolocation knowledge related XCO_2 errors

Very good geolocation knowledge is required for a number of reasons, which are related to the XCO_2 retrieval algorithm (e.g., proper use of high spatial resolution auxiliary data such as a Digital Elevation Model (DEM) used to, for example, surface pressure computation) and to the interpretation of the XCO_2 observations / images via inverse modelling (e.g., use of XCO_2 images to obtain emission estimates).

For example it has been shown in **/CS L1L2-II TN nadir, 2015/** using a high resolution DEM for a scene covering large parts of China that the mean surface elevation (Δz) may change by 50 m at 2x2 km^2 resolution for a horizontal shift (geolocation error Δx) of 200 m, i.e., for a slope (= Δz/Δx) 25% (of course, the slope depends on spatial position and may be much less elsewhere but also higher in regions with mountains). The lowest 50 m of the atmosphere contain typically approximately 0.5% of the air mass corresponding to a 0.5% error of the surface pressure if not corrected for. This relative error may propagate directly into a relative error of XCO_2 **/Kiel et al., 2018/**, i.e., 0.5% surface pressure error may result in a 0.5% (2 ppm) XCO_2 error. In order to reduce the XCO_2 error to below 0.5 ppm (see error budget) the surface pressure error must be less than 0.1%, which corresponds to 1 hPa or 8 m at sea level. For a geolocation error of 200 m this implies a maximum slope of 4% (=8/200) or, for 300 m, a slope of 2.7% (=8/300).

To further investigate this error source we have performed simulations using the Jänschwalde power plant scene (see **Figure 3**). **Figure 27** shows the corresponding results if a surface elevation error of Δz = 10 m (corresponding to an approximately 0.1% surface pressure change) has been added to each ground pixel. The comparisons of the results shown in **Figure 27** (with error) and **Figure 3** (without error) confirms the findings of **/Kiel et al., 2018/**:

The XCO_2 errors for Δz = 10 m are (compare **Figure 27** with **Figure 3**):

- Minimum XCO_2: 0.49 ppm (= 0.15 – (-0.34))
- Maximum XCO_2: 0.48 ppm (= 0.97 – 0.49)
- Maximum – minimum XCO_2: -0.01 ppm (= 0.82 – 0.83)

The XCO_2 errors for Δz = 50 m are (compare **Figure 28** with **Figure 3**):

- Minimum XCO_2: 2.18 ppm (= 1.84 – (-0.34))
- Maximum XCO_2: 2.45 ppm (= 2.94 – 0.49)
- Maximum – minimum XCO_2: 0.27 ppm (= 1.10 – 0.83)

As expected, the XCO_2 errors are approx. five times larger for the five times larger Δz error.

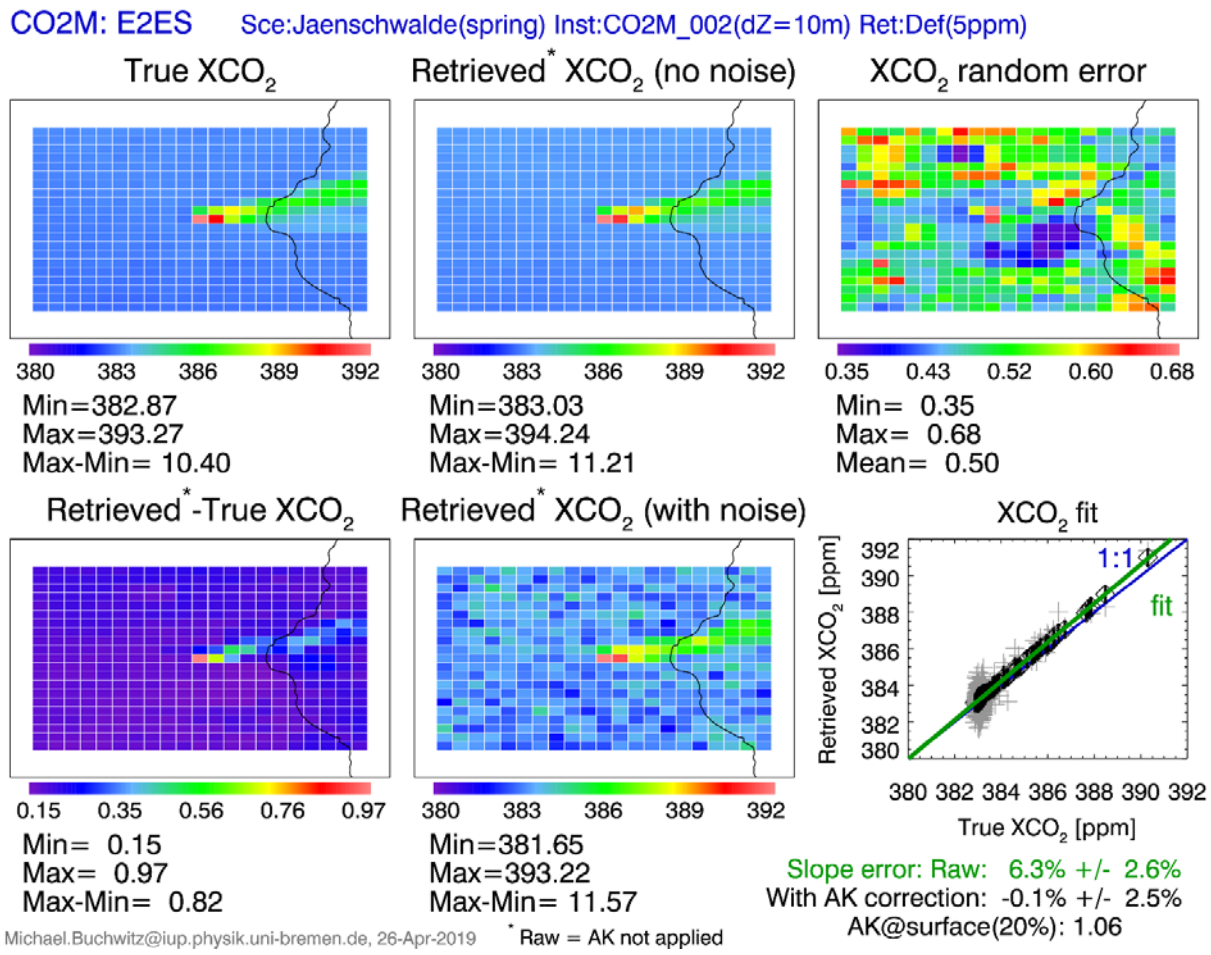

Figure 27: As **Figure 3** but for adding a surface elevation error (Δz) of 10m.

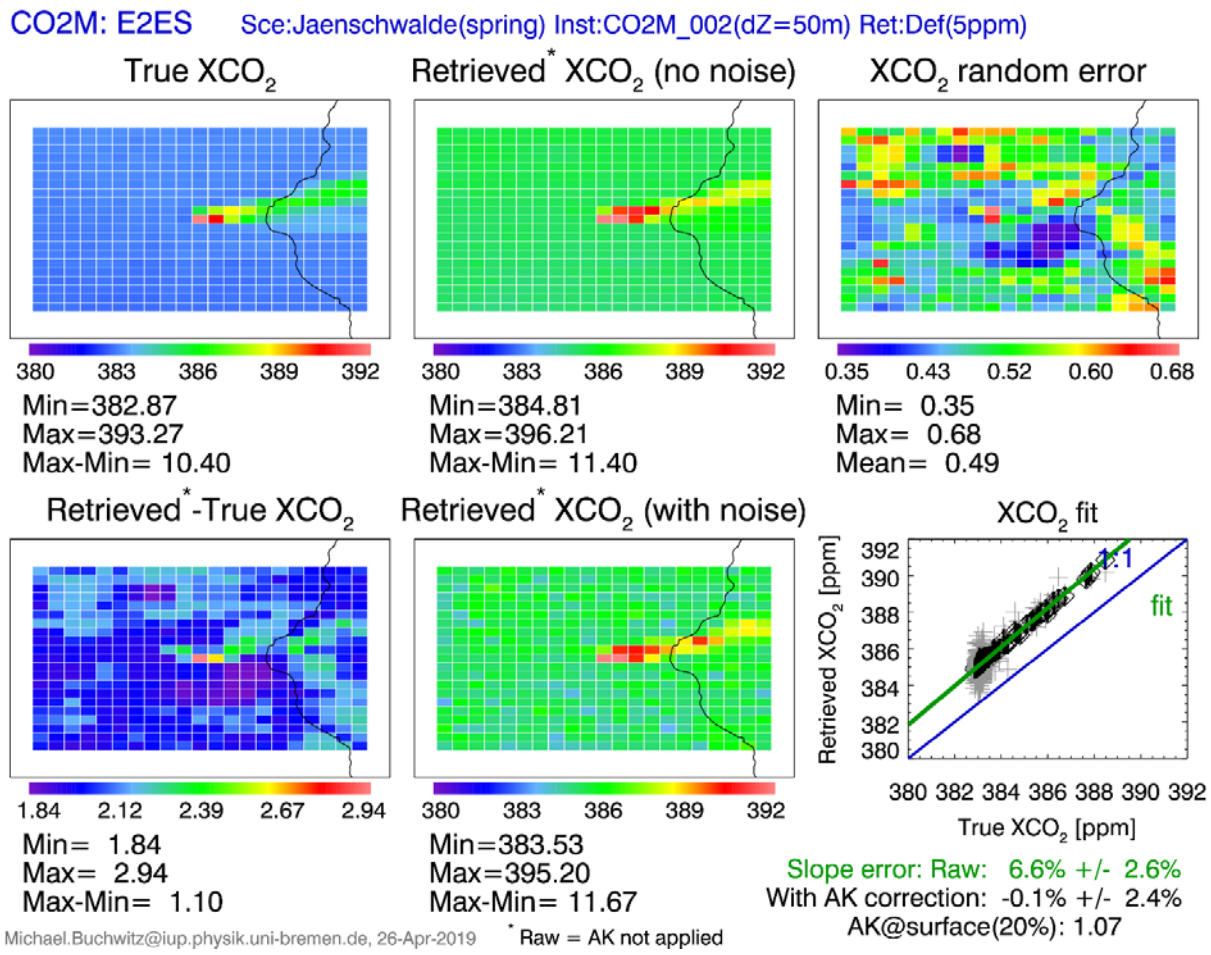

Figure 28: As Figure 27 for adding a surface elevation error (Δz) of 50m.

5. Analysis results for Tropospheric NO_2

5.1. Analysis results for SNR

We assume that the instrument is shot noise limited (see **Table 38**). This means that we can define the SNR performance by an SNR value and the reference spectrum belonging to this value. The SNR reference spectrum is shown in **Figure 29** and is calculated for the tropics and for a dark surface (2% albedo). The noise is calculated using the reference spectrum and the specified SNR. This noise is used for all scenarios, but scaled assuming shot noise. This means that for cloudy scenes the actual SNR can be much larger than the SNR for the reference spectrum. The SNR listed here is the SNR for the reference spectrum, not the actual SNR for a scene.

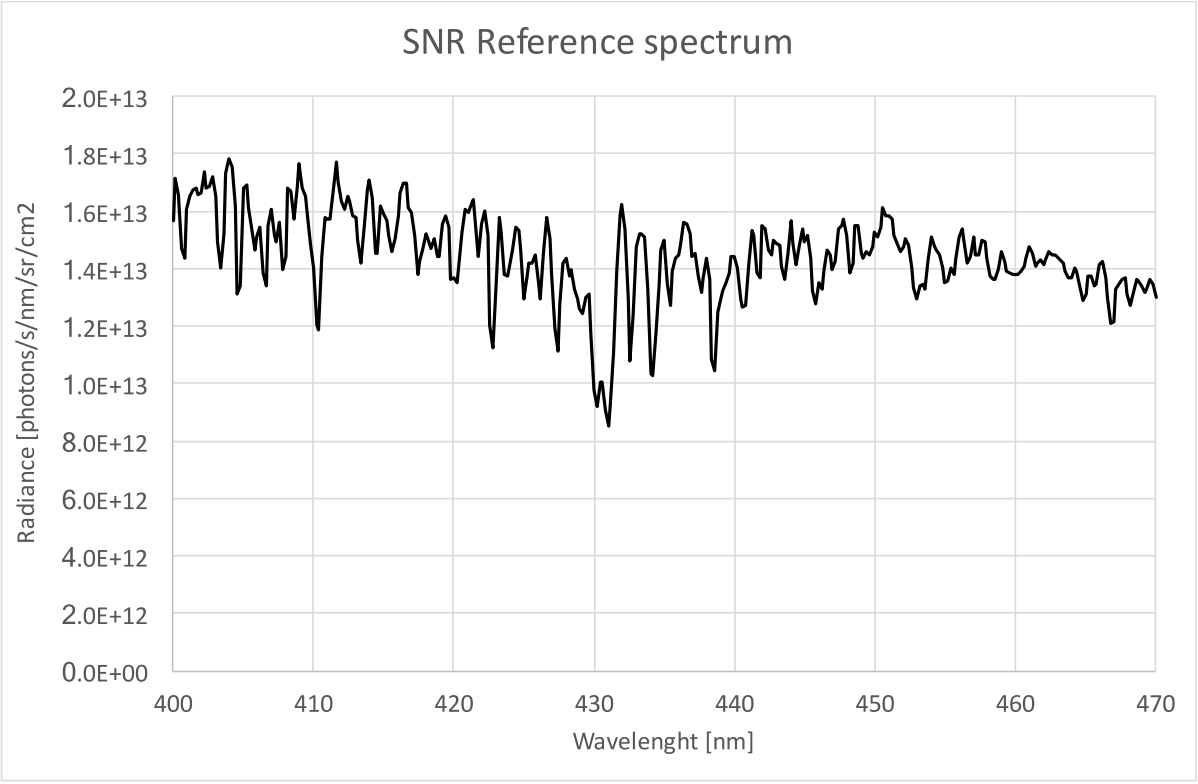

Figure 29: Reference spectrum used for the SNR calculations. This spectrum is derived for SZA=0, VZA=0 and surface albedo of 2%.

When the SNR increases the retrieved NO_2 column will generally be more accurate (other error sources, e.g. stray light, excluded). In **Figure 30** we present the noise precision in the retrieved tropospheric NO_2 column as a function of SNR.

Figure 30 shows that the impact of the surface albedo is larger than of the viewing geometry. For the low surface albedo of 0.02 the requirement of a noise error less than 20% ($2x10^{15}$ molec. cm^{-2}) is only met if the SNR is larger than 1000. For a surface albedo of 0.05 it is met for an SNR of 500, except for cases with a very high SZA. Based on this analysis we recommend using an SNR requirement of 750 for the reference spectrum shown in Figure 29. This value should be interpreted as an average SNR value over the fit window.

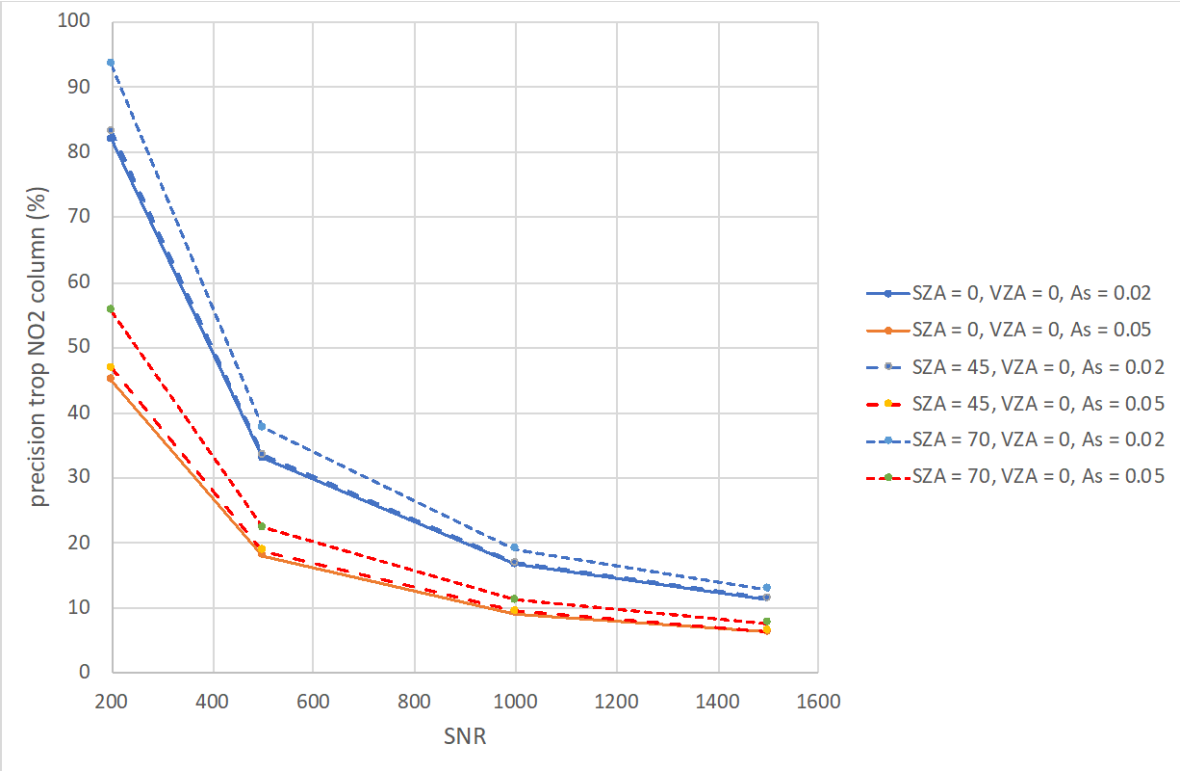

Figure 30: Precision of the retrieved tropospheric NO_2 column plotted as a function of the SNR for three VZAs (0, 45 and 70°) and two surface albedos (0.02 and 0.05). For these simulations, a tropospheric NO_2 column of 1.0E16 molecules/cm^2 was used. For the other parameters the default values listed in **Table 38** were used here.

For the EB we use a noise error of 15% for a tropospheric column amount of 1.0×10^{16} molec cm^{-2}, which corresponds to SNR 750, surface albedo 0.05 and SZA 45°.

5.2. Analysis results for spectral calibration

Errors in the retrieved tropospheric NO_2 column due to imperfect wavelength calibration are investigated by applying artificial wavelength shifts. These shifts are the same for the entire spectral range, 405 – 465 nm. **Figure 31** shows the bias in the retrieved tropospheric NO_2 column as a function of the applied spectral shift in nm.

The figure shows that large errors can occur when there is little NO_2 in the atmosphere. It is noted that no shift still gives a (small) bias because the retrieval method, DOMINO, is not perfect. For instance, a wavelength has to be selected where the air mass factor is calculated. Based on these results, it seems that the value of 0.002 nm mentioned in requirement S7MR-OBS-550 is reasonable. It is noted that prior to or in the DOAS fit a spectral shift can also be fitted, to further mitigate this error.

In practice, the spectral calibration is performed in the L1-2 retrieval algorithms, by fitting a shift and if needed also a stretch. An important boundary condition for this is that the instrument is spectrally stable, which is covered in requirement S7MR-OBS-560.

The requirement S7MR-OBS-550 should be applicable in-flight and for the Level 1-2 algorithms only. Providing a pre-flight a wavelength map with an accuracy of 1/10th of a spectral pixel is sufficient as a starting point.

For the EB we use a value of 2%, which was evenly distributed over random and systematic errors.

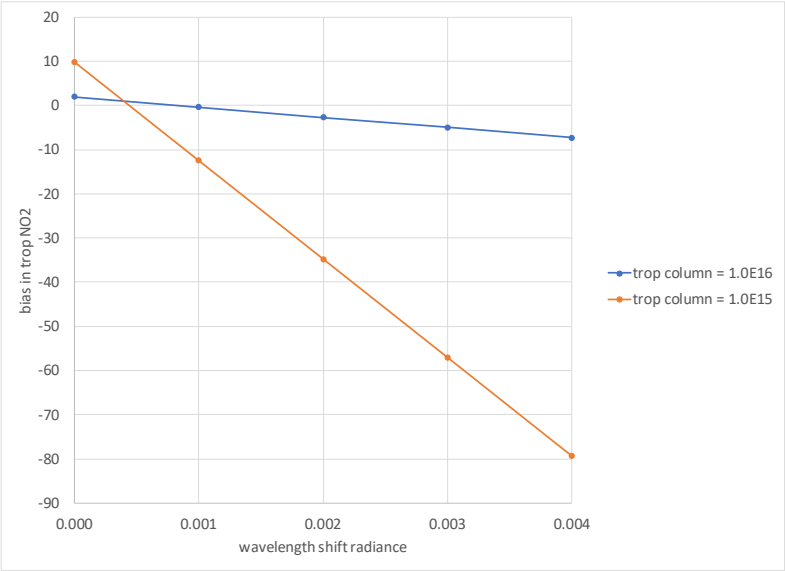

Figure 31: Percent bias in the retrieved tropospheric NO_2 column plotted as a function of the artificial wavelength shift (nm). The viewing direction is nadir and the solar zenith angle is 60 degrees. The surface albedo is 0.05 and there are no clouds or aerosols. Results are given for two values of the tropospheric NO_2 column.

5.3. Analysis results for ISRF

The following requirement on the ISRF shape was investigated and we propose to change the requirement.

S7MR-OBS-570	The ISRF shape shall be known to an accuracy better than 2.0% of the peak value of the ISRF in the spectral range Λ where the ISRF is at least 2% of the peak value.

First we considered perturbation of the ISRF, $s(\lambda_i,\lambda)$, as follows

$$s(\lambda_i,\lambda) = s^n(\lambda_i,\lambda)\left[1+a\sin^2(s\{\lambda_i-\lambda\}+p)\right]$$

where $s^n(\lambda_i,\lambda)$ is the nominal ISRF, a Gaussian or a flat topped function, *a* is the amplitude of the perturbation, *s* is a scale factor, and *p* is a phase factor (in radians). Here λ_i is the nominal wavelength of the ISRF. Next we considered the change in the retrieved tropospheric NO_2 column when perturbations are applied. **Figure 32** shows some results of this exercise, where *b* is the bias in percent of the retrieved tropospheric NO_2 column. It is assumed that the ISRF is wavelength independent. In the simulation of the reflectance the flat-topped ISRF was used (blue curve). When the same ISRF is used in the retrieval we do get a bias (2.6%) because the retrieval algorithm, DOMINO, is not perfect.

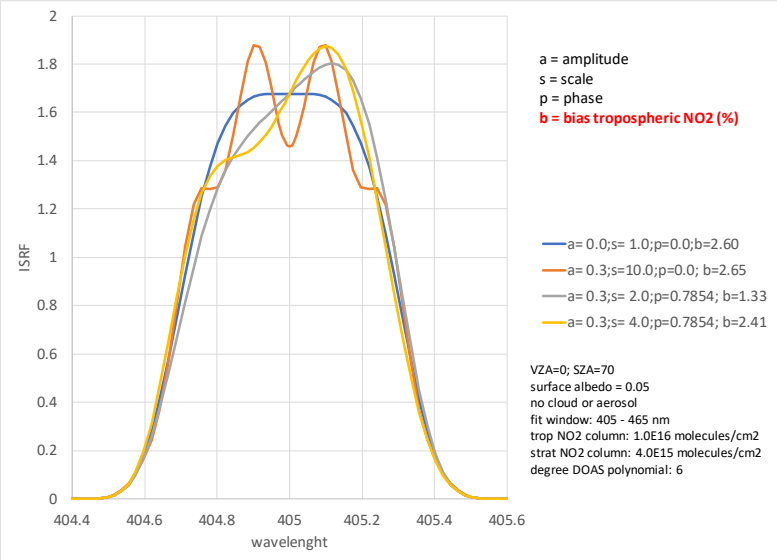

Figure 32. *Bias, b, in percent of the retrieved tropospheric NO2 column for different perturbations of the ISRF.*

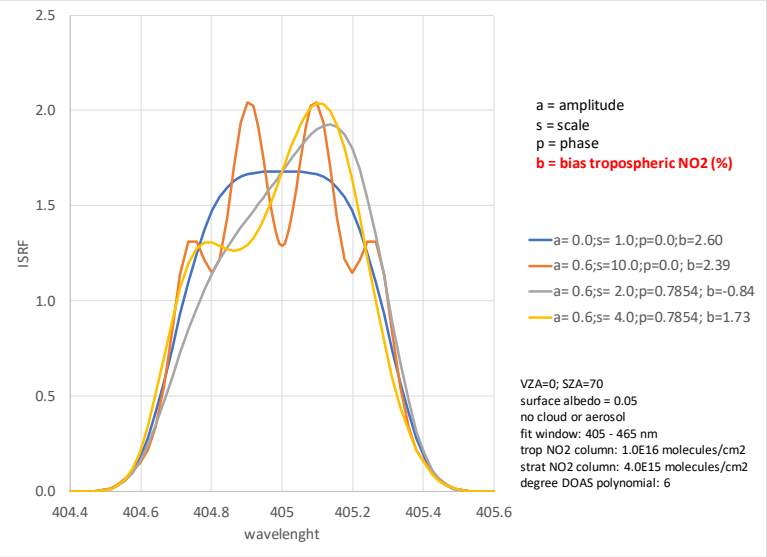

Figure 33. *Same as **Figure 32**, but for a larger amplitude, a, of the perturbation.*

Figure 32 and Figure 33 show that in this case large perturbations of the ISRF do not yield large errors in the retrieved tropospheric NO_2 column. The bias in the retrieved column is of the same order of magnitude as the bias due to the DOAS retrieval.

The perturbation in **Figure 33** are much larger than the 2% mentioned in the requirement S7MR-OBS-570, while the errors in NO_2 are acceptable. *This means that either the requirement is over specified, or wrongly specified.*

Another commonly used way to specify the ISRF shape is by requiring a certain knowledge of the FWHM. To test this approach, we compare results if we use a flat topped ISRF for the simulation and a Gaussian ISRF for the retrieval, having the same value for the FWHM.

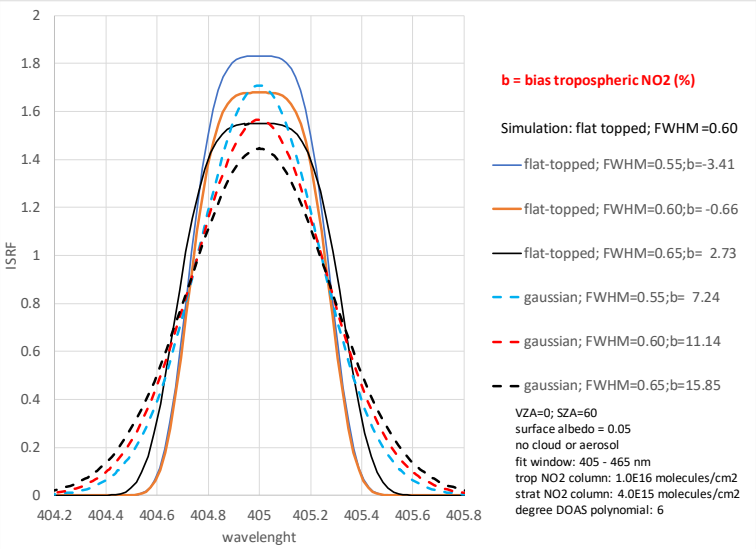

Figure 34. *Bias in the retrieved tropospheric NO_2 column when a flat-topped ISRF is used in the simulation of the reflectance spectrum and a Gaussian ISRF is used in the retrieval. Results for different values of the FWHM used in the retrieval are shown. In addition results are shown when a flat-topped ISRF is used in the retrieval.*

Figure 34 shows that a bias of 11.14% occurs when we use a Gaussian ISRF is used in the retrieval while a flat-topped ISRF is used in the simulation and both have a FWHM of 0.60 nm. Hence, just specifying the FWHM is not a good characterization of the ISRF, as it does not properly account for shape differences, in particular tails of the ISRF.

In DOMINO, a variant of DOAS, the ISRF is used to calculate an effective absorption cross section for NO_2. The effective absorption cross section, $\sigma^{eff}(\lambda_i)$, is calculated as follows

$$\sigma^{eff}(\lambda_i) = \frac{\int \sigma(\lambda) F_0(\lambda) s(\lambda_i, \lambda)\, d\lambda}{\int F_0(\lambda) s(\lambda_i, \lambda)\, d\lambda}$$

where $\sigma(\lambda)$ is the actual absorption cross section of NO_2, $F_0(\lambda)$ is the solar spectrum, and $s(\lambda_i, \lambda)$ is the ISRF for the pixel with wavelength *i*. The solar spectrum occurs here due to the so-called I_0 effect. As only integrated values of the ISRF play a role in the retrieval, it seems logical to consider moments of the ISRF.

In statistics, distribution functions are characterized by their moments, as follows (ignoring the wavelength index λ_i)
Mean

$$m = \int \lambda\, s(\lambda) d\lambda$$

Variance (standard deviation is σ)

$$\sigma^2 = \int (\lambda - m)^2 s(\lambda) d\lambda$$

Skewness

$$sk = \int \frac{(\lambda - m)^3}{\sigma^3} s(\lambda) d\lambda$$

Kurtosis (pointedness)

$$k = \int \frac{(\lambda - m)4}{\sigma^4} s(\lambda) d\lambda - 3$$

here $s(\lambda)$ is the ISRF, normalized so that its integral equals 1.0. The value of -3 occurs so that the kurtosis for a Gaussian ISRF is zero.

The mean is related to the wavelength calibration. When we have two functions $s(\lambda)$ and their moments (variance, skewness, and kurtosis) are nearly the same, the difference in the retrieved tropospheric NO_2 column will be small. In fact, it is mainly the difference in variance that determines the error in the retrieved NO_2 column. As mentioned before, the FWHM is not a good measure to characterize the ISRF because it ignores the tails if the ISRF. The standard deviation, σ, does account for such tails.

To illustrate that the standard deviation yields a better characterization of the ISRF than the FWHM we considered a simulation with a flat topped ISRF with a FWHM of 0.60 nm and a retrieval with a Gaussian ISRF and vary the FWHM of the Gaussian ISRF. Results are shown in **Figure 35**. The standard deviation for the ISRF used in the simulation is 0.1911 and the standard deviation for the ISRF used in the retrieval varies according to the blue line in **Figure 35** (right axis). The Gaussian ISRF has a standard deviation of 0.1911, equal to that for the simulation, when the FWHM of the Gaussian is 0.45. The red line then shows that the bias in the retrieved tropospheric NO_2 column is -1.1% (left axis), much smaller than the 11.1% obtained when the FWHM the simulation and retrieval are the same. Hence, ISRF shapes are nearly equivalent when the standard deviations are nearly the same. The higher moments, such as skewness and kurtosis have some influence on the retrieved NO_2 column, but their influence is of the order of 1%, which is about the same as the accuracy of DOMINO itself.

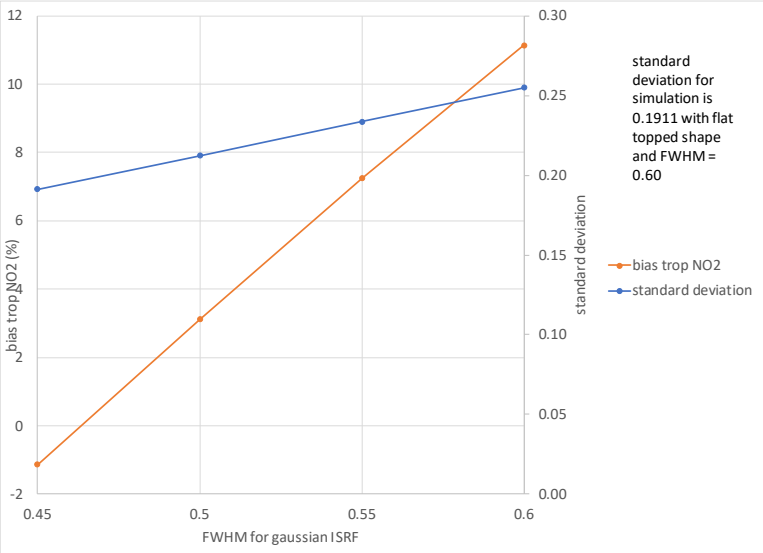

Figure 35. *Bias in the retrieved tropospheric NO2 column when a flat-topped ISRF is used in the simulation of the reflectance spectrum and a Gaussian ISRF is used in the retrieval. Bias and ISRF standard deviation are shown as a function of the FWHM. The simulation uses a flat-topped ISRF with FWHM and standard deviation 0.1911.*

The proposed new requirement is formulated assuming that the ISRF is normalized as follows

$$\int s(\lambda)d\lambda = 1$$

By requiring that the standard deviation of the ISRF is known with an accuracy of 0.01, the bias in NO2 is expected to be within 2%. It is expected that this update of the requirement will avoid a possible over specification. Furthermore, as shown in this section, specifying in term so f the standard deviation has a better physical basis.

S7MR-OBS-570	The standard deviation of the normalized ISRF shall be known to an accuracy better than 0.01

For the EB we use a 2% systematic NO_2 error corresponding to the ISRF standard deviation knowledge of 1%.

5.4. Analysis results for multiplicative radiometric errors

Multiplicative errors in the reflectance do not affect the DOAS slant column amounts, because of the polynomial used in DOAS. However, if the cloud parameters (effective cloud fraction and cloud pressure) are derived from the reflectance spectrum, multiplicative errors will have an impact through the air mass factor.

We recommend to always derive the effective cloud fraction from the VIS spectrum itself, even when the cloud pressure is retrieved from the NIR band, or when a geometrical cloud fraction is used form the cloud imager. The cloud imager could be used to determine cloud-free scenes, for which an explicit aerosol correction could be implemented.

The error is simulated by using a different cloud fraction in the simulation and retrieval. In **Figure 36** the error in the tropospheric NO_2 column is shown as a function of the error in the reflectance. Compared to the sensitivity for additive errors, the error due to multiplicative error is less. However, for certain cloud altitudes, i.e. when the cloud layer is just inside the planetary boundary layer, the error sensitivity can be significantly increased.

Requirement S7MR-OBS-610 states: The multiplicative radiometric error of the radiance measurement at the TOA shall be better than 5% in VIS including polarization sensitivity with max 60% degree of polarization. Based on **Figure 36** the 5% threshold gives rise to a bias in the retrieved NO_2 column of about 5%, because of an error in the air mass factor. This is considered acceptable.

For the EB we use a total error of 5%. Because the polarisation varies quasi randomly, the fraction random:systematic used is 0.3:0.7.

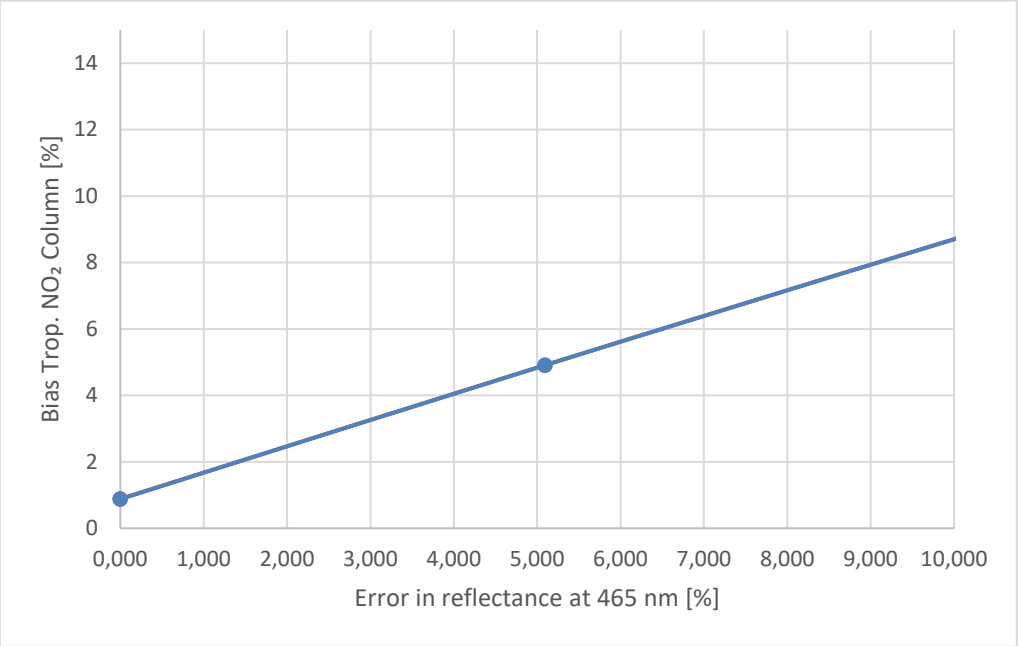

Figure 36: Bias in the tropospheric NO_2 column due to a multiplicative error in the reflectance. The tropospheric NO_2 column is 1.0E16 molecules/cm^2.

5.5. Analysis results for additive radiometric errors

We consider multiplicative and additive offsets. If DOAS is used as retrieval method, multiplicative offsets are absorbed in the DOAS polynomial, but additive offsets give rise to bias in the retrieved NO_2 column. There are variants of DOAS where one tries to compensate for such biases, but they are not considered here.

Here we estimate the bias due to additive offsets using the DOAS algorithm as implemented in DISAMAR/DOMINO. The additive offset is independent of the wavelength and it is expressed as a percentage of the radiance at a particular wavelength. Here this wavelength is chosen to be 405 nm while the fit window is 405-465 nm. Note that the differential absorption due to NO_2 is at most a few percent of the radiance. It is therefore sensitive to small errors.

The requirement S7MR-OBS-620 states: The additive error of the radiance measurement at the TOA shall be better than $2.0 \cdot 10^{11}$ photons/s/nm/sr/cm^2. Note that this offset is 1.5% of the radiance at 405 nm. **Figure 37** shows that this may lead to errors in the tropospheric NO_2 column of about 7% - 10% for a polluted atmosphere with a tropospheric column of 1.0E16 molecules/cm^2 and significantly larger at lower concentrations.

It is recommended to modify this requirement by using the gain matrices. Also, part of this error can be mitigated by fitting the Ring effects, which is not done here. Also, it should be analysed which part of this error is constant over a scene with an NO_2 plume, and hence isn't significant for plume detection.

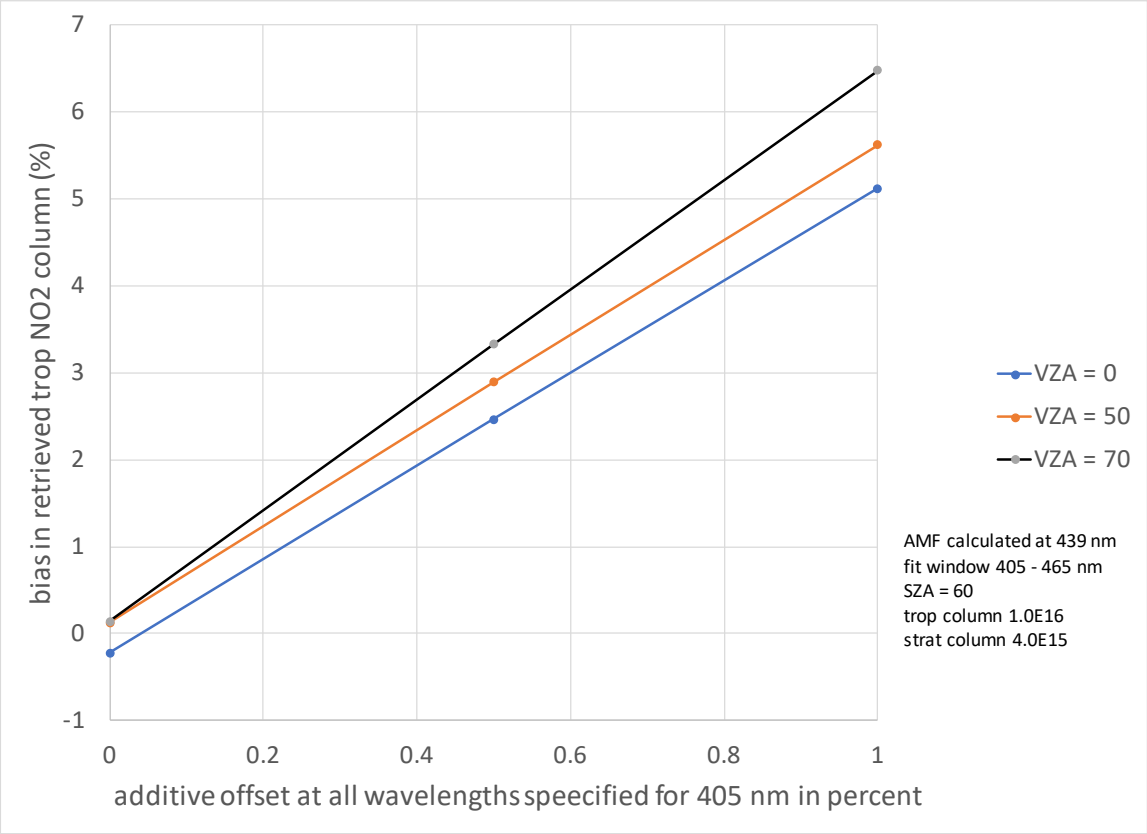

Figure 37: Bias in the retrieved tropospheric NO_2 column due to additive offsets in percent. Results are plotted for three viewing directions. Although two of the VZAs are beyond the range of this study, it shows that the dependency on VZA is not very large. Negative values mean that the retrieved NO_2 column is too small.

To test this for a realistic case, we used TROPOMI zoom measurements, for which a limited dataset is available from the commissioning phase. These measurements have a spatial sampling of approximately 1.8 x 2.6 km^2, which is comparable to the CO2M requirements. We selected a cloud-free scene over Poland for 2 March 2018, which shows a plume from the Belchatov power plant. The data were processed using a modified version of the operational processor. We processed the scene three times: with the original L1B data, with a radiance offset of $2.0 \cdot 10^{11}$ photons/s/nm/sr/cm^2 and for a radiance offset of $5.0 \cdot 10^{11}$ photons/s/nm/sr/cm^2. The original image and the difference plots are shown in **Figure 38**. From visual inspection of this figure we conclude that there is now apparent spatial correlation between the plume (top panel) and the difference plots (middle and lower panel).

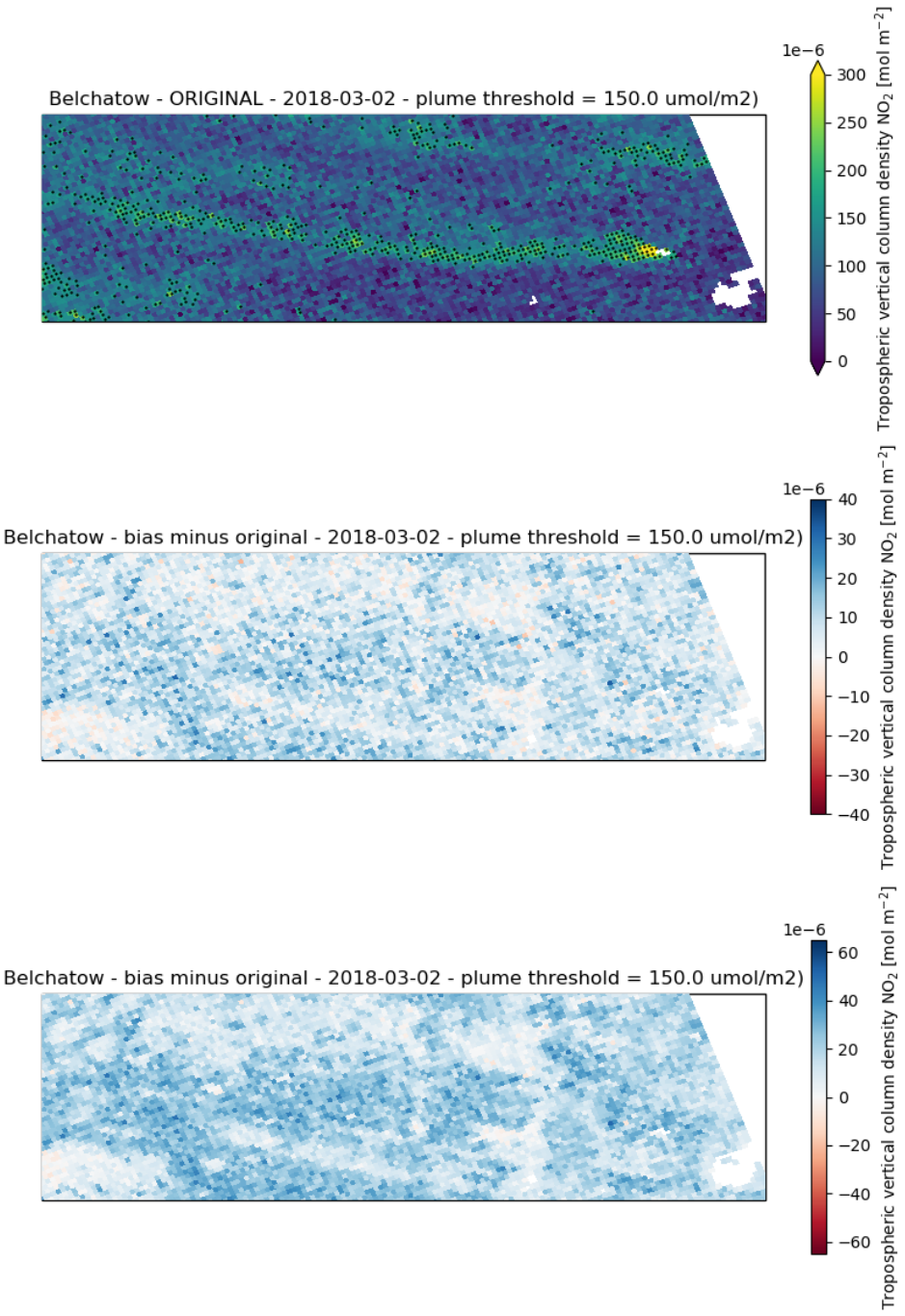

Figure 38. Top panel: TROPOMI NO_2 zoom data for an overpass over Poland on 2 March 2018. The black symbols indicate where the NO_2 column amount exceeds the threshold of 150 µmol m^{-2}. Middle panel: bias in NO_2 resulting from a radiance offset of $2.0 \cdot 10^{11}$ photons/s/nm/sr/cm^2. Lower panel: bias in NO_2 resulting from a radiance offset of $5.0 \cdot 10^{11}$ photons/s/nm/sr/cm^2. Note that 166 µmol m^{-2} corresponds to 10^{16} molec. cm^{-2}.

To identify pixels inside the plume, a simple threshold on NO_2 of 150 µmol m^{-2} (0.9 x 10^{16} molec. cm^{-2} was used. Histograms of the difference of NO_2 columns between the perturbed and original case are shown in **Figure 39**. This figure shows that for a radiance offset of $2.0 \cdot 10^{11}$ photons/s/nm/sr/cm^2 the mean error is approximately 5% and for $5.0 \cdot 10^{11}$ photons/s/nm/sr/cm^2 more than 10%.

The mean error of 5% is somewhat smaller compared to 7-10% found from synthetic cases. This may be due to the additional fitting parameters used in the TROPOMI retrievals, such as the Ring spectra, which can absorb part the error. However, this is not a large effect.

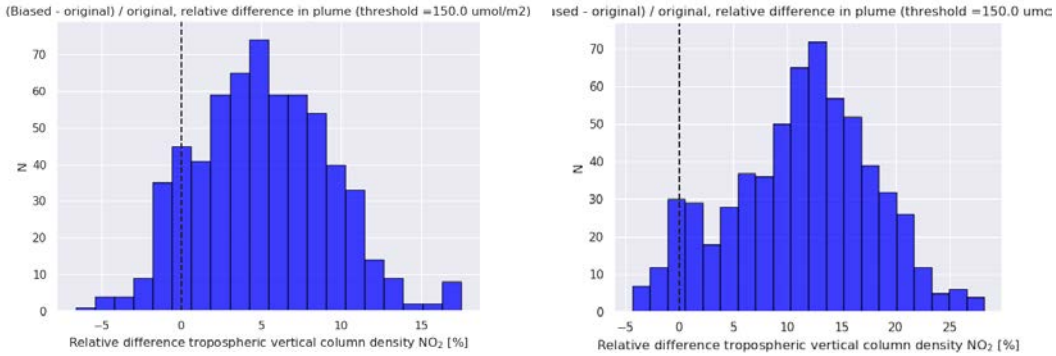

Figure 39. Histograms of the relative difference between the original and the perturbed NO_2 columns. Left panel is for a radiance offset of $2.0 \cdot 10^{11}$ photons/s/nm/sr/cm^2; right panel for $5.0 \cdot 10^{11}$ photons/s/nm/sr/cm^2.

It is recommended to modify this requirement by using the gain matrices. This give the ability to check for a wider range of errors, including wavelength dependent offsets.

For the EB we use 7% error, in line with the requirement. We estimate that half of this error can be calibrated out through an offset correction.

5.6. Summary and conclusions

Assessments of the MRD requirements for the NO_2 observations of CO2M are presented. This has strong heritage from other missions, including S5P/TROPOMI, S4/UVN and S5/UVNS. However, the primary use of the NO_2 data is different than for these heritage missions; for CO2M the primary use is plume detection. For this application observation requirements have to be formulated, especially regarding the systematic errors. We presented a new analysis using TROPOMI zoom data, to show that that the error in the tropospheric NO_2 column doesn't show spatial correlation with the NO_2 column itself.
For several of the requirements we propose modifications, which often is an update of the values. For the ISRF we propose a new approach, which we consider a relaxation compared to the original requirement. Furthermore, we want to highlight the importance of the SNR requirement. The requirement for SNR is currently set at 750 for the provided reference scenario specified for 2% surface albedo. This results in errors in the tropospheric NO_2 column of approximately 1.5 10^{15} molec. cm^{-2}. A further improvement of the SNR towards 1000 for the provided reference spectrum would enable the detection of even smaller plumes, which is judged to be very important for the envisaged application of obtaining CO_2 emission from observed XCO_2 plumes.

6. Analysis results for SIF

To analyse the sensitivity of the SIF retrieval to the requirements for CO2M specified in the MRD, we have made an assessment based on available literature, first-order considerations on the expected impact of the instrument-related source on the SIF retrieval and linear error analysis studies using the UoL algorithm. We assume that the SIF retrieval approach will be based on the change of the depth of known solar lines **/Frankenberg et al., 2011/**.

Furthermore, we assume that systematic errors can be substantially reduced (to 10% of its uncorrected value) by evaluating areas without vegetation such as deserts, bare areas and snow/ice covered areas. This approach has been successfully introduced for the GOSAT SIF retrieval to compensate a non-linearity effect in the detector response which leads to a zero-level offset signal and thus to a SIF bias (**/Frankenberg et al., 2011/**). A similar approach is used for most current SIF retrievals.

There **MRDv1.0** for CO2M gives no requirements on random and systematic errors for SIF. MRDv.2 now states a requirement on the precision of the SIF retrieval (S7MR-DAT-040) of better than 0.7 mW/m^2/sr/nm. Assuming a typical SIF signal of 1 mW/m^2/sr/nm, this represents a single-sounding precision of 70% ensuring the usefulness of the inferred SIF data. This is also roughly consistent with previous missions such as GOSAT /**Frankenberg et al., 2012/.**

Although not a requirement, MRDv2.0 states that systematic errors of the SIF retrieval shall not exceed a value of 0.2 mW/m^2/sr/nm (after applying above correction), which reflects the need to sufficiently well correct the SIF effects in the XCO_2 retrieval and the potential usage of the retrieved SIF to constrain the gross primary productivity **/CO2M-REB TN-3000, 2019/**.

The main spectral range for the SIF retrieval uses a wavelength range with wavelength smaller than the O_2 A Band. SIF can also be retrieved from the larger wavelength end of the O_2 A Band, but here the SIF signal is smaller and there are significant interference from O_2 absorption lines. Consequently, this second wavelength range is commonly used for verification purposes only and we focus here on the SIF retrieval from the smaller wavelength range only.

6.1. Signal-to-noise ratio (SNR)

The noise-related errors (1-σ and single sounding) for the SIF retrievals have been estimated to be between 0.5 – 1 W/m^2/sr/micron for GOSAT and 0.3 – 0.5 W/m^2/sr/micron for OCO-2. Both, OCO-2 and GOSAT have higher spectral resolution than CO2M. The CO2M mission has comparable SNR to OCO-2 and higher SNR as GOSAT. However, CO2M covers a larger spectral range in the NIR band providing extra solar lines that can be used for the SIF retrieval.

To evaluate the impact of the measurement noise on the SIF retrieval, we have simulated CO2M spectra with the UoL algorithm according to the specifications from the MRDv2.0. Noise has been simulated using **Eq. 1** from **Sect. 4.3.1** with the parameters given in **Table 7**.

The spectra have been calculated for a solar zenith angle of 30° and nadir view and aerosol optical depth of 0.1. To obtain a range of radiance levels of the simulated spectra, we have used values for surface albedo between 0.1 and 0.7 varied in steps of 0.1. In addition, we have used a very dark surface with albedo of 0.05.

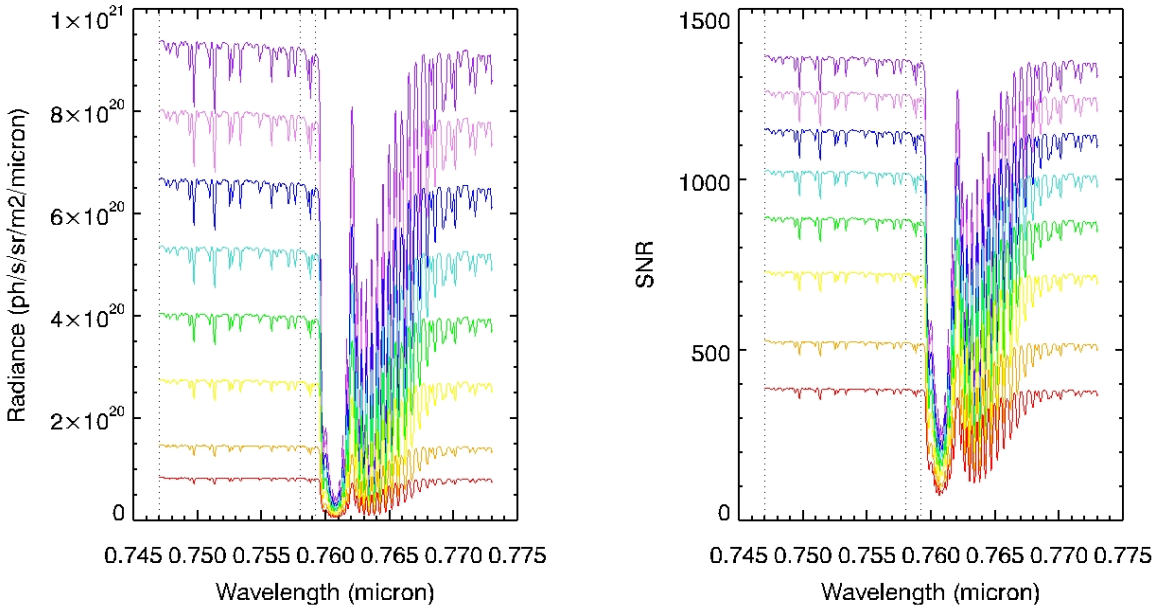

Figure 40: Simulated CO2M radiance spectra (left) and Signal-to-noise SNR (right) in the NIR used to evaluate the SIF precision error. The surface albedo has been varied between 0.1 (orange line) and 0.7 (purple line) in steps of 0.1. Additionally, albedo of 0.05 has been used (red line). The dotted lines indicate range used for the CO2M SIF retrieval (large range) and for the OCO-2 SIF retrieval (small range)

To evaluate the SIF precision, we have applied a SIF retrieval over the spectral ranges shown in **Figure 40**. The retrieval uses a fast non-scattering forward model that only evaluates Lambert-Beer law to account for atmospheric absorption by O_2. The state vector of this SIF retrieval includes zero level offset (equivalent to SIF), dispersion and surface albedo (equivalent to multiplicative scaling in this case). The SIF retrieval precisions has been inferred from the calculated a posteriori error covariance matrix **S** given by:

$$\mathbf{S} = \left(\mathbf{K}^{\mathrm{T}}\mathbf{S}_{\mathbf{e}}^{-1}\mathbf{K} + \mathbf{S}_{\mathbf{a}}^{-1}\right)^{-1}$$

Specifically, we have taken the square root of the variance of the zero-level offset given by corresponding diagonal elements of **S**.

The inferred estimates of the SIF retrieval precision for the smaller and full window (as indicated in **Figure 40**) is given in **Figure 41**. As expected, we find that the precision is much improved due to the enhanced spectral range for the retrieval. We find a modest increase in the precision error with radiance level due to the increase of the measurement noise. Overall, the SIF retrieval precision as a result of measurement noise is well within the precision

requirement stated in MRDv2.0. However, there are additional error components that will contribute to the overall precision of the SIF retrieval as will be discussed later on.

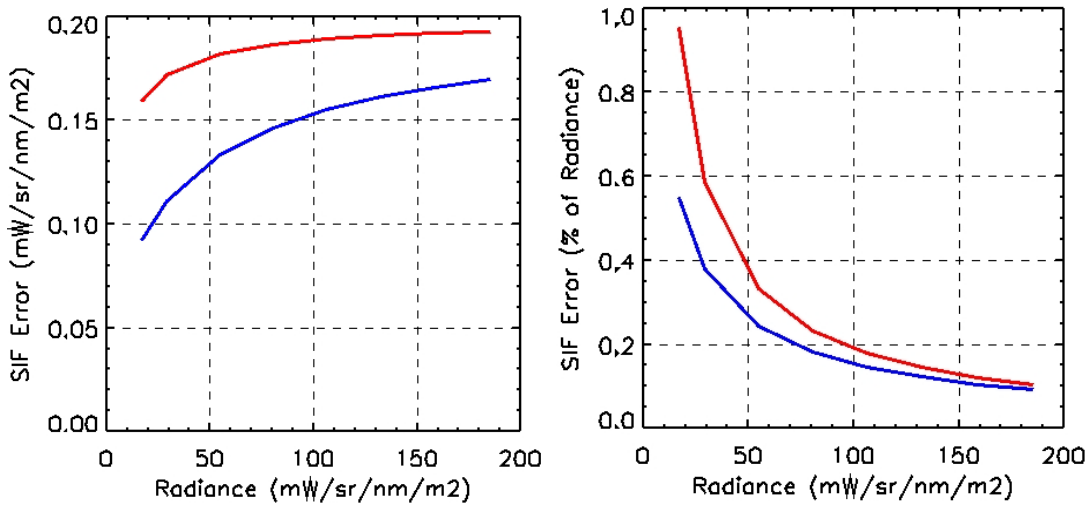

Figure 41: Estimated precision of the SIF retrieval as a function of continuum radiance level in radiance units (left) and relative to continuum radiance (right). The red line gives the precision when using the smaller (OCO-2 like) wavelength range and the blue line indicates a retrieval that uses the larger range as shown in **Figure 40**.

To evaluate the impact of the SIF error on the XCO_2 retrieval, we have computed the spectral radiance signal from the Jacobian for SIF $\mathbf{K_{SIF}}$ (corrected for atmospheric absorption) and the assumed SIF error σ_{SIF} and combined it with the Gain matrix $\mathbf{G_{CO2}}$ of the XCO_2 3-band retrieval to infer the associated error σ_{XCO2} in XCO2:

$$\sigma_{XCO2} = \mathbf{G_{CO2}} \cdot \mathbf{K_{SIF}} \cdot \sigma_{SIF}$$

This has been carried out for the 10 reference scenarios and the resulting XCO_2 errors are given in **Figure 42** for SIF errors representing the SIF precision requirement (blue symbols) and for SIF errors estimated from the measurement noise according to the requirements (green symbols). The requirement allows relatively large precision errors of 70% of the SIF signal and accordingly the CO_2 retrieval uncertainty is as large as 0.9 ppm in the most extreme case. A realistic estimate of the SIF precision based on the measurement noise is much and the subsequent XCO2 errors are reduced to typically less than 0.4 ppm when using the current estimate of the measurement noise.
Note that this statement is related to the derivation of XCO_2 errors from a gain matrix approach using the precision estimate of SIF. This means that it is a random error component. This approaches uses a CO_2 gain matrix so that this value is dependent on the setup of the XCO_2 retrieval, for example for IUP/FOCAL retrieval one might find a different value. Here, a setup that is similar to the UoL GOSAT "C3S setup" has been used, where the retrieval does not retrieve SIF itself in the CO_2 retrieval but retrieves a zero level offset in the O_2 A Band. Also, the value of 0.4 ppm is the maximum value obtained for any of the scenarios. Clearly, for an overall XCO_2 error budget one would use a more representative

value, for example the mean error, which is 0.22 ppm. In principal, one could consider this error to be part of the interference error in the XCO_2 error budget.

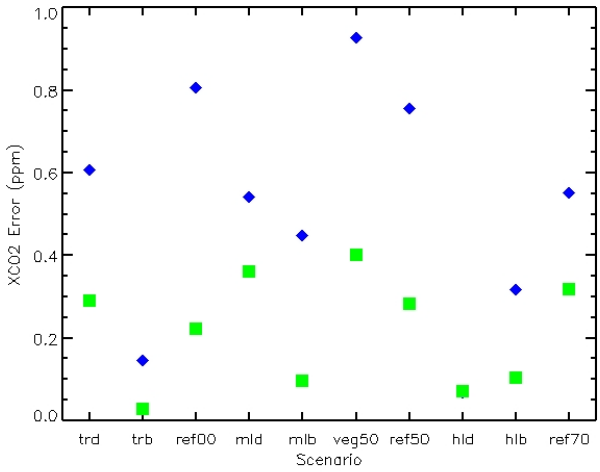

Figure 42: Estimated errors in the XCO_2 retrieval from uncertainties in SIF for the 10 reference scenarios. Blue symbols are for a SIF error of 70% of the SIF signal (assumed to be 1% of continuum radiance) which is representing the requirements on the SIF precision. Green symbols are for SIF precision estimated from the measurement noise.

6.2. Radiometric: Multiplicative

The absolute Radiometric Accuracy (ARA) (S7MR-OBS-180) requirement given in the MRD is 3% of the continuum radiance. As mentioned above, the SIF signal is derived from the depth of solar lines which will not depend on the absolute, multiplicative gain. Therefore, the effect of absolute radiometric calibration will effectively cancel out. Since small residual errors might persist, a small error of 0.01 mW m^{-2} sr^{-1} nm^{-1} might still be present. However, overall, the requirement on multiplicative, absolute radiometric accuracy has little significance for the SIF retrieval.
The MRD also specifies several radiometric relative error sources:

- ESRA, the Effective Spectral Radiometric Accuracy
- RSRA, the Relative Spectral Radiometric Accuracy
- RXRA, the Relative Spatial Radiometric Accuracy

ESRA covers errors resulting from erroneous “spectral features” including polarization, non-linearity, straylight, diffuser speckles etc. Polarisation will be small and relatively homogenous across the retrieval range and thus be well compensated by the multiplicative factor. Non-linearity can also be expected to be small in the NIR. Thus, the analysis for ESRA has focussed on straylight. Straylight has been calculated for the 10 reference scenes (see **Table 36**) using a straylight kernel provided by ESA (B. Sierk, private communication). This straylight kernel has been normalised for a total Internal Scatter (TIS) of 0.9%, which means that 99% of the light reaches the centre pixel while 1% is scattered away. This means

that even for a homogenous and clear scene, straylight will lead to a smoothing of solar lines and thus impact the SIF retrieval.

We have used linear error analysis to infer the error in the SIF retrieval. Here we use the scene-dependent gain matrix **G** for the SIF retrieval calculated with the UoL retrieval algorithm to translate a spectral error from straylight into a SIF error. The resulting errors in the SIF retrieval are given in **Figure 43**. Green symbols show the SIF error for a homogeneous and clear scene. Errors increase from about 0.1 mW/sr/nm/m^2 for low radiance values to 0.45 mW/sr/nm/m^2 for high radiance values in a well predictable manner as long as the straylight kernel itself remains constant.

In addition, we also simulated straylight effects in the presence of cloudy pixels. We have assumed that half of the field of view is cloud and one half is cloud-free. This is shown in blue symbols. In this case, we find that SIF errors show a much larger scatter and will be less correctable. This can be avoided by more rigorous filtering for clouds.

We assign a systematic error of 0.4 mW/sr/nm/m^2 and a random component of 0.1 mW/sr/nm/m^2 to this error source.

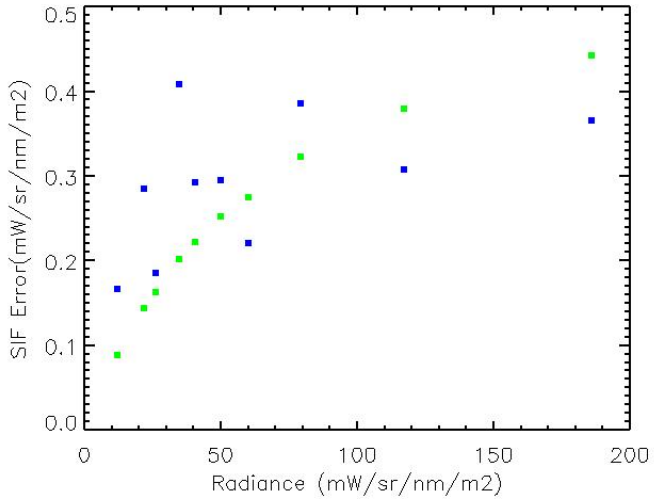

Figure 43: SIF error from straylight as a function of continuum radiance level. The green symbols are for a clear (and homogenous) scene while the blue symbols are for a scene that is half clear and half cloudy.

RSRA covers relative intra-band radiometric errors, which are required to be less than 0.5% peak-to-peak according to MRDv2.0. In the worst case, this could translate into a calibration error of 0.5% in the centre of a solar line with no error in the continuum. This would then lead to an estimated SIF error of 0.5% of the continuum signal. In reality, it is unlikely that intra-band radiometric errors would match the shape of a solar line and we can safely assume this is a large overestimate. Furthermore, assuming that only a fraction is truly systematic and that we can conduct the correction described above then the resulting error is well within the requirement for the SIF bias.

RXRA covers radiometric errors across the swath and is not further discussed here. Potential errors in SIF could be well evaluated over homogenous non-vegetation surfaces (e.g. ice, desert or ocean sunglint) and the bias correction procedure mentioned above should effectively minimise this error source.

6.3. Radiometric: Additive (ZLO)

The requirement for the additive radiometric errors or Zero Level Offsets (ZLO) for the NIR band is given as 8.4 x 10^9 ph/s/nm/cm^2/sr in MRDv1.0 (S7MR-OBS-230) which has been reduced to 6 x 10^9 ph/s/nm/cm^2/sr in MRDv2.0. An uncorrected additive offset will linearly lead to an error in the retrieved SIF signal as the SIF signal itself is also treated as an additive offset. Therefore, this will lead to a SIF bias of 0.02 mW m^{-2} sr^{-1} nm^{-1} (for MRDv1.0) or 0.015 mW m^{-2} sr^{-1} nm^{-1} (MRDv2.0), respectively.

6.4. Instrument Spectral Response Function (ISRF)

The MRD of CO2M provides requirement for the ISRF for homogeneous scenes. S7MR-OBS-110 states a knowledge requirement of better than 2% of the peak value of the ISRF and S7MR-OBS-130 gives a requirement on the ISRF FWHM knowledge of better than 1%.

To estimate the error from the FWHM knowledge requirement, we have perturbed the ISRF (assumed to be Gaussian-shaped) of the simulations for the reference scenes by 1% but maintained the Gaussian shape. The resulting error in the ISRF is shown **Figure 44**. We have also perturbed the shape of the ISRF using eq. 6 from **/Landgraf et al., 2017a/** with parameters k_0=2, a_1=0.03, k_1=0.09 and a_2=k_2=0 (see right panel in **Figure 44**).

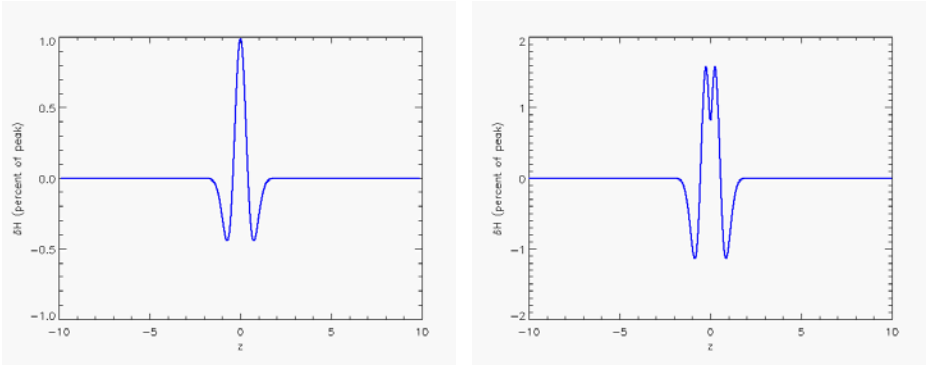

Figure 44: Left: Relative error in a Gaussian-shaped ISRF when perturbing the FWHM by 1%. Right: Relative error in the ISRF when perturbing a Gaussian-shaped ISRF. z is spectral sampling in units of FWHM.

The derivation of errors in the SIF retrieval from perturbing the FWHM or shape of the ISRF has been derived using linear analysis. The results are shown in **Figure 45**. We find SIF errors vary between 0.2 to 0.6 mW m^{-2} sr^{-1} nm^{-1} for the investigated ISRF shape error and

between 0.06 and 0.25 mW m^{-2} sr^{-1} nm^{-1} for FWHM error. SIF errors show a clear relationship with continuum radiance level which should allow a good correction of the SIF error terms.

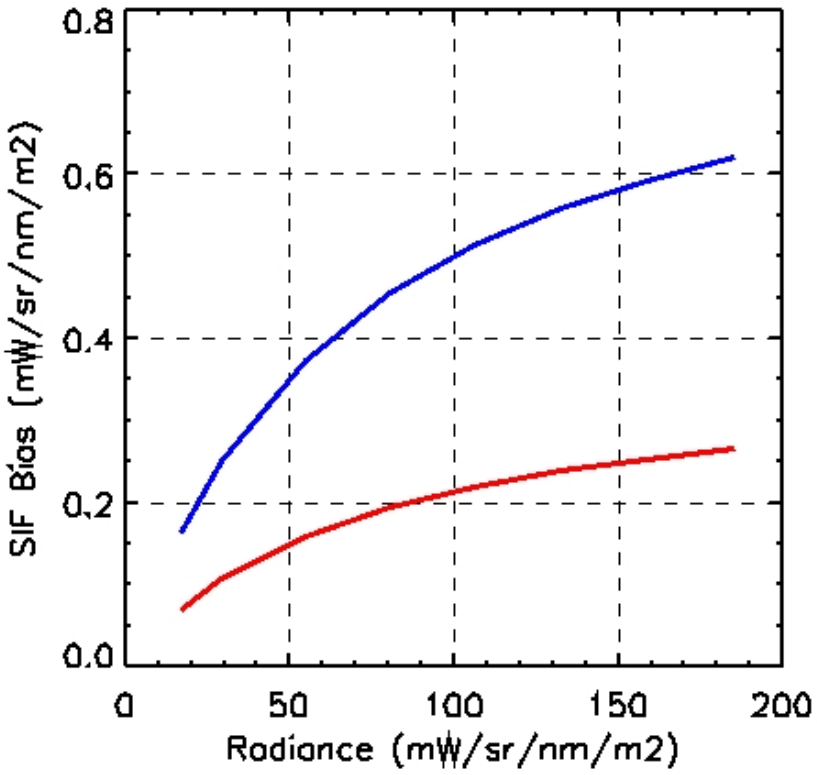

Figure 45: SIF error from uncertainties in the ISRF shape (blue) and FWHM (red).

Heterogeneous scenes may also result in (unknown) ISRF variations caused by inhomogeneous slit illumination. According to S7MR-OBS-120, the requirement for ISRF variations is 1.5% of the peak value of the ISRF. Following the consideration for S7MR-OBS-110 (for homogenous scenes), we assign an error of 0.75% of the continuum level. Errors from inhomogeneous scenes will have a large random fraction. However, it is likely that the requirement for heterogeneous scenes will be largely over-fulfilled by the CO2M instrument due to the planned implementation of a hardware component to mix the scene illumination. This would probably render the impact heterogeneous scene on the ISRF negligible.

6.5. Spectral calibration

The MRD requires a spectral knowledge of 1/20 of a detector pixel (S7MR-OBS-090) corresponding to 2×10^{-6} μm (for the required Spectral Sampling Ratio of 3).

To evaluate this requirement, we have simulated the 10 reference spectra but with a perturbed dispersion. This perturbation uses a second order polynomial which leads to a maximum wavelength error of 2×10^{-6} μm (see **Figure 46**) over the spectral range of the SIF retrieval. Note that the SIF retrieval only fits a linear dispersion so that this applied spectral error can only be partly compensated in the retrieval.

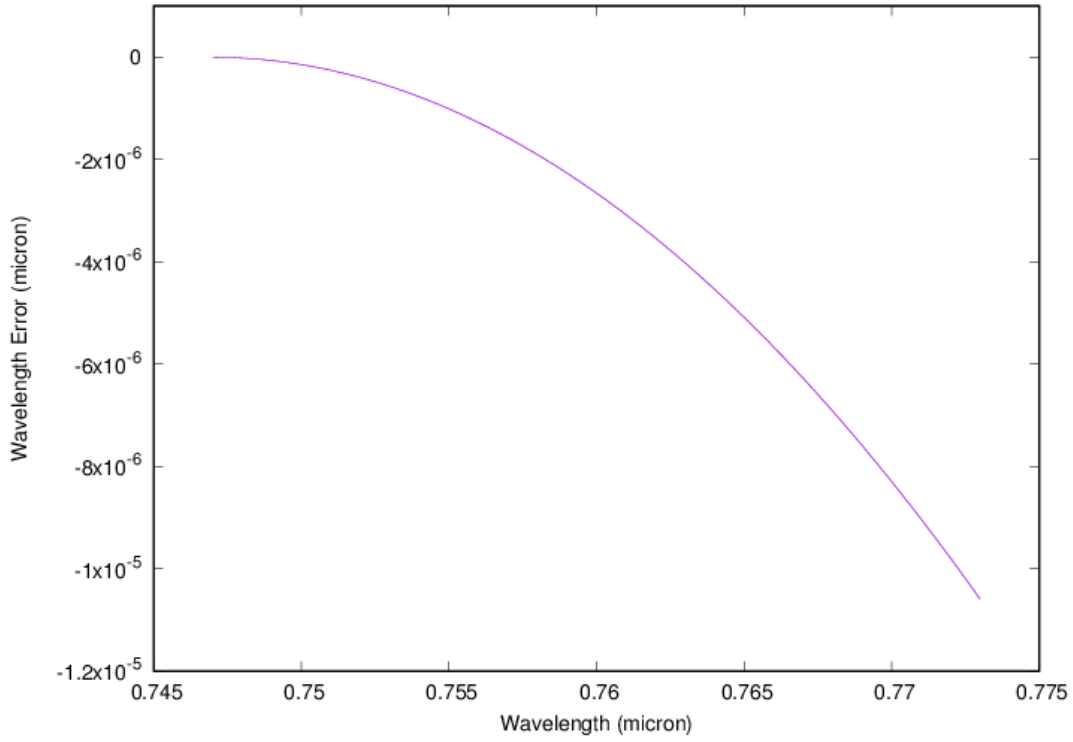

Figure 46: Wavelength error introduced by perturbing the dispersion with a second order polynomial such that the maximum wavelength error equals 2×10^{-6} μm over the SIF window (between 0.747 and 0.759 μm)

The error in the SIF retrieval from an error in the spectral calibration has been inferred using linear error analysis and is shown in **Figure 47**. We find that he SIF error is small in all cases and it will not represent a significant contribution to the error budget.

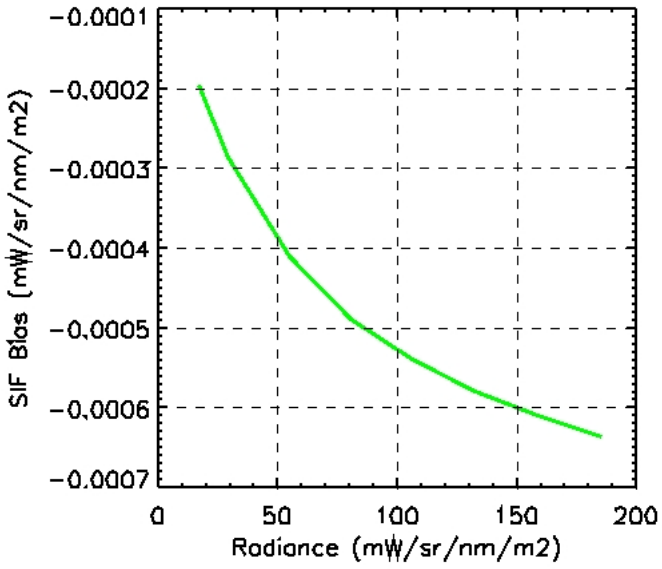

Figure 47: SIF errors from spectral calibration uncertainties as a function of continuum radiance.

6.6. Summary and conclusions

The CO2M requirements have been analyzed for the retrieval of Solar Induced Fluorescence SIF based on available literature, first-order considerations and on linear error analysis using the UoL retrieval algorithm. The results are assessed against the requirements given in the MRD for the precision of the SIF retrieval of better than 0.7 mW m^{-2} sr^{-1} nm^{-1} and for systematic errors of less than 0.2 mW m^{-2} sr^{-1} nm^{-1}. The considered CO2M requirements include SNR, multiplicative radiometric gain, additive zero level offset, relative radiometric gain, ISRF, spectral calibration errors. The analysis show that it can be expected that the random errors from measurement noise are much lower than the requirements. The most significant other error sources are ISRF uncertainties and straylight contributions. If we assume that both error sources can be well corrected using SIF-free retrieval over bare and snow areas then systematic errors will reduce to below the bias requirement. However, this assumes that ISRF errors and straylight characteristics does only slowly change (or in a well predictable manner) over time. Also, clouds within the field of view can contribute additional, more random straylight which can not be easily corrected.

7. Reference cases for Aerosols from the MAP instrument

We use three aerosol cases that represent different atmospheric scenes in this requirement study. In all cases, we assume a bimodal lognormal size distribution of aerosols consisting of a coarse and a fine mode. All of the fine-mode particles are assumed spherical while the coarse mode is a mixture of spheroids and spheres. The aerosol particles of each mode are distributed vertically following a Gaussian distribution parametrized by a mean height and a full width at half maximum (FWHM). The latter is fixed at 2 km. The size distribution, parametrized by the effective radius and effective variance, is assumed constant with height. Case 1 represents boundary layer aerosols in which both modes are located at 1 km height. The coarse mode of Case 2 is representative of an elevated cirrus layer at 8 km. In Case 3, the coarse mode aerosols are located at an intermediate height of 4 km and the size of the fine-mode particles are slightly greater than in Case 1 or 2. For each aerosol case, we study the effect of changing the aerosol column concentration. This is done by varying the fine-mode aerosol optical thickness in Case 1, or by varying the coarse-mode optical thickness in Case 2 and Case 3, to 5 different values (see **Table 27**). **Figure 48** provides the sketches of the aerosol height distributions in Case 1, 2 and 3.

To take the Earth surface reflection into account, we consider a 'vegetation' and a 'soil' type surface. They are Lambertian surfaces with albedo (0.13, 0.30, 0.26) for soil and (0.44, 0.23, 0.06) for vegetation at 3 wavelengths (765, 1600, 2000 nm). Solar zenith angle (SZA) is fixed to either 30 or 60 degrees. Given the variety in aerosol cases, optical thickness (τ_{tot}) values, surface types, and SZAs, there is a total of 60 scenarios, based on which the requirements are derived.

Table 27: Aerosol properties adopted in study cases 1 and 2.

Aerosol parameter	**Case 1**		**Case 2**	
	fine mode	coarse mode	fine mode	coarse mode
effective radius [micron]	0.12	1.6	0.12/0.2	1.6
effective variance	0.2	0.6	0.2	0.6
spherical fraction	1.0	0.05	1.0	0.05
ref. index @ 765nm	(1.5,10-7)	(1.53,2.54·10-3)	(1.5,10-7)	(1.53,2.54·10-3)
ref. index @ 1600nm	(1.5,10-7)	(1.40,1.56·10-3)	(1.5,10-7)	(1.40,1.56·10-3)
ref. index @ 2000nm	(1.5,10-7)	(1.30,2.00·10-3)	(1.5,10-7)	(1.30,2.00·10-3)
layer width (FWHM) [m]	1000	1000	1000	8000/4000
layer width (FWHM) [m]	2000	2000	2000	2000
optical thickness @ 765nm	0.05, 0.1, 0.15, 0.25, 0.5	0.02	0.2	0.02, 0.04, 0.06, 0.10, 0.15

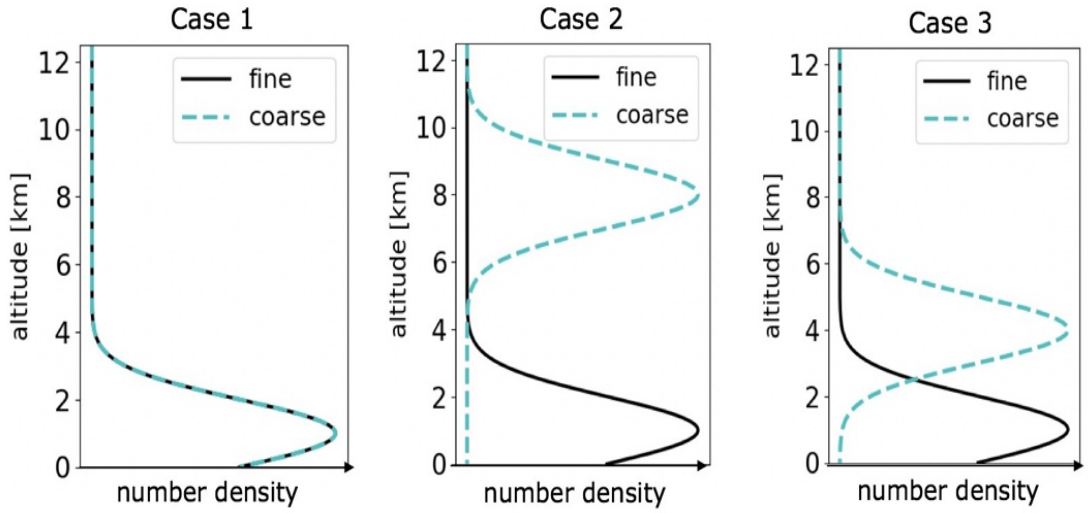

Figure 48: Sketches of the vertical distribution of the coarse- and fine-mode aerosols in Case 1, 2 and 3.

8. Analysis results for Aerosols from the MAP instrument

This chapter addresses the requirements for the Multi-Angle-Polarimeter (MAP) for aerosol and cirrus cloud observations in support of the CO_2 monitoring (CO2M) mission. The presence of aerosol and cirrus leads to scattering that modifies the atmospheric light path and so the depth of telluric absorption lines in the spectral radiance. The MAP collects the necessary information on aerosol properties to describe the light path in the forward simulation of measurements and so helps to mitigate aerosol induced errors in the XCO_2 product. Therefore, MAP observations as a part of the CO2M mission are required to improve the accuracy of the mission products. In this Section, we derive the requirements for the MAP using study cases, where we consider multiple geophysical and atmospheric scenarios as presented in **Sect. 7**.

8.1. Measurement setups

The MAP provides radiance and polarization (degree of linear polarization or DLP) measurements at multiple wavelengths and at multiple observation/viewing zenith angles (VZA). The composition of these measurements is determined by the MAP setup, which is the subject of this requirement study.

Regarding the setup for the CO_2 instrument (spectrum sizing point B of the CO2M-spectral sizing study), the relevant aspects are given in **Table 28** and

Table 29. We employ the noise model in which the signal-to-noise ratio (SNR) of the top-of-atmosphere

radiance *I* follows

$$SNR = \frac{AI}{\sqrt{AI + B^2}}$$

For each spectral window, the coefficients A and B are provided in the Table 29 and 30**.** Here, the different noise specification belong to different instrument settings as they have changed during the course of the project, where Table 30 reflects the settings as specified in Sec. 4. The different instrument settings lead only to marginally different results, as will be shown below.

Table 28: Setup of the CO_2 instrument following SRONCSS-TN-2016-002.

	units	NIR	SW1	SW2
Spectral band width	nm	747-773	1590-1675	1993-2095
Spectral resolution	nm	0.1	0.3	0.57
Spectral oversampling ratio	-	3.14	3.14	3.29
A	(s cm^2 nm sr)/ ph.	4.47 E-08	2.29 E-07	3.91 E-07
B	-	400.7	577.3	568.9

Table 29: Setup of the CO_2 instrument using settings 2 (see also Sec 4).

	units	NIR	SW1	SW2
Spectral band width	nm	747-773	1590-1675	1990-2095
Spectral resolution	nm	0.12	0.30	0.35
Spectral oversampling ratio	-	3	3	3
A	(s cm^2 nm sr)/ ph.	2.0E-08	1.32E-7	1.54E-07
B	-	140	450	450

8.2. State vector definition

For the data reduction of the CO2M mission, we retrieve aerosol properties, together with surface attributes, and the total columns of CH_4, H_2O and CO_2. We take the input vertical profiles of the trace gases as a given and retrieve the total columns via scaling factors. Here, the prior and first guess of the scaling factor for each gas species are always 1.0, corresponding to the input total column. The majority of aerosol properties as given in **Table 27** are included in the state vector; there are only 4 aerosol parameters that are not retrieved. These are the fraction of spherical particles and the layer height of the fine-mode, and layer width for both modes. We assume that non-spherical particles are primarily dust particles which belong the coarse mode. Most critical assumption is that the fine model is located in the boundary layer. For example, smoke includes fine mode particles located also at higher altitudes. To evaluate the statistical relevance of corresponding induced errors, we propose to perform ensemble analysis for global measurement data sets. For the time being, in our retrieval we consider that the four parameters are known and are fixed to the true values. Apart from the aerosol parameters, the MAP state vector also contains surface BRDF and BPDF parameters.

8.3. Linear error analysis

We compute the error in XCO_2 by linearly propagating the measurement errors of MAP and of the CO_2 instrument (spectrometer), taking the prior errors into account. This is done in a two-step approach. The first step represents the aerosol retrieval using MAP and the second step corresponds to the XCO_2 retrieval using the prior knowledge of aerosol from MAP. It follows that the derived XCO_2 error reported here is the aerosol-induced error, and it includes the random and systematic error components. In this framework, the error of the retrieved aerosol properties comprises the part that comes from the prior errors and the part that is propagated from the MAP measurement errors. The error component due to the prior uncertainties is formulated as follow

$$\boldsymbol{S}_{aer}^{sm} = (\boldsymbol{G}_{MAP}\boldsymbol{K}_{MAP} - \boldsymbol{I})\boldsymbol{S}_{a,MAP}(\boldsymbol{G}_{MAP}\boldsymbol{K}_{MAP} - \boldsymbol{I})^T \quad \text{(E8.1)}$$

while the error component due to the measurement errors is written as

$$\boldsymbol{S}_{aer}^{ns} = \boldsymbol{G}_{MAP}\boldsymbol{S}_{y,MAP}\boldsymbol{G}_{MAP}^T \quad \text{(E8.2)}$$

$\boldsymbol{S}_{a,MAP}$ is the covariance matrix of the MAP prior error. The off-diagonal elements are zero and the diagonal elements consist of the squared prior errors of the state vector elements, which include aerosol parameters. The prior errors of these aerosol parameters are assumed to be approximately 100% of their prior values. $\boldsymbol{S}_{y,MAP}$ is the covariance matrix of the MAP measurement error. The diagonal elements consist of the squared radiometric and the polarimetric (degree of linear polarisation) errors. We assume no correlation among the measurements. $\boldsymbol{K}_{MAP}$ is the Jacobian matrix that describes the sensitivity of the MAP measurements to changes in the MAP state variables. $\boldsymbol{K}_{MAP}$ is calculated for each scenario and for a particular MAP measurement setup. $\boldsymbol{G}_{MAP}$ is the gain matrix that relates the MAP measurement errors with the noise in MAP state parameters and it is formulated as

$$\boldsymbol{G}_{MAP} = (\boldsymbol{K}_{MAP}^T\boldsymbol{S}_{y,MAP}^{-1}\boldsymbol{K}_{MAP} + \boldsymbol{S}_{a,MAP}^{-1})^{-1}\boldsymbol{K}_{MAP}^T\boldsymbol{S}_{Y,MAP}^{-1} \quad \text{(E8.3)}$$

The total error on the retrieved aerosol parameters is then represented by the sum of $\boldsymbol{S}_{sm}$ and $\boldsymbol{S}_{ns}$, i.e.

$$\boldsymbol{S}_{aer}^{tot} = \boldsymbol{S}_{aer}^{ns} + \boldsymbol{S}_{aer}^{sm} \quad \text{(E8.4)}$$

The total aerosol uncertainties from Eq. 7.4 are then passed on to the CO_2 retrieval step. At this stage, they are mapped into spectrometer measurement errors using the CO_2 Jacobian matrix for the aerosol parameters $\boldsymbol{K}_{CO2,aer}$, and the measurement errors are in turn mapped into the errors on the CO_2 state variables using the CO_2-instrument gain matrix $\boldsymbol{G}_{CO2}$. Mathematically, this error propagation is expressed as

$$\boldsymbol{S}_{CO2}^{aer} = \boldsymbol{G}_{CO2}\boldsymbol{K}_{CO2,aer}\boldsymbol{S}_{aer}^{tot}\boldsymbol{K}_{CO2,aer}^T\boldsymbol{G}_{CO2}^T \quad \text{(E8.5)}$$

The XCO_2 error reported in this document follows from taking the square root of the diagonal element of $\boldsymbol{S}_{CO2}^{aer}$ that is associated with the CO_2 column concentration. This approach of linear error analysis mimics as close as possible the joint retrieval of aerosol and CO_2 using MAP and spectrometer simultaneously.

8.4. Requirements

We investigate requirements for three aspects of the MAP observations, i.e. the measurement accuracy (radiometric and polarimetric uncertainties), number of viewing angles, and wavelength range. These requirements are derived based on the stringent precision and accuracy target of the CO2M mission, i.e. < 0.7 ppm precision and 0.5 ppm accuracy. The overall CO2M error budget assigns an uncertainty of 0.5 ppm (0.125 % for 400 pm XCO_2) to aerosol and cloud induced errors. In this work, we use a goal requirement of 0.4 ppm (0.1 %) and a threshold requirement 0.6 ppm (0.15 %) for the aerosol-induced XCO_2 error (Eq. 8.5), which includes both the systematic and random errors due to the MAP observations but excludes any error contribution of the spectrometer. XCO_2 errors are calculated using the linear error analysis in **Sect. 8.3** for the geophysical and aerosol scenarios in **Sect. 7**, from which the requirements follow. The results for the two MAP concepts are presented separately below.

8.4.1. Modulation concept (MAP-mod)

Baseline setup

As a reference, we define a baseline setup for MAP-mod. This is specified in **Table 30**.

Table 30: MAP-mod baseline setup.

Features	Baseline setup
Number of VZAs	5 (-60 to 60 degrees)
Spectral range	385-770 nm
Radiance spectral resolution	5 nm
DLP spectral resolution	15nm@395nm, 40nm@755nm
Number of radiance measurements	77
Number of DLP measurements	19
Total number of measurements	480

Radiometric and polarimetric uncertainties

This section addresses requirements S7MR-OBS-380M, S7MR-OBS-390M, S7MR-OBS-400M, and S7MR-OBS-410M in the **MRDv1.0**. To derive requirements for MAP measurement uncertainties, we perform the error analysis by varying $\boldsymbol{S}_{y,MAP}$ (Eq. 8.2). The radiance errors are varied to 0.5%, 1%, 2%, 4% and degree of linear polarization (DLP) errors are set to values ranging from 0.001 to 0.005. For this exercise, the baseline setup (**Table 30**) is used in which the five VZAs consist of 0, +/-40, +/-57 degrees.

The results of the error analysis are displayed in **Figure 49**, which shows that XCO_2 accuracy decreases with increasing DLP and radiance errors in the three aerosol cases. For large radiance and DLP uncertainties, XCO_2 error can be as high as ~0.6%. When radiance and DLP errors are not greater than 2% and 0.003, respectively, XCO_2 errors do not increase beyond 0.15%; in most cases, the target XCO_2 error of 0.1% is in fact met. Relaxing the radiance and DLP errors to 0.003 and 0.0035 still results in XCO_2 errors of $\leq$ 0.15% for the majority of the study cases. The reported radiance and DLP errors are the total errors. Assuming equal contributions from random and systematic components, the 0.0035 DLP errors can be broken down to a noise component of ~0.0025 (or SNR=400) and a systematic error of ~0.0025. Similarly, the radiance error of 3% comprises ~1.7% (SNR~50) noise and ~1.7% systematic component. However, since the required DLP error is smaller, the total SNR requirement is driven by DLP. For a radiometric precision of ~0.0025 (SNR=400), the systematic component is then the dominant part of the total radiance error.

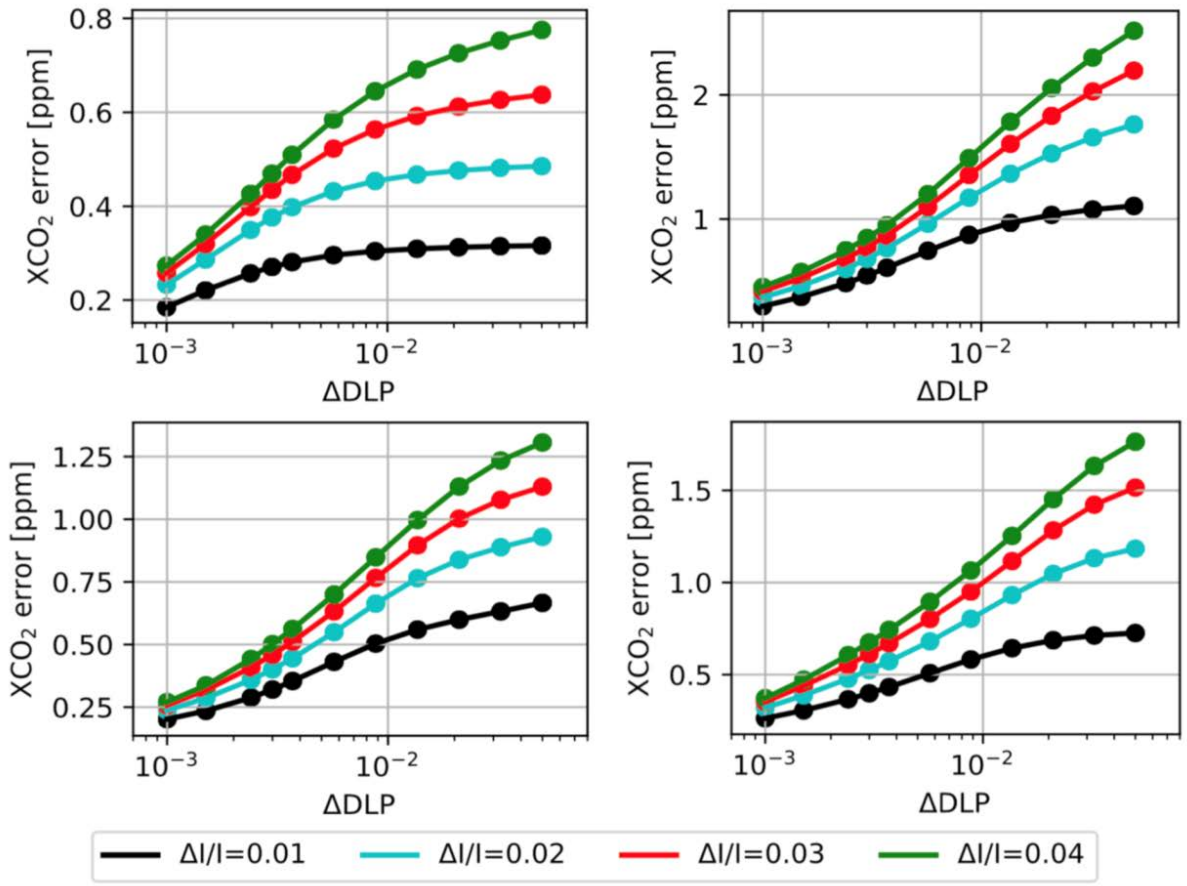

Figure 49: Performance of the MAP-mod baseline setup for four selected study cases, using settings 1 for the spectrometer. Each panel represents one study case where XCO_2 errors are shown as a function of DLP uncertainties (ΔDLP) for different values of radiance errors ($\pm\Delta$I/I). SZA is 60 degrees for all cases shown. Further specifications: Top left: case 1, τ_{tot}=0.07, vegetation. Top right: case 1, τ_{tot}=0.52, vegetation. Bottom left: case 2, τ_{tot}=0.24, soil. Bottom right: case 3, τ_{tot} = 0.24, vegetation. Note the varying scale range of the y-axis.

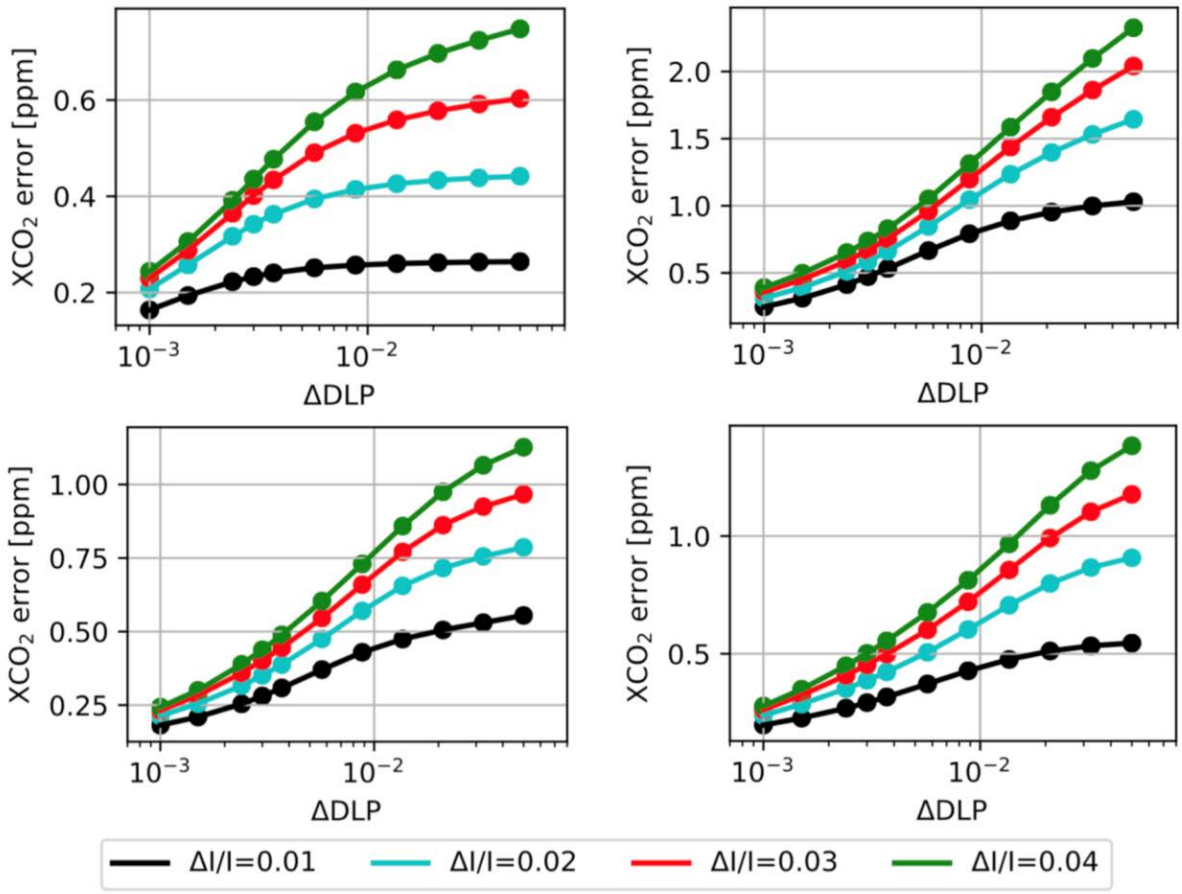

Figure 50: As the previous figure but using the setting 2 for the CO_2 spectrometer.

Number of viewing angles

This section addresses requirement S7MR-OBS-340M in the MRD. For this investigation, the spectral range and resolution of the baseline setup are adopted. Changing the number of viewing angles implies adding or removing measurements, which would influence the aerosol and hence the CO_2 retrieval. To study this effect, we vary the number of VZAs from 3 to 8 and compute a Jacobian matrix $\boldsymbol{K}_{MAP}$ for each. The viewing angles are limited to between -60 and 60 degrees**.Table 31** specifies the viewing angles and the corresponding number of measurements.

Table 31: Number of viewing angles studied for MAP-mod.

Number of VZA	VZAs	Total number of measurements
3	0, ±57	288
4	±19, ±57	384
5	±0, ±20, ±57	480
6	±11, ±34, ±57	576
7	0 ±19, ±38, ±57	672
8	±8, ±24, ±41, ±57	768

Following the discussion above, we assume a radiance error of 2% and a DLP error of 0.3% in the error analysis. **Figure 51** shows the resulting XCO_2 errors as a function of number of viewing angles for several selected cases. The plots in **Figure 51** show that there is a sharp drop of XCO_2 error from 3 to 4 viewing angles. From 4 to 8 viewing angles, XCO_2 errors decrease more mildly. The baseline setup has 5 viewing angles and this choice meets the target XCO_2 error. Having more than 5 viewing angles leads only to a marginal improvement in XCO_2 accuracy. This behavior is seen not just in the selected cases shown here, but also in all the other study cases. An odd number of viewing angles is preferred to an even number to allow for the inclusion of nadir view.

One can then conclude that 5 viewing angles is the minimum necessary to achieve the target XCO_2 error.

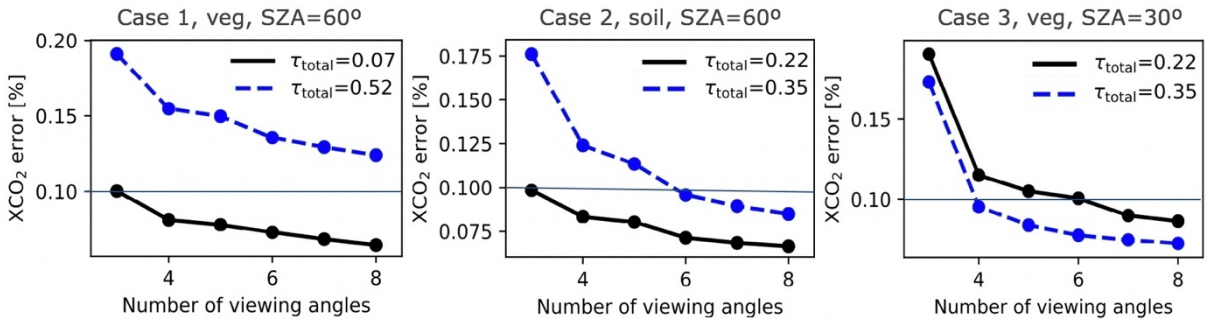

Figure 51: XCO_2 errors as a function of number of viewing angles assuming a radiance error of 2% and a DLP error of 0.003 for the MAP-mod concept. Each panel shows the XCO_2 errors for a particular study case.

Spectral range

This section addresses requirements S7MR-OBS-350M, S7MR-OBS-360M and S7MR-OBS-370M in the MRD. To assess the effect of changing the spectral range on the XCO_2 accuracy, we explore three options, i.e.

- expand the baseline spectral range so it extends further into the UV down to 350 nm ('≥350 nm'),
- truncate the baseline spectral range at 490 nm to exclude UV ('≥490nm'),
- extend the baseline spectral range to include SWIR, i.e. add a single spectral radiance and DLP measurements at 1640 and 2250 nm ('with SWIR'). So, referring to the spectral range 385-2250 nm actually means the continuous spectral coverage 385-765 nm with two additional bands at 1640 and 2250 nm, respectively.

Table 32 summarizes the setups that represent the three options, along with the baseline for comparison. For this exercise, all of the setups include 5 viewing angles at 0, +/-40, and +/-60 degrees to conform to requirement S7MR-OBS-350M. The baseline DLP spectral resolution is retained when excluding or including more UV wavelengths. In the error analysis, the radiance and DLP errors are assumed at 3% and 0.003, respectively.

Table 32: Spectral ranges studied for MAP-mod.

Setup	Spectral range [nm]	Number of radiance measurements	Number of DLP measurements	Total number of measurements
≥350nm	350-765	84	22	530
≥490nm	490-765	56	12	340
with SWIR	385-2250	79	21	500
baseline	385-765	77	19	480

Figure 52 shows the resulting XCO_2 errors as a function of optical depth for all the study cases using the three setups above, compared with the baseline setup. It can be seen in **Figure 52** that when compared to the baseline setup, including more UV wavelengths down to 350nm leads to little gain in XCO_2 accuracy, while removing UV wavelengths altogether leads to a considerable loss of XCO_2 accuracy. Excluding UV can increase XCO_2 error to around 0.25% for Case 3, vegetation with SZA=60 degrees.

Figure 53 shows that XCO_2 accuracy improves with the additional SWIR channels, but only marginally, which might not justify the added financial cost of including them. One can then conclude that the optimal choice of setup for MAP-mod is the baseline setup with spectral range from 385 to 765 nm.

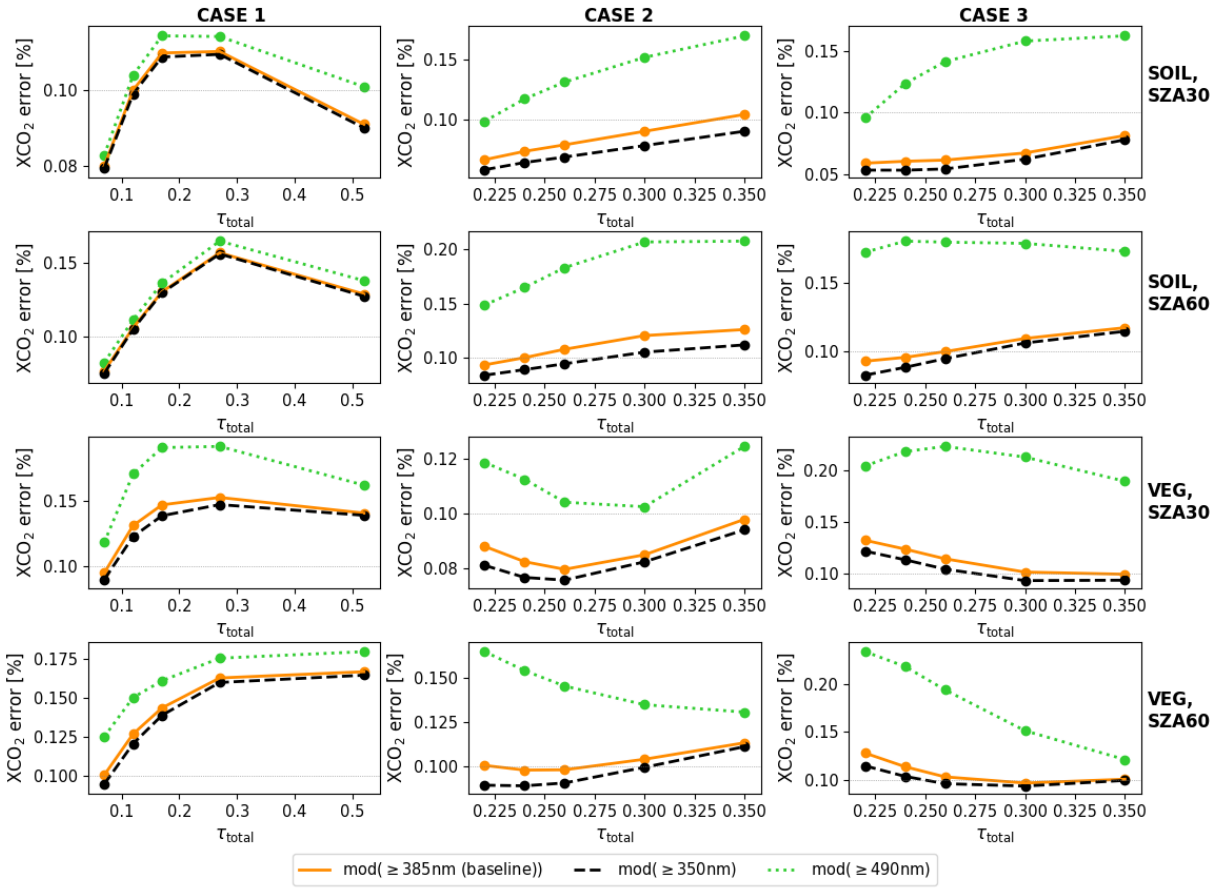

Figure 52: Performance comparison among the baseline, ≥350nm, ≥490nm setups of MAP-mod, represented by the different lines. XCO_2 errors as a function of aerosol total optical thickness is shown for all the study cases as indicated at the top and on the right side. The magnitude of the radiance and DLP uncertainties are assumed 3% and 0.003, respectively.

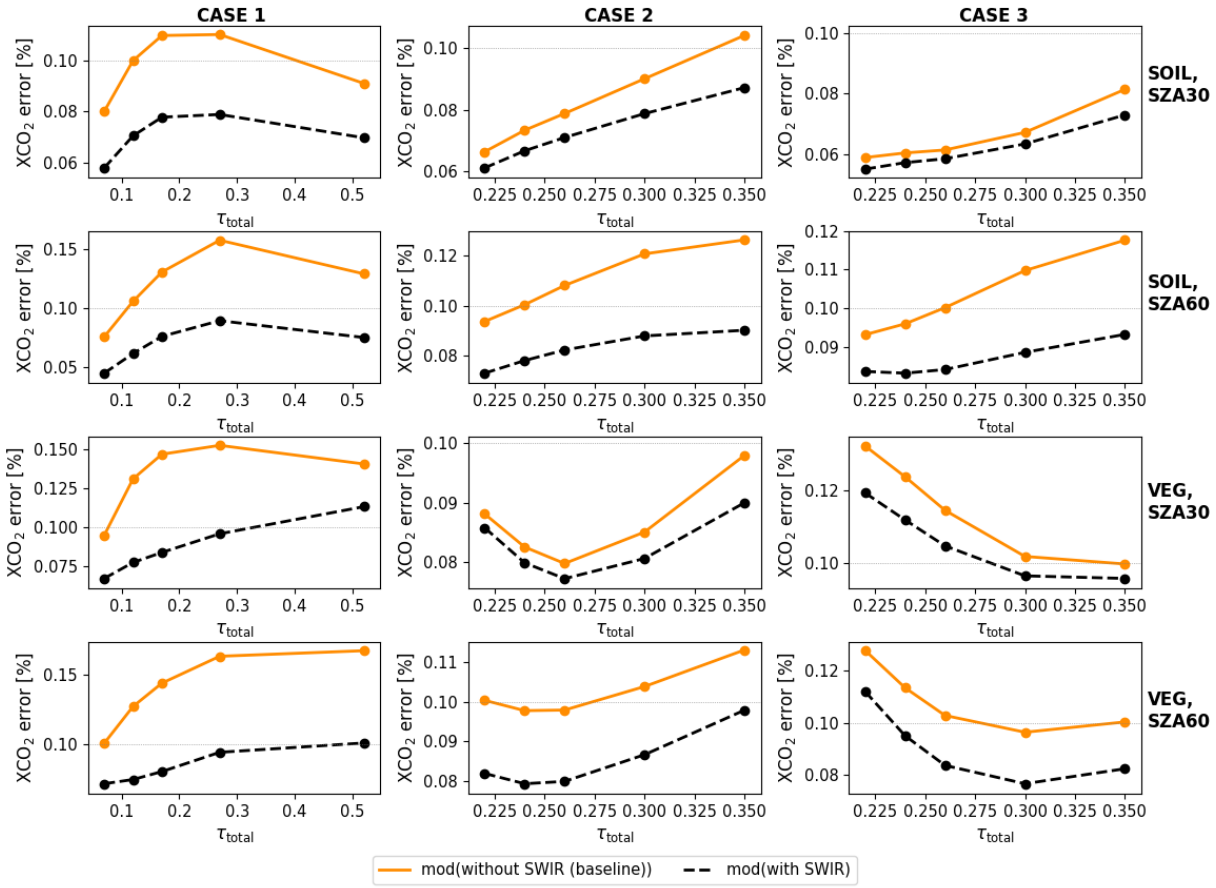

Figure 53: Performance comparison between baseline and with-SWIR setups of MAP-mod concept, represented by the different lines. XCO_2 errors as a function of aerosol total optical thickness is shown for all the study cases as indicated at the top and on the right side. The magnitude of the radiance and DLP uncertainties are assumed 3% and 0.003, respectively.

8.4.2. Bandpass concept (MAP-band)

Baseline setup

As a reference, we define a baseline setup for MAP-band. This is specified in **Table 33**. In this bandpass concept, both radiance and DLP measurements are taken at each bandpass or wavelength.

Table 33: MAP-band baseline setup.

Feature	Baseline setup
Number of VZAs	13
Viewing angles [degrees]	0, ±10, ±20, ±30, ±40, ±50, ±60
Bandpass/wavelengths [nm]	410, 440, 490, 550, 669.9, 863.4, 1640, 2250
Number of radiance measurements	8
Number of DLP measurements	8
Total number of measurements	208

Radiometric and polarimetric uncertainties

This section addresses requirements S7MR-OBS-380B, S7MR-OBS-390B, S7MR-OBS-400B, and S7MR-OBS-410B in the MRD. To derive requirements for MAP measurement uncertainties, we perform the error analysis by varying $\boldsymbol{S_{y,MAP}}$ (Eq. 7.2).

The radiance errors are varied to 0.5%, 1%, 2%, 4% and degree of linear polarization (DLP) errors are set to values ranging from 0.1% to 5%. For this exercise, the baseline setup (**Table 33**) is used.

The results of the error analysis are displayed in **Figure 54**, which shows that XCO_2 accuracy decreases with increasing DLP and radiance errors in the three aerosol cases. For large radiance and DLP uncertainties, XCO_2 error can be as high as ~0.6%. When radiance and DLP errors are not greater than 2% and 0.003, respectively, XCO_2 errors do not increase beyond 0.15%; in most cases, the target XCO_2 error of 0.1% is in fact met. Relaxing the radiance and DLP errors to 3% and 0.0035 still results in XCO2 errors of ≤0.15% for the majority of the study cases. The reported radiance and DLP errors are the total errors. Assuming equal contributions from random and systematic components, the 0.0035 DLP errors can be broken down to a noise component of ~0.0025 (or SNR=400) and a systematic error of _0.0025. Similarly, the radiance error of 3% comprises ~1.7% (SNR~40) noise and ~1.7% systematic component. However, since the required DLP error is smaller, the total SNR requirement is driven by DLP. For a radiometric precision of ~0.0025 (SNR=400), the systematic component is then the dominant part of the total radiance error

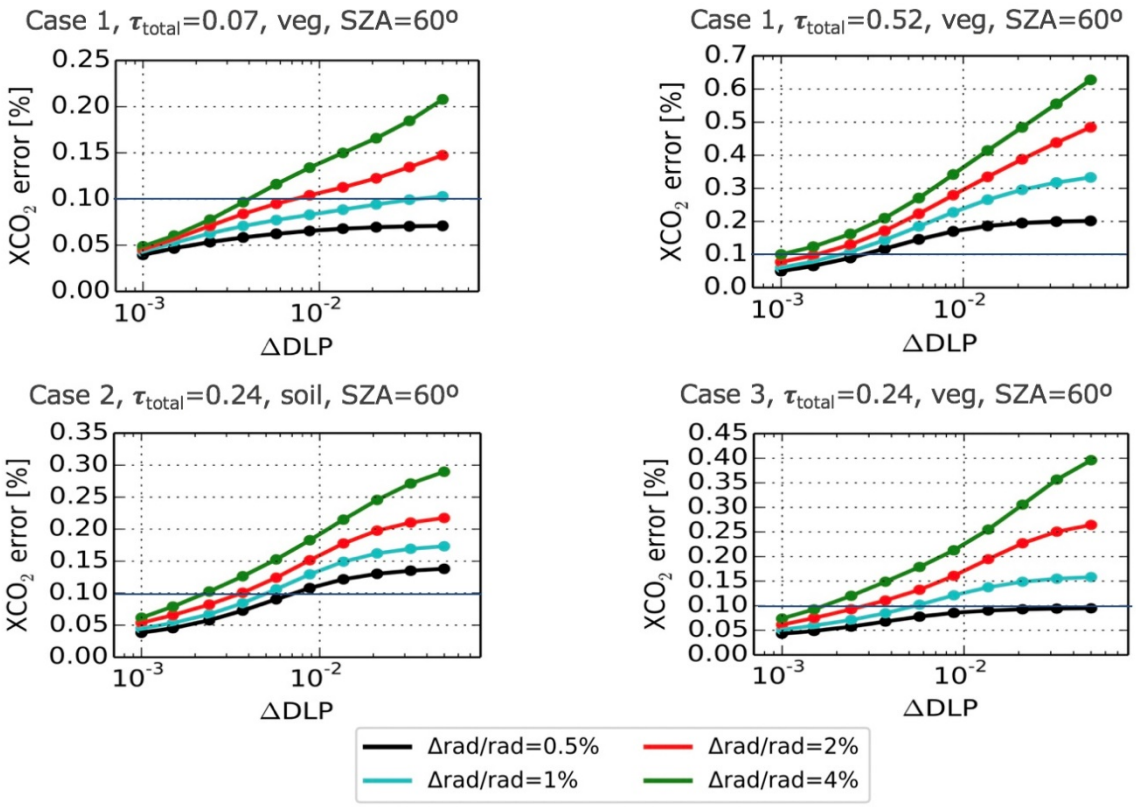

Figure 54: Performance of baseline MAP-band setup for four selected study cases. Each panel represents one study case where XCO_2 errors are shown as a function DLP uncertainties for different values of radiance errors.

Number of viewing angles

This section addresses requirements S7MR-OBS-340B and S7MR-OBS-350B in the MRD. For this investigation, the bandpass/wavelength selection of the baseline setup (**Table 33**) is adopted. Changing the number of viewing angles implies adding or removing measurements, which would influence the aerosol and hence the CO_2 retrieval. To study this effect, we vary the number of VZAs from 10 to 16 and compute a Jacobian matrix $\boldsymbol{K}_{mat}$ for each. The viewing angles are equally spaced and the outermost angles are fixed to -60 and 60 degrees to conform to requirement S7MR-OBS-350B. **Table 34** specifies the individual viewing angles along with the corresponding number of measurements.

Table 34: Number of viewing angles studied for MAP-band.

Number of VZAs	VZAs	Number of measurements
10	±7, ±20, ±33, ±47, ±60	160
11	0, ±12, ±24, ±36, ±48, ±60	176
12	±5, ±16, ±27, ±38, ±49, ±60	192
14	±5, ±14, ±23, ±32, ±42, ±51, ±60	224
15	0, ±9, ±17, ±26, ±34, ±43, ±51, ±60	240
16	±4, ±12, ±20, ±28, ±36, ±44, ±52, ±60	256

Following the discussion above, we assume a radiance error of 2% and a DLP error of 0.003 in the error analysis. **Figure 55** shows the resulting XCO_2 errors as a function of number of viewing angles for several selected cases. The plots in **Figure 55** show that XCO_2 accuracy improves with increasing number of viewing angles in an almost linear fashion. From 10 to 16 angles, the improvement in XCO_2 accuracy is quite small. With ten viewing angles, the target XCO_2 error is in fact already met. This behavior is seen not just in the selected cases shown here, but also in all the other study cases.

An odd number of viewing angles is preferred to an even number to allow for the inclusion of nadir view. One can conclude that, given the baseline bandpass selection, having 11 viewing angles is sufficient to deliver the desired XCO_2 accuracy. Note that the requirement on the number of viewing angles is coupled with the requirement on the bandpass/ wavelength range. Here, the number of viewing angles is assessed for a given set of wavelengths and in the following section, the wavelengths selection is assessed for a given number of viewing angles. We also provide examples of how the interplay between these two aspects affects XCO_2 accuracy.

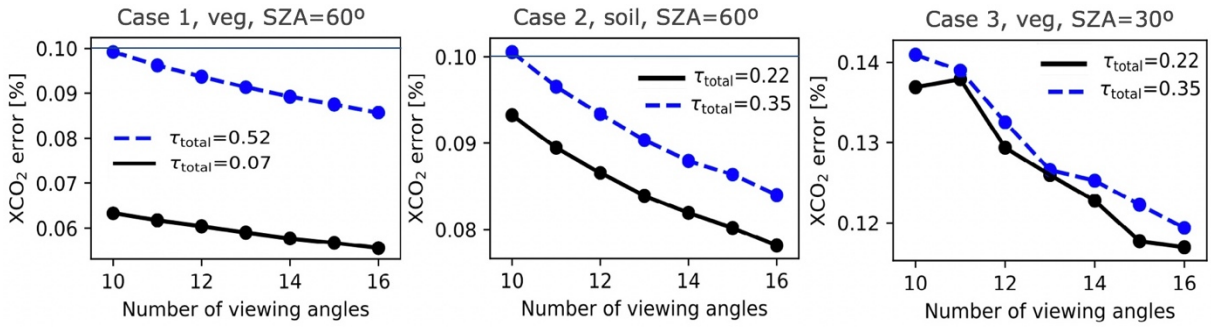

Figure 55: XCO_2 errors as a function of number of viewing angles for a radiance error of 2% and a DLP error of 0.003, for the MAP-band concept. Each panel shows the XCO_2 errors for a particular study case.

Wavelength range

This section addresses requirements S7MR-OBS-360B in the MRD. To assess the effect of changing the wavelength range, we explore three options, i.e.

- expand the baseline wavelength range so it extends further into the UV down to 350nm ('≥ 350nm'),
- truncate baseline wavelength range at 490 nm to exclude UV ('≥490nm'),
- narrow down the baseline wavelength range by excluding SWIR wavelengths, i.e. remove radiance and DLP measurements at 1640 and 2250 nm.

Table 35 summarizes the setups that represent the three options, along with the baseline for comparison. Radiance and polarization measurements are taken at each of the selected wavelengths. Following the results in **Sect. 8.2.3**, in this exercise we use 11 viewing angles in all three setups and the baseline setup. The individual angles are given in **Table 35**.

Table 35: MAP-band bandpass selections for a variety of wavelength ranges

Setup	Bandpass selections	Total number of measurements
≥ 350nm	350, 380, 410, 440, 490, 550, 669.9, 863.4, 1640, 2250	220
≥490nm	490, 550, 669.9, 863.4, 1640, 2250	132
without SWIR	410, 440, 490, 550, 669.9, 863.4	132
baseline	410, 440, 490, 550, 669.9, 863.4, 1640, 2250	176

In the error analysis, the radiance and DLP errors are assumed at 3% and 0.003, respectively. **Figure 56** and **Figure 57** show the resulting XCO_2 errors as a function of optical depth for all the study cases for the three setups above, compared with the baseline setup.

It can be seen in **Figure 56** that when compared to the baseline setup, including more UV wavelengths down to 350 nm leads to little gain in XCO_2 accuracy, while removing UV wavelengths altogether leads to a considerable loss of XCO_2 accuracy. Excluding UV can increase XCO_2 error to around 0.25% for Case 3, vegetation with SZA=60 degrees.

Figure 57 shows that XCO_2 accuracy drops considerably when the SWIR channels (1640 and 2250 nm) are removed. For Case 3, vegetation, SZA=60 degrees, the XCO_2 error can even increase to 0.51%. It is therefore important to keep the SWIR measurements in place.

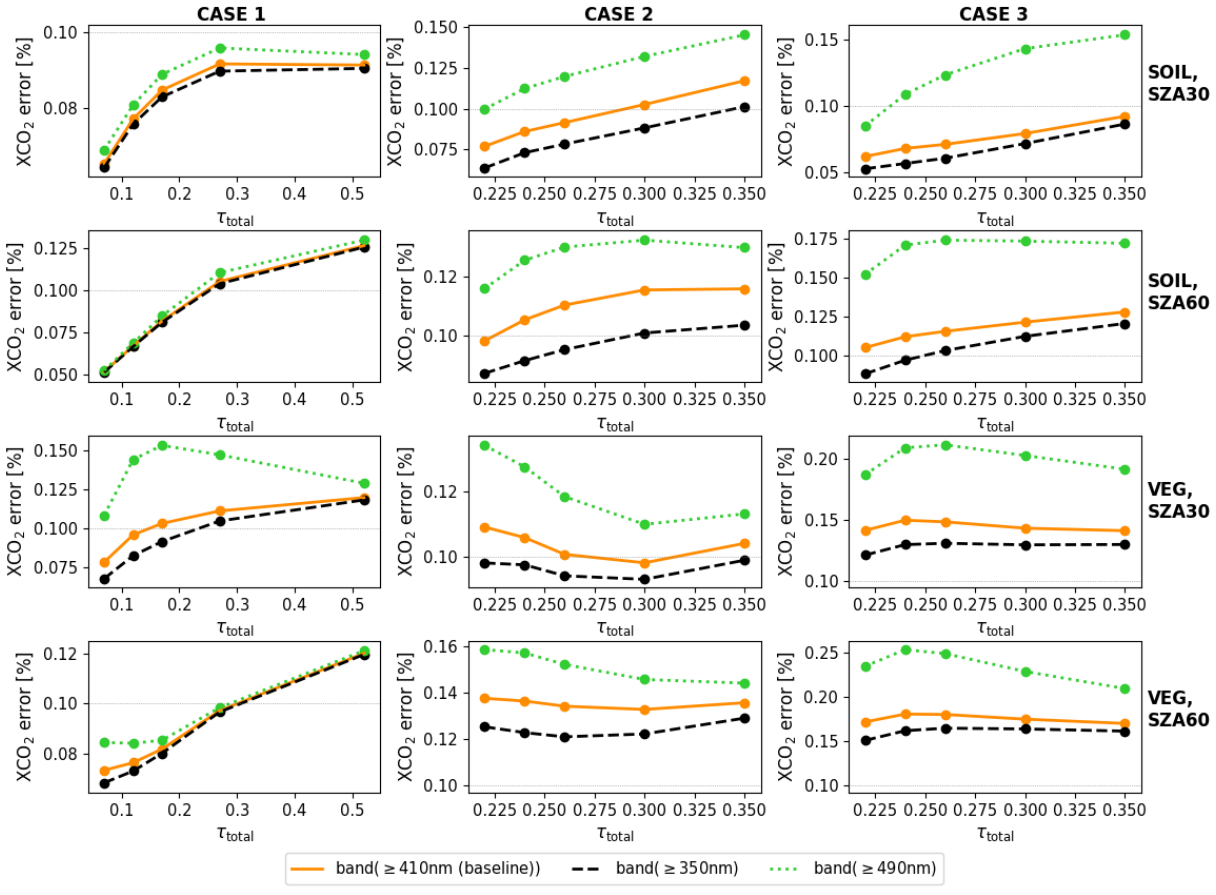

Figure 56: Performance comparison among the baseline, ≥350nm, ≥490nm setups of MAP-band, represented by the different lines. XCO_2 errors as a function of aerosol total optical thickness is shown for all the study cases as indicated at the top and on the right side. The magnitude of the radiance and DLP uncertainties are assumed 3% and 0.003, respectively.

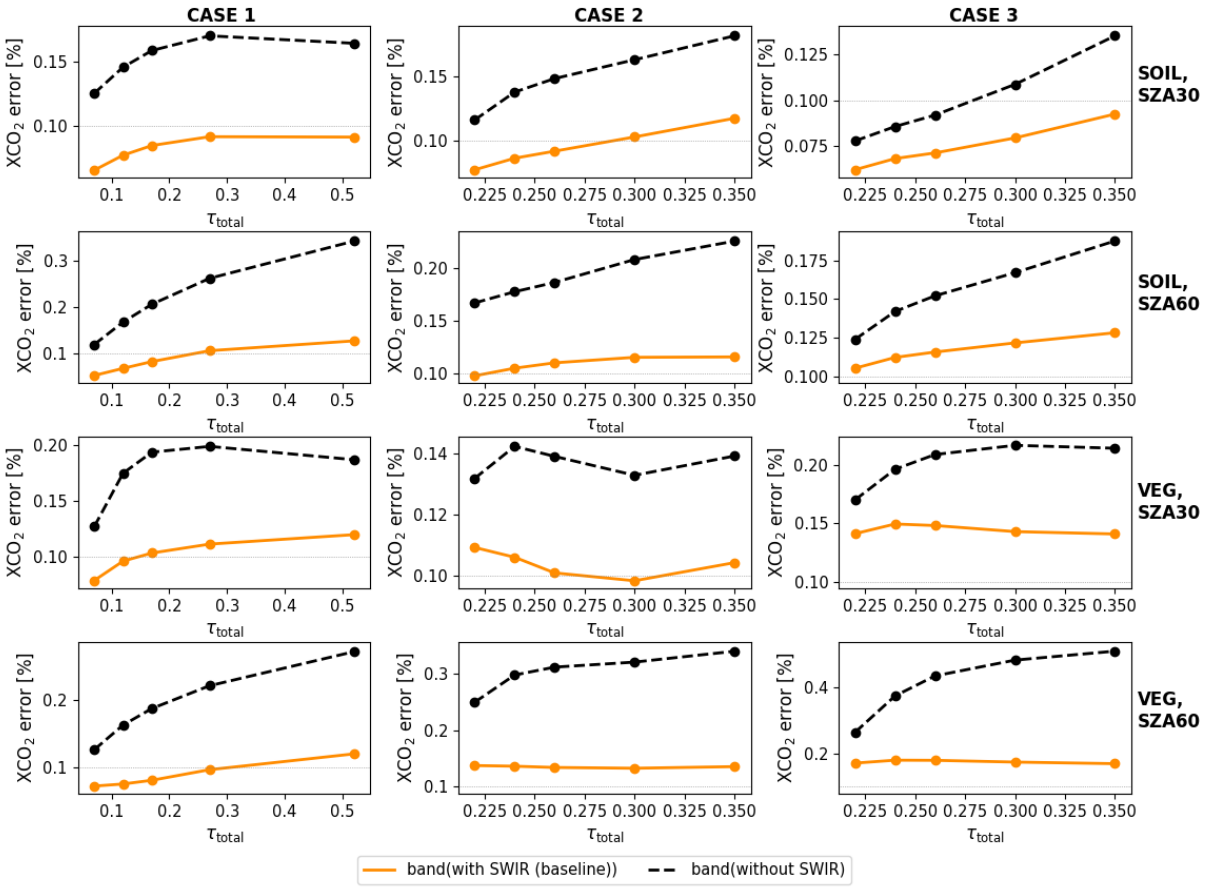

Figure 57: Performance comparison between baseline and without-SWIR setups of MAP-band, represented by the different lines. XCO_2 errors as a function of aerosol total optical thickness is shown for all the study cases as indicated at the top and on the right side. The magnitude of the radiance and DLP uncertainties are assumed 3% and 0.003, respectively.

8.4.3. Alternative setups to MAP-band

Given the analysis regarding the spectral/wavelength range shown in previous sub-sections, it appears that the SWIR channels hold a greater importance in the MAP-band than in the MAP-mod concept. We experiment with the possibility of removing the SWIR channels in MAP-band without compromising the retrieved XCO_2 accuracy significantly. This is done by increasing the number of viewing angles to a point where the total number of measurements approximately matches that of the baseline setup of MAP-mod. The total number of measurements in the baseline MAP-mod is used as reference here because in this setup SWIR channels are not present. The baseline MAP-mod has a total of 480 measurements. With only 6 wavelengths (after the removal of SWIR bands), 40 viewing angles are needed to arrive at the same number of measurements (this setup is referred to as 'band40' in the rest of this document). The resulting XCO_2 errors as a function of optical depth is shown in **Figure 58**. The plots show that the XCO_2 errors obtained using the setup 'band40' are comparable with those obtained using the baseline setup of MAP-mod or MAP-band. This means that the substantial loss of performance when SWIR channels in MAP-band are removed can be prevented by adding more viewing angles.

We extend this experiment to investigate what we call the hybrid setup. Here we increase the number of wavelengths and decrease the number of viewing angles while maintaining approximately the same total number of measurements as the baseline MAP-mod or as the band40 setup (i.e. 480). More specifically, this hybrid setup has 11 wavelengths (at 410, 440, 465, 490, 520, 550, 610, 669, 735, 800, 863 nm), at which both radiance and DLP are measured, and 21 viewing angles (equally spaced from -60 and 60 degrees and includes nadir). The total number of measurements is then equal to 462. It is shown in **Figure 58** that the hybrid setup results in XCO_2 errors that are very similar to those in the band40 setup. To summarize, there are 3 possible implementations for the MAP-band concept. The first is the baseline setup with 8 wavelengths that include SWIR. The second is the removal of 2 SWIR wavelengths while having 40 viewing angles (band40), and the third solution is the setup with 11 wavelengths and 21 viewing angles (hybrid). One common feature here is the total number of measurements that is kept approximately the same.

8.4.4. Inclusion of 753-nm wavelength

To allow for a cross-calibration between MAP and the CO_2 instrument, radiance measurement at a common wavelength is needed. This particular wavelength is expected to be at 753 nm. We investigate the accuracy of XCO_2 when this wavelength is used in place of one the 6 wavelengths in the band40 setup. For this exercise we experiment with replacing the last three wavelengths (555, 669.9, 863.4 nm), with 753 nm one by one, keeping the viewing angles and the total number of measurements in the band40 setup intact. It is assumed that both radiance and DLP are measured at 753 nm.

XCO_2 errors are plotted as a function of aerosol optical depth for the different sets of wavelengths in **Figure 59** and **Figure 60**.

Figure 59 shows that having 753 nm replace 670 nm degrades the performance noticeably for the vegetation scenes. The surface albedo for vegetation at 753 nm is high, resulting in small DLP and this appears to have a negative effect on the XCO_2 accuracy.

Figure 60 compares the other two sets of wavelengths where we replace either 550 nm or 863 nm with 753 nm. It is evident that in most of our study scenarios, replacing 550 nm leads to smaller XCO_2 errors compared to substituting 863 nm. It can then be concluded that among the three wavelengths (550, 670, 865 nm), replacing 550 nm would deliver the highest XCO_2 accuracy.

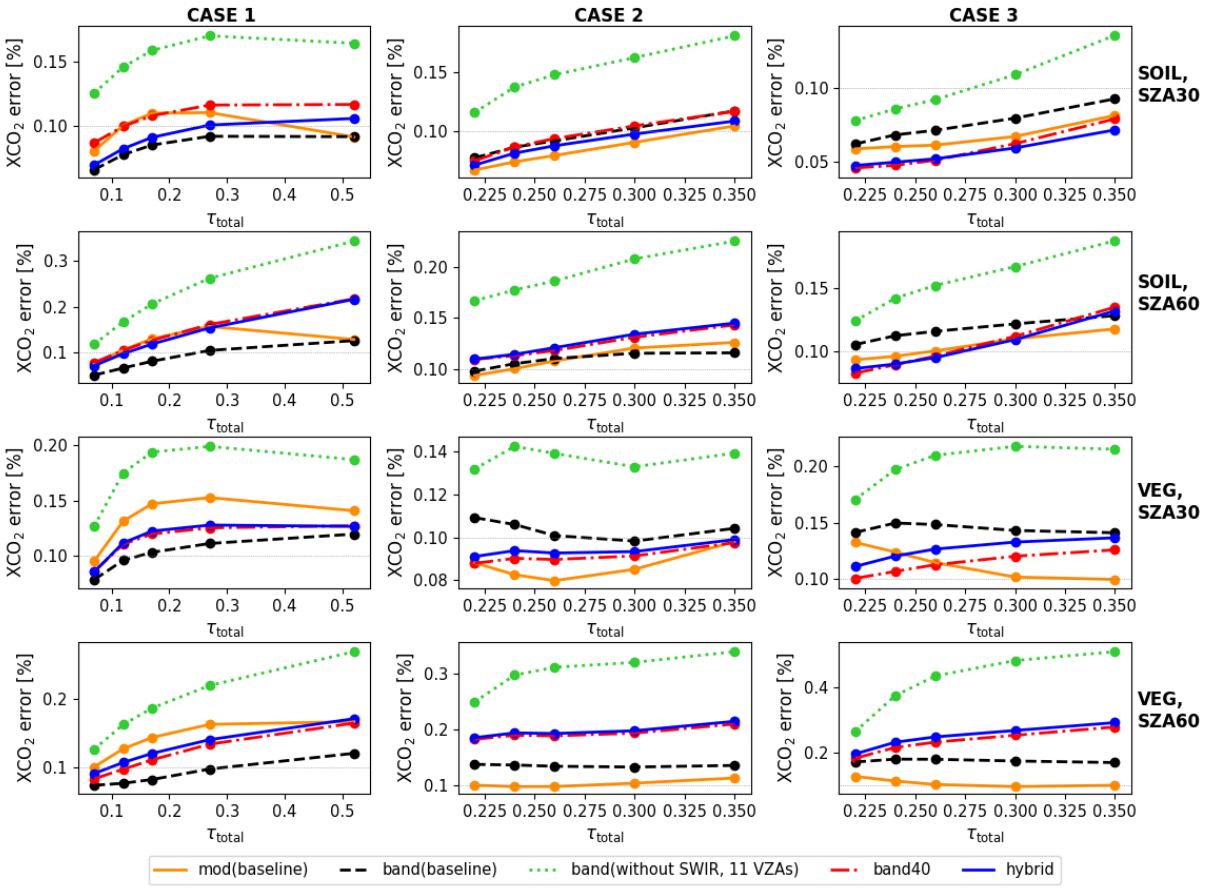

Figure 58: Performance comparison among the baseline setups, without SWIR, and the alternative setups without SWIR, represented by the different lines. XCO_2 errors as a function of aerosol total optical thickness is shown for all the study cases as indicated at the top and on the right side. The magnitude of the radiance and DLP uncertainties are assumed 3% and 0.003, respectively.

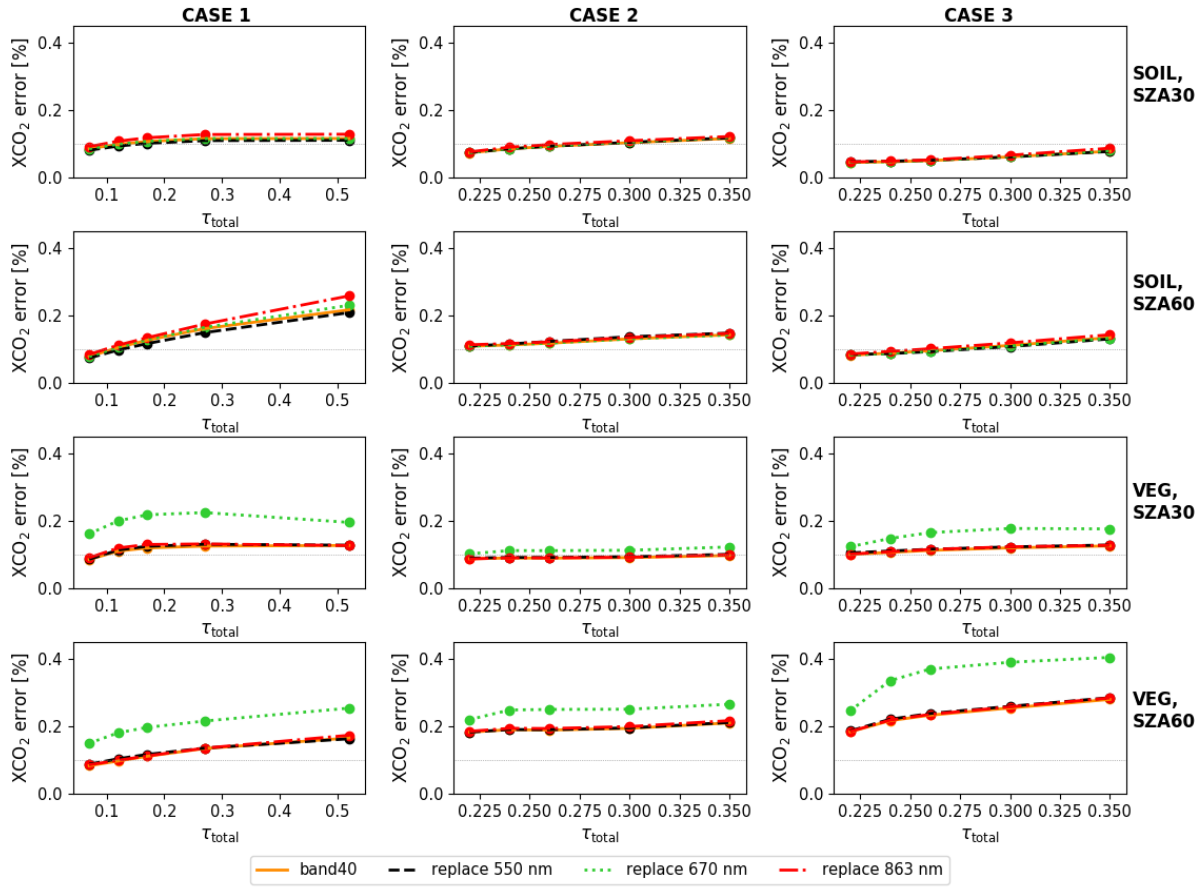

Figure 59: Performance comparison among the different bandpass selections for the band40 setup, represented by the different lines. XCO_2 errors as a function of aerosol total optical thickness is shown for all the study cases as indicated at the top and on the right side. The magnitude of the radiance and DLP uncertainties are assumed 3% and 0.003, respectively.

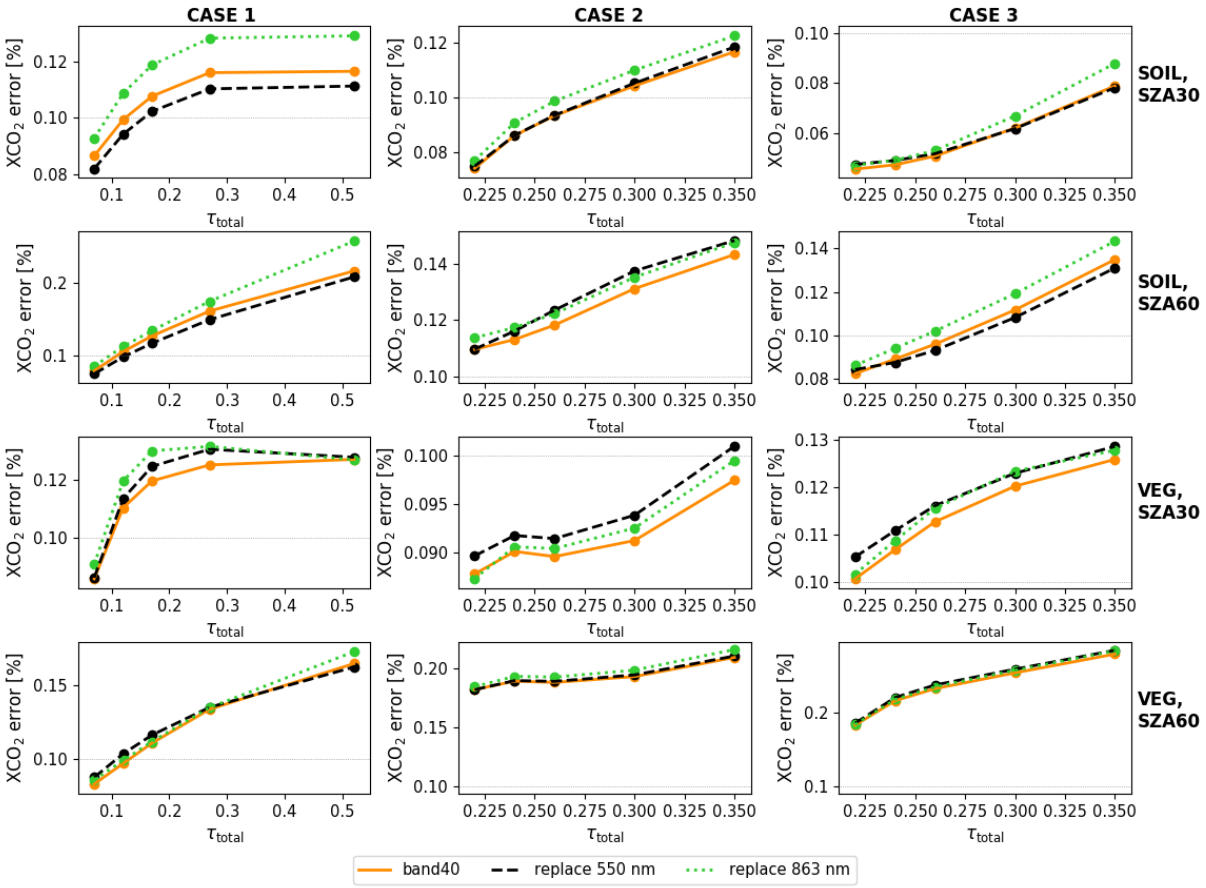

Figure 60: Performance comparison among the different bandpass selections for the band40 setup, represented by the different lines. XCO_2 errors as a function of aerosol total optical thickness is shown for all the study cases as indicated at the top and on the right side. The magnitude of the radiance and DLP uncertainties are assumed 3% and 0.003, respectively.

8.5. Spatial oversampling

To estimate the error induced by spatial resampling of radiance and polarization measurements, we consider two scene examples: first a randomized chess-board scenario and second a Sentinel-2 scene in the Northwest of Shanghai.

8.5.1. Chess-board scenario

The chess-board scenario assumes a 16×16 km^2 spatial domain with an underlying sampling of 20×20 m^2, which are combined to 300×300 m^2 homogeneous spatial scenes. The fine 20×20 m^2 sampling is required by the convolution of the top-of-atmosphere (TOA) radiometric quantities to the spatial resolution of the MAP instrument. Next, we assume that the scene consists of a randomly assigned radiometric pattern of three reference spectra, calculated for five different viewing angles, VZA = 0, ±40, ±60 degrees. The radiometric allocation is depicted in **Figure 61**. As reference scene, we selected a vegetation, soil, and sand BDRF to describe different types of surface reflection.

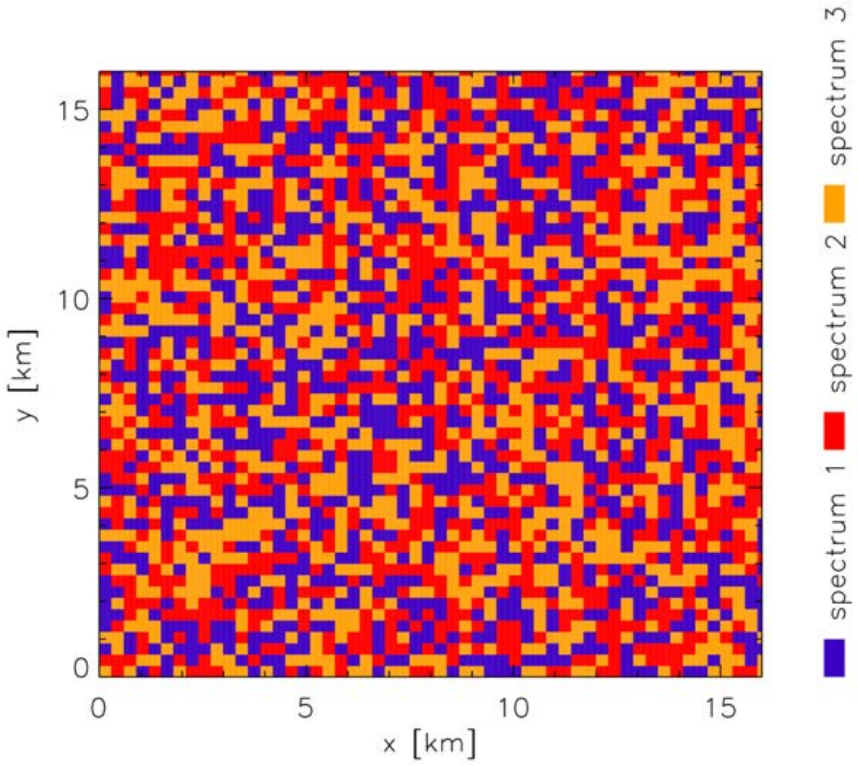

Figure 61: Randomized chess-board scenario where three radiometric scenes are randomly assigned to 300×300 nm homogenous ground scenes. In this study we assume that spectrum 1 represents a vegetation scene and spectrum 2 and 3 a soil and sand scene, respectively.

Figure 62 shows examples of the radiance and degree of linear polarization (DLP) spectra for VZA = +60 degree. In the remaining of the study, the radiometric scene is investigated in more detail for four wavelengths λ = 350, 450, 550, 800 nm.

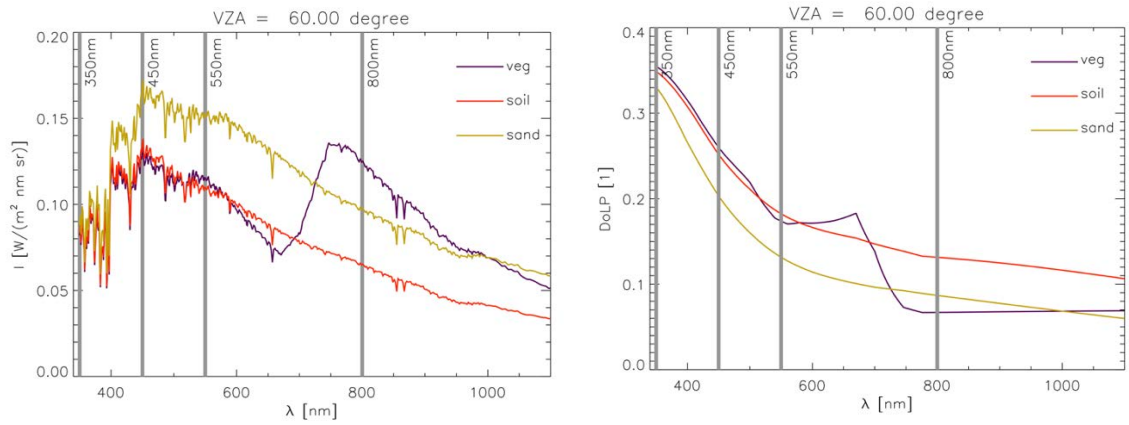

Figure 62: Radiance (left) and DLP (right) reference scene for a vegetation (veg), soil and sand surface BDRF. The depicted simulations are performed for a solar zenith angle of 50 degree and a VZA = 60 degree. Four wavelength λ = 350, 450, 550 and 800 nm are selected for further investigations.

Subsequently, the TOA radiometric scene is convolved with a two-dimensional Gaussian to degrade the scene to the spatial resolution of the MAP. Currently, we assume a full width at half maximum (FWHM) of 2 km in both spatial dimensions. **Figure 63** shows the smoothed radiometric scene sampled on a 20×20 m spatial grid.

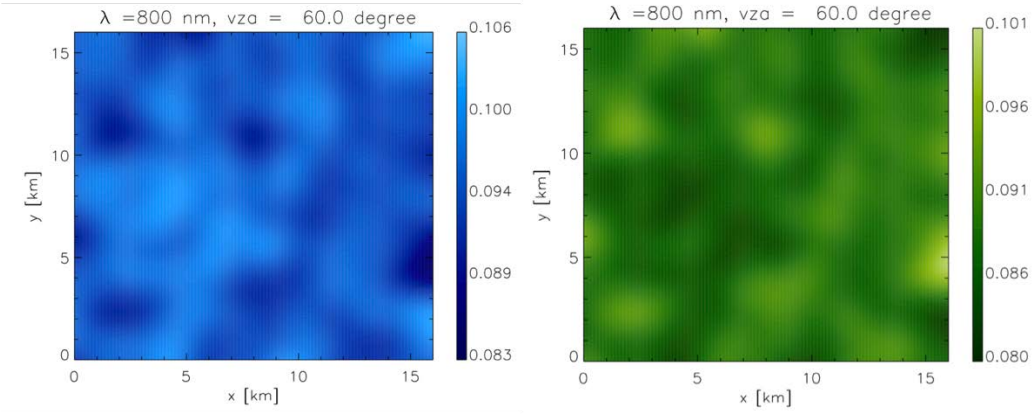

Figure 63: Convolved radiance (left) and DLP (right) radiometric scenes for λ =800 nm and VZA = 60 degree.

Obviously, the MAP measurements will be sampled on a much coarser grid and based on the generated data set any sampling scheme can be applied. This study considers two regular sampling schemes with a sampling distance of 2 km (1 FWHM) and 1 km (0.5 FWHM), so a spatial oversampling ratio of 1 and 2 in both spatial directions. Subsequently, the sampled data set is used as input for a bilinear interpolation scheme to fill the gaps between the sampling point. Thus, comparing the interpolated radiance scene with those of **Figure 62** can be used to estimate resampling error of this simple scheme.

Figure 64 shows an example of the resampling error of the radiance and DLP fields for a VZA of 60 degree at 800 nm for the two sampling distances. Errors are substantial, exceeding ±4 % in the radiance and ±0.004 in the DLP. Enhancing the sampling ratio to 2 reduces the error significantly with a resampling error ≤ 2 % in the radiance field and ≤0.001 in the DLP field.

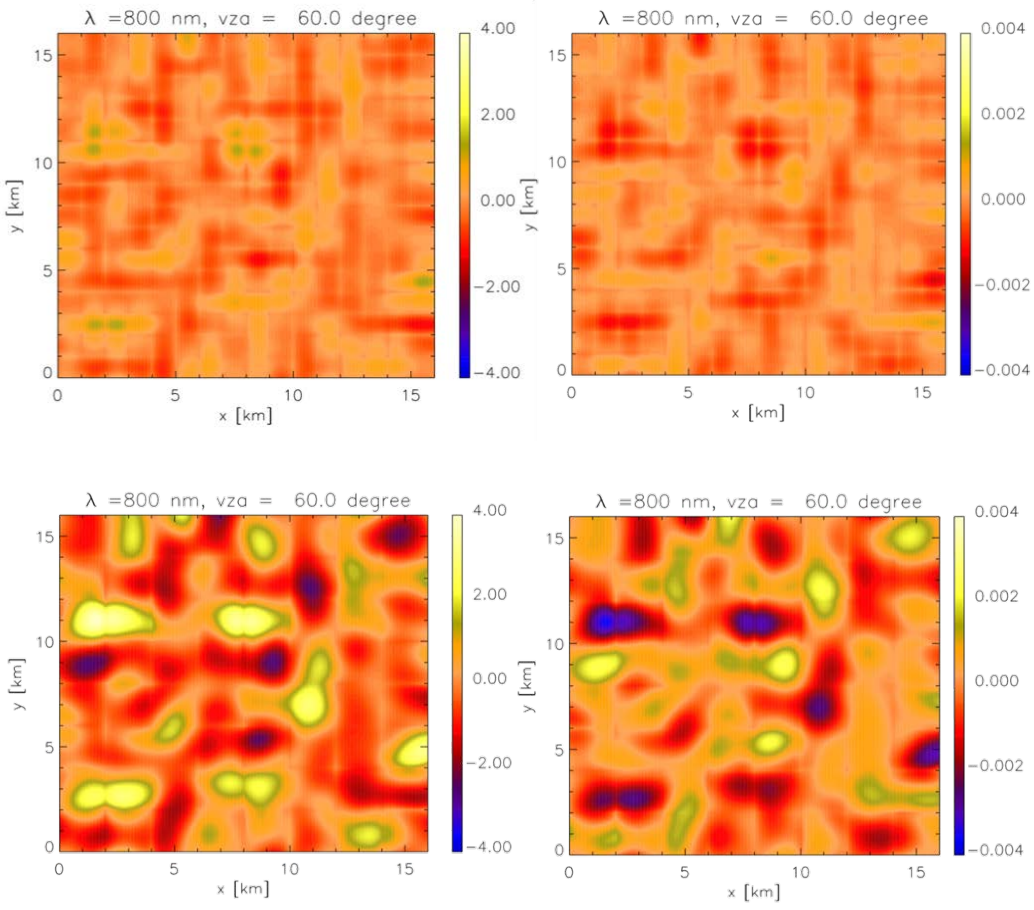

Figure 64: Resampling error for the radiance (left) and DLP (right) for an oversampling ratio of 2 (upper) and 1 (lower).

Finally, **Figure 65** summarizes the resampling error for the chess-board experiment. It shows the maximum and the error standard deviation for the ensemble of resampled radiance and DLP error for all VZAs and for the different wavelengths. Considering the standard deviation as the relevant quantity to formulate MAP requirements, we conclude that for the sampling ratio of 1, errors are too large requiring too large contribution from the radiometric error budget. However for a spatial oversampling ratio of 2, the induced radiance error standard deviations are < 0.5 % and the corresponding DLP errors are <0.0006, which is acceptable.

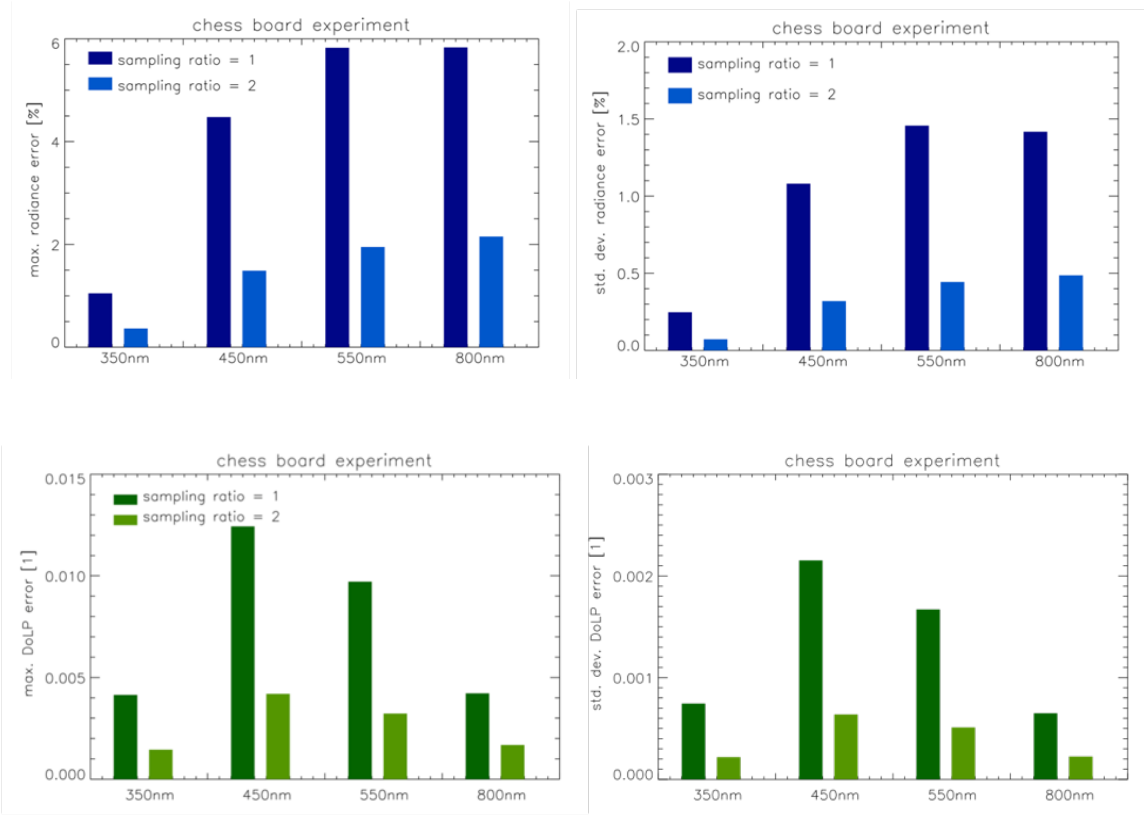

Figure 65: Overview of the resampling errors for the chess-board experiment for all VZAs and the two sampling ratios as indicated in the legend. Maximum error (left), error standard deviation (right), radiance (top) and DLP (bottom).

Google map

8.5.2. Sentinel 2 scenario

The chees-board experiment has a major shortcoming. The radiometric gradients of the ensemble are randomly selected and so introduces a certain arbitrariness in our analysis. To address this problem, a first preliminary analysis was performed for the scenario observed by Sentinel-2 around Shanghai, depicted in **Figure 66**. It comprises nine tiles of surface albedo around 780 nm (band 7), which is used to derive a near-infrared (NIR) surface albedo map for the surrounding of Shanghai with a spatial sampling of 20×20 m^2, shown in **Figure 67**.

The ensemble is much too large for any analysis of the resampling error, and so we selected an area in the Northwest of Shanghai for further investigation. **Figure 67** shows the RGB zoom-in region given by the Apple maps service and the corresponding S2 data and indicates that the area includes mainly crop vegetation with a village in the upper left corner.

To assign model spectra to each Sentinel-2 pixel depending on the NIR albedo, we simulated vegetation reference spectra assuming the surface BDRF

$$BDRF(\lambda, \vartheta_{in}, \vartheta_{out}, \Delta\varphi) = A(\lambda) + \sum_{i=1}^{2} f_i \; R_i(\vartheta_{in}, \vartheta_{out}, \Delta\varphi)$$

which comprises the two spectral independent vegetation kernels R_1 and R_2 with corresponding weights f_i. Here, $A(\lambda)$ is the spectral dependent Lambertian albedo. Using this model for surface reflection, we calculated reference spectra scaling the albedo term to cover the range $0.0 < A(\lambda_{NIR}) < 1.0$ in steps of 0.025. **Figure 68** illustrates two examples for an NIR surface albedo of 0.10 and 0.25. With the albedo map of **Figure 67**, we can assign to each ground pixel a corresponding model spectra and so could generate radiometric scenes, which corresponds to the spatial scales as observed by Sentinel-2.

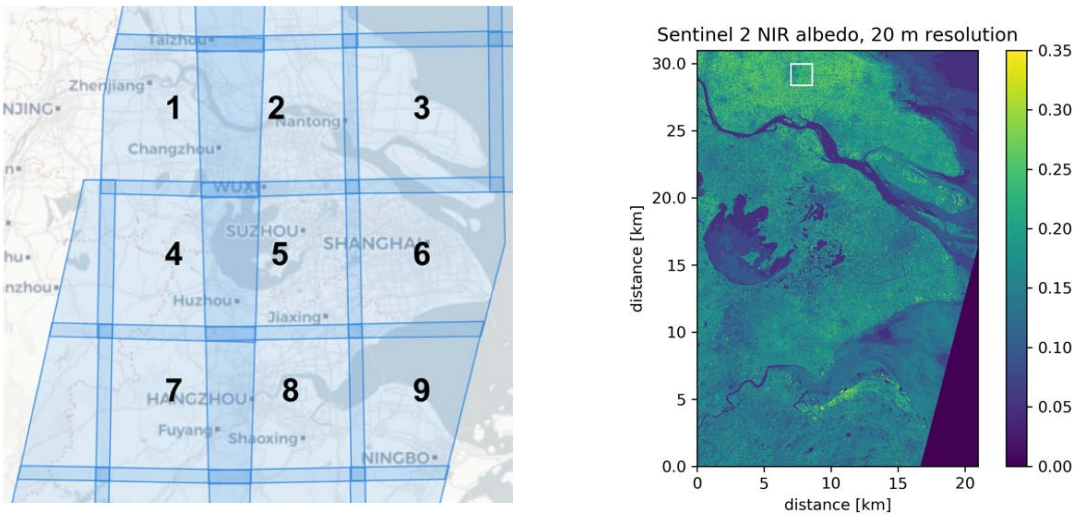

Figure 66: (Left) Nine Sentinel-2 tiles over the Shanghai region (right) Sentinel 2 NIR albedo.

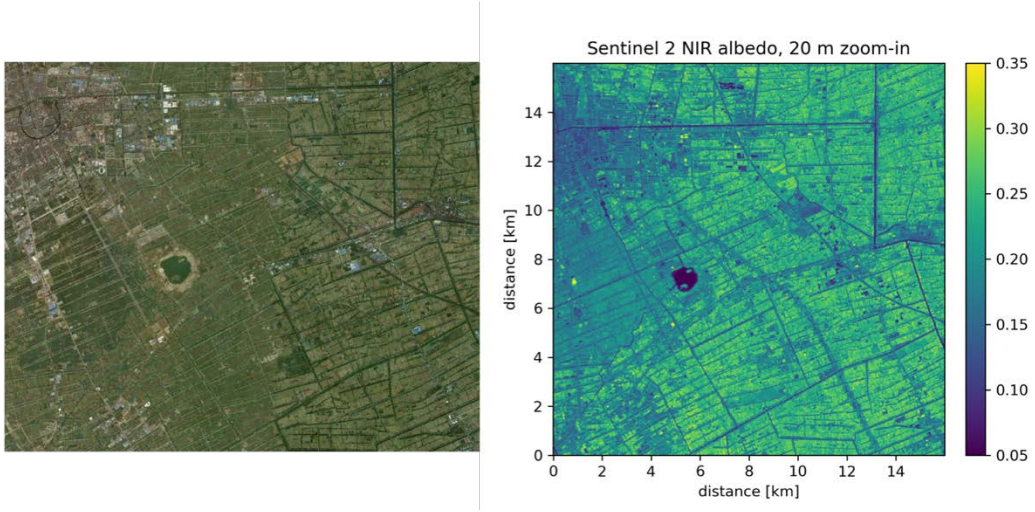

Figure 67 (Left) RGB Apple map service image of the zoom-in, (right) Sentinel 2 NIR albedo for zoom-in.

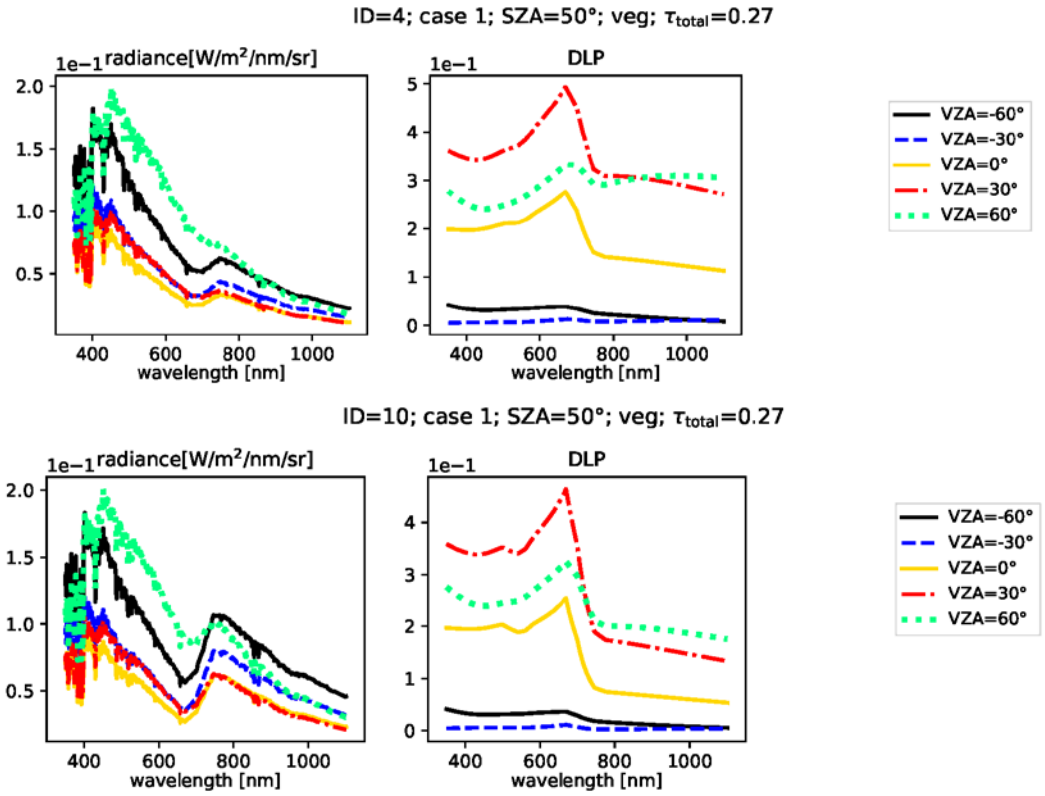

Figure 68: Example of MAP reference spectra for five viewing angles 0, ±30, ±60 degree and two NIR albedo values 0.1 (top) and 0.25 (bottom).

Finally, we apply the same analysis as already described in **Sect. 8.5.1**. **Figure 69** shows the 800 nm radiance scene on Sentinel 2 resolution, convolved with the two-dimensional Gaussian response function, and resampled with a spatial sampling ratio of 1 and 2, analogous to **Sect. 8.5.1**.

For a sampling ratio of 1 and a mean radiance of 7.6 W/(m^2 nm sr), the mean error is 0.048 % (2.4 $\times 10^{-5}$ W/(m^2 nm sr)) with a standard deviation of 0.79 % (5.82×10^{-4} W/(m^2 nm sr)) whereas for a sampling ratio of 2 the mean error is 0.008 % (2.54 $\times 10^{-6}$ W/(m^2 nm sr)) with a standard deviation of 0.23% (1.69×10^{-4} W/(m^2 nm sr)). Thus, the error standard deviation is about a factor 2 smaller than for the chess-board experiment. Here, the mean error is defined as the mean of the individual relative errors.

Figure 70 shows the corresponding results for the sampling error of DLP. Also for the polarization measurements a spatial oversampling ratio of 2 is required to reduce the resampling errors of up to 0.01 to the required accuracy range <0.02.

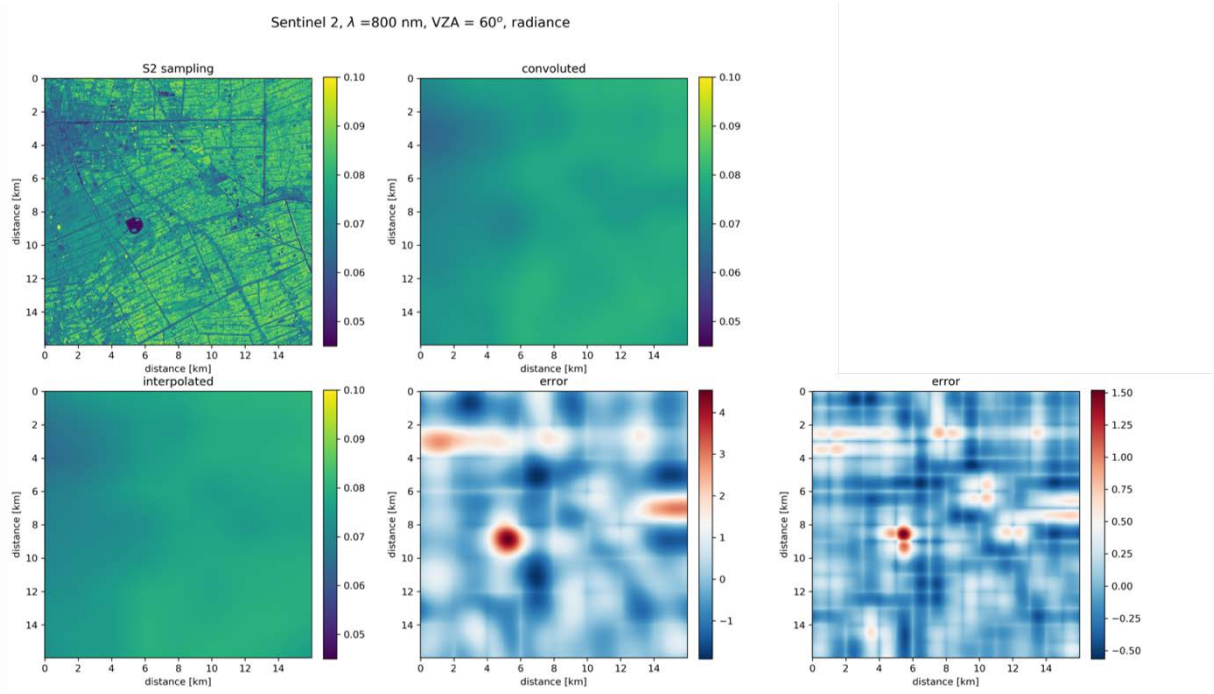

Figure 69: Radiance resampling error for the Sentinel 2 ensemble of **Figure 67**. (Top left) Radiance ensemble at 800 nm and for a VZA of 60 degree [W/(m^2 nm sr)], (top middle) convolved radiances assuming a 2D Gaussian spatial response of the MAP instrument with a FWHM of 2 km in both dimensions, (bottom left) resampled radiances assuming an spatial oversampling ratio of 1 in both directions, (bottom middle) radiance resampling error for an oversampling ratio of 1, (bottom right) radiance resampling error for an oversampling ratio of 2.

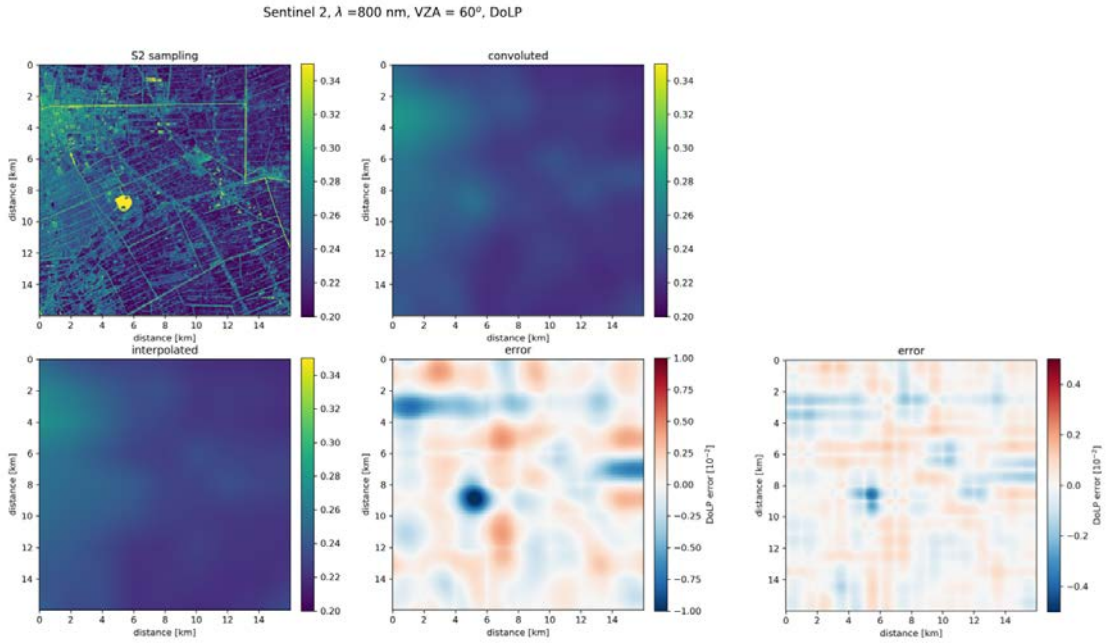

Figure 70: Same as **Figure 69** but for DLP.

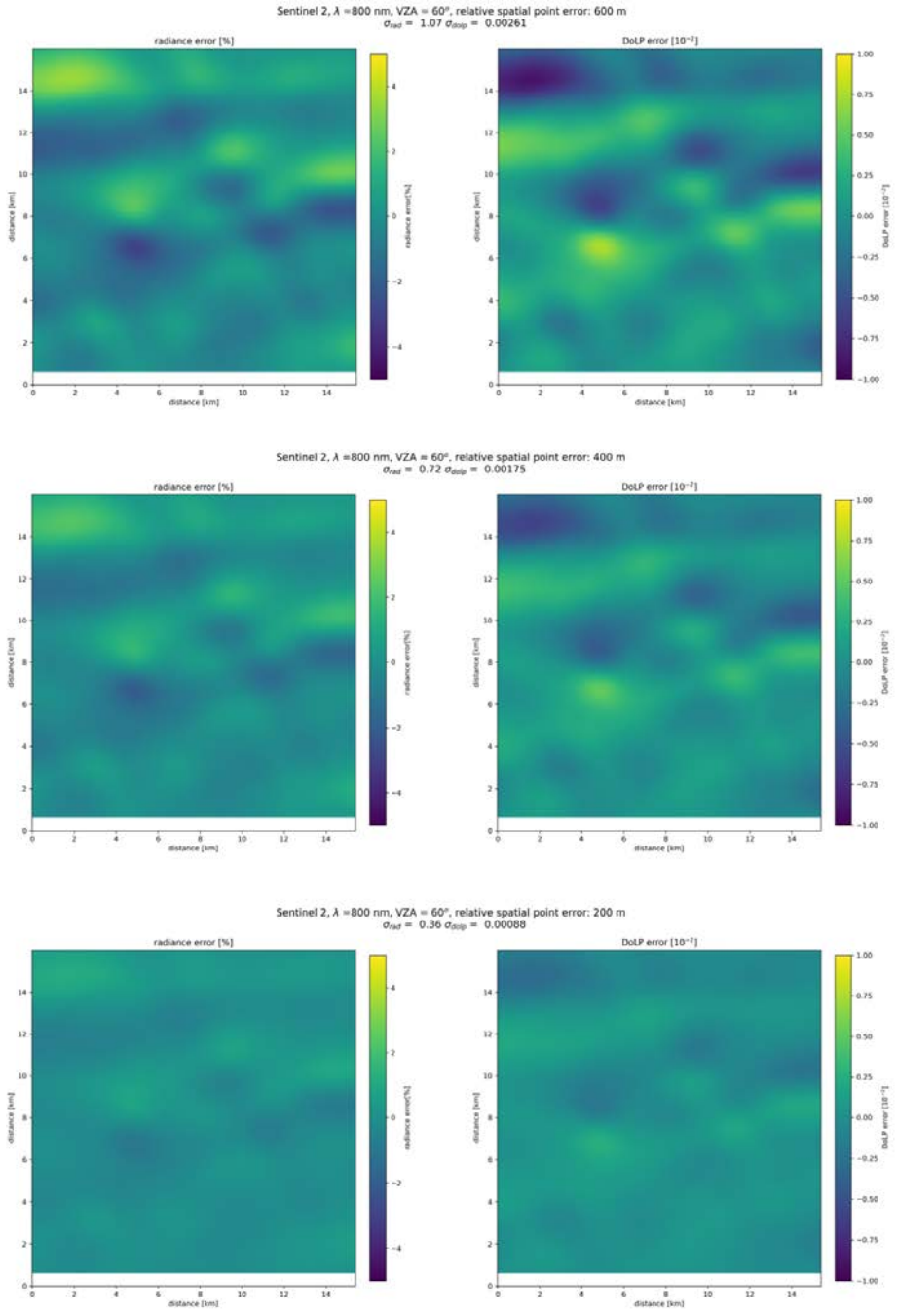

Figure 71: Radiance (left) and DLP (right) error due to a horizontal spatial displacement of the Sentinel-2 scene by 600m (top), 400m (middle), 200m (bottom).

8.6. ISRF knowledge requirement

Overall, the ISRF knowledge is less relevance for the MAP instrument than for the CO_2 spectrometer. To demonstrate this, we consider radiance error induced by ISRF knowledge errors between 1% and 6% as depicted in **Figure 72**. The induced radiance error increases from 0.02% to 0.14% with a maximum error between 0.1% and 0.6% at the Calcium K and L Fraunhofer lines at 382 nm and 393 nm (**Figure 73**). We consider this error as a minor contribution to the total error budget and thus propose an overall knowledge error of the ISRF to be better than 4% of its maximum value, which causes a standard deviation of the radiance error of 0.1%.

Particular attention must be given to the ISRF knowledge in the NIR. Here measurements around the O_2 A band are intended to be used for cross calibration between the CO_2 and MAP instrument. In the light of the required accuracy of the MAP radiance measurements of 3%, we assume that radiance errors induced by ISRF knowledge uncertainties must be < 1%, which leads to a dedicated requirement on the ISRF knowledge of the MAP instrument in the spectral range of the O_2 A band. **Figure 74** shows the ISRF induced radiance error due to uncertainties between ±5% in the FWHM of the ISRF. Here, the radiance error, given with respect to the continuum value, shows maxima at the center and in the wings of the O_2 A band. Hence, considering the error at 761.5 nm and 757.5 nm in **Figure 75**, we conclude that the FWHM of the ISRF must be known with an accuracy of 2% for instrument cross calibration. The analogous analysis of the MAP-band concept is shown in **Figure 76** and results in same requirement for band 6 with the narrow bandwidth of 10 nm. For band 7 with a bandwidth of 40 nm a knowledge requirement of 4% is sufficient.

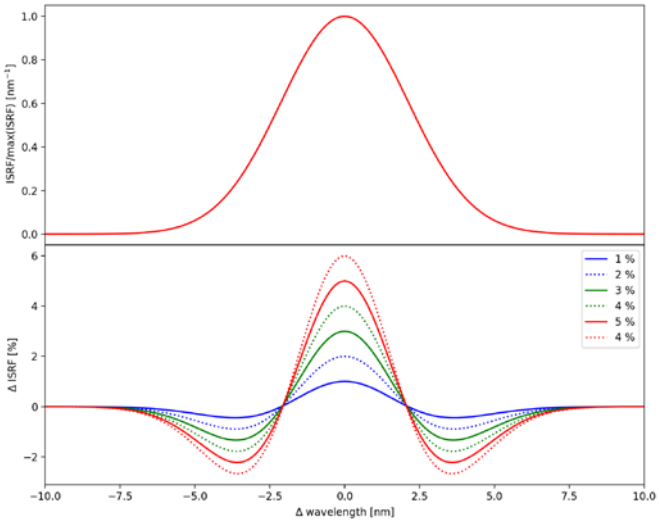

Figure 72: ISRF distortion. (Top) Gaussian ISRF with a FWHM of 5 nm and (bottom) different ISRF distortions with knowledge error between 1-6% (bottom).

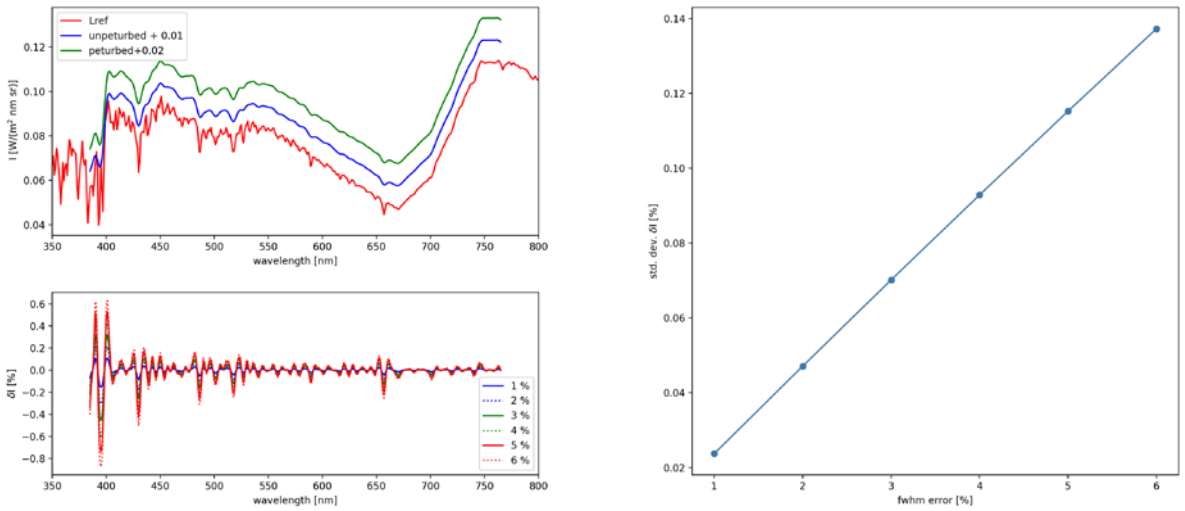

Figure 73: (Left) Radiance error due to ISRF knowledge error shown in **Figure 72**. (Right) Standard deviation of the ISRF radiance error as a function of the ISRF knowledge error.

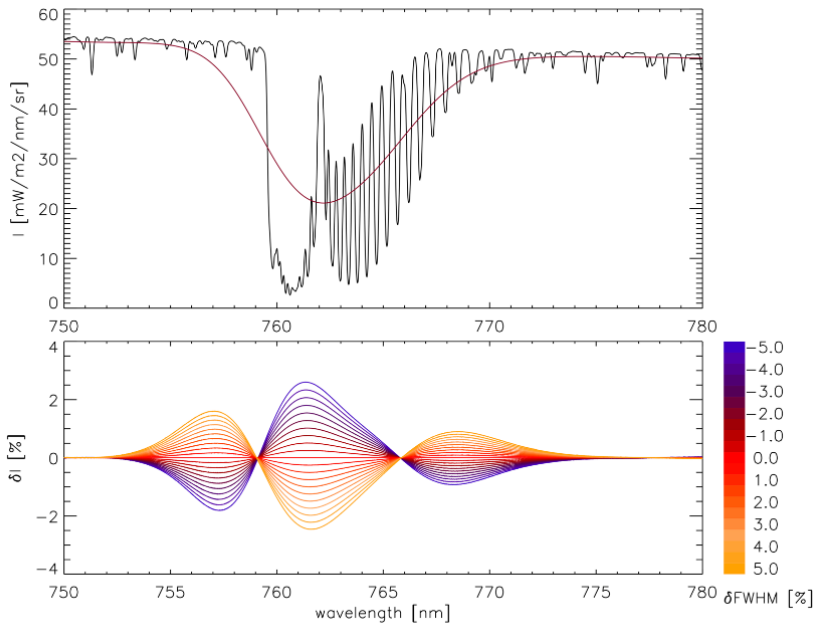

Figure 74: MAP-mod radiance error in the NIR. (Top) Simulation of the MAP-mod radiance measurement from line-by-line radiance simulation assuming a spectral resolution of 5 km. (Bottom) Radiance errors for errors in the FWHM of the ISRF between ±5% calculated with respect to the maximum radiance in the spectrum.

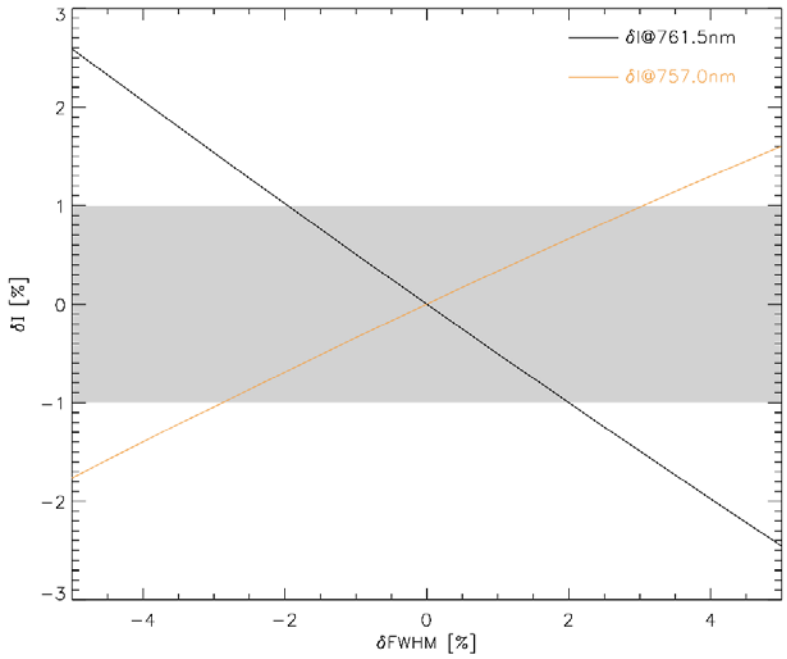

Figure 75: MAP-mod radiance error at 761.5 nm and 757.5 nm as a function of the FWHM error.

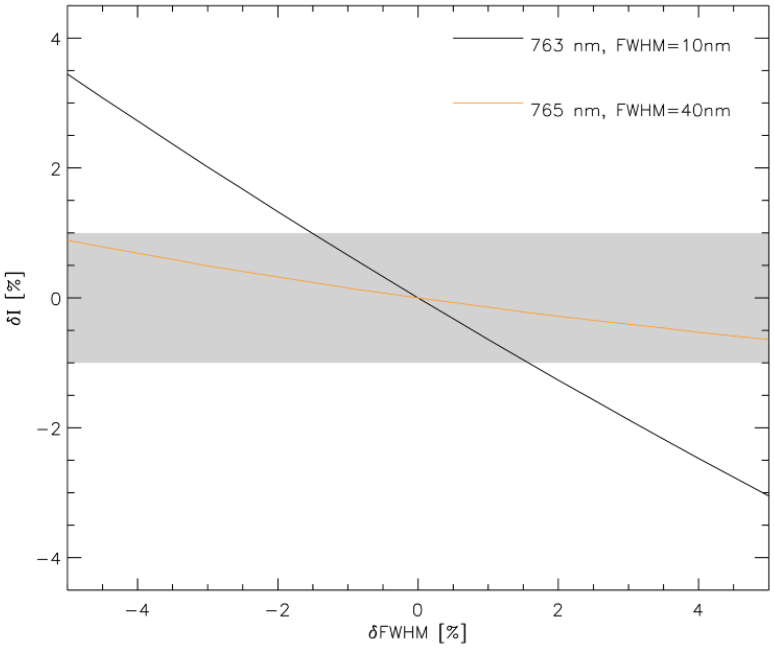

Figure 76: Same as **Figure 75** but for band 6 and 7 of the MAP-band concept as defined in MRDv1.0.

8.7. Summary and conclusions

The CO2M requirements of the MAP instrument have been analyzed with respect to the XCO_2 performance. The analysis accounts for two different instrument concepts using the spectral modulation technique and bandpass polarimetry.

For the modulation concept, we conclude that the radiance uncertainty must be < 3% and the DLP uncertainty < 0.0035. We have broken down this requirement to a radiance precision and bias requirement to be 0.2 % and 3%, respectively, and a DLP precision and bias requirement to be < 0.0025. The instrument must measure radiance and DLP in at least 5 viewing angles in the spectral range 385-765 nm.

For the bandpass concept, the same radiometric requirements hold, i.e., the radiance uncertainty must be < 3% and the DLP uncertainty < 0.0035 with the corresponding breakdown to radiometric and polarization precision and biases. This instrument concept must measure radiance and DLP in a least 40 viewing angles at 7 wavelengths (410, 443, 490, 555, 670, 735, 865 nm). For instrument cross calibration, it is desirable to have one particular radiance measurement at 753 nm. In case an already existing band must be omitted for this implementation, replacing the 555 nm has the smallest impact on the CO2M performance.

Independent on the MAP concept, the radiance and polarization measurements must the spatially resampled, both for a consistent interpretation of the different viewing angles and for a co-alignment with the CO_2 measurements. For this purpose, a spatial oversampling of a factor 2 is required.

9. Reference spectra incl. gain vectors: XCO_2 and XCH_4

9.1. Scenarios and instrument configurations

Reference spectra and gain vectors have been generated for a number of scenarios. Note that spectra for glint observations are not yet part of the data base.

The scenarios are described in **Table 36**. Other (common) parameters: No clouds, background aerosols (low; AOD approx. 0.1 @ 765 nm), XCO_2 400 ppm, XCH_4 1800 ppb, H_2O column approx. US Standard Atmosphere (column: 1.43 g/cm^2; 4.8x10^{22} molecules/cm^2), meteorological data ERA Interim, Berlin (latitude 52.5^{o}N; longitude 13.5^{o}E) 21-March-2008 (surface pressure 971.17 hPa, surface temperature 276.99 K).

Scenario ID	SZA [deg]	Albedo NIR / SW1 / SW2	Comments
TRD	0	0.1 / 0.05 / 0.05	Tropical Dark
TRB	0	0.6 / 0.4 / 0.4	Tropical Bright
REF00	0	0.25 / 0.2 / 0.1	Reference scenario Berlin
MLD	50	0.1 / 0.05 / 0.05	Mid-latitude Dark
MLB	50	0.6 / 0.4 / 0.4	Mid-latitude Bright
VEG50	50	0.2 / 0.1 / 0.05	Vegetation albedo
REF50	50	0.25 / 0.2 / 0.1	Reference scenario Berlin
HLD	70	0.1 / 0.05 / 0.05	High Latitude Dark
HLB	70	0.6 / 0.4 / 0.4	High Latitude Bright
REF70	70	0.25 / 0.2 / 0.1	Reference scenario Berlin

Table 36: Scenarios for reference spectra and gain vectors. No clouds, low aerosols (AOD 0.1).

The CO2M instrument configurations are listed in **Table 37**.

Instrument ID	Description
CO2M_001	SWIR-2: B and C (sub)bands (only) with spectral resolution 0.35 nm. SNR (threshold; radiance unit: photons/s/nm/cm^2/sr): • NIR: *SNRref* = 260, *Lref* = 4.2x10^{12}; formula: Eq. 1 from Draft 1 • SWIR-1: *A* = 0.86 x 10^{-7}, *B* = 200; formula: Eq. 2 from Draft 1 • SWIR-2: *A* = 1.00 x 10^{-7}, *B* = 200; formula: Eq. 2 from Draft 1
CO2M_002	SWIR-2: B and C (sub)bands (only) with spectral resolution 0.35 nm. Identical with CO2M_001 except for SNR: SNR: • NIR: *A* = 0.2 x 10^{-7}, *B* = 140; formula: Eq. 1 (this document) • SWIR-1: *A* = 1.32 x 10^{-7}, *B* = 450; formula: Eq. 1 (this document) • SWIR-2: *A* = 1.54 x 10^{-7}, *B* = 450; formula: Eq. 1 (this document)

Table 37: Instrument configurations for reference spectra and gain vectors.

9.2. Univ. Bremen reference spectra for XCO_2 and XCH_4

The University of Bremen data, i.e., the gain vector (GV) files and high resolution radiance and irradiance spectra, have been generated with FOCAL.

Reference spectra are shown in **Figure 77** - **Figure 80** for the scenarios listed in **Table 36** and using instrument configuration CO2M_002 described in **Table 37**.

The data format is the same as defined and used for CarbonSat **/CS L1L2-II TN nadir, 2015/**. For each scenario a gain vector file and 3 high resolution radiance and irradiance files have been generated.

The reference spectra are stored on the project ftp server in the following subdirectories:

- RefSpecs/FOCAL/CO2M_002_HLB/
- RefSpecs/FOCAL/CO2M_002_HLD/
- RefSpecs/FOCAL/CO2M_002_REF50/
- RefSpecs/FOCAL/CO2M_002_VEG50/
- RefSpecs/FOCAL/CO2M_002_TRB/
- RefSpecs/FOCAL/CO2M_002_TRD/
- …

For example, for VEG50 the following files are stored in its subdirectory:

- 1 gain file: CO2M_002_GM_VEG50_12Dec2018.focalGM
- 3 high resolution radiance files: rad_hr_NIR.dat, rad_hr_SWIR1.dat, rad_hr_SWIR2.dat
- 3 high resolution solar irradiance files: irr_hr_NIR.dat, irr_hr_SWIR1.dat, irr_hr_SWIR2.dat

All files are in ASCII format with a header followed by a table with the data.

CO2M_002_GM_VEG50_12Dec2018.focalGM:

```
* GHGE2ES gain matrix (FOCAL)
* Generated by Stefan.Noel@iup.physik.uni-bremen.de on 2018-12-12
* Number of wavelengths:
  2336
* Wavelength index start - end NIR band:
  0 795
* Wavelength index start - end SW1 band:
  796 1740
* Wavelength index start - end SW2 band:
  1741 2335
* Wavelength range NIR band [nm]:
    747.0000   772.9700
* Wavelength range SW1 band [nm]:
   1590.0000  1674.9600
* Wavelength range SW2 band [nm]:
   1990.0000  2094.9400
* Spectral resolution FWHM NIR band [nm]:
  0.12
* Spectral resolution FWHM SW1 band [nm]:
  0.3
* Spectral resolution FWHM SW2 band [nm]:
  0.35
* IDX Wavelength[nm] G0(XCO2)[-] G1(XCH4)[-] Radiance[phot/s/nm/cm2/sr]
SolarIrrad[phot/s/nm/cm2]
   0   747.0000 -1.95191360269e-01 -4.67867437770e-04  2.10268785343e+13  4.96232555290e+14
   1   747.0327 -1.92402771780e-01 -4.61179020892e-04  2.10051178722e+13  4.95721977796e+14
   2   747.0653 -1.89628039999e-01 -4.54501597727e-04  2.09952816307e+13  4.95492817095e+14
...
2333  2094.5867  3.06828169420e+00  9.83554683888e-03  9.93914073602e+11  1.02676518463e+14
2334  2094.7634  2.25606216025e+00  8.94350794242e-03  9.84840878993e+11  1.02741850447e+14
2335  2094.9400  1.59968246535e+00  7.69894450779e-03  9.71497148136e+11  1.02715970546e+14
```

The radiance and irradiance files all have the same format (a 3 lines header followed by a table with data).

Example: rad_hr_NIR.dat:

```
#  GHGE2ES / FOCAL SGM spectra v2.0
#  Contents: Wavelength [nm], Radiance [phot/s/cm^2/nm/sr]
#  Band NIR, no Doppler shift
  745.0000  1.90805034702e+13
  745.0010  1.93283535688e+13
  745.0020  1.95764076501e+13
…
  774.9980  2.04520828519e+13
  774.9990  2.04489481257e+13
  775.0000  2.04450774853e+13
```

The gains can be used to compute XCO_2 and XCH_4 retrieval errors, given an appropriate error spectrum. This corresponds to "linear error analysis" and if errors shown in this document with this approach then this is referred to as "FOCAL/GV" (e.g., in the header of the corresponding tables).

In order to compute the XCO_2 error in ppm, one has to compute the scalar product of the XCO_2 gain vector *GAIN_XCO2* and the relative error spectrum vector *rel_err_spec*:

$$XCO2_{error} = \sum_{i}^{N} GAIN_XCO2_i \cdot rel_err_spec_i$$

Here *i* is the spectral index of wavelength λ_i and the sum refer to all *N* spectral points covering all three spectral bands.

The dimensionless radiance or reflectance error spectrum *rel_err_spec* is defined as follows:

rel_err_spec = spectrum_with_error / spectrum_without_error – 1.0

The radiance or reflectance error is therefore the relative error spectrum, computed using a spectrum with error divided by an error free spectrum.

The same approach is valid for XCH_4. Here, however, the XCH_4 gain vector needs to be multiplied by 1000, in order to get the XCH_4 error in ppb. Without this scaling, the XCH_4 error is in ppm.

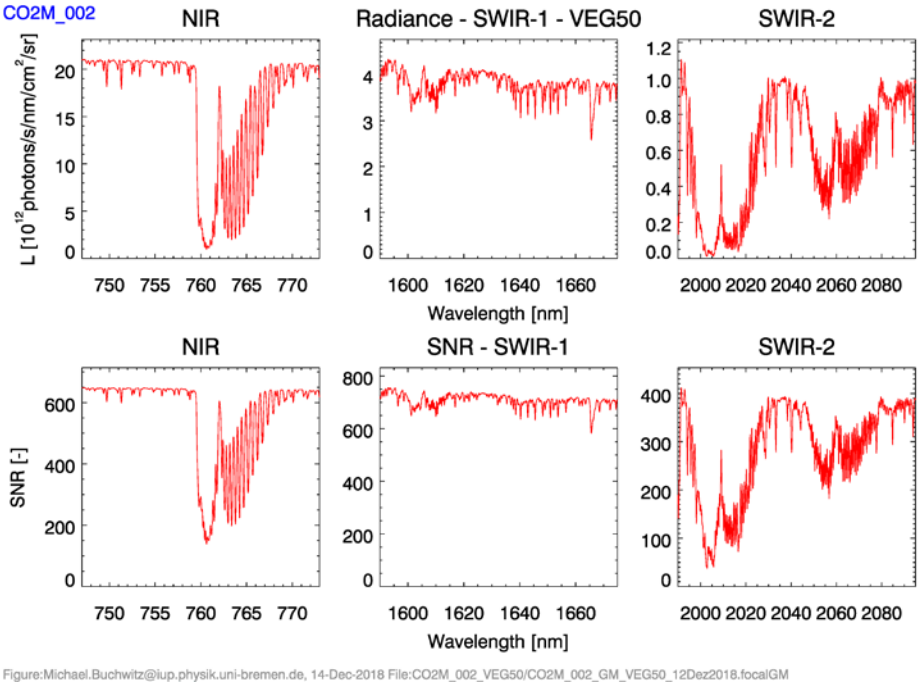

Figure 77: Radiance spectrum (top) and SNR (bottom) for scenario VEG50.

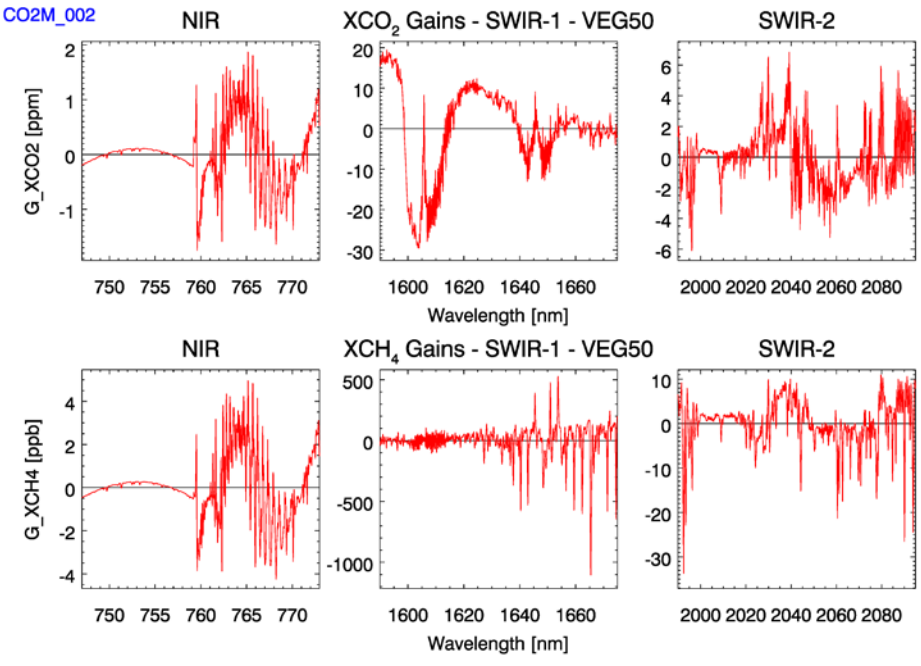

Figure 78: Gains for XCO_2 (top) and XCH_4 (bottom) for VEG50.

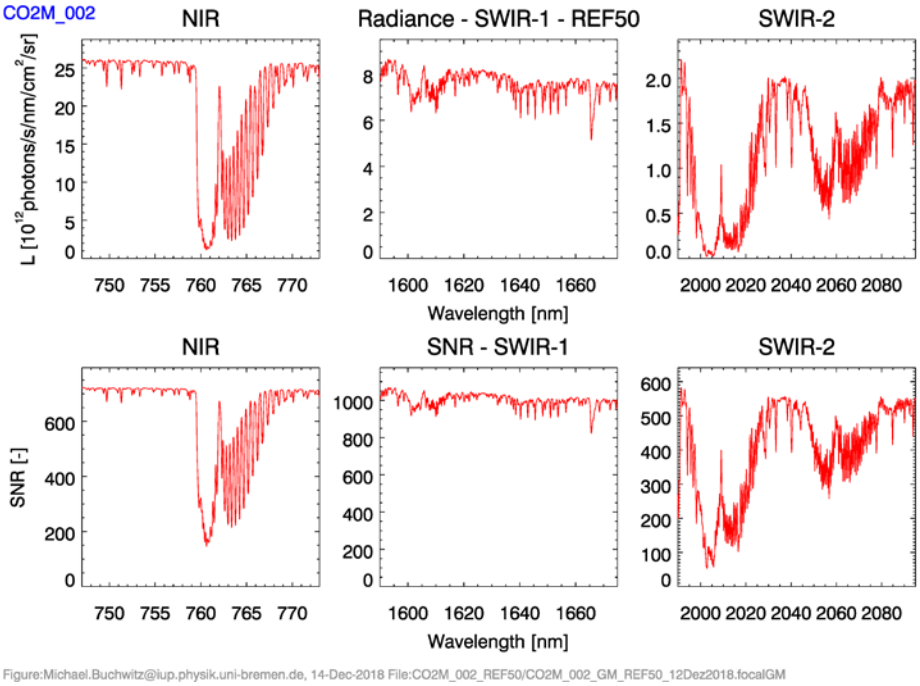

Figure 79: Radiance spectrum (top) and SNR (bottom) for scenario REF50.

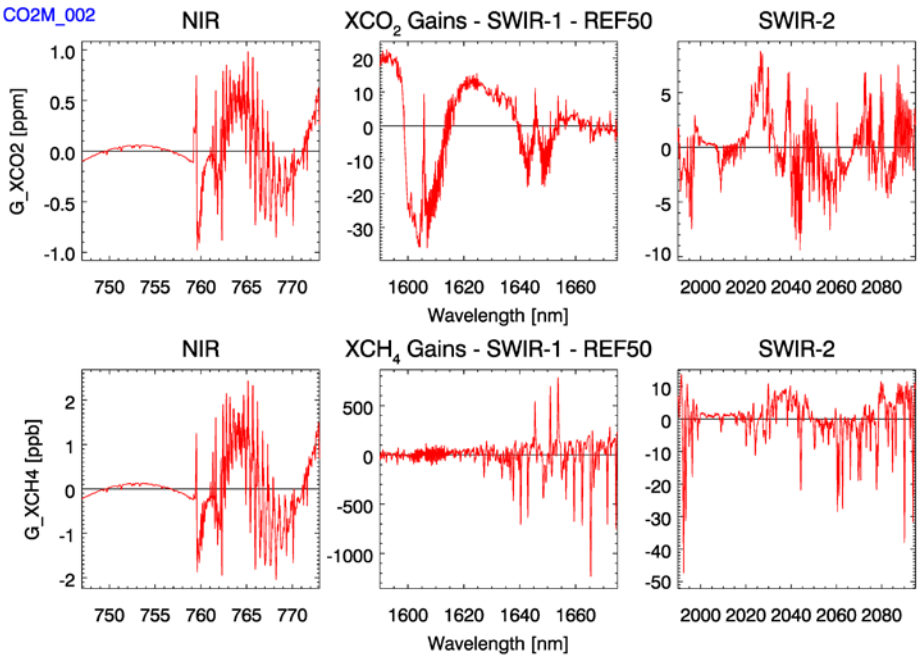

Figure 80: Gains for XCO_2 (top) and XCH_4 (bottom) for REF50.

10. Reference spectra incl. gain vectors: Tropospheric NO_2

10.1. Scenarios and instrument configurations

The default settings for DOMINO are listed in **Table 38**. When other settings are used, they are specified for that particular case. It is noted that the reference spectrum that is used differs from the default settings. This is not problem, as long as the SNR numbers and SNR reference spectrum are used together.

Table 38. Default simulation and retrieval setup.

Noise Model	SNR is defined with respect to a reference spectrum (dark surface with albedo 0.02 for SZA = 0 and VZA = 0, no aerosols, no clouds).
	SNR varies according to shot noise
	SNR for irradiance is set to 5000
Spectral	Spectral range is 405 – 465 nm
	Spectral sampling 0.20 nm
	FWHM 0.60 nm and slit function is a flat-topped Gaussian
Instrument errors	No offsets, no stray light, no added spectral features
Geometry	SZA = 60, VZA varies
Geophysical setup	NO_2 profile shape is taken from the CAMELOT project: European polluted
	No aerosol
	No cloud
	Surface albedo 0.05
	Tropospheric NO_2 column 1.0E16 or 1.0E15 molecules/cm^2
	Stratospheric NO_2 column 4.0E15 molecules/cm2
	300 Dobson units of ozone (shape from European polluted model)
Fit parameters	Total NO_2 column
	Polynomial coefficients (degree polynomial is 6)

10.2. KNMI data: ESRA and Gain: S7MR-OBS-650

Requirement S7MR-OBS-650 reads: The ESRA (Effective Spectral Radiometric Accuracy) correlating with atmospheric spectral structures shall be constrained using the Gain Matrix Method. The systematic NO2 error due to ESRA shall be lower than 10%.

The errors in the retrieved parameters can be calculated from the gain vector, G, using the expression

$$\Delta x = \sum_{i=1}^{N} G(\lambda_i)\,\Delta R(\lambda_i) \qquad (1)$$

where Δx is the error in the retrieved parameter *x*, $G(\lambda_i)$ is the gain matrix calculated for the instrument wavelengths λ_i, and $\Delta R(\lambda_i)$ is the error in the sun-normalized radiance for the instrument wavelengths λ_i . The summation extends over all wavelength in the fit window considered.

Results for the bias in the total column of NO_2 in molecules/cm^2 are presented here. These gain vectors are also delivered to ESA in an Excel spreadsheet, along with the DISAMAR configuration file.

In the DOMINO retrieval approach, used here, we assume that the stratospheric NO_2 is known, therefore the bias presented here is the bias for the tropospheric NO_2 column.

Figure 81 shows that the gain varies little with the viewing direction, and **Figure 82** shows that it changes little when the degree of the DOAS polynomial varies.

Figure 83 shows that the gain varies with the tropospheric NO_2 column. Gain values are significantly larger when the troposphere contains more NO_2. **Figure 84** shows that the gain depends on the surface albedo and is larger for smaller values of the surface albedo.

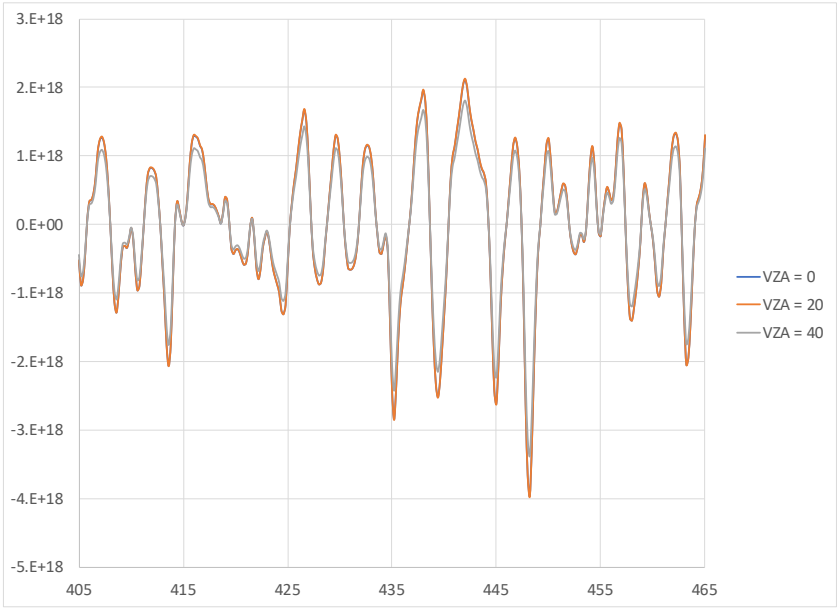

Figure 81. Gain plotted as function of the wavelength for different viewing directions. The tropospheric NO_2 column is 1.0E16 molecules/cm^2, the surface albedo is 0.05, the solar zenith angle is 60 degrees, the azimuth difference is 0 degrees, and the degree of the DOAS polynomial is 6.

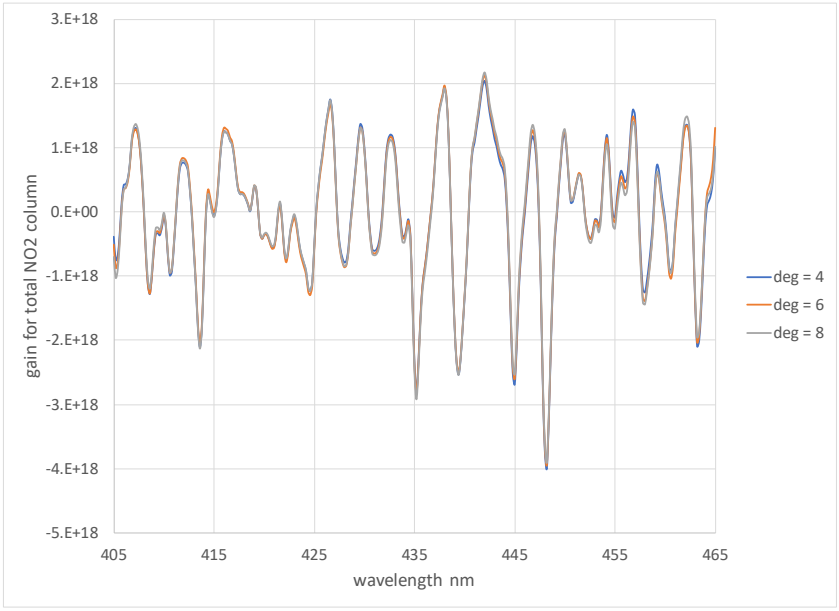

Figure 82. Same as **Figure 81** but for different values of the degree of the DOAS polynomial. Here VZA is 0.

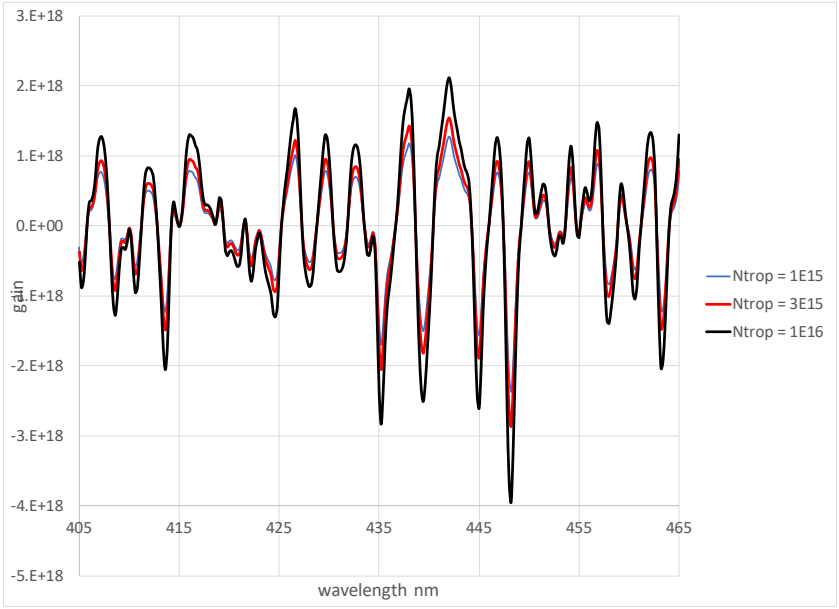

Figure 83. Same as **Figure 81** but for different values of the tropospheric NO_2 column.

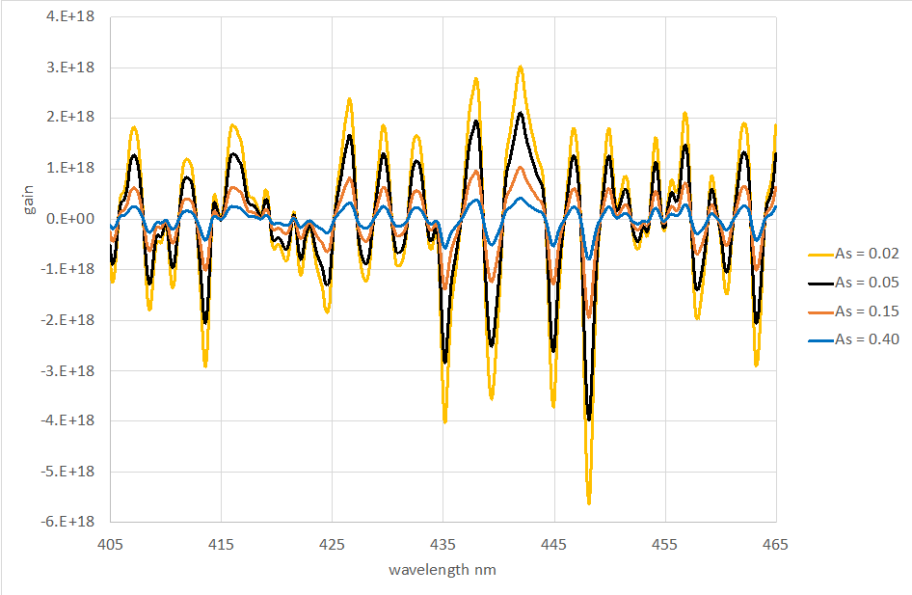

Figure 84. Same as **Figure 81** but for different values of the surface albedo.

10.3. Summary and conclusions

In this section, the NO_2 gain vectors are discussed. These gain vectors vary significantly with the amount of NO_2 and the surface albedo. We recommend using the gain vector for the tropospheric column NO_2 of 3 x 10^{15} molec cm^{-2} and surface albedo 0.05.

11. Reference spectra incl. gain vectors: RemoTeC XCO_2 and MAP aerosols

11.1. Gain vector and reference spectra using RemoTeC

This section describes the delivered XCO_2 gain vectors and reference spectra for the CO_2 spectrometer as generated by SRON.

11.1.1. Scenarios and instrument configurations

For the simulations of the provided data set, we consider eight different reference scenes with the solar geometry and surface albedo given in **Table 39**. Simulations are performed for ground pixels at sub-satellite point, so the viewing zenith angle VZA = 0°. Additional atmospheric parameters, which are common to all scenarios, are summarized in **Table 40**.

Table 39: Solar zenith angle (SZA) and surface albedo for the eight reference scenarios of this study. Note that these are the same as listed in **Table 36**, apart from REF70 and REF0.

scenario	SZA [degree]	Albedo		
		NIR	SW1	SW2
High-Latitude Dark (HLD)	70	0.10	0.05	0.05
High-Latitude Bright (HLB)	70	0.60	0.40	0.40
Tropical Dark (TRD)	0	0.10	0.05	0.05
Tropical Bright (TRB)	0	0.60	0.40	0.40
Mid-Latitude Dark (MLD)	50	0.10	0.05	0.05
Mid-Latitude Bright (MLB)	50	0.60	0.40	0.40
Reference (REF50)	50	0.25	0.20	0.10
Veg50	50	0.20	0.10	0.05

Table 40: Atmospheric constituents applicable for all simulations of this study.

atmospheric constituent	unit	Amount
air column	molec./cm^2	2.14E+25 (corresponds to a surface pressure of 1013 hPa)
XCO_2	ppm	400
XCH_4	ppb	1800
water column	molec./cm^2	2.00E23
aerosol optical thickness@765 nm	-	0.1
aerosol layer height	m	2000
aerosol size distribution parameter $\boldsymbol{\alpha}$	-	4

For the simulations, we consider one instrument concept (equal resolving power), which differ in the spectral sizing of the three bands (NIR, SW1, SW2) and the noise model, specified and **Table 41**. The tables include coefficients a and b of the signal to noise ratio (SNR) model

$$\mathrm{SNR} = \frac{AI}{\sqrt{AI + B^2}} \qquad \text{(E10.1)}$$

where I is the spectral radiance and A and B parametrizes the signal dependent and independent SNR performance of a spectral sizing concept **/Sierk and Caron, 2012/**.

Table 41: Instrument concept ER (Equal Resolving power).

	units	NIR	SW1	SW2
Spectral band width	nm	747-773	1590-1675	1990-2095
Spectral resolution	nm	0.12	0.30	0.35
Spectral oversampling ratio	-	3	3	3
A	(s cm^2 nm sr)/ ph.	2.0E-08	1.32E-7	1.54E-07
B	-	140	450	450

11.1.2. SRON data

A data set of the XCO_2 gain and the radiance spectrum is provided for each atmospheric scenario in **Table 39**. **Figure 85** depicts an example for the Mid-Latitude-Bright scenario.

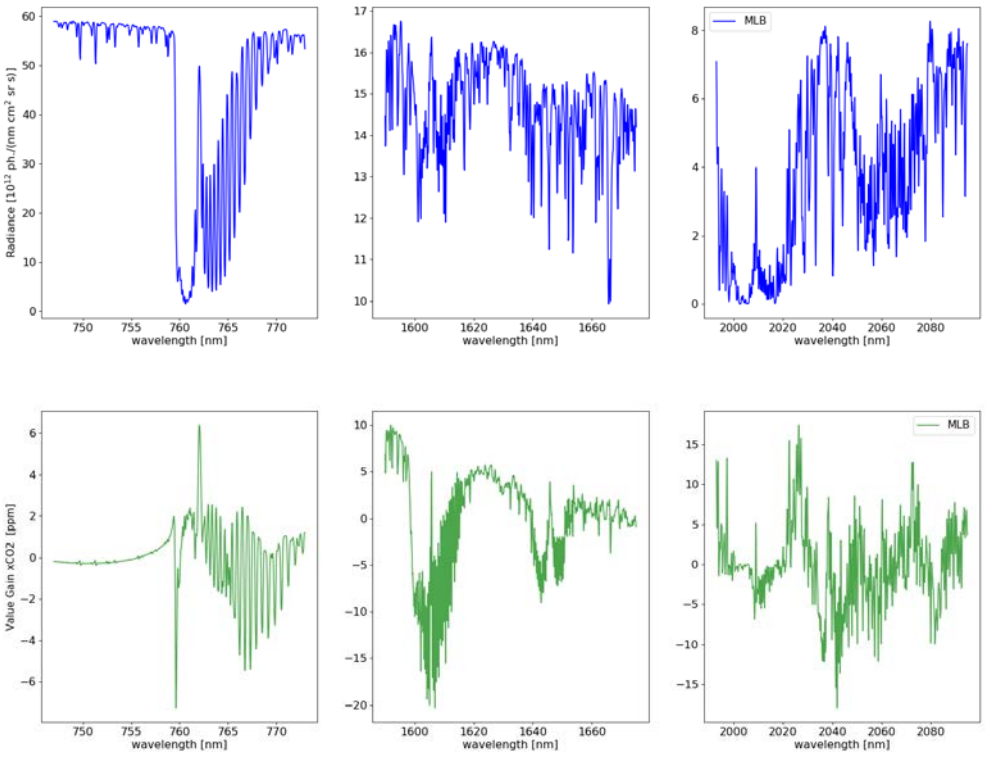

Figure 85: Radiance (top row) and Gain vector (bottom row) for the three different windows (left to right); for the MLB scenario. The gain vector is plotted multiplied with the radiance to be consistent with the description in **Sect. 9.2**.

These reference spectra are also available via the project ftp server. They are stored in the following subdirectory: RefSpecs/SRON/Gain_20190129_scatt/

The directory contains three types of (ASCII) reference spectra files:

- gain files (gain*.dat)
- spec files (spec*.dat)
- LBL files (LBL*.dat)

Gain files:

For each scenario, three gain files exist, one for each of the three bands.
Spectral resolution and sampling corresponds to CO2M (see instrument CO2M_002 in **Table 37**).

The gain files contain a header (2 lines) and 5 columns with data:

- Column 1: Wavelength [nm]
- Column 2: XCO_2 gain for radiance [ppm / (photons/s/nm/cm^2/sr)]
- Column 3: XCH_4 gain for radiance [ppb / (photons/s/nm/cm^2/sr)]
- Column 4: XCO_2 gain for sun normalized radiance [ppm / (1/sr)]
- Column 5: XCH_4 gain for sun normalized radiance [ppb / (1/sr)]

Spec files:

For each scenario, three spec files exist, one for each of the three bands.
Spectral resolution and sampling is the same as for the gain files.
The spec files contain a header (2 lines) and 4 columns with data:

- Column 1: Wavelength [nm]
- Column 2: Radiance [photons/s/nm/cm^2/sr]
- Column 3: Irradiance [photons/s/nm/cm^2]
- Column 4: Reflectance [-] (defined as π x Radiance/Irradiance/cos(SZA))

LBL files:

These files contain high spectral resolution and sampling radiance, irradiance and reflectance data. The format is the same as for the spec files.

In order to compute the XCO_2 error in ppm, one has to compute the scalar product of the XCO_2 gain vector *(as given in the gain file)* and the absolute radiance error spectrum or the error spectrum of the sun-normalized radiance.

The difference to the use of the FOCAL gains (described in **Sect. 9.2**) is that

- the error spectrum has to be specified in radiance or sun-normalized radiance units (in contrast, the FOCAL gains are valid for relative error spectra) and that
- separate gains are provided for (sun-normalized) radiance errors
- the XCO2 is directly given in ppm without any need to convert the error to ppm.

The XCH_4 gains can be used analogously. The XCH_4 error is given in ppb.

SRON also computed reference spectra incl. gains neglecting atmospheric scattering. These "non-scattering" reference spectra are also available via the project ftp server. They are stored in the following subdirectory: RefSpecs/SRON/Gain_20192810_noscatt/
These data have been used to compute the "SRON(non-scatt)" results shown in **Table 27**.

11.2. MAP reference spectra

To formulate radiometric requirements of the MAP instrument, a set of reference spectra are simulated for a minimum, nominal and maximum radiometric scene. Additionally, spectra for an ocean glint scene and a cloudy scene for different solar zenith angles are provided. All spectra include the spectral Stokes parameter I, Q and U and the solar irradiance in the spectral range 350-1100 nm on a 1 nm spectral grid.

11.2.1. Atmospheric Scenarios

For the simulation of MAP reference spectra, we assume a bi-modal aerosol size distribution with a fine and coarse mode. Here, the log-normal size distribution of each mode is characterized by an effective radius and variance. For the fine mode, we assume purely spherical aerosol particles, whereas for the coarse mode both spherical and spheroidal aerosol particles are possible. The optical properties of spherical and spheroidal aerosol particles are calculated using the tabulated kernels of **/Dubovik et al. 2006/**.

For the simulation of the spectra, we assume the micro-physical aerosol properties to be altitude independent, whereas the number of aerosol particles for each mode is described by a Gaussian height profile with a centre height and a width parameter. The values for refractive indexes are based on values for inorganic material for the fine mode, and dust for the coarse mode as reported by **/d'Almeida et al 1991/,**

Finally, to account for surface reflection we employ the BDRF kernel, which is parametrized by five kernel terms, namely

$$\boldsymbol{\rho}(\Omega_{in},\Omega_{out}) = c_0(\lambda)\boldsymbol{K}_0(\Omega_{in},\Omega_{out}) + c_0(\lambda)c_1\boldsymbol{K}_1(\Omega_{in},\Omega_{out}) + c_0(\lambda)c_2\boldsymbol{K}_2(\Omega_{in},\Omega_{out}) + c_3\boldsymbol{K}_3(\Omega_{in},\Omega_{out}) + c_4\boldsymbol{K}_4(\Omega_{in},\Omega_{out}) \quad \text{E10.2}$$

Here ρ is the 4×4 surface BDRF that maps the four Stokes parameters I, Q, U and V of the incident light to the corresponding Stokes parameters of the reflected light as a function of the solid angles Ω_{in},Ω_{out}. The BDRF kernels empirically describe the bidirectional reflection of the Earth surface, where kernel $\boldsymbol{K_i}$ with $i = 0,1,2$ simulates the radiance reflection with a wavelength dependent coefficient $c_0(\lambda)$ and two spectrally independent coefficients c_1 and c_2. Here, the kernel $\boldsymbol{K}_0$ models Lambertian isotropic reflection and so coefficient c_0 corresponds to the spectral Lambertian albedo.

To study the synergy between MAP and CO2I we considered a soil-type surface with Lambertian albedo of (0.13, 0.30) at (765, 1600) nm and a vegetation-type surface with Lambertian albedo of (0.44, 0.23) at (765,1600) nm (for the NIR, SWIR1 and SWIR2 windows of the CO2 spectrometer). Kernel K_1 and K_2 are adapted from the Ross-Li BDRF model describing anisotropic scalar reflection of land surfaces **/Strahler et al., 1999/**, where K_1 simulates reflection of dense leaf canopy and K_2 the radiance reflection of a sparse ensemble of surface objects casting shadows on the background, which is assumed Lambertian. Finally, the polarizing effect of surface reflection is expressed by the kernels K_3 and K_4 representing reflection properties of vegetation and soil surfaces. Here, the polarizing

effect is nearly independent of wavelength as validated with RSP aircraft measurements **/Litvinov P. et al., 2012/**. For the radiative transfer simulation, we used the vector model V-Lintran as described by **/Hasekamp et al., 2002/** and **/Hasekamp et al. 2005/**.

Overall, for the MAP performance analysis we consider three generic cases:

Case 1: Coarse and fine mode of atmospheric aerosol is located in the tropospheric boundary layer. The coarse mode has a fixed small optical depth of 0.02, the optical depth pf the fine mode varies.

Case 2: The Gaussian profile of the coarse mode is at 8 km altitude, whereas the fine mode is located in the boundary layer as for case 1. The fine mode has a fixed optical depth of 0.2, the optical depth of the coarse mode varies.

Case 3: Same as case 2 but for a 4 km layer height of the coarse mode instead of at 8 km.

For the three scenarios, the micro-physical properties are summarized in **Table 42**.

Table 42: Micro-physical properties of the aerosol scenarios.

Aerosol parameters	Case 1		Case 2 / 3	
	Fine mode	Coarse mode	Fine mode	Coarse mode
spherical fraction	1.0	0.05	1.0	0.05
refractive index @765nm	(1.50, 1E-7i)	(1.53, 2.54E-3i)	(1.50, 1E-7i)	(1.53, 2.54E-3i)
refractive index @1600nm	(1.50, 1E-7i)	(1.40, 1.56E-3i)	(1.50, 1E-7i)	(1.40, 1.56E-3i)
refractive index @2000nm	(1.50, 1E-7i)	(1.30, 2.00E-3i)	(1.50, 1E-7i)	(1.30, 2.00E-3i)
effective radius [micron]	0.12	1.6	0.12	1.6
effective variance	0.2	0.6	0.2	0.6
z_center [m]	1000	1000	1000	8000/4000
width (FWHM) [m]	2000	2000	2000	2000
aerosol optical thickness@765 nm	varies	0.02	0.2	varies

11.2.2. Reference Spectra

To investigate the radiometric performance of different MAP instrument concepts we simulated six reference spectra:

Lmin	case 1 with total AOT=0.12, SZA=70°, VZA = 30°, soil BDRF
Lref	case 3 with total AOT=0.3, SZA=50°, VZA = 50°, vegetation BDRF
Lmax	Case 3 for total AOT = 0.3, SZA = 1°, VZA = -20°, maximum spectral radiance of a vegetation and sand spectrum including 20 % margin
Lglint	case 1 with total AOT=0.12, SZA=60°, ocean, wind speed=3 m/s
Lcld_50	Lambertian surface reflection of A=1.1 and SZA = 50°
Lcld_25	Lambertian surface reflection of A=1.1 and SZA = 25°

For each spectrum, the radiance I, the relative Stokes parameters Q/I and U/I, the degree of linear polarisation (DLP) and the solar irradiance spectra are provided for the range 350-1100 nm with a 1 nm spectral sampling. Because of its little contribution, Stokes parameter V is not reported. The spectra L_{min}, L_{ref} and L_{max} are shown in the **Figure 86 - Figure 88**, including corresponding spectra for the range of viewing zenith angles between $\pm 60^{o}$. Here L_{min} comprises a relatively low radiance level with a high degree of linear polarization, whereas L_{max} reflects a spectrum with high clear-sky radiance with a small degree of linear polarization. The figures also depict the corresponding reference values of the 3MI mission **/Schlüssel et al., 2010/**, which overall are more challenging. For L_{max} this can be explained by the choice of a different reference scene, which is a cloudy scene for 3MI and a cloud-free scene in case of the MAP instrument. The much lower L_{min} for 3MI can be explained by that these are defined by ocean scenes, while ocean scenes are not driving requirements for CO2M.

Additionally, spectra are provided for a typical glint scene L_{glint} and for Lambertian reflection at a cloud surface with an albedo A = 1.1 and a solar angle of SZA = 25 and 50 degree, L_{cld_25} and L_{cld_50}. For stray light analyses with a radiometric contrast within an instrument swath, we propose the use of L_{min} and L_{cld_25} to describe the transition between a dark scene with high DLP and a bright scene with low (zero) DLP (see **Figure 89**).

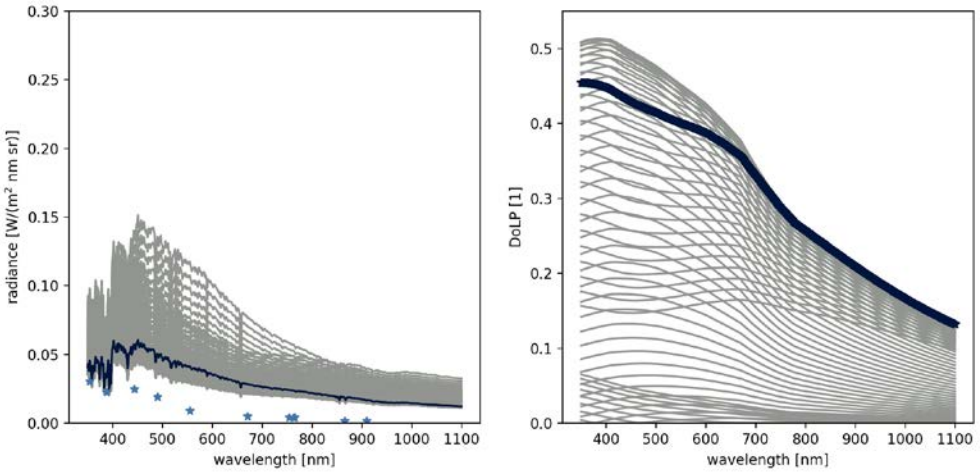

Figure 86: Minimum reference spectrum Lmin for a SZA of 70º and VZA of 30º (black line, left panel: radiance, right panel: degree of linear polarization, DLP). The grey lines show the ensemble of spectra for -60º <VZA<60º in steps of 2º, the blues asterix indicates corresponding reference values of the 3MI instrument. MAP band selection is based on the 3MI selection, but is not identical to it

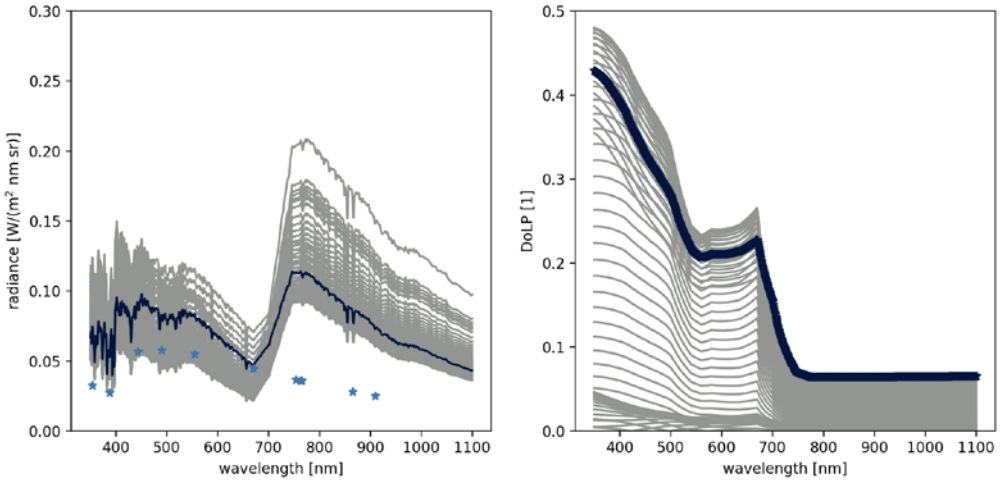

Figure 87: Same as **Figure 86** but for the reference spectra Lref (SZA=50º, VZA = 50º).

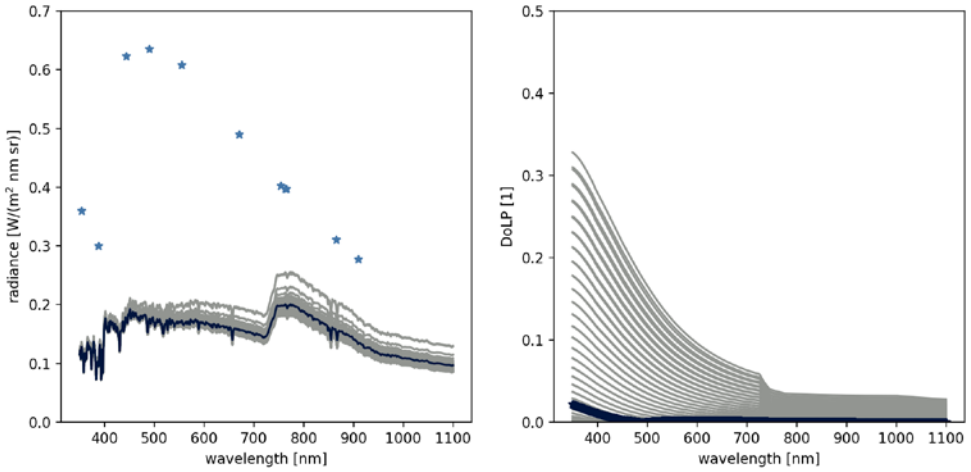

Figure 88: Same as **Figure 86** but for the the reference spectrum Lmax (SZA = 1°, VZA = -20°).

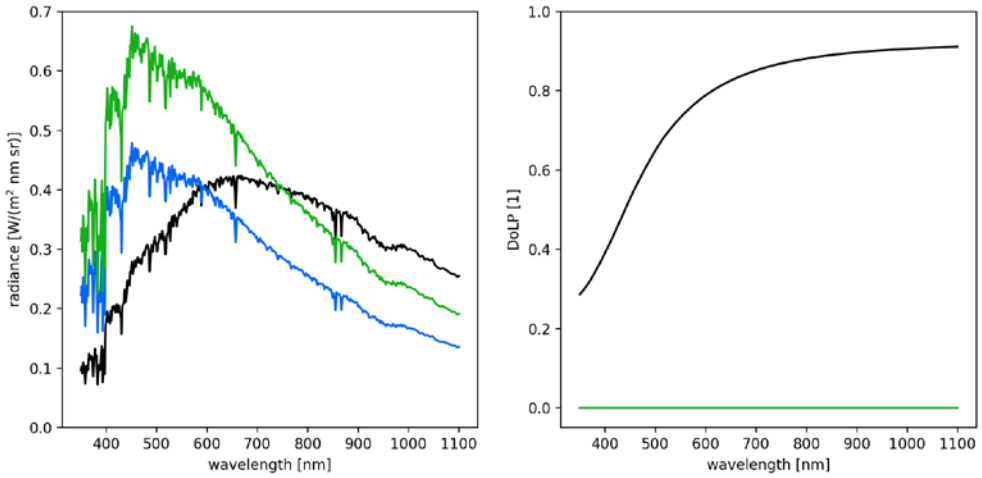

Figure 89: Reference spectra L_{glint} (black) and L_{cld_25} (green) and L_{cld_50} (blue). For both, L_{cld_50} and L_{cld_25}, the degree of linear polarization is zero due to the assumption of a Lambertian reflector.

12. Reference spectra incl. XCO_2 gain vectors from Univ. Leicester

Univ. Leicester has also generated reference spectra and XCO_2 gains vectors computed using the UoL-FP retrieval algorithm and related RTM.

The files have been computed for CO2M instrument CO2M_002 (see **Table 37**) and for the following ten scenarios (see **Table 36**):

- HLB
- HLD
- MLB
- MLD
- TRB
- TRD
- VEG50
- REF00
- REF50
- REF70

These reference spectra are also available via the project ftp server. They are stored in the following subdirectory: RefSpecs/UoL/

This directory contains three sub-directories:

- Radiance files:
  - Sub-directory: outputs_radiance/
- Gains v1:
  - Sub-directory: gains_v1/
  - Contains gain files without ZLO in NIR and with p_surf as state vector elements
- Gains v2:
  - Sub-directory: gains_v2/
  - Contains gain files with ZLO in NIR and without p_surf as state vector elements

Radiance files:

Radiance files at instrument spectral resolution and sampling:

- SSS_rad_meas.dat: ASCII files where SSS indicates the scenario
  - These files consist of a header followed by 4 columns with data:
    - Column 1: Wavelength [nm]
    - Column 2: Wavenumber [cm^{-1}]
    - Column 3: Radiance [photons/s/m^2/µm/sr]
    - Column 4: Radiance error [photons/s/m^2/µm/sr]

Reflectance files at high spectral resolution and sampling:

- SSS_highres_BBB.dat: ASCII files where SSS indicates the scenario and BBB one of the three bands (NIR, SWIR1, SWIR2)
    - These files consist of a header followed by 2 columns with data:
        - Column 1: Wavenumber [cm^{-1}]
        - Column 2: Sun-normalized radiance [-]

Solar irradiance files at high spectral resolution and sampling:

- SSS_solar_highres_BBB.dat: ASCII files where SSS indicates the scenario and BBB one of the three bands (NIR, SWIR1, SWIR2)
    - These are ASCII files consist of a header followed by 2 columns with data:
        - Column 1: Wavelength [nm]
        - Column 2: Solar irradiance [photons/s/m^2/µm]

Gain files:

Gains files at instrument spectral resolution and sampling:

- SSS_gain*.dat: ASCII files where SSS indicates the scenario
    - These files consist of 1 column with data:
        - Column 1: XCO_2 gain [ppm/(photons/s/m^2/µm/sr)]
- ASCII file wl.dat:
    - This file consist of 1 column with data:
        - Column 1: Wavelength [µm]

To compute the XCO_2 error in ppm one has to compute the scalar product of the gain vector with the radiance error vector given in radiance units, i.e., photons/s/m^2/µm/sr.

13. Acronyms and abbrevations

Acronym	Meaning
AOD/AOT	Aerosol Optical Depth/Thickness
ATBD	Algorithm Theoretical Basis Document
AOLP	Angle of linear polarisation
BESD	Bremen optimal EStimation DOAS
BESD/C	BESD algorithm used for CarbonSat assessments
BL	Boundary Layer
BRDF/BDRF	Bidirectional reflectance distribution function
CA	Continental Average (aerosol scenario)
CarbonSat	Carbon Monitoring Satellite
CC	Continental Clean (aerosol scenario)
CCI	Climate Change Initiative (of ESA)
CL	Close Loop
CNES	Centre national d'études spatiales
CO2M	Anthropogenic CO_2 Monitoring Mission
CO2M-REB	Anthropogenic CO_2 Monitoring Mission Requirements Consolidation and Error Budget study
COD	Cloud Optical Depth
CP	Continental Polluted (aerosol scenario)
CS	CarbonSat
CS-L1L2-II	CarbonSat Earth Explorer 8 Candidate Mission Level-1 Level-2 (L1L2) Performance Assessment Study No. 2
CTH	Cloud Top Height
DE	Desert (aerosol scenario)
DISAMAR	Determining Instrument Specifications and Analysing Methods for Atmospheric Retrieval
DES	Desert (surface albedo)
DLP	Degree of linear polarization
DOAS	Differential Optical Absorption Spectroscopy
DOF	Degrees of Freedom
DLP	Degree of linear polarization
E2ES	End-to-end-simulator
EB	Error Budget
EE8	Earth Explorer No. 8 (satellite)
ENVISAT	Environmental Satellite
ESA	European Space Agency
FOCAL	Fast atmOspheric traCe gAs retrievaL
FR	Final Report
FWHM	Full Width at Half Maximum
GHG	Greenhouse Gas
GHG-CCI	Greenhouse Gas project of ESA's Climate Change Initiative (CCI)
GM	Gain Matrix

GMM	Gain Matrix Method
GOSAT	Greenhouse Gases Observing Satellite
GV	Gain Vector
GVM	Gain Vector Method
ISRF	Instrument Spectral Response Function
IUP-UB	Institute of Environmental Physics (Institut für Umweltphysik), University of Bremen, Germany
L1	Level 1
L2	Level 2
MAP	Multi Angle Polarimeter
MC	Monte Carlo
MLS	Mid-latitude summer (profiles)
MODIS	Moderate resolution Imaging Spectrometer
MRD	Mission Requirements Document
NIR	Near Infra Red (band)
OCO	Orbiting Carbon Observatory
OE	Optimal Estimation
OPAC	Optical Properties of Aerosol and Clouds
RfMS	Report for Mission Selection
RMS	Root Mean Square
RMSE	Root Mean Square Error
RSS	Root Sum Square
RTM	Radiative Transfer Model
SCIAMACHY	Scanning Imaging Absorption Spectrometers for Atmospheric Chartography
SCIATRAN	Radiative Transfer Model under development at IUP
SIF	Sun-Induced Fluorescence
SNR	Signal to Noise Ratio
SSI	Spectral Sampling Interval
SSP	Spectral Sizing Point
SSR	Spectral Sampling Ratio
SW1 or SWIR-1	SWIR 1 band
SW2 or SWIR-2	SWIR 2 band
SWIR	Short Wave Infrared
SZA	Solar Zenith Angle
TCCON	Total Carbon Column Observing Network
TOA	Top of atmosphere
VCF	Vegetation Chlorophyll Fluorescence
VEG	Vegetation (surface albedo)
VIIRS	Visible Infrared Imaging Radiometer Suite
VMR	Volume Mixing Ratio
VZA	Viewing Zenith Angle
ZLO	Zero-Level-Offset

14. References

/Boersma et al., 2004/ Boersma, K. F., H. J. Eskes, E. J. Brinksma, Error analysis for tropospheric NO2 retrieval from space, J. Geophys. Res., Vol. 109, issue D4, https://doi.org/10.1029/2003JD003962, 2004.

/Boesch et al., 2006/ Boesch, H., Toon, G. C., Sen, B., Washenfelder, R. A., Wennberg, P. O., Buchwitz, M., de Beek, R., Burrows, J. P., Crisp, D., Christi, M., Connor, B. J., Natraj, V., and Yung, Y. L.: Space-based near-infrared CO_2 measurements: Testing the Orbiting Carbon Observatory retrieval algorithm and validation concept using SCIAMACHY observations over Park Falls, Wisconsin, J. Geophys. Res., 111, D23302, doi:10.1029/2006JD007080, 2006.

/Boesch et al., 2011/ Boesch, H., D. Baker, B. Connor, D. Crisp, and C. Miller, Global characterization of CO_2 column retrievals from shortwave-infrared satellite observations of the Orbiting Carbon Observatory-2 mission, Remote Sensing, 3 (2), 270-304, 2011.

/Boesch, 2018/ Boesch, H., WP2300: Optimizing Spectral Sizing Concepts, Technical Report ESA „Study on Spectral Sizing for CO_2 Observations“, Issue 1, 15-Mar-2018, Doc ID: UOL-CO2SIZ-TN-2018-WP2300, pp. 17, 2018.

/Bovenmann et al., 2010/ Bovensmann, H., Buchwitz, M., Burrows, J. P., Reuter, M., Krings, T., Gerilowski, K., Schneising, O., Heymann, J., Tretner, A., and Erzinger, J., A remote sensing technique for global monitoring of power plant CO_2 emissions from space and related applications, Atmos. Meas. Tech., 3, 781-811, 2010.

/Bovenmann et al., 2014/ Bovensmann, H., M. Buchwitz, M. Reuter, T. Krings, J. Heymann, H. Boesch, J. Landgraf, CarbonSat Earth Explorer 8 Candidate Mission “Level-2 and Level-1B Requirements Consolidation Study“, Final Report ESA Study CarbonSat Earth Explorer 8 Candidate Mission “Level-2 and Level-1B Requirements Consolidation Study “, ESA Contract No 4000105676/12/NL/AF, Version 2.2, Date: 18. July 2014, Doc.ID: IUP-CS-L1L2-FR-01, 2014.

/Bovenmann et al., 2015/ Bovensmann, H., M. Buchwitz, M. Reuter, T. Krings, J. Heymann, H. Boesch, J. Landgraf, CarbonSat Earth Explorer 8 Candidate Mission “Level-1 Level-2 (L1L2) Performance Assessment Study “, Final Report ESA Study, ESA Contract No 4000109814/13/NL/FF/lf, Version 1.0, Date: 11. December 2015, Doc.ID: IUP-CS-L1L2-II-FR-01, 2015.

/Buchwitz, 2011/ Buchwitz, M., CarbonSat Reference Spectra, Technical Report, Version: 2.0, Doc ID: IUP-CS-RS-TN-001, Date: 25 Nov 2011, 2011.

/Buchwitz et al., 2013a/ Buchwitz, M., M. Reuter, H. Bovensmann, D. Pillai, J. Heymann, O. Schneising, V. Rozanov, T. Krings, J. P. Burrows, H. Boesch, C. Gerbig, Y. Meijer, and A. Loescher, Carbon Monitoring Satellite (CarbonSat): assessment of atmospheric CO_2 and CH_4 retrieval errors by error parameterization, Atmos. Meas. Tech., 6, 3477-3500, 2013.

/Buchwitz et al., 2013b/ Buchwitz, M., H. Bovensmann, M. Reuter, J. Heymann, O. Schneising, et al., CARBONSAT: ERROR ANALYSIS FOR PRIMARY LEVEL 2 PRODUCTS XCO_2 AND XCH_4 AND SECONDARY PRODUCT VEGETATION CHLOROPHYLL FLUORESCENCE FOR NADIR OBSERVATIONS OVER LAND, ESA Living Planet Symposium, Sept 9-13, 2013, Edinburgh, UK, conference proceedings ESA Special

Publication SP-722 (on CD-ROM), link: http://www.iup.uni-bremen.de/sciamachy/NIR_NADIR_WFM_DOAS/2846996buchwitz.pdf, 2013.

/Buchwitz et al., 2015/ Buchwitz, M., Bovensmann, T. Krings, M. Reuter, V. V. Rozanov, P. Liebing, J. Landgraf, F. Alkemade, Mission Requirements Analysis and Level 2 Error Characterization for CarbonSat Nadir Observations over Land - WP 1100, 2000 & 4100 Report, ESA Study CarbonSat Earth Explorer 8 Candidate Mission "Level-1 Level-2 (L1L2) Performance Assessment Study" ESA Contract No 4000109814/13/NL/FF/lf, Version 1.2, 3 Dec 2015, Doc ID: IUP-CS-L1L2-II-TNnadir, 2015.

/Buchwitz et al., 2017/ ESA Climate Change Initiative (CCI) Product Validation and Intercomparison Report (PVIR) for the Essential Climate Variable (ECV) Greenhouse Gases (GHG) for data set Climate Research Data Package No. 4 (CRDP#4), Version 5.0, 9. Feb. 2017, link: http://www.esa-ghg-cci.org/?q=webfm_send/352, 2017.

/Buchwitz, 2018/ Buchwitz, M., Error analysis for CarbonSat scenarios and different spectral sizing, Technical Report ESA „Study on Spectral Sizing for CO_2 Observations", Version 4.0, 30-Apr-2018, Doc ID: IUP-CO2SS-TN-5, pp. 93, 2018.

/Buchwitz and Reuter, 2018/ Buchwitz, M., and M. Reuter, Level 2 error files, Technical Report ESA Study of Assessing thresholds for a space borne observation system to monitor fossil CO_2 emissions (PMIF study), Version 2.1, 30-Jan-2018, Doc ID IUP-PMIF_L2e_S7-c, pp. 100, 2018.

/Butz et al., 2017/ Butz, A., K. Graf, J. Landgraf, J. ann den Brugh, D3 – CO_2 errors due to measurement noise and atmospheric scattering for the different spectral sizing concepts of a CO_2 instrument, Technical Report ESA „Study on Spectral Sizing for CO_2 Observations", Version 1.1, 23-May-2017, pp. 24, 2017.

/Ciais et al., 2015/ Ciais, P., et al.: Towards a European Operational Observing System to Monitor Fossil CO_2 emissions - Final Report from the expert group, http://www.copernicus.eu/main/towards-european-operational-observing-system-monitor-fossil-co2-emissions, pp. 68, October 2015, 2015.

/CO2M-REB TN-1000 v1.1, 2019/ Buchwitz, M., M. Reuter, S. Noël, H. Bovensmann, A. Richter, J. Landgraf, P. Vefking, J. de Haan, H. Boesch, Requirements Justification Report for anthropogenic CO_2 Monitoring Mission (CO2M), Technical Report ESA Study on Consolidating Requirements and Error Budget for CO_2 Monitoring Mission (CO2M-REB), version 1.1, 25-April-2019, 74 pages, Doc ID: IUP-CO2M-REB-TN-1000, 2019.

/CO2M-REB TN-2000 v1.2, 2019/ Buchwitz, M., M. Reuter, S. Noël, H. Bovensmann, A. Richter, J. Landgraf, P. Vefking, J. de Haan, H. Boesch, Requirements Sensitivity Analysis for anthropogenic CO_2 Monitoring Mission (CO2M), Technical Report ESA Study on Consolidating Requirements and Error Budget for CO_2 Monitoring Mission (CO2M-REB), version 1.1, 26-April-2019, 133 pages, Doc ID: IUP-CO2M-REB-TN-2000, 2019.

/CO2M-REB TN-3000 v1.1, 2019/ Buchwitz, M., M. Reuter, S. Noël, H. Bovensmann, A. Richter, J. Landgraf, P. Vefking, J. de Haan, H. Boesch, Error Budgets and Performance for anthropogenic CO_2 Monitoring Mission (CO2M), Technical Report ESA Study on Consolidating Requirements and Error Budget for CO_2 Monitoring Mission (CO2M-REB), version 1.1, 25-April-2019, 46 pages, Doc ID: IUP-CO2M-REB-TN-3000, 2019.

/CO2M-REB TN-1000 v2, 2020/ Buchwitz, M., M. Reuter, S. Noël, H. Bovensmann, A. Richter, J. Landgraf, P. Vefking, J. de Haan, H. Boesch, Requirements Justification Report

for anthropogenic CO_2 Monitoring Mission (CO2M), Technical Report ESA Study on Consolidating Requirements and Error Budget for CO_2 Monitoring Mission (CO2M-REB), version 2, Doc ID: IUP-CO2M-REB-TN-1000, 2020.

/CO2M-REB TN-3000 v2, 2020/ Buchwitz, M., M. Reuter, S. Noël, H. Bovensmann, A. Richter, J. Landgraf, P. Vefking, J. de Haan, H. Boesch, Error Budgets and Performance for anthropogenic CO_2 Monitoring Mission (CO2M), Technical Report ESA Study on Consolidating Requirements and Error Budget for CO_2 Monitoring Mission (CO2M-REB), version 2, Doc ID: IUP-CO2M-REB-TN-3000, 2020.

/CO2M-REB TN-1000 v2.1, 2020/ Buchwitz, M., M. Reuter, S. Noël, H. Bovensmann, A. Richter, J. Landgraf, P. Vefking, J. de Haan, H. Boesch, Requirements Justification Report for anthropogenic CO_2 Monitoring Mission (CO2M), Technical Report ESA Study on Consolidating Requirements and Error Budget for CO_2 Monitoring Mission (CO2M-REB), version 2.1, Doc ID: IUP-CO2M-REB-TN-1000, 2020.

/CO2M-REB TN-3000 v2.1, 2020/ Buchwitz, M., M. Reuter, S. Noël, H. Bovensmann, A. Richter, J. Landgraf, P. Vefking, J. de Haan, H. Boesch, Error Budgets and Performance for anthropogenic CO_2 Monitoring Mission (CO2M), Technical Report ESA Study on Consolidating Requirements and Error Budget for CO_2 Monitoring Mission (CO2M-REB), version 2.1, Doc ID: IUP-CO2M-REB-TN-3000, 2020.

/CO2M MRD v1.0, 2018/ Copernicus CO_2 Monitoring Mission Requirements Document, ESA, v1.0, EOPSM/3088/YM-ym, 2018.

/CO2M MRD v2.0, 2019/ Copernicus CO_2 Monitoring Mission Requirements Document, ESA, v2.0, date of issue: 27/09/2019, EOP-SM/3088/YM-ym, 2018.

/CS L1L2-I study FR, 2014/ Bovensmann, H., M. Buchwitz, M. Reuter, T, Krings, J. Heymann, H. Boesch, J. Landgraf, Final Report ESA study “CarbonSat Earth Explorer 8 Candidate Mission “Level-2 and Level-1B Requirements Consolidation Study“, Technical Report, ESA Contract No. 4000105676/13/NL/AF, Version 2.2, 18-July-2014, Doc ID: IUP-CS-L1L2-FR-01, pp. 188, 2014.

/CS L1L2-II study FR, 2015/ Bovensmann, H., M. Buchwitz, M. Reuter, T, Krings, H. Boesch, J. Landgraf, Final Report ESA study “CarbonSat Earth Explorer 8 Candidate Mission “Level-1 Level-2 (L1L2) Performance Assessment Study“, Technical Report, ESA Contract No. 4000109814/13/NL/FF/lf, Version 1.0, 11-Dec-2015, Doc ID: IUP-CS-L1L2-II-FR-01, pp. 43, 2015.

/CS L1L2-II TN nadir, 2015/ Buchwitz, M., H. Bovensmann, T. Krings, M. Reuter, V. V. Rozanov, P. Liebing, J. Landgraf, F. Alkemade, Mission Requirements Analysis and Level 2 Error Characterization for CarbonSat Nadir Observations over Land, Technical Report ESA study “CarbonSat Earth Explorer 8 Candidate Mission “Level-1 Level-2 (L1L2) Performance Assessment Study“, ESA Contract No. 4000109814/13/NL/FF/lf, Version 1.1, 2-Dec-2015, Doc ID: IUP-CS-L1L2-II-TNnadir, pp. 251, 2015.

/CS MRD v1.0, 2011/ ESA, CarbonSat – Candidate Earth Explorer Opportunity Mission – Mission Requirements Document, Issue 1, Revision 0, 8 July 2011, ESA Mission Science Division, Reference EOP-SMA/2232/PI-pi, 2011.

/CS MRD v1.2, 2013/ ESA, CarbonSat – Candidate Earth Explorer Opportunity Mission – Mission Requirements Document, Issue 1, Revision 2, 23 May 2013, ESA Mission Science Division, Reference EOP-SMA/2232/PI-pi, 2011.

/CS RfMS, 2015/ ESA, Report for Mission Selection: CarbonSat, ESA SP-1330/1 (2 volume series), European Space Agency, Noordwijk, The Netherlands. link: http://esamultimedia.esa.int/docs/EarthObservation/SP1330-1_CarbonSat.pdf, 2015.

/Dubovik et al., 2006/ Dubovik, O., Sinyuk, A., Lapyonok, T., Holben, B. N., Mishchenko, M., Yang, P., Eck, T. F., Volten, H., Munoz, O., Veihelmann, B., Zande, v. d. W. J., Leon, J.-F., Sorokin, M., and Slutsker, I.: Application of spheroid models to account for aerosol particle non-sphericity in remote sensing of desert dust, J. Geophys. Res. Atmos., 111, D11208, doi:10.1029/2005JD006619, 2006

/Eldering et al., 2017/ Eldering, A., O'Dell, C. W., Wennberg, P. O., Crisp, D., Gunson, M. R., Viatte, C., Avis, C., Braverman, A., Castano, R., Chang, A., Chapsky, L., Cheng, C., Connor, B., Dang, L., Doran, G., Fisher, B., Frankenberg, C., Fu, D., Granat, R., Hobbs, J., Lee, R. A. M., Mandrake, L., McDuffie, J., Miller, C. E., Myers, V., Natraj, V., O'Brien, D., Osterman, G. B., Oyafuso, F., Payne, V. H., Pollock, H. R., Polonsky, I., Roehl, C. M., Rosenberg, R., Schwandner, F., Smyth, M., Tang, V., Taylor, T. E., To, C., Wunch, D., and Yoshimizu, J.: The Orbiting Carbon Observatory-2: first 18 months of science data products, Atmos. Meas. Tech., 10, 549-563, https://doi.org/10.5194/amt-10-549-2017, 2017.

/Frankenberg et al., 2011/ Frankenberg, C., Butz, A., Toon, G. C., Disentangling chlorophyll fluorescence from atmospheric scattering effects in O2A-band spectra of reflected sun-light. Geophysical Research Letters 38, L03801, doi:10.1029/2010GL045896, 2011

/Frankenberg et al., 2012/ Frankenberg, C., O'Dell, C., Guanter, L., and McDuffie, J.: Remote sensing of near-infrared chlorophyll fluorescence from space in scattering atmospheres: implications for its retrieval and interferences with atmospheric CO_2 retrievals, Atmos. Meas. Tech., 5, 2081-2094, https://doi.org/10.5194/amt-5-2081-2012, 2012

/Galli et al., 2014/ Galli, A., Guerlet, S., Butz, A., Aben, I., Suto, H., Kuze, A., Deutscher, N. M., Notholt, J., Wunch, D., Wennberg, P. O., Griffith, D. W. T., Hasekamp, O., Landgraf, J., The impact of spectral resolution on satellite retrieval accuracy of CO_2 and CH_4, Atmos. Meas. Tech., Volume 7, Issue 4, pp.1105-1119, 2014.

/Guerlet et al., 2013/ Guerlet, S., Butz, A., Schepers, D., et al., Impact of aerosol and thin cirrus on retrieving and validating XCO_2 from GOSAT shortwave infrared measurements, J. Geophys. Res., VOL. 118, 4887–4905, doi:10.1002/jgrd.50332, 2013.

/Hasekamp et al., 2002/ Hasekamp, O. P. and Landgraf, J.: A linearized vector radiative transfer model for atmospheric trace gas retrieval, J. Quant. Spectrosc. Ra., 75, 221–238, 2002.

/Hasekamp et al., 2005/ Hasekamp, O. P. and Landgraf, J.: Linearization of vector radiative transfer with respect to aerosol properties and its use in satellite remote sensing, J. Geophys. Res.-Atmos., 110, D04203, doi:10.1029/2004JD005260, 2005.

/Hess et al., 1998/ Hess, M., P. Koepke, and I. Schult, Optical Properties of Aerosols and Clouds: The software package OPAC, Bull. Am. Met. Soc., 79, 831-844, 1998.

/Heymann et al., 2012/ Heymann, J., H. Bovensmann, M. Buchwitz, J. P. Burrows, N. M. Deutscher, J. Notholt, M. Rettinger, M. Reuter, O. Schneising, R. Sussmann, and T.

Warneke SCIAMACHY WFM-DOAS XCO_2: reduction of scattering related errors, Atmos. Meas. Tech., 5, 2375-2390, 2012.

/Heymann et al., 2015/ Heymann, J., M. Reuter, M. Hilker, M. Buchwitz, O. Schneising, H. Bovensmann, J. P. Burrows, A. Kuze, H. Suto, N. M. Deutscher, M. K. Dubey, D. W. T. Griffith, F. Hase, S. Kawakami, R. Kivi, I. Morino, C. Petri, C. Roehl, M. Schneider, V. Sherlock, R. Sussmann, V. A. Velazco, T. Warneke, and D. Wunch, Consistent satellite XCO_2 retrievals from SCIAMACHY and GOSAT using the BESD algorithm, Atmos. Meas. Tech., 8, 2961-2980, 2015.

/Hu et al., 2016/ Hu, H., O. Hasekamp, A. Butz, A. Galli, J. Landgraf, J. Aan de Brugh, T. Borsdorff, R. Scheepmaker, and I. Aben, The operational methane retrieval algorithm for TROPOMI, Atmospheric Measurement Techniques, 9, 5423-5440, doi: 10.5194/amt-9-5423-2016.

/Kiel et al., 2018/ Kiel, M., O'Dell, C. W., Fisher, B., Eldering, A., Nassar, R., MacDonald, C. G., and Wennberg, P. O.: How bias correction goes wrong: Measurement of X_{CO2} affected by erroneous surface pressure estimates, Atmos. Meas. Tech. Discuss., https://doi.org/10.5194/amt-2018-353, in review, 2018.

/Landgraf et al., 2017a/ Landgraf, J., J. aan de Brugh, A. Butz, K. Graf, Specification of Instrument Spectral Sizing Concepts, Spectral Errors and Geo-Physical Scenarios, Technical Report ESA „Study on Spectral Sizing for CO_2 Observations“, Doc ID: SRON-CSS-TN-2016-002, 15-Aug-2017, issue 5, pp. 24, 2017.

/Landgraf et al., 2017b/ Landgraf, J., J. aan de Brugh, A. Butz, K. Graf, D2 – Instrument related errors for the different spectral sizing of a CO_2 instrument, Technical Report ESA „Study on Spectral Sizing for CO_2 Observations“, Issue 2, 15-Aug-2018, Doc ID: SRON-CSS-TN-2017-001, pp. 39, 2017.

/Litvinov et al., 2012/ Litvinov P., Hasekamp, O.P., Dubovik O., Cairns, B.:, Model for land surface reflectance treatment: physical derivation, application for bare soil and evaluation on airborne and satellite measurements, J. Quant. Spectrosc. Radiat. Transfer, 113, 2023-2039, doi:10.1016/j.jqsrt.2012.06.027, 2012.

/Natraj et al., 2008/ Natraj, V., Boesch, H., Spurr, R. J. D., and Yung, Y. L.: Retrieval of XCO2 from simulated Orbiting Carbon Observatory measurements using the fast linearized R-2OS radiative transfer model, J. Geophys. Res., 113, D11 212, doi:10.1029/2007JD009017, 2008.

/O'Dell, 2010/, O'Dell, C.W.: Acceleration of multiple-scattering, hyperspectral radiative transfer calculations via low-streams interpolation, J. Geophys. Res., 115, D10 206, doi:10.1029/2009JD012803, 2010.

/Rascher et al., 2009/ Rascher, U., Agati, G., Alonso, L., Cecchi, G., Champagne, S., Colombo, R., Damm, A., Daumard, F., de Miguel, E., Fernandez, G., Franch, B., Franke, J., Gerbig, C., Gioli, B., Gomez, J. A., Goulas, Y., Guanter, L., Gutierrez-de-la-Camara, O´ ., Hamdi, K., Hostert, P., Jimenez, M., Kosvancova, M., Lognoli, D., Meroni, M., Miglietta, F., Moersch, A., Moreno, J., Moya, I., Neininger, B., Okujeni, A., Ounis, A., Palombi, L., Raimondi, V., Schickling, A., Sobrino, J. A., Stellmes, M., Toci, G., Toscano, P., Udelhoven, T., van der Linden, S., and Zaldei, A.: CEFLES2: the remote sensing component to quantify photosynthetic efficiency from the leaf to the region by measuring sun-induced fluorescence

in the oxygen absorption bands, Biogeosciences, 6, 1181–1198, doi:10.5194/bg-6-1181-2009, 2009.

/Reuter et al., 2010/ Reuter, M., Buchwitz, M., Schneising, O., Heymann, J., Bovensmann, H., and Burrows, J. P., A method for improved SCIAMACHY CO_2 retrieval in the presence of optically thin clouds, Atmos. Meas. Tech., 3, 209-232, 2010.

/Reuter et al., 2011/ Reuter, M., Bovensmann, H., Buchwitz, M., et al. (2011), Retrieval of atmospheric CO_2 with enhanced accuracy and precision from SCIAMACHY: Validation with FTS measurements and comparison with model results, J. Geophys. Res., 116, D04301, doi:10.1029/2010JD015047.

/Reuter et al., 2017a/ Reuter, M., M. Buchwitz, O. Schneising, S. Noel, V. Rozanov, H. Bovensmann, J. P. Burrows, A Fast Atmospheric Trace Gas Retrieval for Hyperspectral Instruments Approximating Multiple Scattering - Part 1: Radiative Transfer and a Potential OCO-2 XCO_2 Retrieval Setup, Remote Sens., 9, 1159, doi:10.3390/rs9111159, 2017.

/Reuter et al., 2017b/ Reuter, M., M. Buchwitz, O. Schneising, S. Noël, H. Bovensmann, J. P. Burrows, A Fast Atmospheric Trace Gas Retrieval for Hyperspectral Instruments Approximating Multiple Scattering - Part 2: Application to XCO_2 Retrievals from OCO-2, Remote Sens., 9, 1102, doi:10.3390/rs9111102, 2017.

/Reuter et al., 2018/ Reuter, M., H. Bovensmann, S. Noël, K. Bramstedt, H. Bovensmann, Green-House-Gas Total Column Performance Simulations (GHG-TCPS) Validation and Performance Simulation Report, Technical Report Univ. Bremen, version 1.0, 18-June-2018, Doc. ID: IUP-GHG-TCPS-VPSR-01, 2018.

/Rodgers 2000/ Rodgers, C. D.: “Inverse Methods for Atmospheric Sounding: Theory and Practice”, World Scientific, Singapore, 2000.

/Rodgers and Connor, 2003/ Rodgers, C. D. and B. J. Connor, Intercomparison of remote sounding instruments, J. Geophys. Res., Vol. 108, No. D3, 4116, pp. 1-13, 2003.

/Rozanov et al. 2014/ Rozanov, V.V., A.V. Rozanov, A.A. Kokhanovsky, J.P. Burrows: Radiative transfer through terrestrial atmosphere and ocean: Software package SCIATRAN. Journal of Quantitative Spectroscopy and Radiative Transfer, http://dx.doi.org/10.1016/j.jqsrt.2013.07.004, Vol. 133, p. 13–71, 2014.

/Schlüssel et al., 2010/ P. Schlüssel et al., Post-EPS Mission Requirements Document issue V3c, EUM/PEPS/REQ/06/0043, Eumetsat, 25.June 2010.

/Schepers et al., 2016/ Schepers, D., Butz, A., Hu, H., Hasekamp, O.P., Arnold, S.G., Schneider, M., Feist, D.G., Morino, I., Pollard, D.,Aben, I.,Landgraf, J., Methane and carbon dioxide total column retrievals from cloudy GOSAT soundings over the oceans, J. Geophys. Res. 5031-5050, doi: 10.1002/2015JD023389, 2016.

/Somkuti et al., 2017/ Somkuti, P., Boesch, H., Vijay, N., & Kopparla, P., Application of a PCA-based fast radiative transfer model to XCO_2 retrievals in the shortwave infrared. Journal of Geophysical Research: Atmospheres, 122, 10,477–10, 496, 2017.

/Strahler et al., 1999/ A. H. Strahler, J.-P. Muller, MODIS BRDF/Albedo Product: Algorithm Theoretical Basis Document Version 5.0, MODIS Product ID: MOD43 Version 5.0 - April 1999.

/VIIRS Cloud Mask ATBD, 2014/ GSFC JPSS CMO, Joint Polar Satellite System (JPSS) VIIRS Cloud Mask (VCM) Algorithm Theoretical Basis Document (ATBD), Aug. 5, 2014, Revision E, Goddard Space Flight Center, Greenbelt, Maryland, 2014.

***** End of Document *****

Study on Consolidating Requirements and Error Budget for CO_2 Monitoring Mission (CO2M-REB):

Error Budgets and Performance

for anthropogenic CO_2 Monitoring Mission (CO2M)

Technical Note (TN-3000)

ESA Study
"Study on Consolidating Requirements and Error Budget for CO_2 Monitoring Mission"
ESA Contract Nº 4000125122/18/NL/FF/gp

Authors:
Michael.Buchwitz@iup.physik.uni-bremen.de,
Stefan Noël, Maximilian Reuter, Heinrich Bovensmann, Andreas Richter
Institute of Environmental Physics (IUP) / Institute of Remote Sensing (IFE), University of Bremen (UB), Bremen, Germany

Jochen Landgraf, Hein van Heck
SRON, Utrecht, The Netherlands

Pepijn Veefkind, Johan de Haan
KNMI, De Bilt, The Netherlands

Hartmut Boesch
University of Leicester, Leicester, UK

Change log

Version	Date	Status	Authors	Reason for change
1.0	22-Jan-2019	As submitted	CO2M-REB team	New document
1.1	25-Apr-2019	As submitted	-“-	To consider comments from ESA on v1.0
1.2	1-Oct-2019	Intermediate version generated only for project internal use	-“-	To consider remaining open aspects and to document post-MTR results
2.0	25-Feb-2020	As submitted	-“-	Update for MRDv2.0
2.1	8-May-2020	As submitted	-“-	To consider comments from ESA

Table of Contents

1. Abstract 4
2. Executive summary 5
3. Error Budget and Performance: XCO_2 and XCH_4 7
   3.1. Introduction 7
   3.2. Error budget and performance XCO_2 8
   3.3. Error budget and performance XCH_4 23
   3.4. Summary 27
4. Error Budget and Performance: SIF 28
   4.1. Introduction 28
   4.2. Error budget and performance 28
   4.3. Summary 33
5. Error Budget and Performance: Tropospheric NO_2 34
   5.1. Introduction 34
   5.1. Error budget and performance 34
   5.2. Summary 36
6. Error Budget and Performance: Aerosols and clouds 37
   6.1. Introduction 37
   6.2. Error budget and performance 37
   6.3. Summary 39
7. Acronyms and abbrevations 41
8. References 43

1. Abstract

This document is a deliverable of ESA Study "Study on Consolidating Requirements and Error Budget for CO_2 Monitoring Mission". The anthropogenic CO_2 Monitoring satellite mission is referred to as CO2M mission in this document.

This document (technical note 3000, i.e., TN-3000), the "Error Budgets and Performance for CO2M", is one document of three closely related documents. The other two are: the "Requirements Justification Report for CO2M" (TN-1000) and the "Requirements Sensitivity Analysis for CO2M" (TN-2000).

The purpose of this document is to establish Error Budgets (EBs) for the following parameters:

- Carbon dioxide (CO_2) column-averaged dry-air mole fraction, i.e., XCO_2
- Methane (CH_4) column-averaged dry-air mole fraction, i.e., XCH_4
- Solar-induced Fluorescence (SIF)
- Tropospheric NO_2 column
- Aerosol and cloud parameters from the Multi-Angle-Polarimeter (MAP) instrument

This document is an update of the previous version of this documents (version 1.1) which is based on using MRDv1.0 requirements as input.

This updated document refers primarily to MRDv2.0 but also refers to some of the MRDv1.0 requirements (for requirements which did not change between the 2 MRD versions or for completeness, i.e., to document all assessments relevant for this document, which have been carried out in this study).

2. Executive summary

This document is a deliverable of ESA Study "Study on Consolidating Requirements and Error Budget for CO_2 Monitoring Mission". The anthropogenic CO_2 Monitoring satellite mission is referred to as CO2M mission in this document.

This document (technical note 3000, i.e., TN-3000), the "Error Budgets and Performance for CO2M" **/CO2M-REB TN-3000 v2.1, 2020/**, is one document of three closely related documents. The other two are: the "Requirements Justification Report for CO2M" (TN-1000) **/CO2M-REB TN-1000 v2.1, 2020/** and the "Requirements Sensitivity Analysis for CO2M" (TN-2000) **/CO2M-REB TN-2000 v2.1, 2020/**.

The XCO_2 and XCH_4 Error Budget (EB) and performance estimation approach and results can be summarized as follows:

According to the CO2M Mission Requirements Document (MRD, version 2.0) **/CO2M MRD v2.0, 2019/** the most relevant requirements for the XCO_2 EB are the XCO_2 random and systematic error requirements, which are:

- Random error < 0.7 ppm (1-sigma; per single measurement / footprint)
- Systematic error < 0.5 ppm (1-sigma)

Initial EBs are presented for XCO_2 and XCH_4 by listing XCO_2 and XCH_4 errors / uncertainties for all identified error sources. The EBs are based on decomposition of the overall uncertainty into three components relevant for the main application of CO2M, which is to obtain information on CO2 emission sources via XCO_2 imaging.

This approach is also assumed to be at least approximately valid for other applications such as the application to obtain regional fluxes, see for example the GHG-CCI User Requirements Document **/Chevallier et al., 2016/**, where similar requirements are listed. The systematic error requirement is identical but the random error requirement is less demanding as a regional-scale application permits averaging of many data. This shows that the imaging application is more demanding and, of course, the most demanding application is the driver for the required performance.

The three components are (i) random errors (resulting in a noisy image), (ii) relevant systematic errors (XCO2 errors which would result in systematic errors of the CO_2 emissions) and (iii) other errors, i.e., errors which are not random and do not correlate with the emission signal of interest. The individual errors of the various error sources have been summed up quadratically, i.e., assuming uncorrelated errors. The resulting total random and systematic errors have been compared with the required performance. The individual uncertainties stem either from performance assessments or have to be interpreted as requirements. The assessment results are reported in document **/CO2M-REB TN-2000 v2.1, 2020/** where it is either shown that the required performance can be achieved or an improved MRD requirement is proposed to ensure that the required performance can be met.

The SIF EB and performance estimation approach and results can be summarized as follows:

The retrieval of solar induced fluorescence (SIF) provides an important parameter that is needed as input for the full physics CO_2 (and CH_4) retrieval to avoid biases in XCO_2 (XCH_4) as large as 1 ppm. Furthermore, the retrieved SIF is also an interesting by-product providing complementary carbon-cycle information. The SIF signal measurable in the NIR band is typically of the order of 1% of the continuum radiance (or 1 mW m^{-2} sr^{-1} nm^{-1}) at 750 nm and is only present over vegetated surfaces. A detailed Error Budget (EB) including all relevant error sources for the SIF retrieval has been created providing estimates for random and systematic errors. Uncertainties for each component have been estimated based on available literature, first-order considerations on the expected impact of the instrument-related source on the SIF retrieval and linear error analysis studies using the UoL algorithm. This EB has been evaluated against a SIF precision requirement of 0.7 mW m^{-2} sr^{-1} nm^{-1} and a need for systematic errors of less than 0.2 mW m^{-2} sr^{-1} nm^{-1}. For the EB, we assume that systematic errors can be substantially reduced (to 10% of its uncorrected value) by evaluating areas without vegetation such as deserts, bare areas and snow/ice covered areas. We find that the estimated random error is 0.32 mW m^{-2} sr^{-1} nm-1, which is well within the precision requirement. The largest components are measurement noise and assumed random variations of the ISRF. The uncorrected systematic error estimate of 1.26 mW m^{-2} sr^{-1} nm^{-1} which largely exceeds the systematic error requirements of 0.2 mW m^{-2} sr^{-1} nm^{-1}. However, the correction for systematic error is applied, this reduces to 0.08 mW m^{-2} sr^{-1} nm^{-1}, if we assume that each error source is reduced by a factor of 10. If instead we assume that only the combined systematic error can be reduced than this will be 0.13 mW m^{-2} sr^{-1} nm^{-1}. Both values are below the systematic requirement threshold.

The tropospheric NO_2 EB and performance estimation approach and results can be summarized as follows:

Concerning the NO_2 error budget we distinguish instrument related errors and retrieval related errors, and systematic and random error terms. The instrumental errors are dominated by the SNR. The algorithm errors are dominated by air mass factor errors related to clouds, aerosols and surface albedo, and by NO_2 profile shape errors. All of these algorithm errors can be mitigated by improving the information used; especially when better high-spatial resolution information on the surface reflectance is used for cloud-free scenes, the performance is expected to be significantly better than presented in the EB. Also, the use of better, high-resolution model information is expected to improve the performance.

The Aerosols and Clouds EB and performance estimation approach and results can be summarized as follows:

The error budget of the Multi-Angle-Polarimeter (MAP) instrument has also been presented. We distinguish errors on the measured radiance and degree of linear polarization (DoLP), separated further into systematic and (pseudo-)random error terms. Here, the DoLP precision requirements drives stringent SNR requirements on the radiance and so the radiance uncertainty of 3 % can be fully assigned to systematic radiance errors. Moreover, the radiometric biases are divided into errors due to ISRF knowledge errors, spatial resampling errors, pointing errors and other radiometric errors, e.g. due to calibration failure and instrument degradation.

3. Error Budget and Performance: XCO_2 and XCH_4

3.1. Introduction

Detailed Error Budgets (EBs) for satellite retrievals of XCO_2 and XCH_4 have been compiled in the past for CarbonSat in the framework of the ESA study "CarbonSat Earth Explorer 8 Candidate Mission Level-1 Level-2 (L1L2) Performance Assessment Study", in this document referred to as CS-L1L2-II Study **/CS L1L2-II study FR, 2015/**.

The EBs shown in **/CS L1L2-II study FR, 2015/** are valid for nadir observations over land (their Tab. 2) and sun-glint observations over oceans (their Tab. 3). These EBs are based on detailed performance assessments using satellite instrument and (Level 1 (L1) to Level 2 (L2)) retrieval simulations. As can be seen from the two EBs shown in **/CS L1L2-II study FR, 2015/**, many entries (i.e., the numerical values for the various errors) are very similar (often even identical) for nadir/land and ocean/glint. Typically, the random errors are smaller for the ocean/glint mode observations due to higher signal near the glint spot and therefore better signal-to-noise ratios (SNRs). Further away from the glint spot the SNR is expected to be similar as the SNR of nadir mode observations.

This shows that the driver for the XCO_2 EB are the nadir mode observations over land. Therefore, this section focusses on nadir mode observations over land, which is also the main observation mode of the CO2M mission **/CO2M MRD v2.0, 2019/**.

In the following sub-sections, XCO_2 and XCH_4 EBs are presented. They are partly based on assessments carried out in the past for CarbonSat (see EBs show in **/CS L1L2-II study FR, 2015/**). Where required, the CarbonSat EB has been modified for CO2M to consider new or more appropriate knowledge and/or differences between CarbonSat and CO2M. For several error sources the errors/uncertainties as listed in the EBs presented in this document have to be interpreted as performance requirements and it has been investigated if the corresponding requirement as listed in the CO2M Mission Requirements Documents (MRDs) version 1.0 **/CO2M MRD v1.0, 2018/** and version 2.0 **/CO2M MRD v2.0, 2019/** results in the required performance or not and if not then recommendations are given on how to improve the corresponding MRD requirement in order to obtain the desired performance.

3.2. Error budget and performance XCO_2

According to the CO2M Mission Requirements Document (MRD, version 2.0) **/CO2M MRD v2.0, 2019/** the most relevant requirements for the XCO_2 EB are the XCO_2 random and systematic error requirements, which are:

- Random error < 0.7 ppm (1-sigma; per single measurement / footprint)
- Systematic error < 0.5 ppm (1-sigma)

A key feature of the CO2M mission is its imaging capability, which permits to observe the CO_2 emission plume of strong or moderate localized emission sources such as coal-fired power plants and cities. This application requires high XCO_2 precision (i.e., low random error or noise) as the local enhancement of the XCO_2 (e.g., defined as the maximum XCO_2 value of the plume relative to the surroundings of the plume, i.e., relative to background XCO_2) will rarely exceed 1 ppm (for the envisaged 2x2 km^2 ground pixel size). Note that the XCO_2 random error (or precision) requirement is more demanding compared to CarbonSat, where the threshold requirement was 3 ppm **/CS MRD v1.2, 2013/ /CS RfMS, 2015/**.

Of course, also high accuracy is needed. Here, however, the requirement is the same as for CarbonSat (< 0.5 ppm). Note that this is a very challenging requirement (as it corresponds to only 0.125% of the CO_2 column assuming that 1% corresponds to 4 ppm). However, as shown in **/Buchwitz et al., 2017/** and **/Reuter et al., 2019b/**, a "relative accuracy" close to 0.5 ppm has been achieved using real SCIAMACHY and GOSAT XCO_2 retrievals as concluded from comparisons with TCCON ground-based observations, which have an uncertainty of 0.4 ppm (1-sigma). This indicates that achieving 0.5 ppm (1-sigma, root-mean-square error (RMSE) after quality filtering and bias correction) is very challenging but not impossible.

Concerning the application of obtaining emission estimates from single overpass images of localized emission sources (e.g., **/Reuter et al., 2019/**) it is clear that also systematic XCO_2 errors are critical, but typically only if the corresponding relevant systematic XCO_2 error (i.e., after quality filtering and bias correction) correlates significantly with the signal of interest, i.e., the emission plume (as this will lead to an underestimation or overestimation of the derived emission). If systematic XCO_2 errors do not correlate significantly with the emission plume, than they are less relevant (but of course, it also depends on the inversion algorithm, which "extracts" the emission information from the XCO_2, and how it deals with potential systematic errors).

Note that XCO_2 random errors ("precision") are not only due to the instrument SNR. The XCO_2 image may suffer to some extent also from "pseudo noise" caused by errors, which vary quasi randomly from ground pixel to ground pixel such as errors due to inhomogeneous scenes (in terms of variations of surface reflectivity and/or topography, aerosols, clouds) or spatial colocation related errors.

Based on these considerations and considering detailed assessment results obtained for CarbonSat **/CS L1L2-II study FR, 2015/** an initial XCO_2 EB has been compiled and is shown in **Table 1.**

The differences w.r.t. the CarbonSat EB are:

- The required XCO_2 random error is 0.7 ppm (instead of 3 ppm for CarbonSat)
- The additional error sources "Smoothing" and "Interference" for Algorithms (L1 to L2 processing) have been added and by
- explicitly listing the used assumptions concerning "Variance fractions" in terms of random error (RND), systematic error (SYS) and other (OTH) (see detailed explanations given below, esp. **Figure 1**).

The EB has been compiled primarily for the application "Estimating CO_2 emissions from XCO_2 images" for a localized CO_2 emission source as this is the main (and driving) application for CO2M.

This approach is also assumed to be at least approximately valid for other applications such as the application to obtain regional fluxes, see for example the GHG-CCI User Requirements Document **/Chevallier et al., 2016/**, where similar requirements are listed. The systematic error requirement is identical but the random error requirement is less demanding as a regional-scale application permits averaging of many data. This shows that the imaging application is more demanding and, of course, the most demanding application is the driver for the required performance.

As can be seen, the EB (**Table 1**) lists various error sources and the XCO_2 random and systematic error for each error source.

The values listed for random and systematic errors have been computed from the "Total uncertainty" (UNCT, see also **Figure 1**), which is also listed for each error source and the listed "variance fractions" for RND and SYS (see also **Figure 1**). The listed values for total uncertainty are either based on performance simulations (e.g., clouds and aerosols, radiometric) or they are a requirement (e.g., spectroscopy).

Note that the performance not only depends on the instrument and the retrieval algorithm but also on the scene, on the illumination conditions, on the target of interest, etc. Some of these conditions may be very challenging, resulting in errors larger than the EB suggests. These scenes need to be identified and it may be even necessary to filter them out if too challenging. The reported errors are considered "typical errors" for "typical conditions". Depending on the conditions, errors can of course also be smaller or larger.

Of course, it also needs to be demonstrated that the corresponding performance can be achieved. Note however that only the overall random error (0.7 ppm) and systematic error (0.5 ppm) requirements need to be met. If a requirement for a given error source cannot be met, then this can be compensated/rebalanced by making another requirement of another error source stricter (as shown in **Table 1**, the achieved overall performance is then equal (but not better than) the required performance).

The EB has been compiled as follows:

- In a first step all relevant error sources have been identified (and grouped, if appropriate). Details on each error source are given below.
- Then the "Total uncertainty" (UNCT, see above) has been added to the table. The listed values are partially based on the assessments presented in **/CS L1L2-II TN nadir, 2015/**. Details are given below.

- Then the "Variance fractions" have been added such that their sum equals 1.0 (see **Figure 1**). Details are given below.
- It is assumed here that the total error variance is the sum of three variances, the variance of random errors (RND), the variance of relevant (for the application) systematic errors (SYS) and the variance of all "other" remaining (OTH) errors.
- The variance fractions depend on the error source. For example for a pure random error source such as SNR, f_{RND} = 1.0 and the other fractions are 0.0. For an error source which is expected to generate significant "pseudo noise" such as "Heterogeneous scenes" f_{RND} is higher compared to f_{SYS}. For most error sources the following combination has been used: f_{RND} = 0.2, f_{SYS} = 0.2, f_{OTH} = 0.6. Why this is assumed to be a reasonable choice is explained below.
- Finally, the XCO_2 random and systematic errors have been computed.

At the bottom of the EB the total random and systematic errors are shown ("Total (RSS)") including comparison with the required performance. The achieved performance has been computed by adding all individual contributions via Root-Sum-Square (RSS).

As motivated by the examples presented below, it is typically assumed that OTH is the dominant contribution to the total uncertainty (the only exception is SNR). In the OTH category are all errors which are expected to have no or only negligible relevance for the envisaged application. Examples are:

- Error contributions which are removed by quality filtering and bias correction
- Errors which do not result in a significant error of the derived quantity such as the targeted emission of a localized emission source (to what extent this is the case also depends, of course, also on the implemented inversion algorithm).

To motivate and to illustrate this approach concrete examples are shown in **Figure 2 - Figure 4**. **Figure 2** shows emission inversion results using simulated observations. Here the error pattern (panel top middle) corresponds to results obtained from an error parameterization and corresponding simulated CO2M satellite data as presented in **/Buchwitz and Reuter, 2018/** (based on the method described in **/Buchwitz et al., 2013a/**) essentially modelling systematic XCO_2 errors due to light path errors caused by not fully accounted radiative transfer effects due to aerosols, clouds and surface reflectance. Also listed are variance fractions denoted RND, SYS and OTH in **Figure 2** (and in the EB). The listed values are not prescribed but have been computed from the XCO_2 total error pattern (EP, **Figure 2** middle) as explained using **Figure 1**. Here some additional details are given:

- First, the total uncertainty (UNCT) has been computed as standard deviation (StdDev) of the XCO_2 errors shown in the error map (see **Figure 1**).
- The random error RND is computed from the error patter (EP) map as StdDev(EP - smooth(EP)), where smooth(EP) is the smoothed EP obtained by smoothing the EP with a 3x3 (footprint) boxcar function. It is assumed here that the subtraction of the smoothed EP removes most of the systematic errors.
- Then the standard deviation of the systematic error is computed. For this several approaches have been investigated. Initially this has been done by fitting the emission plume to the error pattern followed by a computation of the standard deviation of the scaled plume (if the scaling factor is zero then this would indicate that the systematic error is zero). This typically results in very small (too small?) values.

On the other hand it would be useful if the obtained numerical value is clearly related to the resulting emission error, which was rarely the case using the initial method. Therefore, the systematic error is estimated by computing the (relative) systematic error of the inverted emission. To estimate the emission, a simple inversion model is used consisting of an offset (= constant value for entire map/scene) plus a scaling factor of the "true plume". The observed XCO_2 plume is the true plume plus error and the difference of the scaling factor from 1.0 is the emission error (-1.76% for the scenario shown in **Figure 2**).

- Finally, OTH is computed (see **Figure 1**).

As can be seen, OTH dominates the other terms by far (OTH = 0.975). Here, i.e., in this example, the reason is that (i) the systematic error does not correlate significantly with the emission plume and therefore is not relevant and (ii) random errors due to instrument noise have not been added.

Figure 3 shows the corresponding assessment results if a systematic error is added (to the EP used for **Figure 2**) which correlates with the emission plume. This additional error pattern has been computed from the emission plume by multiplying it with -0.1. If only this error would be present than one would obtain a systematic low bias of the retrieved emission of 10%. As can be seen, the emission error is -11.76% (and therefore SYS is 0.118), i.e., the underestimation is even a bit larger. The reason for this is that the background is overestimated due to the initial error pattern (used for **Figure 2**), which has a mean bias of +0.018 ppm (see **Figure 2**). Despite this, OTH is again the dominating term.

Figure 4 shows similar assessment results but here the random error due to instrument noise has been considered as error source. Here RND is the dominating term as it should be.

As can be seen from **Table 1**, very low values for RND and SYS are listed for error source Smoothing (RND=SYS=0.1) and even zero for error source Interference. The reason is that smoothing errors are expected to be mainly in the other (OTH) category as primarily an XCO_2 offset in images is expected **/Reuter et al., 2018/**. Interference errors are assumed to be even less relevant for the EB as a separate error source as interference errors from state vector elements related to scattering parameters and meteorology are already covered by error sources "Clouds & aerosols" and "Meteorology". Furthermore, the a priori uncertainties assigned to state vector elements are often very conservative (large values) in order to constrain the retrieval problem as little as possible. As a result, the a posteriori uncertainty as computed with Optimal Estimation algorithms (which includes the components SNR, Smoothing and Interference) may significantly overestimate the Smoothing and Interference error, especially for XCO_2 images corresponding to scenes which contain much less variability than assumed for the a priori error estimates.

CO2M: Error Budget: XCO2 (v1.1) - XCO2 imaging						
Error source	**Level 2 errors XCO2**		**Total**		Variance fractions	
	Random	**Systematic**	**uncertainty**			
	[ppm]	[ppm]	[ppm]	[-]	[-]	[-]
Instrument				RND	SYS	OTH
Signal-to-Noise Ratio (SNR)	0,50	0,00	0,50	1,0	0,0	0,0
Radiometric: Multiplicative/absolute	0,09	0,09	0,20	0,2	0,2	0,6
Radiometric: Multiplic./rel. (ESRA, RSRA, RXRA)	0,20	0,20	0,45	0,2	0,2	0,6
Radiometric: Additive (ZLO)	0,09	0,09	0,20	0,2	0,2	0,6
Instrument Spectral Response Functions (ISRF)	0,09	0,09	0,20	0,2	0,2	0,6
Spectral calibration	0,09	0,09	0,20	0,2	0,2	0,6
Spatio-temporal co-registration	0,22	0,22	0,50	0,2	0,2	0,6
Heterogeneous scenes	0,16	0,16	0,35	0,2	0,2	0,6
Other	0,05	0,05	0,15	0,1	0,1	0,8
Algorithm (L1 to L2)						
Clouds & aerosols	0,22	0,22	0,50	0,2	0,2	0,6
Smoothing	0,16	0,16	0,50	0,1	0,1	0,8
Interference	0,00	0,00	0,50	0,0	0,0	1,0
Meteorology (p, T, H2O)	0,07	0,07	0,15	0,2	0,2	0,6
Spectroscopy	0,13	0,13	0,40	0,1	0,1	0,8
Other	0,05	0,05	0,15	0,1	0,1	0,8
Total (RSS):	0,70	0,50	1,40			
Required max. error (MRD v1):	0,70	0,50				

Table 1: CO2M Error Budget for XCO_2 imaging.

Note: SIF is not part of the error budget because it is assumed that this error is negligible. This assumes an appropriate retrieval algorithm (e.g., one which considers SIF as state vector element).

As explained, **Table 1** shows the EB for the application "deriving CO_2 emissions of localized emission sources via inversion of XCO_2 images". As also explained, the listed "Variance fractions" are motivated by this application but the listed "Total uncertainty" values are essentially assumed to be application independent.

For other applications such as "regional scale or country scale CO_2 flux inversions" the flux information needs to be extracted from a much larger number of XCO_2 retrievals compared to the imaging application. This implies that the random error will be of much less importance (essentially meaning that one could use smaller values for RND). On the other hand, one may argue that systematic error are more important and therefore the values for SYS need to be enhanced. However, as explained earlier, a performance close to the required 0.5 ppm has been achieved using real SCIAMACHY and GOSAT satellite data (e.g., ***/Buchwitz et al., 2017/***). From this it is concluded that concerning systematic error the EB shown in **Table 1** is appropriate also for other applications than XCO_2 imaging.

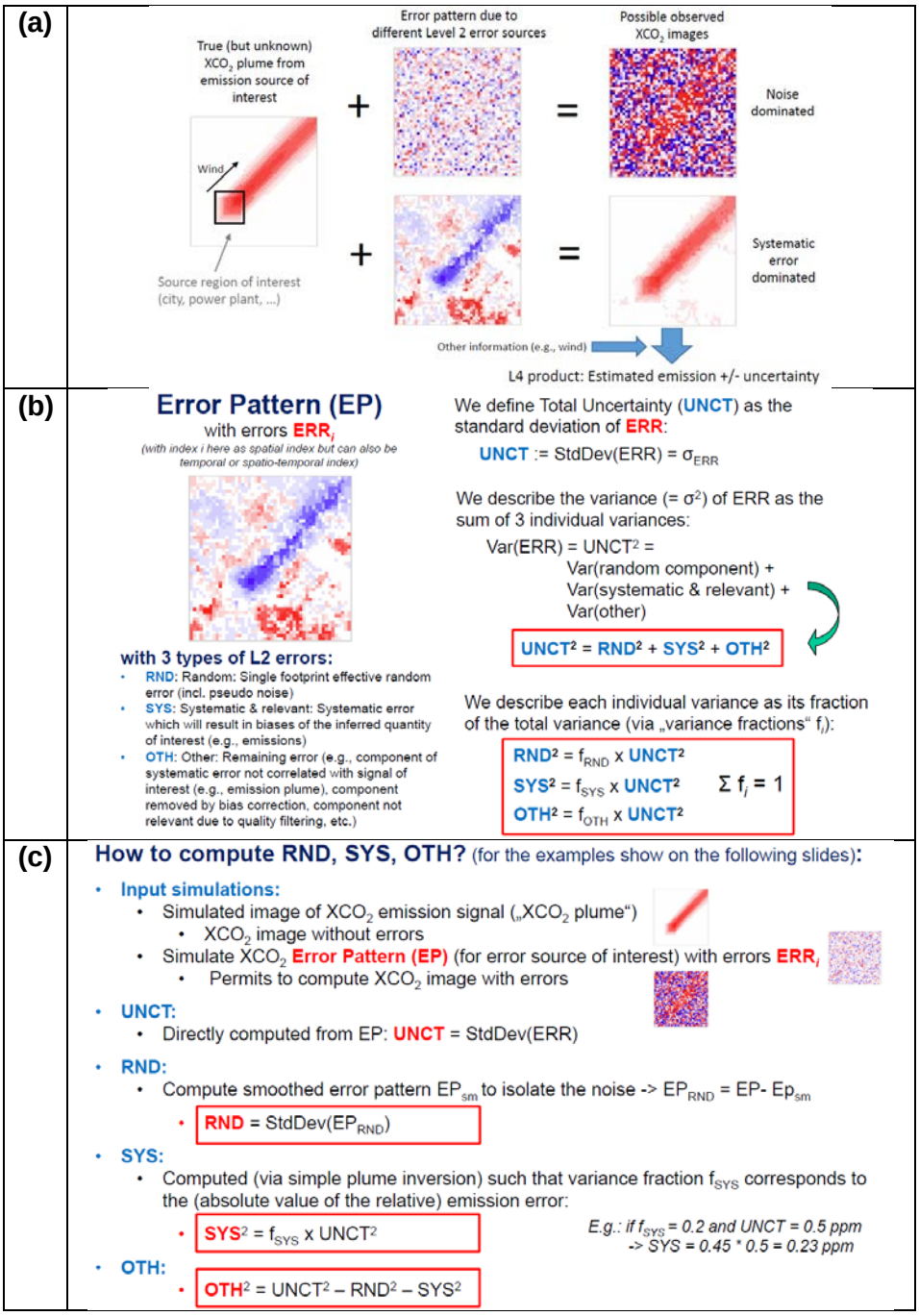

Figure 1: Shows how total uncertainty (UNCT) and the 3 error components (RND, SYS, OTH) have been computed. **Top:** Left: "True plume": Simulated error free CO_2 emission plume (red) originating from a localized source region such as a city (black rectangle). The observed plumes (right) differ from the true plume (left) due to random (middle top) and systematic (middle bottom) errors resulting in an uncertainty of the derived emission. **Middle and bottom:** Explanation of how UNCT, RND, SYS and OTH have been computed.

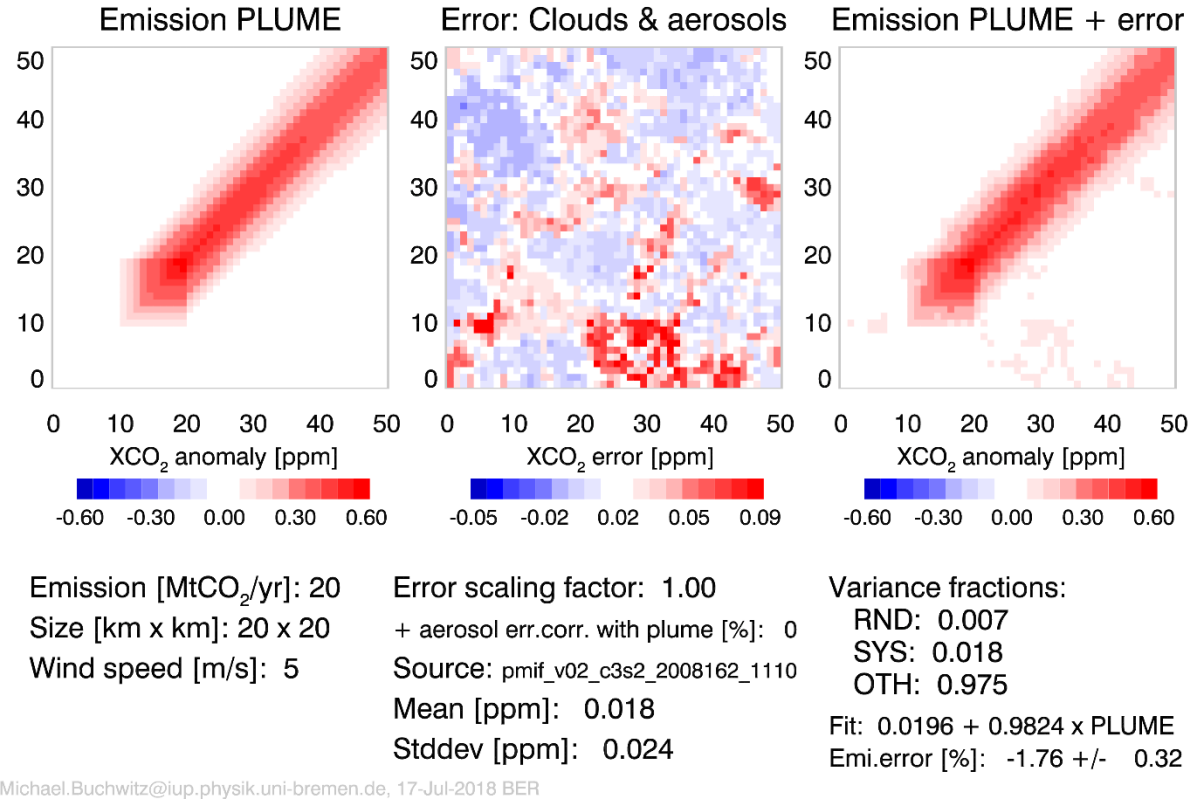

Figure 2: Emission inversion using simulated observations. Left: "True emission plume" of a localized emission source of size 20x20 km² (e.g., a city) observed with an image (of size 100x100 km²) consisting of 50x50 pixels each with a pixel size of 2x2 km². The assumed emission is 20 $MtCO_2$/year and the wind speed is 5 m/s. Middle: Error pattern due to cloud and aerosol related light path errors. Also listed is the mean error (0.018 ppm) and the standard deviation of the error (0.024 ppm). Right: Observed plume, i.e., true XCO_2 plume (left) plus error (middle). The inversion algorithm consists of an offset and a scaling factor of the simulated (true) plume. The retrieved offset is 0.0196 and the retrieved scaling factor is 0.9824. The resulting emission error is -1.76% ± 0.32% (systematic error ± 1-sigma uncertainty). Also listed are the obtained values for (the relative or normalized error components) RND=0.007, SYS=0.018 and OTH=0.975 (their sum equals 1).

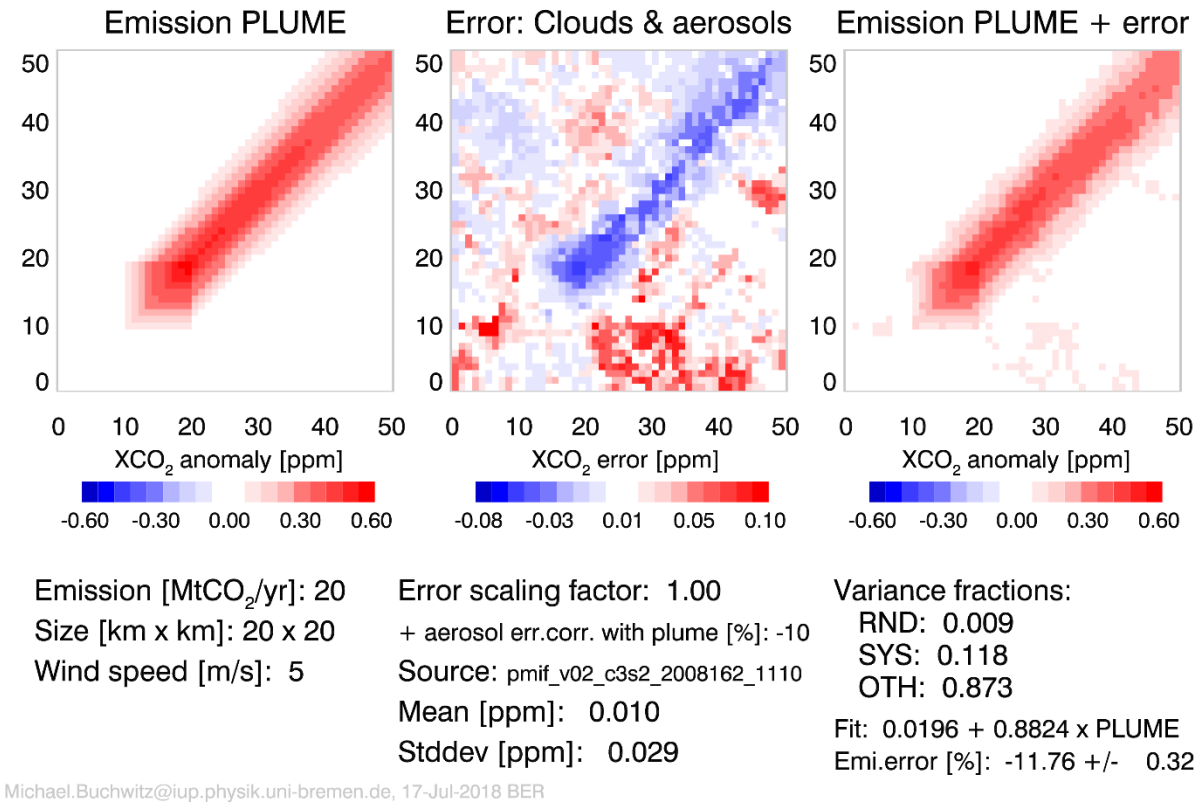

Figure 3: As **Figure 2** but adding a systematic error, which correlates with the emission plume. The amplitude of this error is 10% of the amplitude of the emission plume. As a consequence, the emission is underestimated by approximately 10% (-11.76% as the error pattern also consists of other errors).

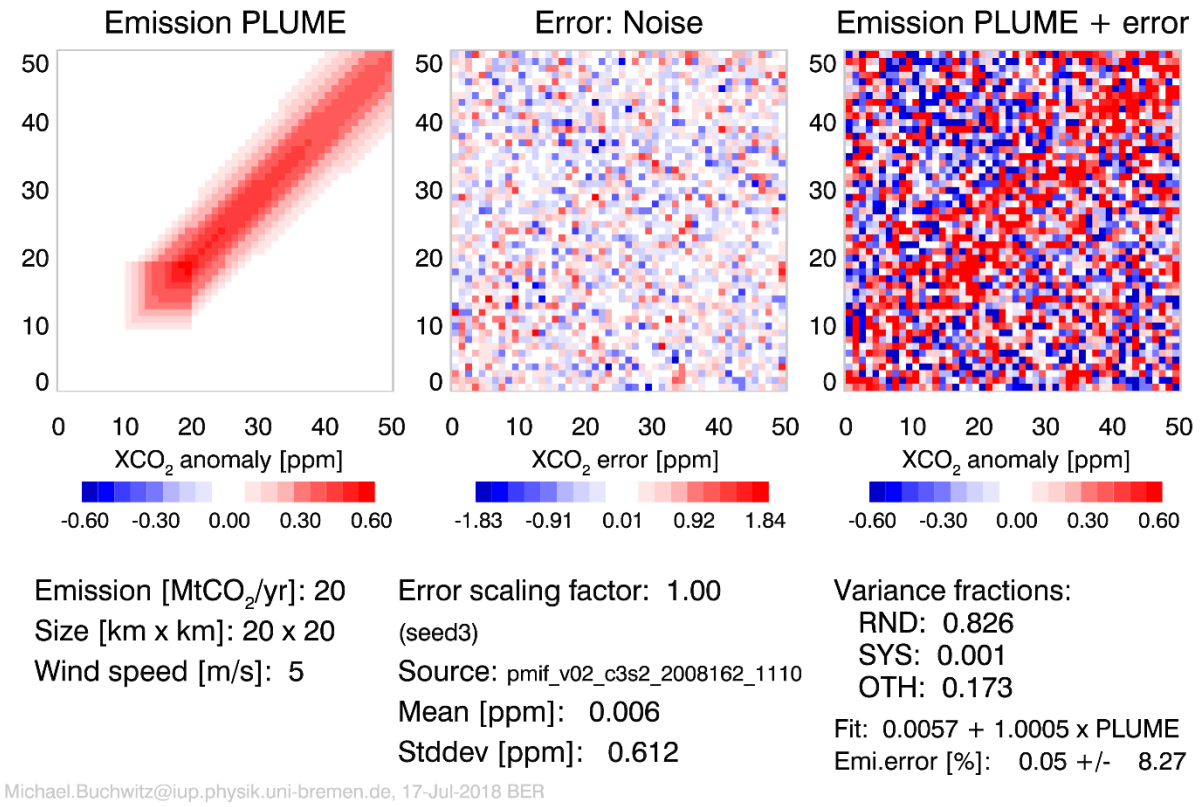

Figure 4: As **Figure 2** but for XCO_2 random errors due to instrument noise.

In the following the individual error sources and corresponding CO2M performance as listed in the EB (**Table 1**) are discussed in detail.

Signal-to-noise ratio (SNR):

This error source originates from the noise of the measured radiance (and irradiance) spectra. For simulations the noise on the radiance can be computed if the SNR is known. The relevant SNR for this study is the SNR requirement as given in the MRD. Noise on the spectra results in a random scatter of the retrieved XCO_2. According to the EB, the total uncertainty must be 0.5 ppm or less. This error source is a pure random error, therefore RND=1.0 and SYS=OTH=0.0 in **Table 1**.

In order to estimate the 1-sigma scatter of the retrieved XCO_2 due to noise on the spectra, simulated retrievals have been carried out. To compute the corresponding XCO_2 error several methods can be (and have been) used (e.g., **/Reuter et al., 2018/**). The retrieval algorithm can be be applied to an ensemble of noisy spectra followed by a computation of the standard deviation of the retrieved XCO_2 (i.e., using a Monte Carlo (MC) approach, e.g., **/Reuter et al., 2018/**) or the XCO_2 a posteriori uncertainty - as computed by optimal estimation (OE) retrieval algorithms (e.g., **/Rodgers 2000/ /Rodgers and Connor, 2003/ /Reuter et al., 2017a, 2017b, 2018/**) can be used.

The OE a posteriori total uncertainty not only depends on the instrument SNR but also on

- the smoothing error, which quantifies the variation of the retrieved XCO_2 due to the (assumed) a priori variabiity of the CO_2 a priori profile and
- the interference error, which quantifies the variation of the retrieved XCO_2 due to the (assumed) a priori variabiity of the non-CO_2 state vector elements.

The latter two aspects are considered by the introduction of error sources “Smoothing” and “Interference” in the EB.

Detailed simulations to quantify “XCO_2 precision” for CarbonSat and for the CO2M mission are reported in documents such as **/CS L1L2-II TN nadir, 2015/ /Butz et al., 2017/ /Buchwitz, 2018/ /Landgraf et al., 2017b/ /Boesch, 2018/**. However, the underlying instrument related assumptions differ somewhat from MRDv1.0 and the SNR-only component has not always been separately quantified. Therefore, new assessments have been carried out as described in **/CO2M-REB TN-2000 v2.1, 2020/** and detailed recommendations are given in that document on how to improve the MRD SNR requirement. These recommendations have been considered for MRDv2.0.

Radiometric: Multiplicative/absolute:

The MRD distinguishes between several types of radiometric errors. One of them is the Absolute Radiometric Accuracy (ARA) (S7MR-OBS-180). Required is an absolute accuracy of 3% of the continuum radiance.

Continuum radiances are typically used in retrieval algorithms to obtain estimates of the surface albedo for each spectral band. Corresponding retrieval simulations are reported in **/CS L1L2-II TN nadir, 2015/** (their Sect. 9.7), where it has been estimated how large the XCO_2 error (and the XCH_4 error) is for various surface albedo errors. Based on these results

it has been concluded that a 3% requirement for ARA is appropriate. The corresponding XCO_2 errors are about 0.1 ppm. Using the FOCAL algorithm and the CO2M instrument specification as given in the MRD this has been confirmed **/CO2M-REB TN-2000 v2.1, 2020/**. This is a factor of 2 smaller than the 0.2 ppm as listed for Total Uncertainty in the EB.

However, also the inter-band relative gain error (S7MR-OBS-200 in MRDv1.0; a "non-numbered requirement" in MRDv2.0) needs to be considered. According to the MRD this error needs to be smaller than 1% between any two bands. The results shown in **/CS L1L2-II TN nadir, 2015/** (their Sect. 9.7) permit to estimate this error (as the multiplicative radiance errors are also listed per band). The corresponding XCO_2 errors are about 0.03 ppm. When (quadratically) adding this to the ARA-related error one obtains a total uncertainty of about 0.1 ppm. Similar results have been obtained using the FOCAL algorithm and the CO2M instrument specification as given in the MRD **/CO2M-REB TN-2000 v2.1, 2020/**. This is somewhat less than the value listed in the EB but it is recommended to have some margin, as the final L1-L2 retrieval algorithm still needs to be defined and it is therefore at present unknown if that algorithm will have a somewhat stronger sensitivity to this type of error or not.

Overall, this indicates that the value listed in the EB for the Total Uncertainty is justified.

Radiometric: Multiplicative/relative (ESRA, RSRA, RXRA):

This error source category combines three error sources:

- ESRA, the Effective Spectral Radiometric Accuracy
- RSRA, the Relative Spectral Radiometric Accuracy
- RXRA, the Relative Spatial Radiometric Accuracy

ESRA covers XCO_2 errors resulting from erroneous "spectral features" (see **/CS L1L2-II TN nadir, 2015/** (their Sect. 9.5)) such as polarization, non-linearity, straylight, diffuser speckles (see also **/CS L1L2-I study FR, 2014/**, e.g., page 9). The MRD (S7MR-OBS-220) requires that the corresponding XCO_2 error does not exceed 0.4 ppm. To achieve this, or to see if this is achieved or not, industry is provided with so called Gain Matrices (see **/CS L1L2-II TN nadir, 2015/**). It is therefore at present assumed that ESRA related errors will not exceed 0.4 ppm.

RSRA (S7MR-OBS-190 in MRDv1.0; a non-numbered requirement in MRDv2.0) covers relative intra-band radiometric errors, which are required to be less than 0.5% peak-to-peak. The corresponding performance assessments are reported in **/CS L1L2-II TN nadir, 2015/** (their Sect. 9.3). As shown in that document, the resulting XCO_2 errors are typically less than about 0.2 ppm.

RXRA (S7MR-OBS-210 in MRDv1.0; a non-numbered requirement in MRDv2.0) covers radiometric errors across the swath, which are required to be less than 0.5%. The corresponding performance assessments are reported in **/CS L1L2-II TN nadir, 2015/** (their Sect. 9.3). As shown in that document, the resulting XCO_2 errors are typically less than about 0.1 ppm.

Adding all three errors (quadratically) gives $\sqrt{(0.4^2 + 0.2^2 + 0.1^2)} = 0.46$ ppm. Taking into account that maximum errors have been used here for RSRA and RXRA this shows that the Total Uncertainty of 0.45 ppm as listed in the EB is justified.

Radiometric: Additive (ZLO):

XCO_2 error due to additive radiometric errors or Zero Level Offsets (ZLO) have been estimated using simulated retrievals. In **/CS L1L2-II TN nadir, 2015/** (their Sect. 9.2) radiance offsets are recommended which are the ones listed in MRDv1.0 S7MR-OBS-230; in MRDv2.0 this is a non-numbered requirement and it has been tightened, as recommended. The corresponding XCO_2 uncertainty is 0.2 ppm (see **/CS L1L2-II TN nadir, 2015/**, their Tab. 1). This indicates that the Total Uncertainty of 0.2 ppm as listed in the EB is justified. However, it is also noted in **/CS L1L2-II TN nadir, 2015/** that the assumptions used are not worse case assumptions and that they may even be somewhat optimistic.

In a follow-on study an additional ZLO-related error analysis has been performed. The results are reported in **/Buchwitz, 2018/.** The focus of that study was on the relative performance of different instrument concepts. The assessments in that study have been conducted using ZLO values, which are smaller than the ones listed in the MRD (50% smaller in the NIR and SWIR-1 bands and 26% smaller in SWIR-2). As shown in **/Buchwitz, 2018/** (their Fig. 42, top) the corresponding XCO_2 errors are approx. 0.07 ppm. Assuming that the error is proportional to the ZLO, then the error would be approx. 0.2 ppm for three times higher ZLOs, which is similar as the results shown in **/CS L1L2-II TN nadir, 2015/** discussed above. However, it is a bit unclear if this scaling approach is appropriate and – even more important – the assessment results presented in **/Buchwitz, 2018/** have been made to compare the performance of different instruments, not to accurately quantify the performance of a single instrument.

Additional ZLO-related assessment results are shown in **/Boesch, 2018/**. Their assessments are based on using the same ZLO values as also used for the results presented in **/Buchwitz, 2018/**. Their main ZLO-related results are shown in their Tab. 8. They report XCO_2 errors as high as 0.5 ppm, which is significantly larger compared to the values given in **/Buchwitz, 2018/**. They used a different inversion algorithm and also studied other scenarios. Using the same ZLO values as used by **/Boesch, 2018/** additional results have been produced using a third retrieval method and a "global ensemble" **/Landgraf et al., 2017b/**. They found (their Fig. 19, top right, instrument B) XCO_2 related errors of about 0.6 ppm, i.e., errors similar as those obtained by **Boesch, 2018/**.

New simulation for CO2M have been carried out as shown in **/CO2M-REB TN-2000 v2.1, 2020/** and the results can be summarized as follows:

The results obtained with FOCAL indicate that XCO_2 errors may exceed the 0.2 ppm as permitted according to the EB if ZLO is not added as state vector elements but are less than 0.2 ppm if ZLO is added as state vector element. This shows that the justification status depends critically on the retrieval algorithm. When FOCAL is applied to real OCO-2 data **/Reuter et al., 2017b/** then ZLO is not added as state vector elements but a ZLO correction is used instead. This indicates that the specified values are appropriate but to be on the safe side it is recommended to add x2 lower values as a goal requirement.

The recommendation to specify somewhat lower ZLO values has been considered for MRDv2.0.

Instrument Spectral Reponse Function (ISRF):

ISRF related XCO_2 errors for homogeneous scenes (note that ISRF related errors for inhomogeneous scenes are covered by error source "Heterogenenous scenes") have been quantified in **/CS L1L2-II TN nadir, 2015/** (their Sect. 10 referring mainly to **/CS L1L2-I study FR, 2014/**). They report worst case errors as large as 1 ppm but argue that this may correspond to approx. 0.2 ppm (1-sigma), which is the Total Uncertainty value for ISRF in the EB. However, here the assumption was that the ISRF shape is known to 1%, which is a factor of two stricter than the 2% requirement in the MRDv1.0 (S7MR-OBS-110); in MRDv2.0 there is a corresponing non-numbered requirement.

ISRF related errors have also been assessed in the framework of an ESA study focussing on "spectral sizing" using three independent analysis. **/Buchwitz, 2018/** obtained errors in the range 0.15 to 0.46 ppm (their Figs. 43 and 44 top) depending on the assumed ISRF shape error. **/Landgraf et al., 2017c/** report mean biases less than 0.35 ppm for a global ensemble and using a different retrieval algorithm. Using another algorithm and other scenarios, **/Boesch, 2018/** reports errors exceeding 1 ppm.

New simulation for CO2M have been carried out as shown in **/CO2M-REB TN-2000 v2.1, 2020/** and the results can be summarized as follows:

Residual errors of the Instrument Spectral Response Function (ISRF) result in errors of the XCO_2 retrievals. According to the Error Budget (EB) 0.2 ppm has been allocated for this error source. Simulated XCO_2 retrievals have been carried out with FOCAL for several types of ISRF errors. The results indicate that the MRD requirement is appropriate.

Spectral calibration:

The MRD requires a spectral knowledge of 1/20 detector pixel (S7MR-OBS-090 in MRDv1.0; a non-numbered requirement in MRDv2.0) corresponding to 1/60 FWHM (for the required Spectral Sampling Ratio of 3).

This requirement originates from retrieval simulations performed in order to quantify XCO_2 biases originating from spectral calibration errors **/CS L1L2-I study FR, 2014/** (Sect. 7.8). As shown in **/CS L1L2-I study FR, 2014/**, the resulting XCO2 errors depend significantly on the retrieval algorithm settings, in particular if a shift & squeeze (sh&sq) correction is used or not and on the assumptions on how the spectral error depends on wavelength. For example, an XCO_2 error of 0.06 ppm has been found if the spectral error is a spectral shift and sh&sq is used. However, assuming a more challenging spectral error the resulting XCO_2 bias can be as large as 0.46 ppm but it has also be shown that this error can be reduced to 0.04 ppm if the retrieval algorithm is used in iterative mode. From this it is concluded that the Total Uncertainty of 0.2 ppm as listed in the EB is reasonable.

Spatio-temporal co-registration:

XCO_2 errors originating from spatio-temporal co-registration related errors have been assessed in **/CS L1L2-II TN nadir, 2015/** (their Sect. 12). It has been found that XCO_2 errors typically do not exceed 0.48 ppm for spatial co-location errors in the range 100-400 m. From this it is concluded that the Total Uncertainty of 0.5 ppm as listed in the EB is justified.

Heterogeneous scenes:

Heterogeneous scenes may result in XCO_2 errors due to (unknown) ISRF variations caused by inhomogeneous slit illumination. Corresponding XCO_2 errors have been investigated in **/CS L1L2-II TN nadir, 2015/** (their Sect. 9.6). It has been found (for the investigated limited amount of shape errors) that a 2% ISRF shape error corresponds to an XCO_2 error of approximately 0.3 ppm. However, it has also been shown that the error can be larger for very challenging scenes The required ISRF error due to non-uniform scenes is 1.5% (MRDv1.0 S7MR-OBS-120; a non-numbered requirement in MRDv2.0). From this it is concluded that the Total Uncertainty of 0.35 ppm as listed in the EB is justified.

Cloud & aerosols:

Typically light-path related errors due to unaccounted variability of aerosols and clouds dominates the XCO_2 error budget as shown in several publications (see, e.g., **/CS L1L2-II TN nadir, 2015/** and references given therein). As shown in **/CS L1L2-II TN nadir, 2015/**, the assumption of a Total Uncertainty of 0.5 ppm as listed in the EB seems reasonable (for essentially cloud free scenes and scenes not moderately contaminated by aerosols (i.e., after very strict quality filtering) and using an algorithm which takes light path variations into account).

Typically light-path related errors due to unaccounted variability of aerosols and clouds dominates the XCO_2 error budget as shown in several publications (see, e.g., **/CS L1L2-II TN nadir, 2015/** and references given therein). To mitigate these errors, CO2M comprises an novel payload combination for syngergistic use of the CO2I spectral meeasurements, the multiangle polarimeter (MAP) and the cloud imager CLIM with a dedicated cirrus channel at 1.38 µm. The MAP instrument in combination with the SWIR measurements of the CO2I spectrometer allows to characterize very accuratly the effect of aerosol on the atmospheric light path, both for boundary layer aerosol and elevated aerosol layers. The CLIM instrument will be used for cloud clearing and dedicated cirrus detection. Currently, it is under investigation how well cirrus properties can be determined by a combination of CO2I, MAP and CLIM(1.38 µm) observations with the object to optimize the data yield of the CO2M mission.

Meteorology (p, T, H_2O):

XCO_2 retrieval algorithms typically use meteorological data as a priori information and also retrieve the most relevant parameters (see, e.g., **/CS L1L2-II TN nadir, 2015/** and references given therein). As explained in **/CS L1L2-II TN nadir, 2015/**, the resulting XCO_2 Total Uncertainty is estimated to be around 0.15 ppm (for scenes where high-quality XCO_2 retrieval are possible, which requires cloud free conditions, etc.). From this it is concluded that the Total Uncertainty of 0.15 ppm as listed in the EB is justified.

Spectroscopy:

The XCO_2 error due to errors of the spectroscopic data is difficult to quantify. In particular it is difficult to guess how large errors in spectroscopic paramters will be around 2025, i.e., the around the time of the planned launch of the satellite, as the improvement of spectroscopic data is an ongoing activity in several laboratories. The Total Uncertainty listed in the EB needs to be interpreted as a requirement rather than an expected performance estimate.

3.3. Error budget and performance XCH_4

The same method as used for XCO_2 has also been used to establish the error budget for XCH_4. It is shown in **Table 2**. As can be seen, the "Variance fractions" are the same as for XCO_2 (for the same reason).

Note that in relative (percentage) terms XCH_4 errors can be somewhat larger than for XCO_2. This is reflected by the required performance:

- Random errors: 0.7 ppm (0.175%) for XCO_2 vs. 10 ppb (0.5%) for XCH_4.
- Systematic errors: 0.5 ppm (0.125%) for XCO_2 vs. 5 ppb (0.25%) for XCH_4.

CO2M: Error Budget: XCH4 (v1.1) - XCH4 imaging						
Error source	**Level 2 errors XCH4**		**Total**		Variance	
	Random	**Systematic**	**uncertainty**		fractions	
	[ppb]	[ppb]	[ppb]	[-]	[-]	[-]
Instrument				RND	SYS	OTH
Signal-to-Noise Ratio (SNR)	8,0	0,0	8	1,0	0,0	0,0
Radiometric: Multiplicative/absolute	0,9	0,9	2	0,2	0,2	0,6
Radiometric: Multiplic./rel. (ESRA, RSRA, RXRA)	2,2	2,2	5	0,2	0,2	0,6
Radiometric: Additive (ZLO)	0,9	0,9	2	0,2	0,2	0,6
Instrument Spectral Response Functions (ISRF)	0,9	0,9	2	0,2	0,2	0,6
Spectral calibration	0,9	0,9	2	0,2	0,2	0,6
Spatio-temporal co-registration	2,2	2,2	5	0,2	0,2	0,6
Heterogeneous scenes	1,8	1,8	4	0,2	0,2	0,6
Other	0,6	0,6	2	0,1	0,1	0,8
Algorithm (L1 to L2)						
Clouds & aerosols	1,8	1,8	4	0,2	0,2	0,6
Smoothing	1,3	1,3	4	0,1	0,1	0,8
Interference	0,0	0,0	4	0,0	0,0	1,0
Meteorology (p, T, H2O)	0,9	0,9	2	0,2	0,2	0,6
Spectroscopy	1,3	1,3	4	0,1	0,1	0,8
Other	0,6	0,6	2	0,1	0,1	0,8
Total (RSS):	9,4	4,9	14,9			
Approx. required:	10,0	5,0				

Table 2: CO2M Error Budget for XCH_4 imaging.

The XCH_4 performance estimates in terms of XCH_4 errors as listed in the EB are presented and discussed in the following for each error source:

Signal-to-noise ratio (SNR):

To quantify this error, the same method has been used as for XCO_2. According to the EB, the total uncertainty must be 8 ppb or less.

Radiometric: Multiplicative/absolute:

The MRD distinguishes between several types of radiometric errors. One of them is the Absolute Radiometric Accuracy (ARA) (S7MR-OBS-180). Required is an absolute accuracy of 3% of the continuum radiance.

Continuum radiances are typically used in retrieval algorithms to obtain estimates of the surface albedo for each spectral band. Corresponding retrieval simulations are reported in **/CS L1L2-II TN nadir, 2015/** (their Sect. 9.7), where it has been estimated how large the XCH_4 error (and the XCO_2 error) is for various surface albedo errors. Based on these results it has been concluded that a 3% requirement for ARA is appropriate. The corresponding XCH_4 errors are less than 1 ppb. Using the FOCAL algorithm and the CO2M instrument specification as given in the MRD, this has been confirmed **/CO2M-REB TN-2000 v2.1, 2020/**. This is less than the 2 ppb as listed for Total Uncertainty in the EB.

However, also the inter-band relative gain error (S7MR-OBS-200 in MRDv1.0; in MRDv2.0 this is a non-numbered requirement) needs to be consider. According to the MRD this error needs to be smaller than 1% between any two bands. The results shown in **/CS L1L2-II TN nadir, 2015/** (their Sect. 9.7) are also appropriate to estimate this error as the errors are listed per band. The corresponding XCH_4 errors are about 0.4 ppb. When (quadratically) adding this to the ARA-related error one obtains a total uncertainty of about 1.1 ppb. Similar results have been obtained using the FOCAL algorithm and the CO2M instrument specification as given in the MRD (see **/CO2M-REB TN-2000, 2019/**). This is somewhat less than the value listed in the EB but it is recommended to have some margin, as the final L1-L2 retrieval algorithm still needs to be defined and it is therefore at present unknown if it will have a somewhat stronger sensitivity to this type of error or not.

Overall, this indicates that the value listed in the EB for the Total Uncertainty is justified.

Radiometric: Multiplicative/rel. (ESRA, RSRA, RXRA):

This error source category combines three error sources:

- ESRA, the Effective Spectral Radiometric Accuracy
- RSRA, the Relative Spectral Radiometric Accuracy
- RXRA, the Relative Spatial Radiometric Accuracy

ESRA covers XCH_4 errors resulting from erroneous “spectral features” (see **/CS L1L2-II TN nadir, 2015/** (their Sect. 9.5)). The MRD (S7MR-OBS-220) requires that the corresponding XCH_4 error does not exceed 5 ppb. To achieve this, or to see if this is achived or not, industry is provided with so called Gain Matrices (see **/CS L1L2-II TN nadir, 2015/**). It is at present assumed that ESRA related errors will not exceed 5 ppb.

RSRA (S7MR-OBS-190 in MRDv1.0; in MRDv2.0 this is a nun-numbered requirement) covers relative intra-band radiometric errors, which are required to be less than 0.5% peak-to-peak. The corresponding performance assessments are reported in **/CS L1L2-II TN nadir, 2015/** (their Sect. 9.3). As shown in that document, the resulting XCH_4 errors are typically less than about 1 ppb.

RXRA (S7MR-OBS-210 in MRDv1.0; in MRDv2.0 this is a non-numbered requirement) covers radiometric errors across the swath, which are required to be less than 0.5%. The corresponding performance assessments are reported in **/CS L1L2-II TN nadir, 2015/** (their Sect. 9.3). As shown in that document, the resulting XCH_4 errors are typically less than about 0.3 ppb.

Adding all three errors (quadratically) gives $\sqrt{(5^2 + 1^2 + 0.3^2)} = 5.1$ ppb. Taking into account that maximum errors have been used here for RSRA and RXRA this shows that the Total Uncertainty of 5 ppb as listed in the EB is justified.

Radiometric: Additive (ZLO):

XCH_4 error due to additive radiometric errors or Zero Level Offsets (ZLO) have been estimated using simulated retrievals. In **/CS L1L2-II TN nadir, 2015/** (their Sect. 9.2) radiance offsets are recommended which are the ones listed in MRDv1.0 S7MR-OBS-230; in MRDv2.0 there is a corresponding non-numbered requirement. The corresponding XCH_4 uncertainty is 1.97 ppb (see **/CS L1L2-II TN nadir, 2015/**, their Tab. 1). This indicates that the Total Uncertainty of 2 ppb as listed in the EB is justified. However, it is also noted in **/CS L1L2-II TN nadir, 2015/** that the assumptions used are not worse case assumptions and that they may even be somewhat optimistic. To be on the save side recommendation have been given on how to improve the MRD requirement in order to obtain the required performance (see **Sect. 3.2**). These recommendations have been considered for MRDv2.0

Instrument Spectral Reponse Function (ISRF):

ISRF related XCH_4 errors for homogeneous scenes (note that ISRF related errors for inhomogeneous scenes are covered by error source “Heterogenenous scenes”) have been quantified in **/CS L1L2-II TN nadir, 2015/** (their Sect. 10 referring mainly to **/CS L1L2-I study FR, 2014/**). They report worst case errors as large as 5-10 ppb but argue that this may correspond to approx. 1-2 ppb (1-sigma), which is similar as the Total Uncertainty value for ISRF in the EB (2 ppb). However, here the assumption was that the ISRF shape is known to 1%, which is a factor of two stricter than the 2% requirement in the MRD (S7MR-OBS-110 in MRDv1.0; in MRDv2.0 there is a corresponding non-numbered requirement). See also **Sect. 3.2** describing the EB for XCO_2.

Spectral calibration:

The MRD requires a spectral knowledge of 1/20 detector pixel (S7MR-OBS-090 in MRDv1.0; in MRDv2.0 there is a corresponding non-numbered requirement) corresponding to 1/60 FWHM (for the required Spectral Sampling Ratio of 3).

This requirement originates from retrieval simulations performed in order to quantify XCH_4 biases originating from spectral calibration errors **/CS L1L2-I study FR, 2014/** (Sect. 7.8). As shown in **/CS L1L2-I study FR, 2014/**, the resulting XCH_4 errors depend significantly on the retrieval algorithm settings, in particular if a shift & squeeze (sh&sq) correction is used or not and on the assumptions on how the spectral error depends on wavelength. For example, an XCH_4 of 0.9 ppb has been found if the spectral error is a spectral shift and sh&sq is used. However, assuming a more challenging spectral error the resulting XCH_4 bias can be as

large as 0.41 ppb. From this it is concluded that the Total Uncertainty of 2 ppb as listed in the EB is reasonable. See also **Sect. 3.2** describing the EB for XCO_2.

Spatio-temporal co-registration:

According to the MRD (S7MR-SYS-040) the geo-location knowledge has to be better than 200 m. In MRDv2.0 the relevant requirements are S7MR-SYS-040 and S7MR-SYS-045. XCO_2 errors originating from spatio-temporal co-registration related errors have been assessed in **/CS L1L2-II TN nadir, 2015/** (their Sect. 12). It has been found that XCO_2 errors typically do not exceed 0.48 ppm (0.12%) for spatial co-location errors in the range 100-400 m. From this it is concluded that the Total Uncertainty of 5 ppb (0.25%) as listed in the EB is justified (note that the XCH_4 accuracy requirement is relaxed compared to the XCO_2 accuracy requirement by a factor of 2 in relative terms (XCO_2: the 0.5 ppm accuracy requirement corresponds to 0.125%; XCH_4: the 5 ppb accuracy requirement corresponds to 0.25%, i.e., 2 x 0.125%)).

Heterogeneous scenes:

Heterogeneous scenes may result in XCO_2 errors due to (unknown) ISRF variations caused by inhomogeneous slit illumination. Corresponding XCO_2 errors have been investigated in **/CS L1L2-II TN nadir, 2015/** (their Sect. 9.6). It has been found that a 2% ISRF shape error corresponds to an XCO_2 error of approximately 0.3 ppm. However, it has also been shown that the error can be larger for very challenging scenes The required ISFR error due to non-uniform scenes is 1.5% (MRDv1.0 S7MR-OBS-120; in MRDv2.0 there is a corresponding non-numbered requirement). From this it is concluded that the Total Uncertainty of 0.35 ppm as listed in the EB for XCO_2 is justified. 0.35 ppm corresponds to about 0.1% of the CO_2 column and 0.1% corresponds to 2 ppb for XCH_4. From this it is concluded that the Total Uncertainty of 4 ppb as listed in the EB for XCH_4 is justified (note that the XCH_4 accuracy requirement is relaxed compared to the XCO_2 accuracy requirement by a factor of 2 in relative terms (XCO_2: the 0.5 ppm accuracy requirement corresponds to 0.125%; XCH_4: the 5 ppb accuracy requirement corresponds to 0.25%, i.e., 2 x 0.125%)).

Cloud & aerosols:

As shown in **/CS L1L2-II TN nadir, 2015/**, the assumption of a Total Uncertainty of 4 ppb as listed in the EB seems reasonable (for essentially clouds free scenes and scenes not strongly contaminated by aerosols (i.e., after very strict quality filtering) and using an algorithm which takes light path variations into account). From this it is concluded that the Total Uncertainty of 4 ppb as listed in the EB for XCH_4 is justified.

Meteorology (p, T, H_2O):

XCH_4 retrieval algorithms typically use meteorological data as a priori information and also retrieved the most relevant parameters (see, e.g., **/CS L1L2-II TN nadir, 2015/** and references given therein). As explained in **/CS L1L2-II TN nadir, 2015/**, the resulting XCH_4 Total Uncertainty is estimated to be around 1.2 ppb (for scenes where high-quality XCH_4 retrieval are possible, which requires cloud free conditions, etc.). From this it is concluded that the Total Uncertainty of 2 ppb as listed in the EB is justified.

Spectroscopy:

The XCH_4 error due to errors of the spectroscopic data is difficult to quantify. In particular it is difficult to guess how large errors in spectroscopic paramters will be around 2025, i.e., the around the time of the planned launch of the satellite, as the improvement of spectroscopic data is an ongoing activity in several laboratories. The Total Uncertainty listed in the EB needs to be interpreted as a requirement rather than an expected performance estimate.

3.4. Summary

The XCO_2 and XCH_4 Error Budget (EB) and performance estimation approach and results can be summarized as follows:

According to the CO2M Mission Requirements Document (MRD, version 2.0) **/CO2M MRD v2.0, 2019/** the most relevant requirements for the XCO_2 EB are the XCO_2 random and systematic error requirements, which are:

- Random error < 0.7 ppm (1-sigma; per single measurement / footprint)
- Systematic error < 0.5 ppm (1-sigma)

Initial EBs are presented for XCO_2 and XCH_4 by listing XCO_2 and XCH_4 errors / uncertainties for all identified error sources. The EBs are based on decomposition of the overall uncertainty into three components relevant for the main application of CO2M, which is to obtain information on CO2 emission sources via XCO_2 imaging. The three components are (i) random errors (resulting in a noisy image), (ii) relevant systematic errors (XCO2 errors which would result in systematic errors of the CO_2 emissions) and (iii) other errors, i.e., errors which are not random and do not correlate with the emission signal of interest. The individual errors of the various error sources have been summed up quadratically, i.e., assuming uncorrelated errors. The resulting total random and systematic errors have been compared with the required performance. The individual uncertainties stem either from performance assessments or have to be interpreted as requirements.

The assessment results are reported in documents **/CO2M-REB TN-2000 v1.2, 2019/** and **/CO2M-REB TN-2000 v2.1, 2020/** where it is either shown that the required performance can be achieved or an improved MRD requirement is proposed to ensure that the required performance can be met.

4. Error Budget and Performance: SIF

4.1. Introduction

In this section, a detailed Error Budget (EB) for the solar induced fluorescence (SIF) retrieval will be described. SIF will only occur over vegetated land surfaces and thus the error budget is limited to those scenarios of the CO2M mission.

The SIF retrieval approach is based on the change of the depth of known solar lines **/Frankenberg et al., 2011/**. It has been shown that this approach results in little sensitivity to aerosols and other atmospheric variations (as long as the atmosphere is sufficiently transparent) **/Frankenberg et al., 2012/**. The main focus of the EB is therefore on instrument parameters but we make also an assessment of algorithm uncertainties related to aerosols+clouds.

4.2. Error budget and performance

The SIF signal measurable in the NIR band of the CO2M mission is of the order of 1% of the continuum radiance for a strong SIF signal over a vegetated scene. This roughly corresponds to a value of 1 mW m^{-2} sr^{-1} nm^{-1} at 750 nm and it will drop off towards larger wavelength.

The SIF signal can be inferred from the spectral ranges without O_2 absorption on either side of the O_2 A Band (around 750 nm and 770 nm) but here we will focus only on the 750 nm range which is the primary range for SIF retrievals and includes several absorption-free solar lines as well as a stronger SIF signal.

From past missions, it is known that the SIF retrievals exhibit a 1-σ single sounding precision error of around 0.5% of the continuum level radiance **/Frankenberg et al., 2012/.** Systematic errors in the SIF retrieval, e.g. from instrument calibration uncertainties, have not been studied in detail and it is generally assumed that systematic errors can be largely reduced by bias correction methods (see below).

Two main applications for the SIF retrieval are considered when creating the EB. The full physics (FP) CO_2 (and CH_4) retrievals make use of the O_2 A Band region to infer information on aerosols and surface pressure. The SIF signal in the NIR band contributes to the observed top-of-atmosphere radiance spectra and, if not corrected for, will bias the retrieval of aerosols and surface pressure and subsequently XCO_2. **/Frankenberg et al., 2012/** found a mean relationship of 1 ppm error per 1% relative (to continuum) SIF signal while **/Somkuti, 2018/** found a weaker relationship with errors of 0.5 ppm per 1%, but also pointed out the large spread of values (see **Figure 5**). This is consistent to results shown in section 6 of **CO2M-REB TN-2000 v2.1, 2020/.**

The retrieved SIF data can also provide important carbon cycle information in its own right as it is powerful proxy for photosynthetic productivity (Gross Primary Productivity GPP) and plant health. Thus, SIF can add valuable information that can be used in synergy with net

CO_2 fluxes inferred from the retrieved XCO_2, for example to help disentangling the different components of the total flux.

MRDv2.0 gives a requirement on the precision of the SIF retrieval (S7MR-DAT-040) of better than 0.7 mW/m^2/sr/nm for a typical SIF signal of 1 mW/m^2/sr/nm. For systematic errors, MRDv2.0 states that errors of the SIF retrieval shall not exceed a value of 0.2 mW/m^2/sr/nm (after applying above correction). This accuracy requirement is similar to the requirement for the EE8 FLEX mission (**/ESA 2015/**).

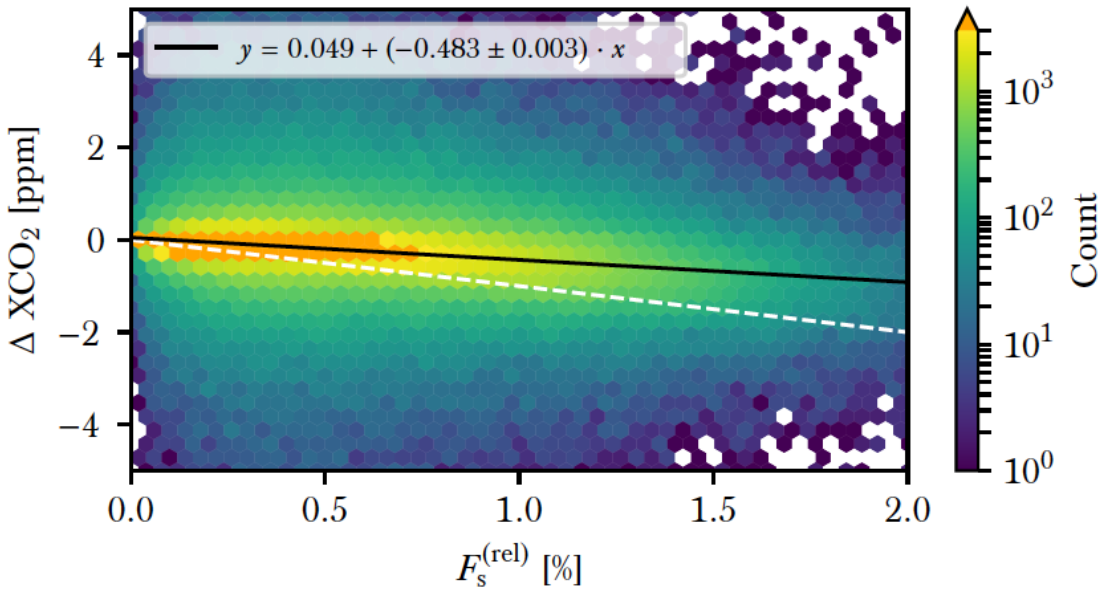

Figure 5: XCO_2 error introduced by an uncorrected SIF (F_s) signal. The SIF signal is given as percentage of the continuum radiance value. Taken from **/Somkuti, 2018/.**

To compile the EB, all relevant error sources have been identified (and grouped, if appropriate). Details on each error source is given below. For each error source, a value for the uncertainty has been estimated based on available literature, first-order considerations on the expected impact of the instrument-related source on the SIF retrieval and linear error analysis studies using the UoL algorithm. For the EB, we also assume that systematic errors can be substantially reduced (to 10% of its uncorrected value) by evaluating areas without vegetation such as deserts, bare areas and snow/ice covered areas. This approach has been successfully adopted for the GOSAT SIF retrieval to compensate a non-linearity effect in the detector response which leads to a zero-level offset signal **/Frankenberg et al., 2011/**. Each error component is split up into a random, systematic and 'other' component adopting the approach taken for CO_2 and CH_4 (Sect. 3).

The overall error budget is given in **Table 3**. The table gives the estimated or assigned total uncertainty, its split into random, systematic and other components and the resulting random and systematic error for each error source. Here, we assume that others is zero.

In total, we find a random error of 0.32 mW m^{-2} sr^{-1} nm^{-1}, which is well below the requirement of the random error of 0.7% of the continuum radiance (or 0.7mW m^{-2} sr^{-1} nm^{1}). The largest components are measurement noise and assumed random variations of the ISRF.
The uncorrected systematic error estimate of 1.26 mW m^{-2} sr^{-1} nm^{-1} largely exceeds the systematic error requirements of 0.2 mW m^{-2} sr^{-1} nm^{-1}. However, once the correction for systematic errors is applied, this reduced to 0.08 mW m^{-2} sr^{-1} nm^{-1}, if we assume that each error source is reduced individually by a factor of 10. If instead we assume that only the combined systematic error can be reduced than this will reduce to 0.13 mW m^{-2} sr^{-1} nm^{-1}. Both values are below the systematic requirement threshold.

CO2M: Error Budget: SIF (v1)						
Error Source	SIF Errors (mW m^{-2} sr^{-1} nm^{-1})		Total Uncertainty	Variance fractions		
Instrument	Random	Systematic with/without correction		RND	SYS	OTH
Signal-to-noise Ratio (SNR)	0.2	0	0.20	1.0	0.0	0.0
Radiometric: Multiplicative/abs.	0.01	0.01/0.01	0.01	0.1	0.9	0.0
Radiometric: Multiplicative/ rel. (RSRA)	0.08	0.02/0.24	0.25	0.1	0.9	0.0
Radiometric: Multiplicative/ rel. (straylight)	0.1	0.04/0.40	0.41	0.05	0.95	0.0
Radiometric: additive	0.01	0.01/0.01	0.015	0.1	0.9	0.0
Spectral calibration	0.01	0.01/0.01	0.01	0.5	0.5	0.0
Instrument Spectral Response Function	0.2	0.06/0.6	0.63	0.1	0.9	0.0
Heterogeneous scenes	0.01	0.01/0.01	0.01	0.5	0.5	0.0
Others	0.03	0.01/0.03	0.04	0.5	0.5	0.0
Algorithm						
Aerosols + Clouds	0.07	0.01/0.07	0.1	0.5	0.5	0.0
Spectroscopy (Solar lines)	0.0	0.01/1.0	1.00	0.0	1	0.00
Other	0.01	0.01/0.01	0.04	0.1	0.5	0.0
Total (RSS)	0.32	0.08/1.26				
Approx. required	0.7	0.2				

Table 3: CO2M Error Budget for SIF. Note that values smaller than 0.01 mW m^{-2} sr^{-1} nm^{-1} are given as 0.01 mW m^{-2} sr^{-1} nm^{-1}

Signal-to-noise ratio (SNR):

The signal-to-noise error describes the random error that originates from the noise of the measured radiance spectra. This error source is a pure random error, therefore RND=1.0 and SYS=OTH=0.0. Using the noise specification from MRDv2.0, we have derived estimates of the SIF precision due to measurement noise using the UoL-FP algorithm. We find a value of 0.17 mW m^{-2} sr^{-1} nm^{-1} for bright scenes decreasing to less than 0.1 mW m^{-2} sr^{-1} nm^{-1} for darker scenes. As a conservative estimate, we use an upper limit of 0.2 mW m^{-2} sr^{-1} nm^{-1} for the SIF error from noise.

Radiometric: Multiplicative/absolute:

The absolute Radiometric Accuracy (ARA) (S7MR-OBS-180) requirement from the MRD is given by 3% of the continuum radiance. The SIF signal is derived from the depth of solar lines. This depth does not depend on the absolute, multiplicative gain and therefore the effect of absolute radiometric calibration will effectively cancel out. However, small residual errors might remain in the retrieval and thus we allow an error of 0.01 mW m^{-2} sr^{-1} nm^{-1}.

Radiometric: Multiplicative/rel. (ESRA, RSRA, RXRA):

The radiometric relative error source includes three components:

- ESRA, the Effective Spectral Radiometric Accuracy
- RSRA, the Relative Spectral Radiometric Accuracy
- RXRA, the Relative Spatial Radiometric Accuracy

ESRA covers errors resulting from erroneous "spectral features" including polarization, non-linearity, straylight, diffuser speckles etc. For the NIR, straylight is expected to be the most significant contributor which has been estimated using the UoL-FP algorithm. For clear scenes, SIF errors from straylight range from 0.1 to 0.45 mW m^{-2} sr^{-1} nm^{-1} in a systematic manner. If partly cloudy scenes are included, then additional scatter roughly with a width of 0.1 mW m^{-2} sr^{-1} nm^{-1} is observed. Consequently, we assign a systematic error of 0.4 mW/sr/nm/m^2 and a random component of 0.1 mW/sr/nm/m^2. However, this is mostly likely an overestimate as it might be possible to correct straylight in the L0-1 processing.

RSRA covers relative intra-band radiometric errors, which are required to be less than 0.5% peak-to-peak according to MRDv2.0. A worst-case error could be as large as 0.5 mW/sr/nm/m^2 ; here we use a more realistic estimate of 0.25 mW/sr/nm/m^2 which is assumed to be mostly systematic.

RXRA (S7MR-OBS-210) covers radiometric errors across the swath, which are required to be less than 0.5%. The resulting SIF error will depend on the nature of the radiometric error. We do not include an explicit SIF error for RXRA as we assume that this error can be absorbed by the 'conservative' error estimates for ESRA and RSRA.

Radiometric: Additive (ZLO):

The requirement for the additive radiometric error or Zero Level Offset (ZLO) for the NIR band is given as 8.4 x 10^9 ph/s/nm/cm^2/sr (S7MR-OBS-230) in MRDv1.1 and as 6 x 10^9 ph/s/nm/cm^2/sr in MRDv2.0. We use the value from MRDv2.0 and assign an error of 0.015 mW m^{-2} sr^{-1} nm^{-1} which is assumed to be largely systematic in nature.

Instrument Spectral Response Function (ISRF):

The MRD of CO2M provides multiple requirements for the ISRF for homogeneous scenes. S7MR-OBS-110 states a knowledge requirement of better than 2% of the peak value while S7MR-OBS-130 gives a requirement on the ISRF FWHM knowledge of better than 1%. The resulting error in the SIF retrieval has been estimated with the UoL-FP retrieval algorithm and errors are found to be as large as 0.6 mW/sr/nm/m^2, again assumed to be largely systematic.

Spectral calibration:

The MRD requires a spectral knowledge of 1/20 detector pixel (S7MR-OBS-090) corresponding to 1/60 FWHM (for the required Spectral Sampling Ratio of 3). We have estimated errors from a spectral mis-calibration using the UoL-FP algorithm and found that errors do not exceed 0.0007 mW/sr/nm/m^2 and thus will not significantly contribute to the error budget.

Spatio-temporal co-registration:

The spatial co-registration between pixels within a band is better than 95%. This means that there is a possibility that some spectral ranges will see slightly different levels of vegetation and thus a stronger SIF signal than others. We do not assign a specific value for this error and instead we assume that this is included under error source 'others' in the error budget.

Heterogeneous scenes:

Heterogeneous scenes may result in (unknown) ISRF variations caused by inhomogeneous slit illumination. We assume that an effective slit homogeniser is applied so that that the effects of heterogeneous scenes becomes small and we only allow a value of 0.01 mW/sr/nm/m^2.

Cloud & aerosols:

The SIF retrieval itself using solar lines has little sensitivity to scattering from aerosols and clouds. However, the retrieved SIF signal represents the top-of-atmosphere (TOA) SIF signal. Scattering in the atmosphere can lead to a variable (diffuse) component (without SIF contributions) to the top-of-atmosphere radiances which can then lead to a difference between retrieved TOA SIF and the bottom-of-atmosphere (surface) SIF signal. **/Frankenberg et al., 2012/** has estimated the error related to aerosols and they found that this can be approximated by ~exp(-0.05xAOD/cos(SZA)). Assuming a SZA of 50^o and an upper limit for AOD of 0.5, then the TOA SIF signal will have a relative error of 4% of the SIF signal itself or 0.04 mW/sr/nm/m^2. However, recent studies point towards somewhat larger differences between top and bottom of atmosphere SIF signals and thus we allow an uncertainty of 0.1 mW/sr/nm/m^2, which we assume to have systematic and random components of equal parts.

Spectroscopy (solar lines):

To fit the solar lines, an empirical list of solar line parameters [G. Toon, private communication] is used. This list derived from FTS solar spectra based on the Atmospheric Trace Molecule Spectroscopy (ATMOS), MkIV balloon spectra, and Kitt Peak ground-based spectra. The accuracy of individual solar lines is hard to estimate and we assign an accuracy of 1%. However, we expect that it will be possible to remove this error

source very effectively by using non-vegetated areas for calibration and we assume that this error source is entirely systematic.

4.3. Summary

The retrieval of solar induced fluorescence (SIF) provides an important parameter that is needed as input for the full physics CO_2 (and CH_4) retrieval to avoid biases in XCO_2 (XCH_4) as large as 1 ppm. Furthermore, the retrieved SIF is also an interesting by-product providing complementary carbon-cycle information.

The SIF signal measurable in the NIR band is typically of the order of 1% of the continuum radiance (or 1 mW m^{-2} sr^{-1} nm^{-1}) at 750 nm and is only present over vegetated surfaces.

A detailed Error Budget (EB) including all relevant error sources for the solar induced fluorescence (SIF) retrieval has been created providing estimates for random and systematic errors for each component. Uncertainties for each component have been estimated based on available literature, first-order considerations on the expected impact of the instrument-related source on the SIF retrieval and linear error analysis studies using the UoL algorithm. This EB has been evaluated against a SIF precision requirement of 0.7 mW m^{-2} sr^{-1} nm^{-1} and a need for systematic errors of less than 0.2 mW m^{-2} sr^{-1} nm^{-1}. For the EB, we assume that systematic errors can be substantially reduced (to 10% of its uncorrected value) by evaluating areas without vegetation such as deserts, bare areas and snow/ice covered areas.

The overall error budget is given in **Table 3**. We find that the estimated random error is 0.32 mW m^{-2} sr^{-1} nm^{-}1, which is well within the precision requirement. The largest components are measurement noise and assumed random variations of the ISRF.

The uncorrected systematic error estimate of 1.26 mW m^{-2} sr^{-1} nm^{-1} largely exceeds the systematic error requirements of 0.2 mW m^{-2} sr^{-1} nm^{-1}. However, once the correction for systematic error is applied, this reduces to 0.08 mW m^{-2} sr^{-1} nm^{-1}, if we assume that each error source is reduced by a factor of 10. If instead we assume that only the combined systematic error can be reduced than this will reduce to 0.13 mW m^{-2} sr^{-1} nm^{-1}. Both values are below the systematic requirement threshold.

5. Error Budget and Performance: Tropospheric NO_2

5.1. Introduction

In this section a detailed Error Budget (EB) for the tropospheric NO_2 retrieval will be described.

5.1. Error budget and performance

The error budget for NO_2 is presented in **Table 4**. This error budget distinguishes instrument related error and algorithm errors. For the algorithm we use the DOAS method, which consists of a spectral fitting part and an air mass factor part. The instrument related errors predominantly act on the slant column retrieval whereas the algorithm errors act on the air mass factors.

For all the errors in the error budget we distinguish random errors (RND), which include pure instrument noise as well as quasi random error terms, systematic errors (SYS) and other errors (OTH). OTH contribution are errors that are no expected to significantly influence the final results. For NO_2 this is the case when errors result in an overall bias, which will drop out when we compute the difference between the NO_2 plumes and their backgrounds. The enhancement wrt the background is what is important to identify pollution plumes and to estimate the emission source strength.
All errors are combined in a root-sum-squared way to compute the total error. This is also done separately for the instrumental and algorithm errors.

CO2M: Error Budget NO2				Date:	25/09/2019
Error Source	Tropospheric Column :		1.00E+16 molec.cm-2		
	Random	**Systematic**	**Total Uncertainty**		
Instrument				RND	SYS OTH
Singal to noise (SNR)	15.0%	0.0%	15.0%	1	0 0
Radiometric: multiplicative	2.7%	4.2%	5.0%	0.3	0.7 0
Radiometric: multiplicative relative (ESRA, RSRA, RXRA)	8.9%	0.0%	10.0%	0.8	0 0.2
Radiometric: additive	0.0%	4.9%	7.0%	0	0.5 0.5
Spectral calibration	1.4%	1.4%	2.0%	0.5	0.5 0
Instrument Spectral Response Function	0.0%	1.4%	2.0%	0	0.5 0.5
Spatio-temporal co-registration	2.0%	0.0%	2.0%	1	0 0
Heterogenous scenes	5.0%	0.0%	5.0%	1	0 0
Other	0.0%	0.0%	0.0%	0.33	0.33 0.33
Algorithm (L1 to L2)					
Clouds, aerosols and surface reflectance	15.0%	21.2%	30.0%	0.25	0.5 0.25
Smoothing (NO2 profile shape)	0.0%	17.9%	20.0%	0	0.8 0.2
Interference	0.0%	4.5%	10.0%	0	0.2 0.8
Meteorology (p,T,NO2)	0.0%	4.5%	5.0%	0	0.8 0.2
Spectroscopy	0.0%	2.2%	5.0%	0	0.2 0.8
Other	0.0%	0.0%	0.0%	0.33	0.33 0.33
Total (RSS)	24%	29%			
Requirement	20%	35%			
Instrumental	18.5%	6.8%			
Algorithm (L1 to L2)	15.0%	28.5%			

Table 4. Error budget for NO_2.

Remarks to the error budget presented in **Table 4**:

CO2M: Error Budget NO2	
Error Source	
	Source / Remarks
Instrument	
Singal to noise (SNR)	Assuming SNR 750 and albedo 0.05
Radiometric: multiplicative	Based on requirement of 5% on the radiance, and comes in through cloud fraction errors. Because the polarization varies quasi randomly an estimate is also provided for the random errors
Radiometric: multiplicative relative (ESRA, RSRA, RXRA)	The random error is directly linked to the requirement using gain vectors. Systematic error is assumed to be negligible after in-flight soft calibration
Radiometric: additive	This is based on a 1.5% radiance offset at 405 nm with no mitigation measures.
Spectral calibration	Based on a 1% spactral pixel knowledge
Instrument Spectral Response Function	This error source assumes standard deviation knowledge of 1%. It is expected to be linked to the thermal stability
Spatio-temporal co-registration	Based on S5 studies.
Heterogenous scenes	This is a worst case estimate, based on OMI experience of a spectral shotft of up to 1/10th of a spectral pixel.
Other	
Algorithm (L1 to L2)	
Clouds, aerosols and surface reflectance	Based on various model and validations studies. Varying cloud fractions will contribute to the quasi random error.
Smoothing (NO2 profile shape)	NO2 profile error can be strongly reduced using regional modelling.
Interference	Stratospheric column estimate
Meteorology (p,T,NO2)	Rough estimate due to temperature variability and orography
Spectroscopy	Rough estimate due to temperature variability and orography
Other	
Total (RSS)	
Requirement	
Instrumental	
Algorithm (L1 to L2)	

The instrumental random errors are dominated by the instrument SNR. The systematic instrumental errors are significantly smaller than the instrumental random errors. Improving the SNR of the instrument is therefore expected to have large performance impact.

The algorithm errors are dominated by the effects of clouds, aerosols and surface albedo, and the NO_2 profile shape errors. For cloud/aerosol and surface reflectance AMF errors we use an error of 30% in the EB. For the CO2M missions, the focus will be on cloud-free scenes. For such scenes, improving the knowledge on the surface albedo by using high-spatial resolution databases can make these errors significantly smaller than the 30% that is used. For cloud-free scenes, explicit aerosol corrections can also make this error significantly smaller. The synergy with the MAP and CLIM observations of CO2M may be used identify such cloud-free ground pixels and to quantify the aerosol properties. The NO_2 profile shape error can be mitigated by using improved model information. This can also be done as a post-processing step, when accurate high-spatial resolution model information is available.

5.2. Summary

In this section the NO_2 error budget is presented. We distinguish instrument related errors and retrieval related errors, and systematic and random error terms. The instrumental errors are dominated by the SNR. Thus, improving the SNR over the threshold requirement is expected to directly improve the instrument performance. The algorithm errors are dominated by air mass factor errors related to clouds, aerosols and surface albedo, and by NO_2 profile shape errors. All of these algorithm errors can be mitigated by improving the information used; especially when better high-spatial resolution information on the surface reflectance is used for cloud-free scenes, the performance is expected to be much better than presented in the EB. Also, the use of better, high-resolution model information is expected to improve the performance.

6. Error Budget and Performance: Aerosols and clouds

6.1. Introduction

This section gives an error budget based on the Multi-Angle-Polarimeter (MAP) instrument performance analysis, which is described in more detail in TN-2000. The analysis considers an allocated XCO_2 uncertainty of 0.5 ppm due to aerosol induced errors (see **Sec. 3.2**) and assumes that all errors add up quadratically to the total aerosol induced uncertainty. In case of low error sensitivities and no major technical constraints, the error gets a smaller contribution to the total budget. For all other cases, we propose equal error partitioning.

6.2. Error budget and performance

The MAP error budget is shown in **Table 5**. In TN-2000, we showed that a radiance uncertainty of 3% and a DoLP uncertainty of 0.0025 complies with an aerosol induced error of ≤ 0.5 ppm. This is the initial assumption for our aerosol induced error budget included in Tab. 3. The DoLP uncertainties are divided equally between precision and systematic errors, requiring a DoLP precision and radiometric biases to be ≤0.0025. The DoLP precision drives the requirement on radiance precision to be $< 0.2\%$, which means that the uncertainty is almost exclusively determined by the systematic errors.

Table 5: MAP error budget for radiance (left) and degree of linear polarization (DoLP, right).

Radiance			DoLP	
3 % uncertainty			0.0035 uncertainty	
Precision	systematic errors (radiometric bias)			Precision
0.2 %	3.0 %		0.0025	0.0025
-	0.2 %	ISRF	-	-
-	0.5 %	resampling	0.001	-
-	0.5 %	pointing	0.001	-
-	2.9 %	other systematic errors	0.002	-

To show this, we consider a bandpass instrument and assume for simplicity reasons that the DoLP is determined by two independent measurements, S_+ and S_-, which determines the Stokes parameters $Q = S_+ - S_-$ and $I = S_+ + S_-$. Stokes parameter U is assumed to be zero. Obviously, the precision of Q and I are the same, $\delta Q = \delta I$, and

$$DoLP = \frac{|Q|}{I}$$

Thus, the precision of DoLP and I are related by

$$\left[\frac{\delta DoLP}{DoLP}\right]^2 = \left[\frac{\delta Q}{Q}\right]^2 + \left[\frac{\delta I}{I}\right]^2$$

and so yields

$$\delta DoLP^2 = \left[\frac{\delta I}{I}\right]^2 (1 + DoLP^2)$$

Thus, for a maximum DoLP of 0.6 the relative radiance precision is driven by the DoLP precision via

$$\frac{\delta I}{I} \approx 0.8\, \delta DoLP\ ,$$

which yields a radiance precision reported in **Table 5**.

Moreover, the allocated radiance and DoLP systematic errors are broken down to three individual radiometric biases due to

1. spatial resampling errors,
2. pointing errors,
3. other systematic errors.

Overall, the error budget indicates that the MAP radiance sensitivity with respect to ISRF errors is minor, leading to a contribution of 0.2 % to the error budget. For the polarimetric budget, we assume that ISRF induced errors cancels out to a large extend in the radiometric ratio of DoLP. So, we omit a corresponding error contribution in the DoLP error budget.
The spatial observations of the MAP instrument have to be resampled on a common grid, which induces radiometric errors depending on the spatial sampling ratio and the regularity of the spatial sampling concept. We assign 0.5 % of the radiance error and a DoLP bias of 0.001 to this error contribution. Similar, errors due to a relative pointing error (relative geolocation knowledge) should be $\leq$ 0.5 % of the radiance signal and $\leq$ 0.001 DoLP.
Finally, this leads to a remaining error contribution of 2.9 % radiance and 0.002 DoLP, which can be attributed to other instrument specific errors due to erroneous radiometric calibration and instrument degradation.

6.3. Summary

The error budget of the Multi-Angle-Polarimeter (MAP) instrument has been presented. We distinguish errors on the measured radiance and degree of linear polarization, separated further into systematic and random error terms. Here, the DoLP precision requirements drives stringent SNR requirements on the radiance and so the radiance uncertainty of 3 % can be fully assigned to systematic radiance errors. Moreover, the radiometric biases are divided into errors due to ISRF knowledge errors, spatial resampling errors, pointing errors and other radiometric errors, e.g. due to calibration failure and instrument degradation.

In TN-2000 Sect. 8.3 it is shown that the error performance of the joint MAP-CO_2 retrieval can be described well with the linear error analysis tools. Based on these findings, all MAP requirements are deduced for the aerosol induced XCO_2 error, which includes the XCO_2 noise contribution due to the MAP measurement noise and the XCO_2 error due to the smoothing error of the retrieved aerosol parameters. The aerosol product of XCO_2 retrieval comprises 11 parameters as defined in Sect. 8.2 of TN-2000, where each parameter has a given uncertainty. Hasekamp et al., 2019, showed that the aerosol product of the required MAP instrument fulfills the Aerosol-Clouds-Ecosystems (ACE) requirements on aerosol parameters also shown in the table below. Here ACE requirements are not formulated for specific reference scenes. For most aerosol parameters, Hasekamp et al., 2019 found a better performance than required but some parameters (e.g. the real refractive index) are non-compliant with the ACE requirements. Larger errors are found for the coarse model, which we expect to improve by a combination of CO_2I and MAP measurements, coving also the SWIR spectral range. Overall, we advise to use as the ACE uncertainty requirement for the auxiliary aerosol product using the CO2M reference scenes.

Property	ACE requirement
AOD (Aerosol optical depth)	Max.(0.02, 5%)
SSA (Single scattering albedo)	0.02
r_eff	10%
v_eff	50%
m_r	0.02
N	100%
Aerosol layer height	500 m

Table 6: Aerosol accuracy requirements as used by the ACE study (Hasekamp et al., 2019)

We note that these requirements do not safeguard the XCO_2 performance as derived in TN-2000 because error correlations must be considered as well to constrain the required accuracy in the atmospheric light path, which is the underlying quantity to be considered for XCO_2. In our opinion, the light path effect can only be evaluated in the manner as presented in TN-2000 Sect. 8.3.

Note: Once the joint MAP-CO_2 retrieval algorithm exists then the impact on the XCO_2 errors (XCO_2 error budget) needs to be established. Also the error budget for the aerosol product itself (e.g., AOD, layer height) needs to be established.

7. Acronyms and abbrevations

Acronym	Meaning
AOD	Aerosol Optical Depth
ATBD	Algorithm Theoretical Basis Document
BESD	Bremen optimal EStimation DOAS
BESD/C	BESD algorithm used for CarbonSat assessments
BL	Boundary Layer
CA	Continental Average (aerosol scenario)
CarbonSat	Carbon Monitoring Satellite
CC	Continental Clean (aerosol scenario)
CCI	Climate Change Initiative (of ESA)
CL	Close Loop
CNES	Centre national d'études spatiales
CO2M	Anthropogenic CO_2 Monitoring Mission
CO2M-REB	Anthropogenic CO_2 Monitoring Mission Requirements Consolidation and Error Budget study
COD	Cloud Optical Depth
CP	Continental Polluted (aerosol scenario)
CS	CarbonSat
CS-L1L2-II	CarbonSat Earth Explorer 8 Candidate Mission Level-1 Level-2 (L1L2) Performance Assessment Study No. 2
CTH	Cloud Top Height
DE	Desert (aerosol scenario)
DES	Desert (surface albedo)
DOAS	Differential Optical Absorption Spectroscopy
DOF	Degrees of Freedom
DoLP	Degree of linear polarization
EB	Error Budget
EE8	Earth Explorer No. 8 (satellite)
ENVISAT	Environmental Satellite
ESA	European Space Agency
FR	Final Report
FLEX	Fluorescence Explorer
FWHM	Full Width at Half Maximum
GHG	Greenhouse Gas
GHG-CCI	Greenhouse Gas project of ESA's Climate Change Initiative (CCI)
GM	Gain Matrix
GMM	Gain Matrix Method
GOSAT	Greenhouse Gases Observing Satellite
GPP	Gross Primary Productivity
ISRF	Instrument Spectral Response Function
IUP-UB	Institute of Environmental Physics (Institut für Umweltphysik), University of Bremen, Germany
L1	Level 1

L2	Level 2
MAP	Multi-Angle-Polarimeter
MC	Monte Carlo (approach)
MLS	Mid-latitude summer (profiles)
MODIS	Moderate resolution Imaging Spectrometer
MRD	Mission Requirements Document
NIR	Near Infra Red (band)
OCO	Orbiting Carbon Observatory
OE	Optimal Estimation
OPAC	Optical Properties of Aerosol and Clouds
OTH	Other errors (as defined for the EB)
RfMS	Report for Mission Selection
RMS	Root Mean Square
RMSE	Root Mean Square Error
RND	Random errors (as defined for the EB)
RSS	Root Sum Square
RTM	Radiative Transfer Model
SCIAMACHY	Scanning Imaging Absorption Spectrometers for Atmospheric Chartography
SCIATRAN	Radiative Transfer Model under development at IUP
SIF	Solar-Induced Fluorescence
SNR	Signal to Noise Ratio
SSI	Spectral Sampling Interval
SSP	Spectral Sizing Point
SSR	Spectral Sampling Ratio
SW1 or SWIR-1	SWIR 1 band
SW2 or SWIR-2	SWIR 2 band
SWIR	Short Wave Infrared
SYS	Systematic errors (as defined for the EB)
SZA	Solar Zenith Angle
TCCON	Total Carbon Column Observing Network
TOA	Top of atmosphere
VCF	Vegetation Chlorophyll Fluorescence
VEG	Vegetation (surface albedo)
VIIRS	Visible Infrared Imaging Radiometer Suite
VMR	Volume Mixing Ratio

8. References

/Boesch, 2018/ Boesch, H., WP2300: Optimizing Spectral Sizing Concepts, Technical Report ESA „Study on Spectral Sizing for CO_2 Observations“, Issue 1, 15-Mar-2018, Doc ID: UOL-CO2SIZ-TN-2018-WP2300, pp. 17, 2018.

/Bovenmann et al., 2010/ Bovensmann, H., Buchwitz, M., Burrows, J. P., Reuter, M., Krings, T., Gerilowski, K., Schneising, O., Heymann, J., Tretner, A., and Erzinger, J., A remote sensing technique for global monitoring of power plant CO_2 emissions from space and related applications, Atmos. Meas. Tech., 3, 781-811, 2010.

/Bovenmann et al., 2014/ Bovensmann, H., M. Buchwitz, M. Reuter, T. Krings, J. Heymann, H. Boesch, J. Landgraf, CarbonSat Earth Explorer 8 Candidate Mission “Level-2 and Level-1B Requirements Consolidation Study“, Final Report ESA Study CarbonSat Earth Explorer 8 Candidate Mission “Level-2 and Level-1B Requirements Consolidation Study “, ESA Contract No 4000105676/12/NL/AF, Version 2.2, Date: 18. July 2014, Doc.ID: IUP-CS-L1L2-FR-01, 2014.

/Bovenmann et al., 2015/ Bovensmann, H., M. Buchwitz, M. Reuter, T. Krings, J. Heymann, H. Boesch, J. Landgraf, CarbonSat Earth Explorer 8 Candidate Mission “Level-1 Level-2 (L1L2) Performance Assessment Study “, Final Report ESA Study, ESA Contract No 4000109814/13/NL/FF/lf, Version 1.0, Date: 11. December 2015, Doc.ID: IUP-CS-L1L2-II-FR-01, 2015.

/Buchwitz et al., 2013a/ Buchwitz, M., M. Reuter, H. Bovensmann, D. Pillai, J. Heymann, O. Schneising, V. Rozanov, T. Krings, J. P. Burrows, H. Boesch, C. Gerbig, Y. Meijer, and A. Loescher, Carbon Monitoring Satellite (CarbonSat): assessment of atmospheric CO_2 and CH_4 retrieval errors by error parameterization, Atmos. Meas. Tech., 6, 3477-3500, 2013.

/Buchwitz et al., 2013b/ Buchwitz, M., H. Bovensmann, M. Reuter, J. Heymann, O. Schneising, et al., CARBONSAT: ERROR ANALYSIS FOR PRIMARY LEVEL 2 PRODUCTS XCO_2 AND XCH_4 AND SECONDARY PRODUCT VEGETATION CHLOROPHYLL FLUORESCENCE FOR NADIR OBSERVATIONS OVER LAND, ESA Living Planet Symposium, Sept 9-13, 2013, Edinburgh, UK, conference proceedings ESA Special Publication SP-722 (on CD-ROM), link: http://www.iup.uni-bremen.de/sciamachy/NIR_NADIR_WFM_DOAS/2846996buchwitz.pdf, 2013.

/Buchwitz et al., 2015/ Buchwitz, M., Bovensmann, T. Krings, M. Reuter, V. V. Rozanov, P. Liebing, J. Landgraf, F. Alkemade, Mission Requirements Analysis and Level 2 Error Characterization for CarbonSat Nadir Observations over Land - WP 1100, 2000 & 4100 Report, ESA Study CarbonSat Earth Explorer 8 Candidate Mission “Level-1 Level-2 (L1L2) Performance Assessment Study“ ESA Contract No 4000109814/13/NL/FF/lf, Version 1.2, 3 Dec 2015, Doc ID: IUP-CS-L1L2-II-TNnadir, 2015.

/Buchwitz et al., 2017/ ESA Climate Change Initiative (CCI) Product Validation and Intercomparison Report (PVIR) for the Essential Climate Variable (ECV) Greenhouse Gases (GHG) for data set Climate Research Data Package No. 4 (CRDP#4), Version 5.0, 9. Feb. 2017, 2017.

/Buchwitz, 2018/ Buchwitz, M., Error analysis for CarbonSat scenarios and different spectral sizing, Technical Report ESA „Study on Spectral Sizing for CO_2 Observations“, Version 4.0, 30-Apr-2018, Doc ID: IUP-CO2SS-TN-5, pp. 93, 2018.

/Buchwitz and Reuter, 2018/ Buchwitz, M., and M. Reuter, Level 2 error files, Technical Report ESA Study of Assessing thresholds for a space borne observation system to monitor fossil CO_2 emissions (PMIF study), Version 2.1, 30-Jan-2018, Doc ID IUP-PMIF_L2e_S7-c, pp. 100, 2018.

/Butz et al., 2017/ Butz, A., K. Graf, J. Landgraf, J. ann den Brugh, D3 – CO_2 errors due to measurement noise and atmospheric scattering for the different spectral sizing concepts of a CO_2 instrument, Technical Report ESA „Study on Spectral Sizing for CO_2 Observations“, Version 1.1, 23-May-2017, pp. 24, 2017.

/Chevallier et al., 2016/ Chevallier, F., et al., User Requirements Document (URD), ESA Climate Change Initiative (CCI) GHG-CCI project, Version 2.1, 19 Oct 2016, link: http://cci.esa.int/sites/default/files/URDv2.1_GHG-CCI_Final.pdf, 2016.

/Ciais et al., 2015/ Ciais, P., et al.: Towards a European Operational Observing System to Monitor Fossil CO_2 emissions - Final Report from the expert group, http://www.copernicus.eu/main/towards-european-operational-observing-system-monitor-fossil-co2-emissions, pp. 68, October 2015, 2015.

/CO2M-REB TN-1000 v1.1, 2019/ Buchwitz, M., M. Reuter, S. Noël, H. Bovensmann, A. Richter, J. Landgraf, P. Vefking, J. de Haan, H. Boesch, Requirements Justification Report for anthropogenic CO_2 Monitoring Mission (CO2M), Technical Report ESA Study on Consolidating Requirements and Error Budget for CO_2 Monitoring Mission (CO2M-REB), version 1.1, 25-April-2019, 74 pages, Doc ID: IUP-CO2M-REB-TN-1000, 2019.

/CO2M-REB TN-2000 v1.2, 2019/ Buchwitz, M., M. Reuter, S. Noël, H. Bovensmann, A. Richter, J. Landgraf, P. Vefking, J. de Haan, H. Boesch, Requirements Sensitivity Analysis for anthropogenic CO_2 Monitoring Mission (CO2M), Technical Report ESA Study on Consolidating Requirements and Error Budget for CO_2 Monitoring Mission (CO2M-REB), version 1.1, 26-April-2019, 133 pages, Doc ID: IUP-CO2M-REB-TN-2000, 2019.

/CO2M-REB TN-3000 v1.1, 2019/ Buchwitz, M., M. Reuter, S. Noël, H. Bovensmann, A. Richter, J. Landgraf, P. Vefking, J. de Haan, H. Boesch, Error Budgets and Performance for anthropogenic CO_2 Monitoring Mission (CO2M), Technical Report ESA Study on Consolidating Requirements and Error Budget for CO_2 Monitoring Mission (CO2M-REB), version 1.1, 25-April-2019, 46 pages, Doc ID: IUP-CO2M-REB-TN-3000, 2019.

/CO2M-REB TN-1000 v2, 2020/ Buchwitz, M., M. Reuter, S. Noël, H. Bovensmann, A. Richter, J. Landgraf, P. Vefking, J. de Haan, H. Boesch, Requirements Justification Report for anthropogenic CO_2 Monitoring Mission (CO2M), Technical Report ESA Study on Consolidating Requirements and Error Budget for CO_2 Monitoring Mission (CO2M-REB), version 2, Doc ID: IUP-CO2M-REB-TN-1000, 2020.

/CO2M-REB TN-2000 v2, 2020/ Buchwitz, M., M. Reuter, S. Noël, H. Bovensmann, A. Richter, J. Landgraf, P. Vefking, J. de Haan, H. Boesch, Requirements Sensitivity Analysis for anthropogenic CO_2 Monitoring Mission (CO2M), Technical Report ESA Study on Consolidating Requirements and Error Budget for CO_2 Monitoring Mission (CO2M-REB), version 2, Doc ID: IUP-CO2M-REB-TN-2000, 2020.

/CO2M-REB TN-1000 v2.1, 2020/ Buchwitz, M., M. Reuter, S. Noël, H. Bovensmann, A. Richter, J. Landgraf, P. Vefking, J. de Haan, H. Boesch, Requirements Justification Report for anthropogenic CO_2 Monitoring Mission (CO2M), Technical Report ESA Study on Consolidating Requirements and Error Budget for CO_2 Monitoring Mission (CO2M-REB), version 2.1, Doc ID: IUP-CO2M-REB-TN-1000, 2020.

/CO2M-REB TN-2000 v2.1, 2020/ Buchwitz, M., M. Reuter, S. Noël, H. Bovensmann, A. Richter, J. Landgraf, P. Vefking, J. de Haan, H. Boesch, Requirements Sensitivity Analysis for anthropogenic CO_2 Monitoring Mission (CO2M), Technical Report ESA Study on Consolidating Requirements and Error Budget for CO_2 Monitoring Mission (CO2M-REB), version 2.1, Doc ID: IUP-CO2M-REB-TN-2000, 2020.

/CO2M MRD v1.0, 2018/ Copernicus CO_2 Monitoring Mission Requirements Document, ESA, v1.0, EOPSM/3088/YM-ym, 2018.

/CO2M MRD v2.0, 2019/ Copernicus CO_2 Monitoring Mission Requirements Document, ESA, v2.0, date of issue: 27/09/2019, EOP-SM/3088/YM-ym, 2018.

/CS L1L2-I study FR, 2014/ Bovensmann, H., M. Buchwitz, M. Reuter, T, Krings, J. Heymann, H. Boesch, J. Landgraf, Final Report ESA study "CarbonSat Earth Explorer 8 Candidate Mission "Level-2 and Level-1B Requirements Consolidation Study", Technical Report, ESA Contract No. 4000105676/13/NL/AF, Version 2.2, 18-July-2014, Doc ID: IUP-CS-L1L2-FR-01, pp. 188, 2014.

/CS L1L2-II study FR, 2015/ Bovensmann, H., M. Buchwitz, M. Reuter, T, Krings, H. Boesch, J. Landgraf, Final Report ESA study "CarbonSat Earth Explorer 8 Candidate Mission "Level-1 Level-2 (L1L2) Performance Assessment Study", Technical Report, ESA Contract No. 4000109814/13/NL/FF/lf, Version 1.0, 11-Dec-2015, Doc ID: IUP-CS-L1L2-II-FR-01, pp. 43, 2015.

/CS L1L2-II TN nadir, 2015/ Buchwitz, M., H. Bovensmann, T. Krings, M. Reuter, V. V. Rozanov, P. Liebing, J. Landgraf, F. Alkemade, Mission Requirements Analysis and Level 2 Error Characterization for CarbonSat Nadir Observations over Land, Technical Report ESA study "CarbonSat Earth Explorer 8 Candidate Mission "Level-1 Level-2 (L1L2) Performance Assessment Study", ESA Contract No. 4000109814/13/NL/FF/lf, Version 1.1, 2-Dec-2015, Doc ID: IUP-CS-L1L2-II-TNnadir, pp. 251, 2015.

/CS MRD v1.0, 2011/ ESA, CarbonSat – Candidate Earth Explorer Opportunity Mission – Mission Requirements Document, Issue 1, Revision 0, 8 July 2011, ESA Mission Science Division, Reference EOP-SMA/2232/PI-pi, 2011.

/CS MRD v1.2, 2013/ ESA, CarbonSat – Candidate Earth Explorer Opportunity Mission – Mission Requirements Document, Issue 1, Revision 2, 23 May 2013, ESA Mission Science Division, Reference EOP-SMA/2232/PI-pi, 2011.

/CS RfMS, 2015/ ESA, Report for Mission Selection: CarbonSat, ESA SP-1330/1 (2 volume series), European Space Agency, Noordwijk, The Netherlands. link: http://esamultimedia.esa.int/docs/EarthObservation/SP1330-1_CarbonSat.pdf, 2015.

/Eldering et al., 2017/ Eldering, A., O'Dell, C. W., Wennberg, P. O., Crisp, D., Gunson, M. R., Viatte, C., Avis, C., Braverman, A., Castano, R., Chang, A., Chapsky, L., Cheng, C., Connor, B., Dang, L., Doran, G., Fisher, B., Frankenberg, C., Fu, D., Granat, R., Hobbs, J., Lee, R. A. M., Mandrake, L., McDuffie, J., Miller, C. E., Myers, V., Natraj, V., O'Brien, D., Osterman, G. B., Oyafuso, F., Payne, V. H., Pollock, H. R., Polonsky, I., Roehl, C. M., Rosenberg, R., Schwandner, F., Smyth, M., Tang, V., Taylor, T. E., To, C., Wunch, D., and Yoshimizu, J.: The Orbiting Carbon Observatory-2: first 18 months of science data products, Atmos. Meas. Tech., 10, 549-563, https://doi.org/10.5194/amt-10-549-2017, 2017.

/ESA 2015/ ESA, Report for Mission Selection: FLEX, ESA SP-1330/2, European Space Agency, Nordwijk, The Netherlands, 2015

/Frankenberg et al., 2011/ Frankenberg, C., Butz, A., Toon, G. C., Disentangling chlorophyll fluorescence from atmospheric scattering effects in O2A-band spectra of reflected sun-light. Geophysical Research Letters 38, L03801, doi:10.1029/2010GL045896, 2011

/Frankenberg et al., 2012/ Frankenberg, C., O'Dell, C., Guanter, L., and McDuffie, J.: Remote sensing of near-infrared chlorophyll fluorescence from space in scattering atmospheres: implications for its retrieval and interferences with atmospheric CO_2 retrievals, Atmos. Meas. Tech., 5, 2081-2094, https://doi.org/10.5194/amt-5-2081-2012, 2012

/Galli et al., 2014/ Galli, A., Guerlet, S., Butz, A., Aben, I., Suto, H., Kuze, A., Deutscher, N. M., Notholt, J., Wunch, D., Wennberg, P. O., Griffith, D. W. T., Hasekamp, O., Landgraf, J., The impact of spectral resolution on satellite retrieval accuracy of CO_2 and CH_4, Atmos. Meas. Tech., Volume 7, Issue 4, pp.1105-1119, 2014.

/Guerlet et al., 2013/ Guerlet, S., Butz, A., Schepers, D., et al., Impact of aerosol and thin cirrus on retrieving and validating XCO_2 from GOSAT shortwave infrared measurements, J. Geophys. Res., VOL. 118, 4887–4905, doi:10.1002/jgrd.50332, 2013.

/Hess et al., 1998/ Hess, M., P. Koepke, and I. Schult, Optical Properties of Aerosols and Clouds: The software package OPAC, Bull. Am. Met. Soc., 79, 831-844, 1998.

/Heymann et al., 2012/ Heymann, J., H. Bovensmann, M. Buchwitz, J. P. Burrows, N. M. Deutscher, J. Notholt, M. Rettinger, M. Reuter, O. Schneising, R. Sussmann, and T. Warneke SCIAMACHY WFM-DOAS XCO_2: reduction of scattering related errors, Atmos. Meas. Tech., 5, 2375-2390, 2012.

/Heymann et al., 2015/ Heymann, J., M. Reuter, M. Hilker, M. Buchwitz, O. Schneising, H. Bovensmann, J. P. Burrows, A. Kuze, H. Suto, N. M. Deutscher, M. K. Dubey, D. W. T. Griffith, F. Hase, S. Kawakami, R. Kivi, I. Morino, C. Petri, C. Roehl, M. Schneider, V. Sherlock, R. Sussmann, V. A. Velazco, T. Warneke, and D. Wunch, Consistent satellite XCO_2 retrievals from SCIAMACHY and GOSAT using the BESD algorithm, Atmos. Meas. Tech., 8, 2961-2980, 2015.

/Landgraf et al., 2017a/ Landgraf, J., J. aan de Brugh, A. Butz, K. Graf, Specification of Instrument Spectral Sizing Concepts, Spectral Errors and Geo-Physical Scenarios, Technical Report ESA „Study on Spectral Sizing for CO_2 Observations“, Doc ID: SRON-CSS-TN-2016-002, 20-May-2017, version 4, pp. 21, 2017.

/Landgraf et al., 2017b/ Landgraf, J., J. aan de Brugh, A. Butz, K. Graf, D2 – Instrument related errors for the different spectral sizing of a CO_2 instrument, Technical Report ESA „Study on Spectral Sizing for CO_2 Observations“, Issue 2, 15-Aug-2018, Doc ID: SRON-CSS-TN-2017-001, pp. 39, 2017.

/Rascher et al., 2009/ Rascher, U., Agati, G., Alonso, L., Cecchi, G., Champagne, S., Colombo, R., Damm, A., Daumard, F., de Miguel, E., Fernandez, G., Franch, B., Franke, J., Gerbig, C., Gioli, B., Gomez, J. A., Goulas, Y., Guanter, L., Gutierrez-de-la-Camara, O´ ., Hamdi, K., Hostert, P., Jimenez, M., Kosvancova, M., Lognoli, D., Meroni, M., Miglietta, F., Moersch, A., Moreno, J., Moya, I., Neininger, B., Okujeni, A., Ounis, A., Palombi, L., Raimondi, V., Schickling, A., Sobrino, J. A., Stellmes, M., Toci, G., Toscano, P., Udelhoven, T., van der Linden, S., and Zaldei, A.: CEFLES2: the remote sensing component to quantify photosynthetic efficiency from the leaf to the region by measuring sun-induced fluorescence in the oxygen absorption bands, Biogeosciences, 6, 1181–1198, doi:10.5194/bg-6-1181-2009, 2009.

/Reuter et al., 2010/ Reuter, M., Buchwitz, M., Schneising, O., Heymann, J., Bovensmann, H., and Burrows, J. P., A method for improved SCIAMACHY CO_2 retrieval in the presence of optically thin clouds, Atmos. Meas. Tech., 3, 209-232, 2010.

/Reuter et al., 2011/ Reuter, M., Bovensmann, H., Buchwitz, M., et al. (2011), Retrieval of atmospheric CO_2 with enhanced accuracy and precision from SCIAMACHY: Validation with FTS measurements and comparison with model results, J. Geophys. Res., 116, D04301, doi:10.1029/2010JD015047.

/Reuter et al., 2017a/ Reuter, M., M. Buchwitz, O. Schneising, S. Noel, V. Rozanov, H. Bovensmann, J. P. Burrows, A Fast Atmospheric Trace Gas Retrieval for Hyperspectral Instruments Approximating Multiple Scattering - Part 1: Radiative Transfer and a Potential OCO-2 XCO_2 Retrieval Setup, Remote Sens., 9, 1159, doi:10.3390/rs9111159, 2017.

/Reuter et al., 2017b/ Reuter, M., M. Buchwitz, O. Schneising, S. Noel, H. Bovensmann, J. P. Burrows, A Fast Atmospheric Trace Gas Retrieval for Hyperspectral Instruments Approximating Multiple Scattering - Part 2: Application to XCO_2 Retrievals from OCO-2, Remote Sens., 9, 1102, doi:10.3390/rs9111102, 2017.

/Reuter et al., 2018/ Reuter, M., H. Bovensmann, S. Noël, K. Bramstedt, H. Bovensmann, Green-House-Gas Total Column Performance Simulations (GHG-TCPS) Validation and Performance Simulation Report, Technical Report Univ. Bremen, version 1.0, 18-June-2018, Doc. ID: IUP-GHG-TCPS-VPSR-01, 2018.

/Reuter et al., 2019/ Reuter, M., Buchwitz, M., Schneising, O., Krautwurst, S., O'Dell, C. W., Richter, A., Bovensmann, H., and Burrows, J. P.: Towards monitoring localized CO_2 emissions from space: co-located regional CO_2 and NO_2 enhancements observed by the OCO-2 and S5P satellites, Atmos. Chem. Phys., https://www.atmos-chem-phys.net/19/9371/2019/, 19, 9371-9383, 2019.

/Reuter et al., 2019b/ Reuter, M., Buchwitz, M., Schneising, O., Noel, S., Bovensmann, H., Burrows, J. P., Boesch, H., Di Noia, A., Anand, J., Parker, R. J., Somkuti, P., Wu, L., Hasekamp, O. P., Aben, I., Kuze, A., Suto, H., Shiomi, K., Yoshida, Y., Morino, I., Crisp, D., O'Dell, C., Notholt, J., Petri, C., Warneke, T., Velazco, V., Deutscher, N. M., Griffith, D. W. T., Kivi, R., Pollard, D., Hase, F., Sussmann, R., Te, Y. V., Strong, K., Roche, S., Sha, M. K., De Maziere, M., Feist, D. G., Iraci, L. T., Roehl, C., Retscher, C., and Schepers, D., Ensemble-based satellite-derived carbon dioxide and methane column-averaged dry-air mole fraction data sets (2003-2018) for carbon and climate applications, Atmos. Meas. Tech. Discuss., https://doi.org/10.5194/amt-2019-398, in review, 2019.

/Rodgers 2000/ Rodgers, C. D.: “Inverse Methods for Atmospheric Sounding: Theory and Practice”, World Scientific, Singapore, 2000.

/Rodgers and Connor, 2003/ Rodgers, C. D. and B. J. Connor, Intercomparison of remote sounding instruments, J. Geophys. Res., Vol. 108, No. D3, 4116, pp. 1-13, 2003.

/Rozanov et al. 2014/ Rozanov, V.V., A.V. Rozanov, A.A. Kokhanovsky, J.P. Burrows: Radiative transfer through terrestrial atmosphere and ocean: Software package SCIATRAN. Journal of Quantitative Spectroscopy and Radiative Transfer, http://dx.doi.org/10.1016/j.jqsrt.2013.07.004, Vol. 133, p. 13–71, 2014.

/Somkuti, 2018/ P. Somkuti, Novel Methods for Atmospheric Carbon Dioxide Retrieval from the JAXA GOSAT and NASA OCO-2 Satellites, PhD thesis, University of Leicester, available from http://handle.net/2381/42868, 2018

/VIIRS Cloud Mask ATBD, 2014/ GSFC JPSS CMO, Joint Polar Satellite System (JPSS) VIIRS Cloud Mask (VCM) Algorithm Theoretical Basis Document (ATBD), Aug. 5, 2014, Revision E, Goddard Space Flight Center, Greenbelt, Maryland, 2014.

***** End of Document *****

Study on Consolidating Requirements and Error Budget for CO_2 Monitoring Mission (CO2M-REB):

Support A/B1 System Activities for anthropogenic CO_2 Monitoring Mission (CO2M)

Technical Note (TN-4000)

ESA Study
"Study on Consolidating Requirements and Error Budget for CO_2 Monitoring Mission"
ESA Contract N^o 4000125122/18/NL/FF/gp

Authors:
Michael.Buchwitz@iup.physik.uni-bremen.de,
Stefan Noël, Maximilian Reuter, Heinrich Bovensmann, Andreas Richter
Institute of Environmental Physics (IUP) / Institute of Remote Sensing (IFE), University of Bremen (UB), Bremen, Germany

Jochen Landgraf, Hein van Heck
SRON, Utrecht, The Netherlands

Pepijn Veefkind, Johan de Haan
KNMI, De Bilt, The Netherlands

Hartmut Boesch
University of Leicester, Leicester, UK

Change log

Version	Date	Status	Authors	Reason for change
Draft 0.1	17-Oct-2018	As submitted	M. Buchwitz and CO2M-REB project team	New document
Draft 0.3	30-Nov-2018	Draft for PM2	-"-	New post PM1 results added
1.0	25-Feb-2020	As submitted	-"-	Post PM2 results added
1.1	8-May-2020	As submitted	-"-	To consider comments from ESA

Table of Contents

Table of Contents 3

1. Executive summary 4
2. Computation of SNR-related XCO_2 errors: Specific instruments and scenarios 5
3. Computation of SNR-related XCO_2 errors: Specific instrument parameters (“B”) to study the impact of temporal oversampling 8
4. Crosstalk between neighbour FOVs 10
   - 4.1. IUP analysis 10
   - 4.2. SRON analysis 14
5. Alternative instrument concept for tropospheric NO_2 retrieval by using a small fit window and a high spectral resolution 19
   - 5.1. Analysis and results 19
   - 5.2. Summary and conclusions 20
6. XCO_2 errors computed using different gains applied to error spectra from industry 21
7. Acronyms and abbreviations 32
8. References and related literature 34

1. Executive summary

This document is a deliverable of ESA Study "Study on Consolidating Requirements and Error Budget for CO_2 Monitoring Mission". The satellite mission is referred to as CO2M (anthropogenic CO_2 Monitoring Mission) in this document.

The purpose of this document is to document assessment results obtained to support phase A/B1 system activities.

The following activities are covered in this document:

For specific instrument concepts and scenarios instrument signal-to-noise (SNR) related XCO_2 random errors have been computed based on specific input provided by ESA.

The XCO_2 error due to crosstalk between neighbour field-of-views (FOVs) has been computed using specific input provided by ESA. It has been found that the resulting XCO_2 is less than 0.1 ppm for cloud-free cases but even a quite thin cloud may result in unacceptably errors of several 0.1 ppm.

For NO_2 retrieval an alternative instrument concept has been evaluated providing data with high spectral resolution in a smaller fit window, 425-450 nm. The analysis shows that this approach improves the precision of the retrieved tropospheric NO_2 column by a factor of 2.0 – 2.5, mainly because many more spectral pixels are used for the small window while maintaining SNR per spectral sample.

ESA has provided CO2M error spectra and these have been used in the gain method to compute the corresponding XCO_2 errors. These errors have been computed using gains of the retrieval algorithms from SRON (using scattering and non-scattering gains), Univ. Bremen and Univ. Leicester.

2. Computation of SNR-related XCO_2 errors: Specific instruments and scenarios

ESA asked for the computation of SNR-related XCO_2 errors for two different instruments and several scenarios (e-mails B. Sierk, 10-11 September 2018). For the SNR computation so-called A and B coefficients have been provided by ESA (see SNR formula and additional explanations as given in **/Sierk et al., 2018/**).

The relevant parameters for the instruments and the scenarios are shown in **Table 1**.

The corresponding XCO_2 errors are shown in **Table 2**.

As can be seen, instrument 2 has smaller SNR-related XCO_2 errors compared to instrument 1, and instrument 2 is better if temporal oversampling = 1.

Instruments:						
ID	**Comment**					
I_01	Instrument 1					
I_02_T1	As I_01 but modified detector (lower FWC and RON), temporal oversampling=1					
I_02_T2	As I_02_T1 but temporal oversampling=2					
Instrument parameters: SNR:						
Instrument	**NIR**		**SWIR-1**		**SWIR-2**	
ID	**A**	**B**	**A**	**B**	**A**	**B**
	(*)	**[-]**	**(*)**	**[-]**	**(*)**	**[-]**
I_01	2,24E-15	21343,81	1,29E-14	228820,79	2,48E-14	232755,13
I_02_T1	2,24E-15	21343,81	1,40E-14	78199,85	2,67E-14	81885,27
I_02_T2	2,24E-15	21343,81	1,40E-14	173057,09	2,67E-14	176713,36
(*) A unit = 1/radiance_unit, where radiance_unit = phot/s/m2/micron/sr (= L_sron)						
(L_iup [phot/s/cm2/nm/sr]-> L_iup = L_sron * 1e-7)						
Instrument parameters: Other:						
Spectral range and resolution [nm]:						
Band	**Start**	**End**	**Resolution**			
NIR	747	773	0,098			
SWIR-1	1590	1675	0,27			
SWIR-2	1925	2095	0,53			
Spectral Sampling Distance (SSD) in pixel per FWHM:					3	
Scenarios:						
ID	**Comment**			**Albedo**		**SZA**
			NIR	**SWIR-1**	**SWIR-2**	**[deg]**
HLD	High latitude dark		0,10	0,05	0,05	75
VEG50	VEG50		0,20	0,10	0,05	50
MLD	Mid latitude dark		0,10	0,05	0,05	50
MLB	Mid latitude bright		0,80	0,60	0,60	50
MLB2	Mid latitude bright 2		0,50	0,40	0,40	50
TRD	Tropical dark		0,10	0,05	0,05	0
TRB	Tropical bright		0,80	0,60	0,60	0
TRB2	Tropical bright 2		0,50	0,40	0,40	0

Table 1: Relevant parameters for instruments and scenarios. Note that in this table SSD is used as abbreviation for Spectral Sampling Distance (i.e., not Spatial Sampling Distance).

SNR-related XCO2 errors (SNR-related precision):				
Scenario		**SNR-related XCO2 error (1-sigma) [ppm]**		
		I_01	**I_02_T1**	**I_02_T2**
HLD		1,32	1,11	1,23
VEG50		0,86	0,74	0,80
MLD		1,02	0,85	0,95
MLB		0,36	0,34	0,35
MLB2		0,42	0,40	0,41
TRD		0,99	0,85	0,93
TRB		0,35	0,34	0,34
TRB2		0,40	0,39	0,39

Table 2: SNR-related XCO_2 errors as computed with FOCAL by Univ. Bremen.

3. Computation of SNR-related XCO_2 errors: Specific instrument parameters ("B") to study the impact of temporal oversampling

SNR-related XCO_2 random errors have been computed according to a specification from ESA (e-mail YM, 26-Oct-2018, "Input to MAG for SNR requirement refinement").

The results as obtained by IUP-UB using the FOCAL retrieval algorithm are shown in **Table 3**, where also the used SNR formula, i.e., SNR(L, A, B), is given including the values for the different A and B pairs (L is the radiance). For SWIR-2 the B and C bands have been used for retrieval assuming a spectral resolution of 0.35 nm. For FOCAL an XCO_2 *a priori* uncertainty of 5 ppm (1-sigma) is assumed.

Case 0 has been added (to the 12 cases 1-12 as specified by ESA) as this is an important reference scenario for application "CO_2 emissions via XCO_2 imaging". Here error is 0.454 ppm, which is better than required for this error source (0.5 ppm according to the Error Budget). For VEG50 errors are in the range 0.553 to 0.595 (+8% for max. coadding) depending on Temporal Oversampling Factor (TOF).

As can be seen, impact of coadding (TOF > 1) on the XCO_2 SNR-related random error is relatively small (< 10% even for the change from no coadding (TOF=1) to largest coadding factors (TOF = 4)).

Identical A values (throughput) have been used for all cases, because of the purpose here is to study the impact of coadding as quantified by different values of the effective detector noise (parameter B).

CO2M: SNR-related XCO_2 random errors

Computation of SNR-related XCO_2 random errors (by IUP-UB) based on ESA specification (e-mail YM 26-Nov-2018 to CO2M MAG):

$$SNR = \frac{A \cdot L}{\sqrt{A \cdot L + B^2}}$$

Note:
- SNR formula with B^2 (not B) !
- Radiance unit: phot/s/nm/cm²/sr (for L and A) !

Case	ID	SZA	Albedo NIR / SW1 / SW2	TOF NIR / SW1 / SW2	A NIR / SW1 / SW2 [10^{-7} / (phot/s/nm/cm²/sr)]	B NIR / SW1 / SW2 [10^{-7} / (phot/s/nm/cm²/sr)]	XCO_2 error (via FOCAL) [ppm]
0 (*)	REF50	50	0.25 / 0.2 / 0.1	1 / 1 / 1	0.432 / 1.16 / 1.50	209 / 207 / 201	0,454
1	VEG50	50	0.2 / 0.1 / 0.05	1 / 1 / 1	- „ -	209 / 207 / 201	0,553
2	VEG50	50	0.2 / 0.1 / 0.05	2 / 2 / 2	- „ -	296 / 294 / 285	0,590
3	VEG50	50	0.2 / 0.1 / 0.05	3 / 3 / 2	- „ -	355 / 353 / 285	0,595
4	MLB50	50	0.5 / 0.4 / 0.4	3 / 3 / 2	- „ -	355 / 353 / 285	0,322
5	VEG25	25	0.2 / 0.1 / 0.05	2 / 1 / 1	- „ -	296 / 207 / 201	0,515
6	VEG25	25	0.2 / 0.1 / 0.05	3 / 3 / 2	- „ -	355 / 353 / 285	0,546
7	VEG25	25	0.2 / 0.1 / 0.05	4 / 4 / 2	- „ -	415 / 411 / 285	0,549
8	MLB25	25	0.5 / 0.4 / 0.4	4 / 4 / 2	- „ -	415 / 411 / 285	0,287
9	VEG00	0	0.2 / 0.1 / 0.05	2 / 1 / 1	- „ -	296 / 207 / 201	0,504
10	VEG00	0	0.2 / 0.1 / 0.05	4 / 4 / 3	- „ -	415 / 411 / 344	0,551
11	TRB	0	0.5 / 0.4 / 0.4	4 / 4 / 3	- „ -	415 / 411 / 344	0,337
12	TRD	0	0.1 / 0.05 / 0.05	4 / 4 / 3	- „ -	415 / 411 / 344	0,733

(*) Case 0 = REF50 added by IUP-UB as this is a relevant reference scenario for application „CO_2 emissions via XCO_2 imaging" (the albedos correspond to typical albedos for the end-to-end simulator Berlin scenes)

From: MB, SN, MR, Univ. Bremen, 29-Oct-2018

Table 3: SNR-related XCO_2 random errors (1-sigma) for different scenarios and instrument parameters (incl. different TOFs) as computed by IUP-UB using the FOCAL retrieval algorithm.

4. Crosstalk between neighbour FOVs

Radiance signals may “leak” to the target spatial sample of interest from the adjacent one (e.g., straylight). This may be an issue for scenes with the large radiometric contrast, e.g., in case of spatial inhomogeneity due to large surface albedo variations or clouds. Requirements have been formulated for non-uniform scenes and strong contrast but for this case an “exclusion zone” of 5 SSD (Spatial Sampling Distance) has been defined (5 SSD = 10 km). It is investigated here if short-range effects are a severe issue taking into account performance estimates provided by industry (**Table 4**).

The following Table 4 has been provided by ESA (BS, mail from 22-Aug-2019, 10:43, subject: “albedo variation within a scene”):

	SWIR2			SWIR1			NIR		
	2095	2042.5	1990	1675	1632.5	1590	773	760	747
ACT Field 1	0.22%	0.24%	0.25%	0.15%	0.15%	0.14%	0.07%	0.06%	0.06%
ACT Field 2	0.20%	0.26%	0.24%	0.16%	0.16%	0.14%	0.06%	0.06%	0.06%
ACT Field 3	0.22%	0.31%	0.27%	0.21%	0.19%	0.15%	0.07%	0.07%	0.08%

Table 4: Total flux contribution from neighbour FOV (performance estimate from industry).

4.1. IUP analysis

To investigate this aspect, several cases have been studied using simulated retrievals and FOCAL gain vectors (for linear error analysis). The target scene corresponds to the “Mid-Latitude Dark” (MLD) scenario (SZA 50^o, albedos in the three bands NIR, SWIR-1 and SWIR-2: 0.1 / 0.05 / 0.05) and the adjacent scene to the “Mid-Latitude Bright” (MLB) scenario (SZA 50^o, albedos: 0.6 / 0.4 / 0.4), where the radiances are approximately a factor of 8 larger compared to MLD. The radiance spectra are shown in **Figure 1**.

Table 4 lists potential (fractional) radiance contributions (for three wavelength per band) from the adjacent spatial sample to the target spatial sample. As can be seen, the contributions are typically largest for row “ACT Field 3”. The values in this row have been interpolated (smoothly, using a second order polynomial) to compute the fractional radiance contribution as a function of wavelength. These fractional contributions together with the radiance of the adjacent scene (MLB) have been used to generate radiance error spectra which have been added to the (otherwise error free) target radiance spectra (MLD) to compute corresponding XCO_2 errors using the gain vector approach. The results are shown in **Table 5**.

As can be seen from **Table 5**, all XCO_2 errors are below 0.1 ppm, even for a (probably) quite extreme scenario with 5 times the error listed in Table 4 and using a target scene with XCO_2 enhanced by 1 ppm relative to the adjacent scene.

However, adjacent scenes can also be cloud covered. To investigate this, radiance spectra with a cloud (with 100% cloud cover) have been computed with FOCAL (see **Figure 1 (c)**). The cloud is located at 500 hPa (approx. 5 km), has an optical depth of 0.72 in the NIR and an Ångstrom coefficient of 1.5. The XCO_2 error assessment results are shown in **Table 6**. As can be seen, the XCO_2 errors are much larger in this case often exceeding the error budget value of 0.2 ppm (allocated for, e.g., radiometric accuracy).

From this it is concluded that XCO_2 errors due to crosstalk from adjacent scenes seems not to be a significant problem (assuming that all assumptions (esp. **Table 4**) are valid) for cloud-free neighbour scenes but in case of a cloud covered neighbour scene the XCO_2 error can be unacceptably large (> 0.2 ppm). >>> Maybe explain here that the CLD contribution is worse due to photons not reaching the surface and hence a contributing spectrum with shallower absorption <<<

Target scene	**Adjacent scene**	**Band**			**XCO_2 error [ppm]**	**Comment**
		NIR	**SWIR-1**	**SWIR-2**		
		Ratio continuum radiance adjacent/target spatial sample				
MLD	MLB	5.6	7.9	8.0		
		Contribution from adjacent spatial sample [%]				For default error scaling factors: 1, 1, 1
		0.08	0.19	0.28		
		Contribution to target spatial sample [%]				
		0.45	1.48	2.28		
		Error scaling factor:				
MLD	MLB	1	1	1	-0.0006	
-“-	-“-	1	0	0	-0.0014	
-“-	-“-	0	1	0	-0.0016	
-“-	-“-	0	0	1	0.0024	
-“-	-“-	0	0	2	0.0047	
MLD + 1 ppm	-“-	0	0	2	-0.0219	
-“-	-“-	0	2	0	-0.0128	
-“-	-“-	2	0	0	-0.0028	
-“-	-“-	0	2	2	-0.0346	
-“-	-“-	0	4	4	-0.0693	
-“-	-“-	4	4	4	-0.0748	
-“-	-“-	5	5	5	-0.0935	

Table 5: XCO_2 errors due to crosstalk from an adjacent spatial sample to the target spatial sample of interest. XCO_2 errors have been computed taking the fractional radiance contributions listed in **Table 4** into account. An “error scaling factor” of 1 in a given band (default value) means that exactly the **Table 4** values have been used (0 means no error, 2 means twice this error). The “MLD + 1 ppm” scene is identical with the MLD scene except that XCO_2 is enhanced by 1 ppm (401 ppm instead of the 400 ppm used for MLD)

Target scene	Adjacent scene	Band			XCO_2 error [ppm]	Comment
		NIR	SWIR-1	SWIR-2		
		Ratio continuum radiance adjacent/target spatial sample				
MLD	CLD	5.6	3.7	2.9		
		Contribution from adjacent spatial sample [%]				For default error scaling factors: 1, 1, 1
		0.08	0.17	0.27		
		Contribution to target spatial sample [%]				
		0.43	0.64	0.80		
		Error scaling factor:				
MLD	CLD	1	1	1	-0.44	
-“-	-“-	1	0	0	0.24	
-“-	-“-	0	1	0	-0.53	
-“-	-“-	0	0	1	0.07	
-“-	-“-	2	2	2	-0.87	
-“-	-“-	2	0	0	0.05	
-“-	-“-	0	2	0	-1.06	
-“-	-“-	0	0	2	0.13	
-“-	-“-	4	4	4	-1.75	
-“-	-“-	4	0	0	0.09	
-“-	-“-	0	4	0	-2.11	
-“-	-“-	0	0	4	0.26	

Table 6: As **Table 5** but for a scenario with a cloud covered adjacent, i.e., neighbour scene. The listed percentage contributions are valid for “Error scaling factor” (ESF) 1. If the ESF for a given band is 0, then the contribution from this band is zero and if the ESC is 2, then the contribution is twice as large as for ESF=1.

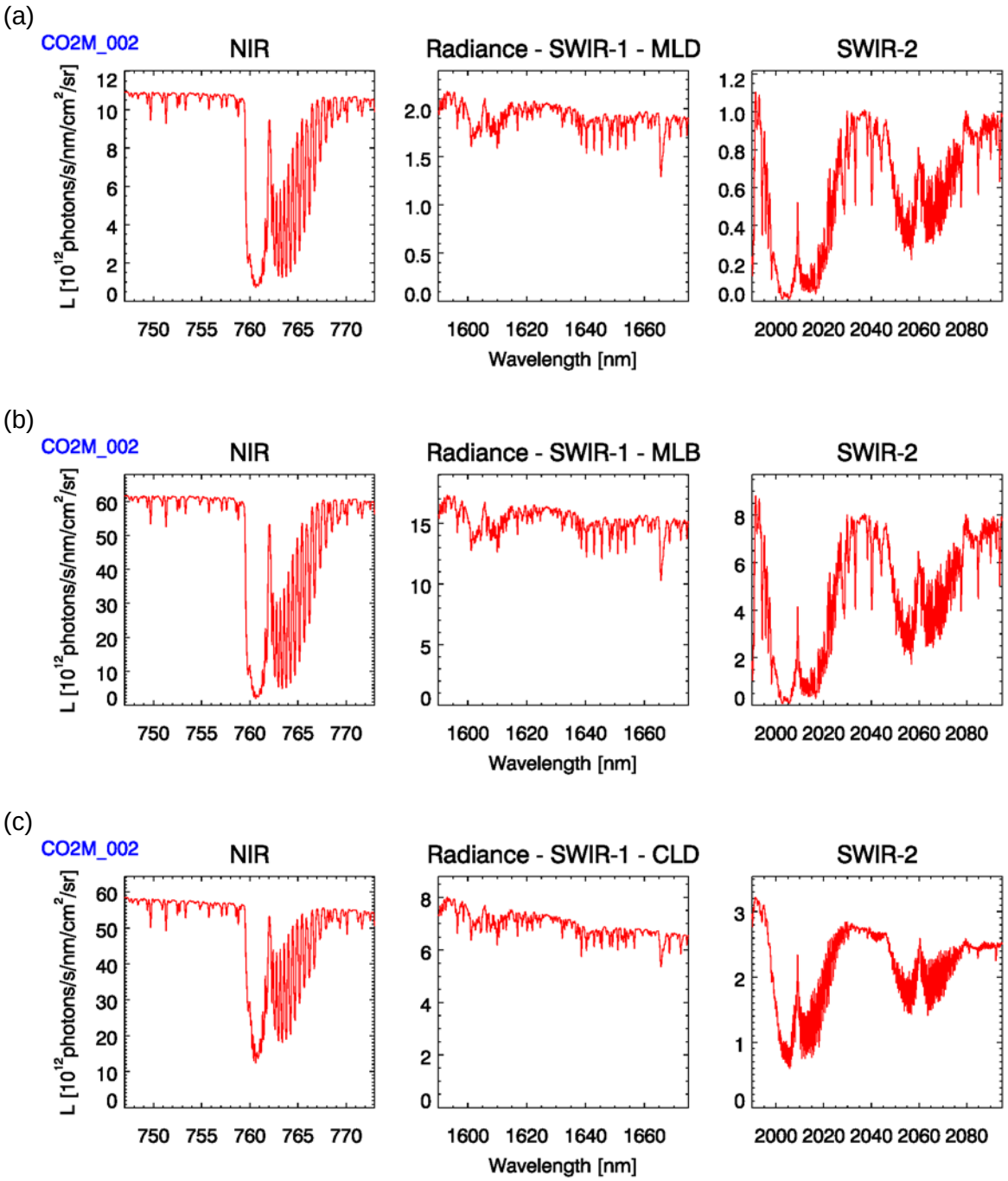

Figure 1: Radiance spectra for scenario MLD (a), MLB (b) and for the scenario with clouds (c).

4.2. SRON analysis

To verify the findings shown in the previous sub-section, SRON performed similar simulations for the pixel crosstalk using the RemoTeC algorithm. First, we estimated the XCO_2 error due to crosstalk between neighbouring field-of-views assuming:

1. The Tropical Dark reference scene for the target pixel and the Tropical Bright reference scene as the interfering pixel. This scenario represents two adjacent scenes with the same solar and viewing geometry but different surface albedo. For each spectral band, we assuming a mixing
$$I(\lambda) = (1 - a)I_{tar}(\lambda) + aI_{adj}(\lambda)$$
where a is the pixel crosstalk factor and I_{tar} and I_{adj} are the radiance spectra for the target and adjacent pixel, respectively. The coefficient a is spectrally independent, so describes a simultaneous mixing over all bands. In our simulations we vary a between 0.01 and 0.10. The error analysis performance nearly linear for small mixing coefficents a and so performance estimates can be derived by linear interpolation for mixing $a < 0.01$.
2. The Mid-Latitude Dark reference scene for both target and adjacent pixel, where the target pixel is assumed to be clear sky and the adjacent pixel is covered by a cloud (type 1 cloud at 5 km altitude with a cloud optical depth of 0.72). For the base case, the pixel crosstalk factors are $a_{NIR} = 0.0008$, $a_{SWIR1} = 0.0017$ and $a_{SWIR2} = 0.0027$. Additionally, we consider cases where these crosstalks are multiplied by a factor of 2, 3, 4 and 5.
3. The Tropical Dark reference scene for both target and adjacent scene. In this case, we assume a clear sky target scene and an adjacent scene fully covered by a stratiform cloud at the top of the tropospheric boundary layer (cloud type 2). Here the cloud optical depth is 20 and the cloud central height is at 2 km. We vary the crosstalk factors a between 0.01 and 0.10 and for $a < 0.01$ reliable performance can be estimated by linear interpolation.

The radiance spectra for these cases are shown in **Figure 2**, the resulting error on XCO_2 in **Figure 3 - Figure 5**, depending on the considered cases 1–3, respectively.

Figure 3 shows that the differences in surface albedo of the adjacent pixels result in a minor XCO_2 contribution of less than 0.1 ppm. This is also expected because of the linearity of radiative transfer in the surface albedo for a non-scattering atmosphere. The figure confirms that in this artificial case, the XCO_2 error is negligible.

Cloud presence increases the error on XCO_2 up to 1 ppm in the case of an optically thin cloud with an AOD of 0.72 at 5 km altitude (**Figure 4**) and the pixel cross talk as indicted in **Table 4**.

This is in line with the findings described in the previous section.

Figure 5 shows that the XCO_2 error quickly rises above 10 ppm in case of a cloud with an optical thickness of 20 and a pixel crosstalk ratio > 0.005. For reported values of $0.008 < a < 0.0027$, linear interpolation estimates a range of XCO_2 errors between 1.6 ppm and 5.4 ppm.

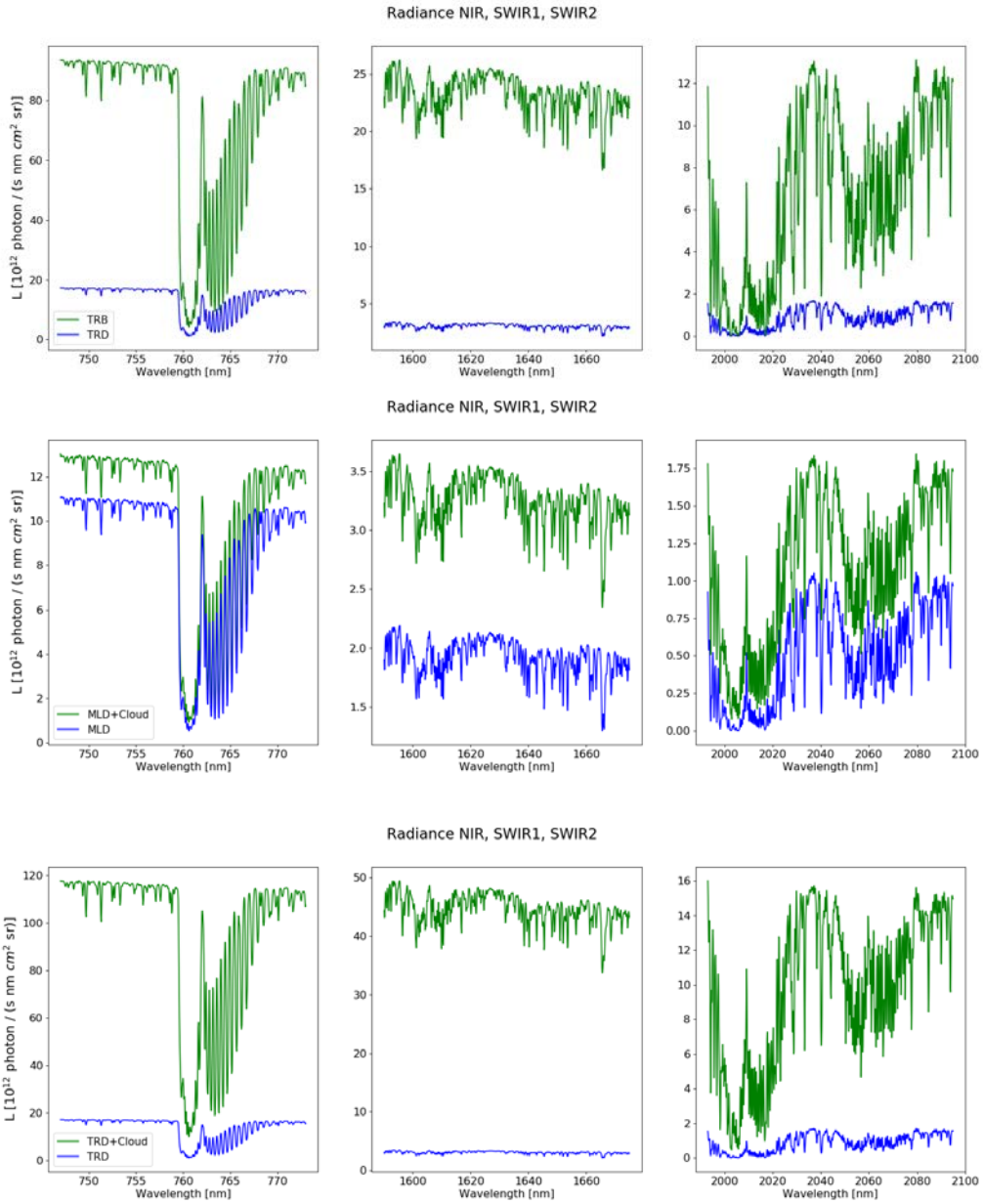

Figure 2: Clear-sky and cloudy radiance spectra for the three investigated cases. Top: Tropical Dark and Tropical Bright; Middle: Mid-Latitude Dark clear-sky and cloudy (cloud type 1); Tropical Dark clear-sky and cloudy (cloud type 2).

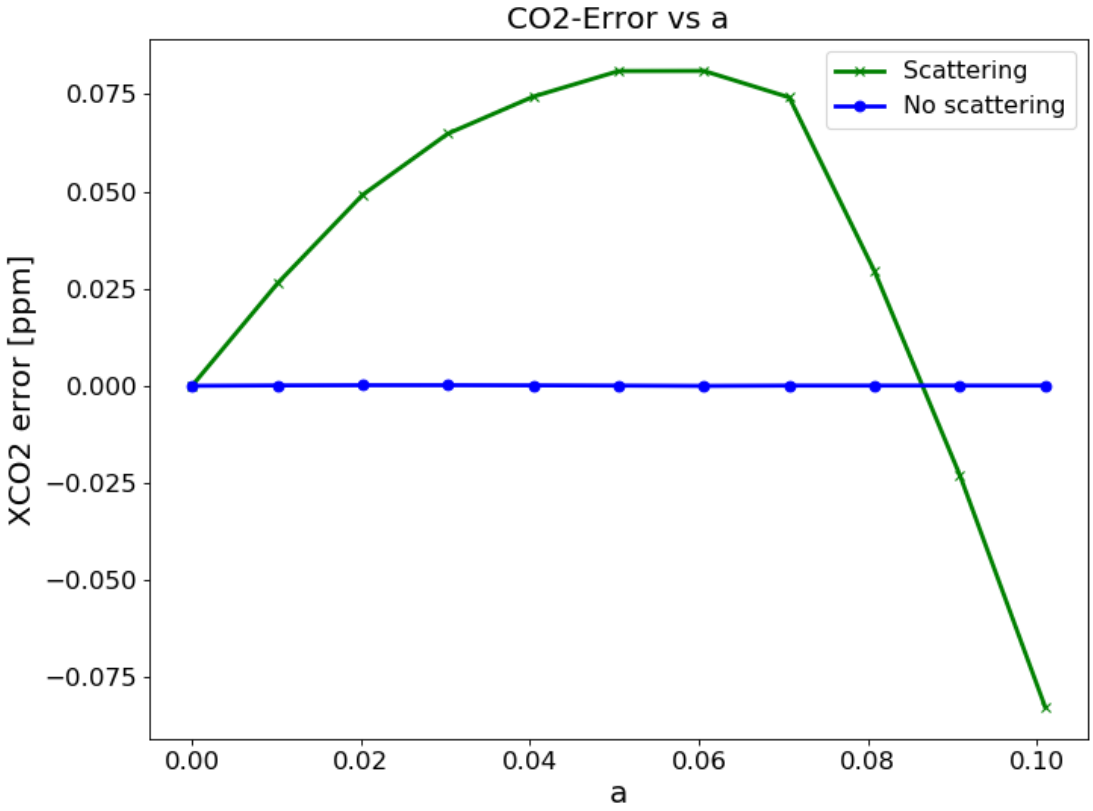

Figure 3: XCO_2 error in ppm as function of the pixel crosstalk $\boldsymbol{a}$ for case 1. A no scattering case is added as a check.

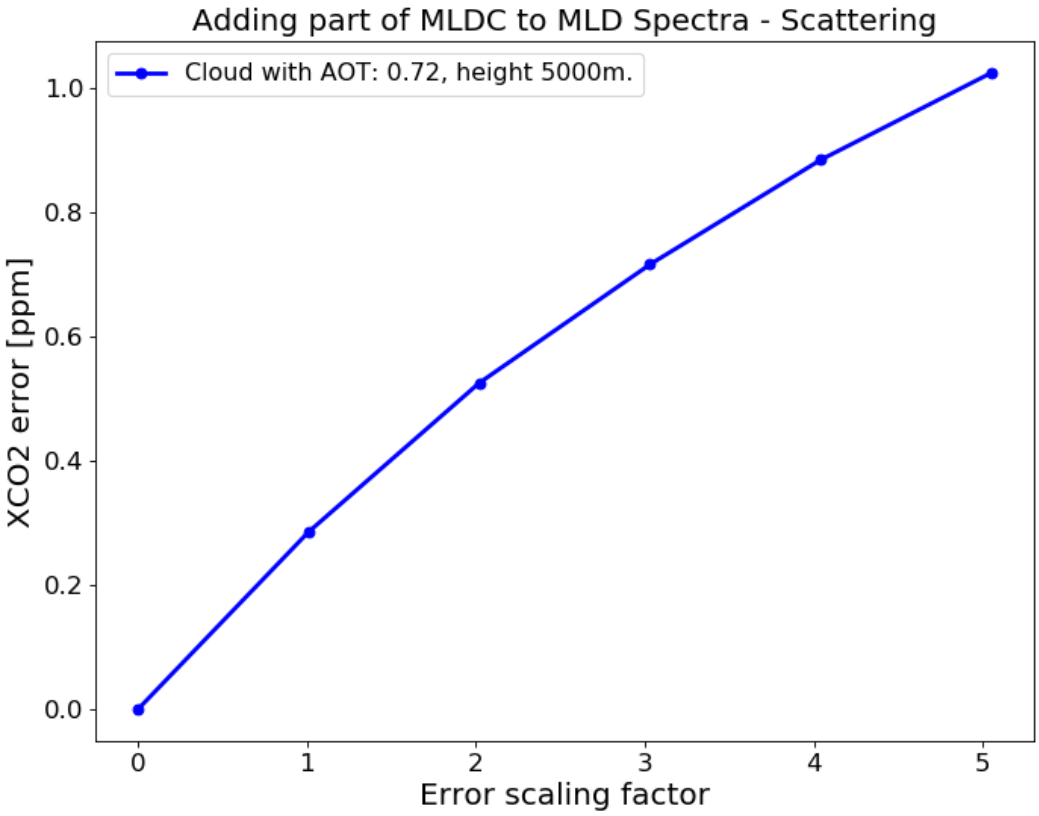

Figure 4: XCO_2 error as a function of the pixel cross talk scaling factor for case 2. A scaling factor of 1 corresponds to mixing ratios of 0.0008 for the NIR, 0.0017 for the SWIR1, and 0.0027 for the SWIR2 as indicated in **Table 4**.

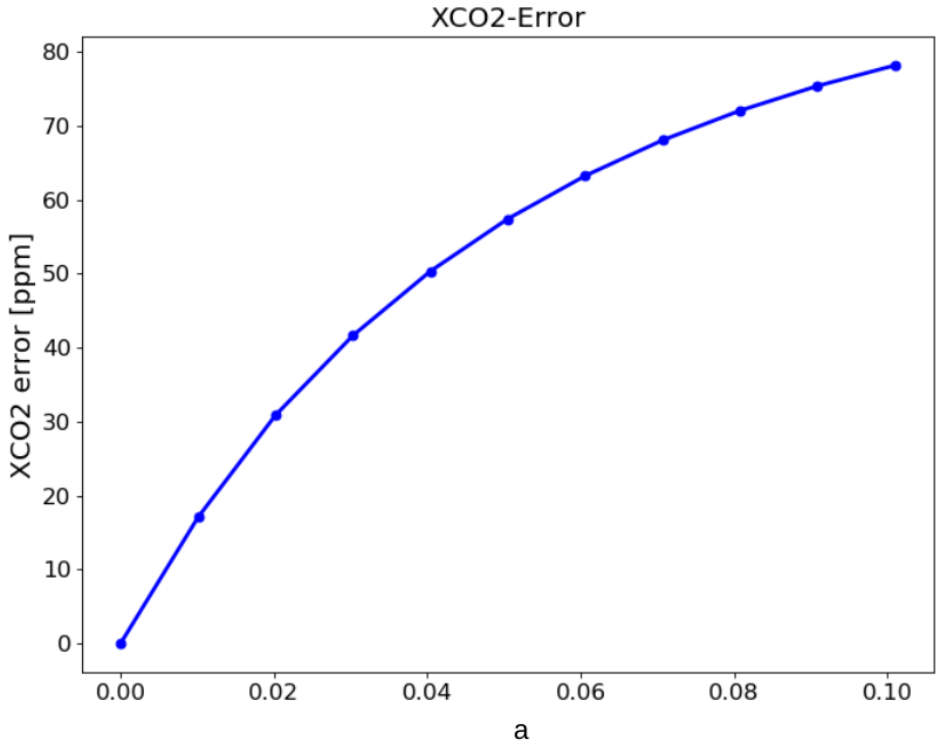

Figure 5: XCO_2 error as a function the crosstalk factor $\boldsymbol{a}$ *for case 3.*

5. Alternative instrument concept for tropospheric NO_2 retrieval by using a small fit window and a high spectral resolution

Previous results for tropospheric NO_2 are based on DOMINO settings involving a large fit window for NO_2 (405-465 nm) and a low spectral resolution (FWHM of 0.60 nm; sampling 0.2 nm).

ESA request: Consider as alternative a small fit window (425 – 450 nm) or (450 – 475 nm) and a high spectral resolution with FWHM = 0.069 (sampling 0.023 nm). As the fit window (425 – 450 nm) contains more pronounced absorption features, the precision of the retrieved NO_2 column is better in this window. Calculations for the second window are not reported here, instead we focus on the comparison of the precision for the wide fit window with relatively low spectral resolution and the small window with high spectral resolution.

The advantage of using the small window would be: perfect spatial co-registration and a much better SNR.

The signal to noise ratio for the wide and small window, SNR, is given by

$$SNR = \frac{LA}{\sqrt{LA + B^2}}$$

where
L is the earth radiance
A and *B* are coefficients provided by ESA
A = 2.10E-10; *B* = 354.3

5.1. Analysis and results

The retrieval method for the tropospheric NO_2 column is the DOMINO algorithm as implemented in DISAMAR.

Calculations have been performed for an atmosphere containing no clouds nor aerosols. The stratospheric column of NO_2 is 4.0E15 molecules/cm2 and the tropospheric NO2 column is 1.0E16 molecules/cm2. The viewing direction is nadir (VZA = 0) and results are obtained for different values of the solar zenith angle and the surface albedo.

Figure 6 shows the precision in percent of the tropospheric NO_2 column plotted as function of the surface albedo for the two fit windows considered and for different values of the solar zenith angle.

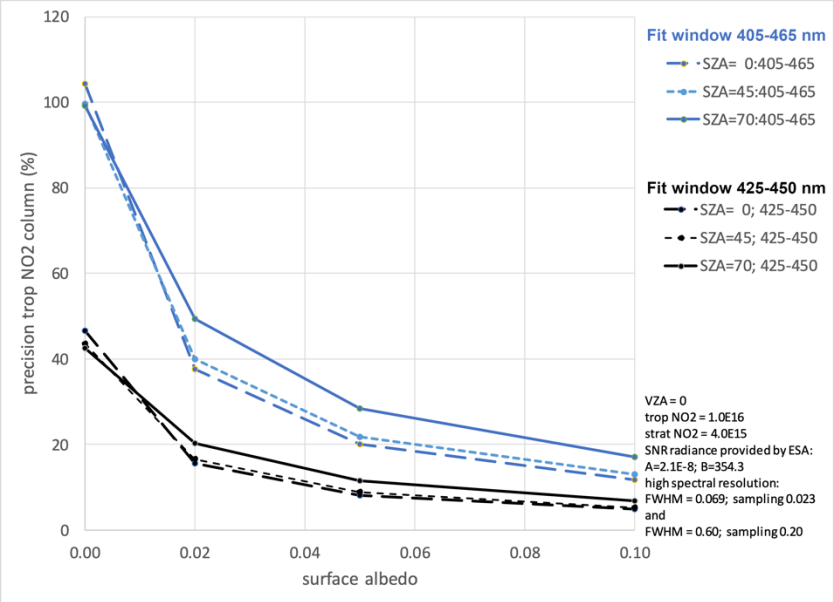

Figure 6. *Precision of the retrieved tropospheric NO_2 column plotted as function of the surface albedo for the two fit windows, 405-465 nm (blue lines) and 425-450 nm (black lines). The spectral resolution differs for the two windows: FWHM is 0.60 for 405-465 nm and 0.069 for 425-450 nm while the sampling is one third of the FWHM. The ISRF is Gaussian and the viewing angle is nadir. Results for three solar zenith angles are shown: SZA = 0, 45, and 70 degrees.*

Figure 6 shows that the precision is about a factor of 2 – 2.5 better for the small 425 – 450 nm window than for the wide 405 - 465 nm. This is mainly due to the large number of spectral pixels in the 425 - 450 window, about 1100, whereas the wide window has just 300 spectral pixels. As the SNR for the pixels is assumed to be the same, using a small fit window with a high spectral resolution has the potential to improve the precision of NO_2 retrievals significantly. Off-course, if the SNR is not maintained for the spectral pixels of the smaller window, this will impact the results.

5.2. Summary and conclusions

For NO_2 retrieval an alternative approach has been evaluated, using a high spectral resolution and a small fit window, 425-450 nm. The analysis shows that this approach improves the precision of the retrieved tropospheric NO_2 column by a factor of 2.0 – 2.5, mainly because much more spectral pixels are used for the small window, while the SNR of the spectral samples is maintained.

6. XCO_2 errors computed using different gains applied to error spectra from industry

This sub-section shows (self-explaining) slides from a presentation given on 10-Feb-2020 by M. Buchwitz at a videoconference with ESA and participation of SRON and Univ. Leicester.

Shown are results from CO2M gain comparisons by applying them to error spectra from industry provided by ESA to the study team members.

The purpose of the presentation was to

(i) Present comparison results using gains provided by Univ. Bremen, SRON (scattering and non-scattering gains) and Univ. Leicester.

(ii) To compute XCO_2 errors using the error spectra provided by industry.

The following has been done: SRON used error spectra (for sun-normalized radiance) from industry (straylight & polarization) and computed XCO_2 errors using 4 sets of gains: SRON-NS, SRON-S, IUP, UoL. The same analysis has been done by IUP-UB to verify that both groups are able to use the input data in an identical way and obtain reliable and robust conclusions.

The conclusions from this activity are:

- The SRON and IUP-UP results showed good agreement using the SRON-NS, SRON-S and IUP gains
- For the UoL gains IUP-UB obtained somewhat different errors compared to SRON likely due to a different approach to deal with limitations of the UoL gains when applied to errors given for sun-normalized radiance

Institute of Environmental Physics and Remote Sensing
IUP/IFE-UB

Department 1
Physics/Electrical Engineering

CO2M Requirements & Error Budget Study (CO2M-REB):
Gain Comparisons Meeting, 10-Feb-2020, VideoCon

CO2M gain comparisons including error spectra from industry

Michael Buchwitz, Stefan Noël, Maximilian Reuter (IUP-UB)

Institute of Environmental Physics (IUP), Institute of Remote Sensing (IFE)
University of Bremen, Bremen, Germany

and
project partner / sub-contractor:
J. Landgraf (SRON), H. van Heck (SRON),
H. Boesch (Univ. Leicester)

Universität Bremen
buchwitz@uni-bremen.de

Purpose of presentation

- Activity is related to CO2M-REB PM4 actions (see next slide)
- Gain comparisons:
  - Check if SRON-analysis results as shown in SRON file CO2M-Gain_comparison.pptx (e-mail JL, 8-Jan-2020) can be reproduced by IUP-analysis

- Provide answers to (IUP/FOCAL related) questions from ESA (e-mail BS, 9-Jan-2020) to e-mail from SRON (e-mail JL, 8-Jan-2020)

Related CO2M-REB PM4 actions

AI_PM4_01: On MB, JL, HB: On MB to check all gains (including computation of several instrument related errors), put them on the project ftp server and add a description on how to use them in TN-2000. Afterwards JL and HB to independently repeat the error computations. Due: 17 Dec 2019.

- MB: ftp & TN-2000: done
- JL: Used SRON, IUP & UoL gains for AI_PM4_03 industry errors (mail 8-Jan-2020)
- MB: Compared SRON results with IUP results (see this presentation)

TN-2000

AI_PM4_02: On JL to make a proposal on how to use the non-scattering gains to be discussed by all study members. Due: 17 January 2020.

- JL: Mail 8-Jan-2020 (see also AI_PM4_04)

AI_PM4_03: On ESA to make available instrument related error spectra (especially for straylight). Due: 12 Dec 2019.

- BS: Done (e-mail 11-Dec-2019)

TN-4000

AI_PM4_04: On MB, JL, HB to use the output from AI_PM4_03 to compute XCO2 errors using gains. Due: 20 Jan 2019 ~~X~~ 2020

- JL: Mail 8-Jan-2020
- MB: This presentation

(new Section to be added)

Universität Bremen ife KNMI UNIVERSITY OF LEICESTER SRON 3

CO2M XCO_2 errors

ZLO

Universität Bremen ife KNMI UNIVERSITY OF LEICESTER SRON 4

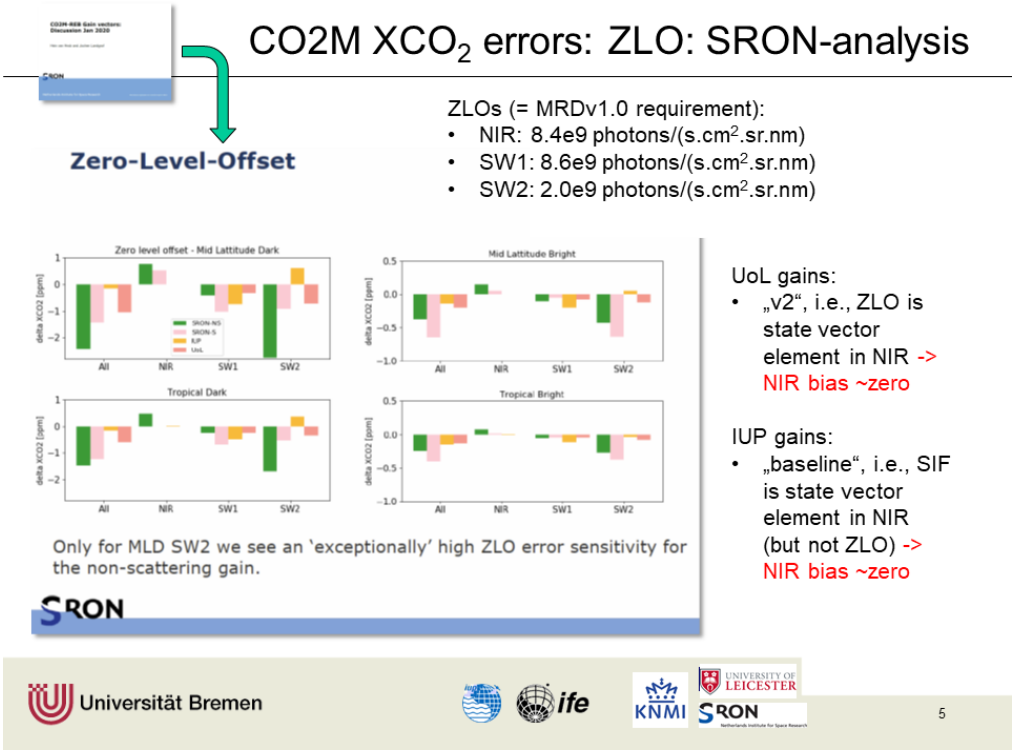
CO2M XCO2 errors: ZLO: SRON-analysis
Zero-Level-Offset
ZLOs (= MRDv1.0 requirement):
• NIR: 8.4e9 photons/(s.cm2.sr.nm)
• SW1: 8.6e9 photons/(s.cm2.sr.nm)
• SW2: 2.0e9 photons/(s.cm2.sr.nm)
Zero level offset - Mid Lattitude Dark
Mid Lattitude Bright
Tropical Dark
Tropical Bright
Only for MLD SW2 we see an 'exceptionally' high ZLO error sensitivity for the non-scattering gain.
SRON
UoL gains:
• „v2“, i.e., ZLO is state vector element in NIR -> NIR bias ~zero
IUP gains:
• „baseline“, i.e., SIF is state vector element in NIR (but not ZLO) -> NIR bias ~zero
Universität Bremen
ife
KNMI
UNIVERSITY OF LEICESTER
SRON
5

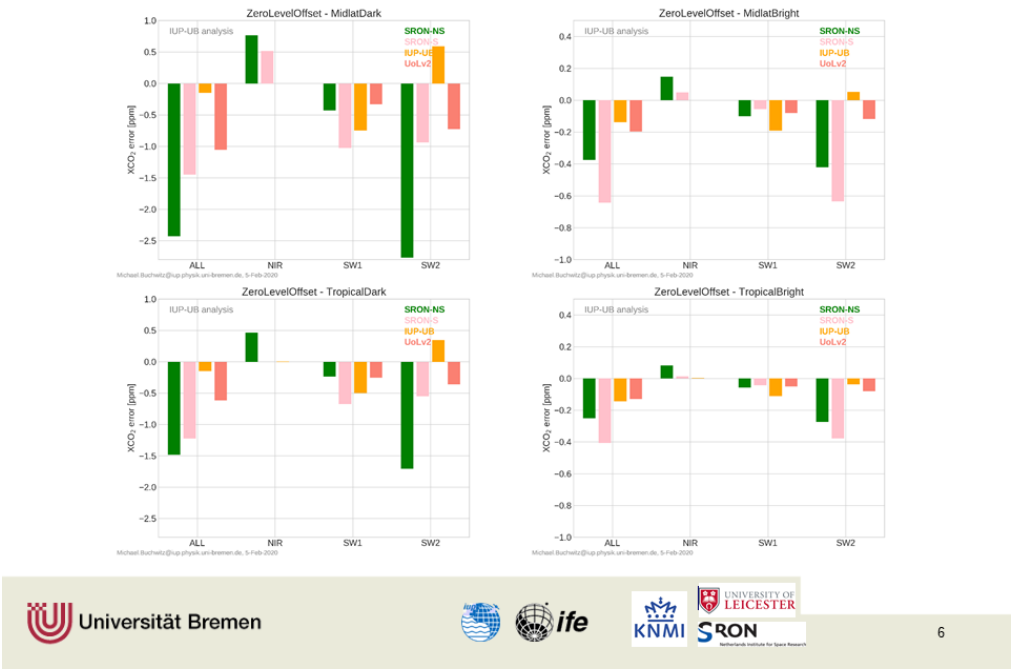
CO2M XCO2 errors: ZLO: IUP-analysis
ZeroLevelOffset - MidlatDark
ZeroLevelOffset - MidlatBright
ZeroLevelOffset - TropicalDark
ZeroLevelOffset - TropicalBright
IUP-UB analysis
SRON-NS
SRON-S
IUP-UB
UoLv2
Universität Bremen
ife
KNMI
UNIVERSITY OF LEICESTER
SRON
6

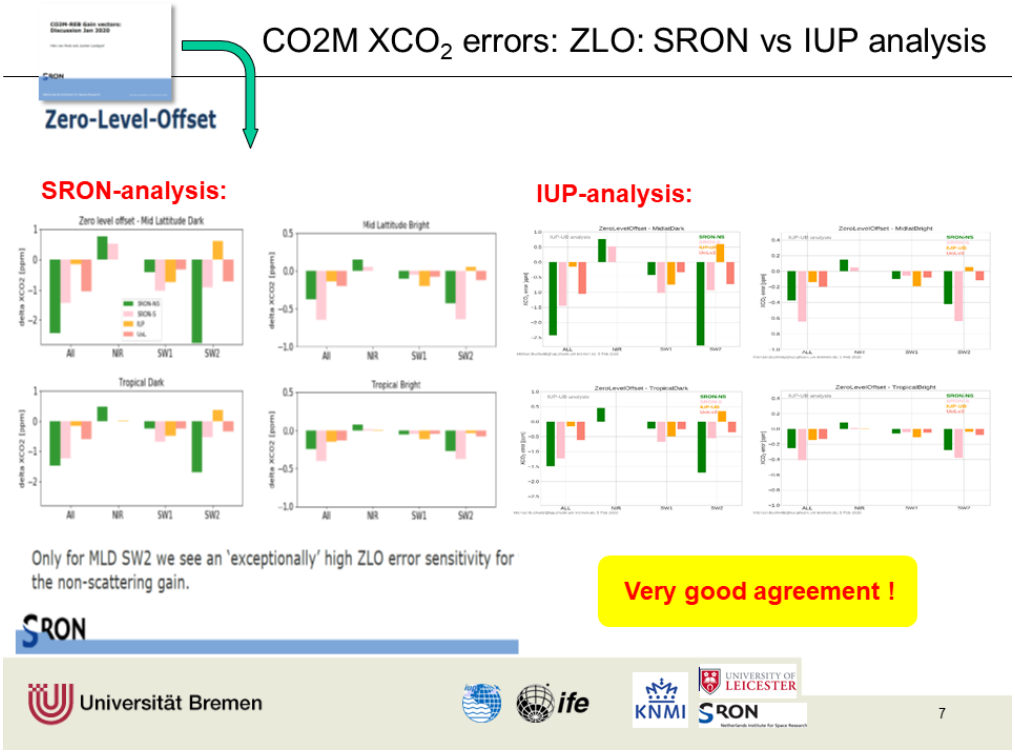
CO2M XCO2 errors: ZLO: SRON vs IUP analysis
Zero-Level-Offset
SRON-analysis:
IUP-analysis:
Zero level offset - Mid Latitude Dark
Mid Latitude Bright
Tropical Dark
Tropical Bright
Only for MLD SW2 we see an 'exceptionally' high ZLO error sensitivity for the non-scattering gain.
Very good agreement !
SRON
Universität Bremen
ife
KNMI
UNIVERSITY OF LEICESTER
SRON
7

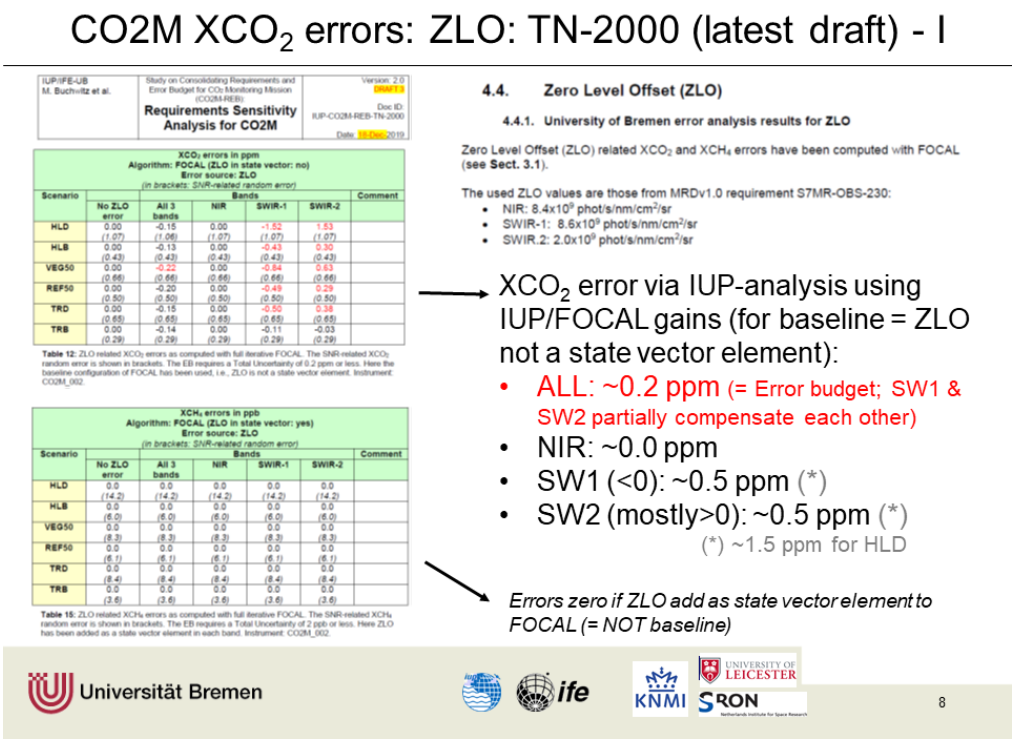
CO2M XCO2 errors: ZLO: TN-2000 (latest draft) - I
IUP/IFE-UB
M. Buchwitz et al.
Requirements Sensitivity Analysis for CO2M
4.4. Zero Level Offset (ZLO)
4.4.1. University of Bremen error analysis results for ZLO
Zero Level Offset (ZLO) related XCO2 and XCH4 errors have been computed with FOCAL (see Sect. 3.1).
The used ZLO values are those from MRDv1.0 requirement S7MR-OBS-230:
NIR: 8.4x10^9 phot/s/nm/cm^2/sr
SWIR-1: 8.6x10^9 phot/s/nm/cm^2/sr
SWIR.2: 2.0x10^9 phot/s/nm/cm^2/sr
XCO2 error via IUP-analysis using IUP/FOCAL gains (for baseline = ZLO not a state vector element):
ALL: ~0.2 ppm (= Error budget; SW1 & SW2 partially compensate each other)
NIR: ~0.0 ppm
SW1 (<0): ~0.5 ppm (*)
SW2 (mostly>0): ~0.5 ppm (*)
(*) ~1.5 ppm for HLD
Errors zero if ZLO add as state vector element to FOCAL (= NOT baseline)
Universität Bremen
ife
KNMI
UNIVERSITY OF LEICESTER
SRON
8

CO2M XCO_2 errors: ZLO: TN-2000 (latest draft) - II

Scenario	ZLO added to band:	XCO2 error [ppm] IUP	SRON	UoL(*)
VEG50	All 3	-0,191	➡ -1,287	➡ -1,384
VEG50	NIR	0,002	➡ 0,502	0,000
VEG50	SW1	➡ -0,839	➡ -0,736	➡ -0,622
VEG50	SW2	➡ 0,646	➡ -1,038	➡ -0,762
MLD	All 3	-0,152	➡ -1,446	➡ -1,056
MLD	NIR	0,001	➡ 0,518	0,000
MLD	SW1	➡ -0,746	➡ -1,027	➡ -0,329
MLD	SW2	➡ 0,593	➡ -0,937	➡ -0,727
MLB	All 3	-0,138	➡ -0,643	-0,197
MLB	NIR	0,001	0,048	0,000
MLB	SW1	-0,192	-0,056	-0,079
MLB	SW2	0,052	➡ -0,635	-0,117

Red: largest error
Green: smallest error

➡ Error > 0.2 ppm

Universität Bremen ife KNMI UNIVERSITY OF LEICESTER SRON 9

CO2M XCO_2 errors: ZLO: TN-1000 (latest draft)

IUP/IFE-UB M. Buchwitz et al.	Study on Consolidating Requirements and Error Budget for CO_2 Monitoring Mission (CO2M-REB): **Requirements Justification Report for CO2M**	Version: 2.0 DRAFT 2 Doc ID: IUP-CO2M-REB-TN-1000 Date: 18-December-2019

The EB /CO2M-REB TN-3000 v1.1, 2019/ /CO2M-REB TN-3000 v2, 2019/ lists in Tab. 2 a Total Uncertainty of 5 ppb for this error source for XCO_2 (5 ppb for ESRA, RSRA, RXRA).

This shows that this requirement is consistent with the EB.

The following is written in MRDv2.0 w.r.t. Zero-Level-Offset (ZLO):

As unknown small additive offsets on the radiance have a severe impact on XCO_2 retrievals, there is a need to define the offset correction accuracy.

The offset (zero-level baseline) correction accuracy (in photons/s/nm/cm^2/sr) of the radiance should be known to
- 6.0 x 10^9 in NIR,
- 3.0 x 10^9 in SWIR-1,
- 1.5 x 10^9 in SWIR-2.

According to the Error Budget (EB) /CO2M-REB TN-3000 v2, 2019/ a Total Uncertainty of 0.2 ppm has been allocated for this error source.

Simulation for CO2M have been carried out and are reported in /CO2M-REB TN-2000 v2, 2019/. These simulations have been done using ZLO errors as specified in MRDv1.0. The results obtained with FOCAL indicate that XCO_2 errors may exceed the 0.2 ppm as permitted according to the EB if ZLO is not added as state vector elements but are less than 0.2 ppm if ZLO is added as state vector element. This shows that the justification status depends critically on the retrieval algorithm. When FOCAL is applied to real OCO-2 data /Reuter et al., 2017b/ then ZLO is not added as state vector elements but a ZLO correction is used instead. This indicates that the values specified in MRDv1.0 are appropriate but to be on the save side it was recommended to specify somewhat lower values compared to the values specified in MRDv1.0. This recommendation has been considered for MRDv2.0.

MRDv1:
- NIR: 8.4x10^9 photons/s/nm/cm^2/sr
- SW1: 8.6x10^9 photons/s/nm/cm^2/sr
- SW2: 2.0x10^9 photons/s/nm/cm^2/sr

MRDv2:
- 6.0 x 10^9 in NIR,
- 3.0 x 10^9 in SWIR-1,
- 1.5 x 10^9 in SWIR-2.

Universität Bremen ife KNMI UNIVERSITY OF LEICESTER SRON 10

IUP-UB As to ESA Qs (e-mail BS 9-Jan-2020): ZLO

ZLO:

- BS: 1) ZLO errors are shockingly high. Did you apply the offsets in our spec?:
- - 6.0 E9 photons/(s.cm2.sr.nm) in NIR — No, used ZLO errors are larger: 8.4e9
- - 3.0 E9 photons/(s.cm2.sr.nm) in SWIR-1 — 8.6e9
- - 1.5 E9 photons/(s.cm2.sr.nm) in SWIR-2 — 2.0e9
- If so, and the errors are so high, isn't the above spec too relaxed ? Is this an option ?

- BS: 3) The error from ZLO seems to be almost (or even exactly) zero in the NIR for IUP and UoL gains.
  - How is this possible ?
    - IUP:
      - The IUP FOCAL algorithm baseline gains have been used here, i.e., ZLO is not a state vector element (if ZLO is added, then the biases would be zero (see TN-2000)).
      - The low FOCAL errors due to ZLO-error in the NIR are because SIF is a state vector element in the NIR.
  - Could it be that these gains are from a retrieval which introduces constant offsets in the state vector ?
    IUP: Yes for FOCAL (SIF is state vector element in NIR and therefore also accounts for ZLO).

- BS: 4) For IUP gains, the XCO2 error is positive in SWIR-2 for a (positive) ZLO, for the other providers (SRON, UoL) it is negative. Would you know the reason (I would always expect a negative error, unless SWIR-2 is used for light path correction only, and therefore behave like NIR) ? IUP: All algos include corrections for "disturbing spectral features" (e.g., via aerosol or albedo, which may compensate also for other errors). For a given error source the bias can therefore be positive or negative. Apparently for FOCAL the bias is positive here for ZLO in SWIR-2.

Universität Bremen ife KNMI UNIVERSITY OF LEICESTER SRON 11

XCO_2 errors using industry spectra

Stray light and polarization

Universität Bremen ife KNMI UNIVERSITY OF LEICESTER SRON 12

XCO_2 errors using industry spectra - I

- Comparison not trivial because of different units and different quantities:
  - **Industry errors:** absolute error of sun-normalized radiance
  - **SRON gains:** for absolute radiance and absolute sun-normalized radiance errors
    - Note: In contrast to what is written in the headers of the SRON gain files, gains are for (radiance) and sun-norm-radiance (NOT reflectance)
  - **IUP gains:** for relative radiance error (or relative sun-normalized radiance or reflectance error)
  - **UoL gains:** for absolute radiance errors
    - Note: No solar irradiance at CO2M resolution provided, irregular wavelength grid, …; -> different approaches to deal with this likely explain differences of SRON and IUP analysis results (see following slides)

Universität Bremen ife KNMI UNIVERSITY OF LEICESTER SRON 13

XCO_2 errors using industry spectra - II

FoV#: 75

Stray light ghost

SRON analysis:

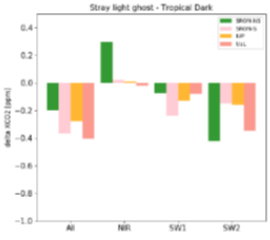

IUP-UB analysis:

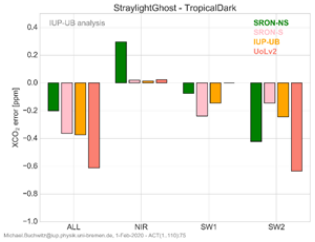

Findings:

- Errors similar but not identical
- **SRON-NS errors:**
  - Very good agreement
- **SRON-S errors:**
  - Some differences
- **IUP errors:**
  - Some differences
- **UoL errors:**
  - ALL & SW2: larger for IUP
  - NIR: small differences
  - SW1: smaller for IUP

Universität Bremen ife KNMI UNIVERSITY OF LEICESTER SRON 14

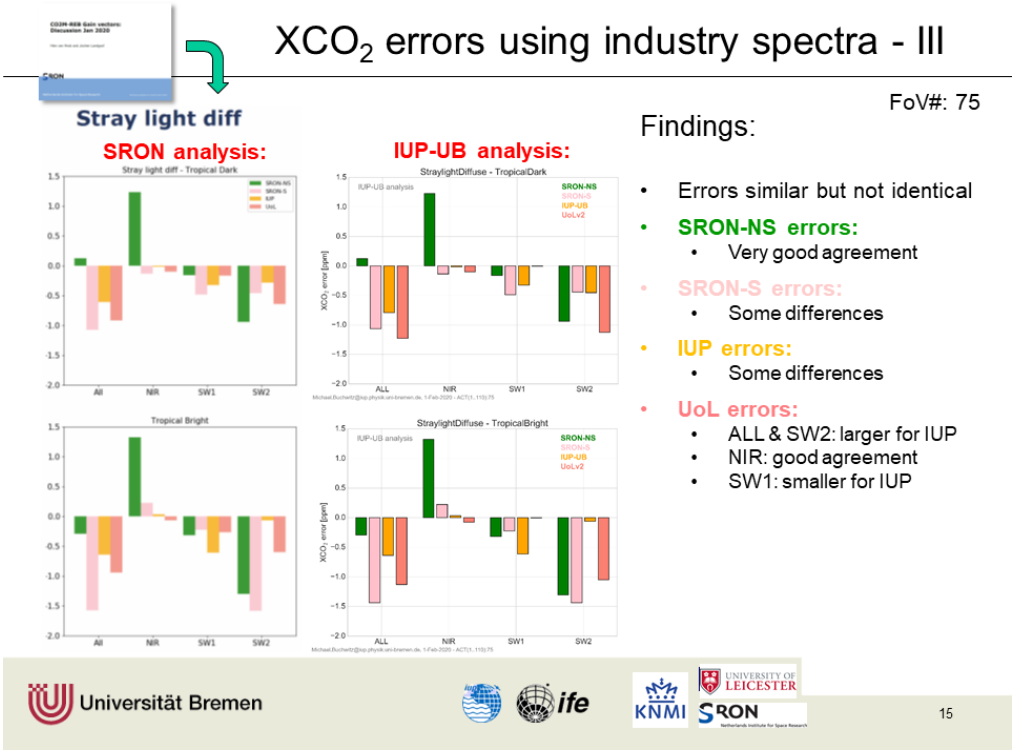
XCO2 errors using industry spectra - III
Stray light diff
SRON analysis:
IUP-UB analysis:
FoV#: 75
Findings:
Errors similar but not identical
SRON-NS errors:
Very good agreement
SRON-S errors:
Some differences
IUP errors:
Some differences
UoL errors:
ALL & SW2: larger for IUP
NIR: good agreement
SW1: smaller for IUP
Universität Bremen
ife
KNMI
UNIVERSITY OF LEICESTER
SRON
15

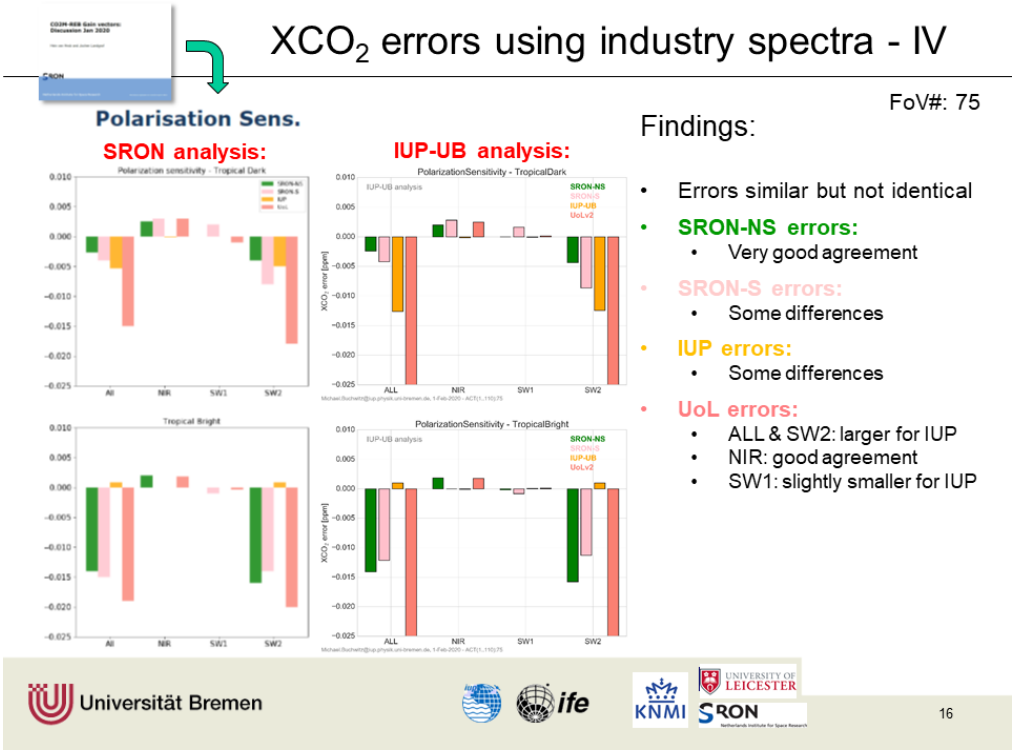
XCO2 errors using industry spectra - IV
Polarisation Sens.
SRON analysis:
IUP-UB analysis:
FoV#: 75
Findings:
Errors similar but not identical
SRON-NS errors:
Very good agreement
SRON-S errors:
Some differences
IUP errors:
Some differences
UoL errors:
ALL & SW2: larger for IUP
NIR: good agreement
SW1: slightly smaller for IUP
Universität Bremen
ife
KNMI
UNIVERSITY OF LEICESTER
SRON
16

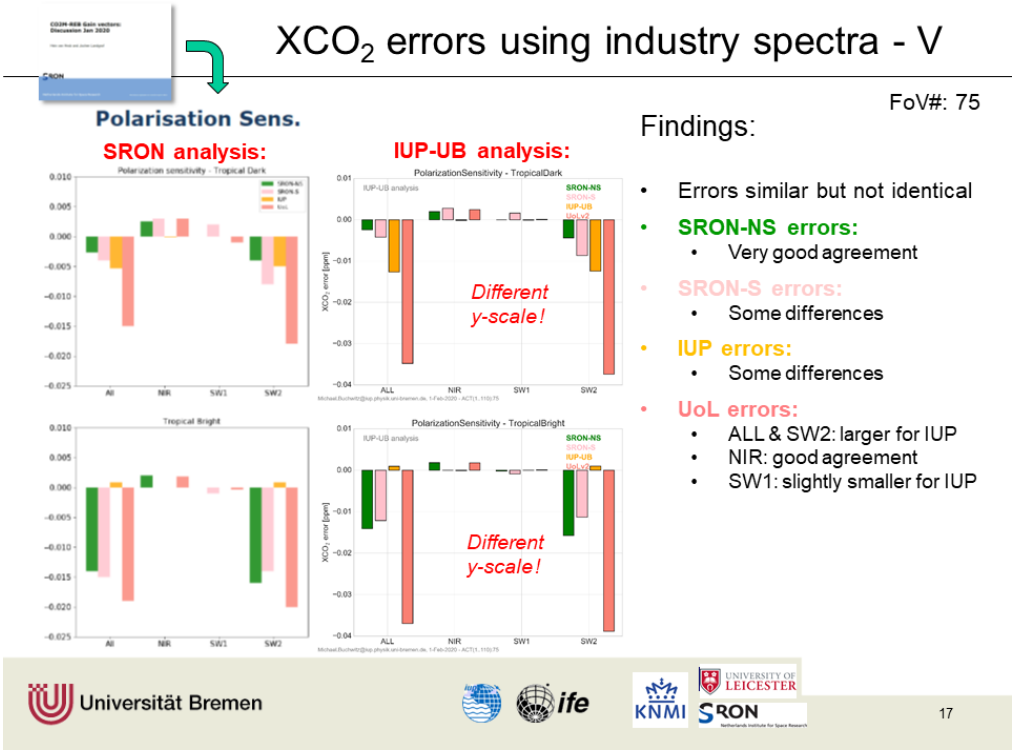
XCO2 errors using industry spectra - V
Polarisation Sens.
SRON analysis:
IUP-UB analysis:
FoV#: 75
Findings:
Errors similar but not identical
SRON-NS errors:
Very good agreement
SRON-S errors:
Some differences
IUP errors:
Some differences
UoL errors:
ALL & SW2: larger for IUP
NIR: good agreement
SW1: slightly smaller for IUP
Different y-scale!
Different y-scale!
Universität Bremen
ife
KNMI
UNIVERSITY OF LEICESTER
SRON
17

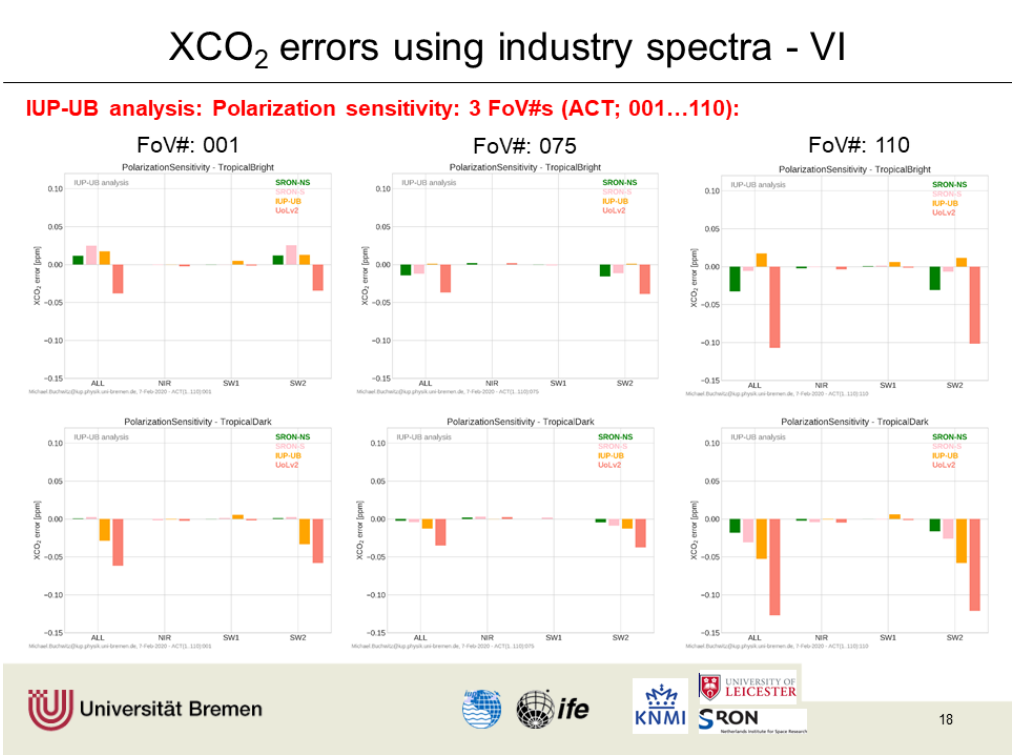
XCO2 errors using industry spectra - VI
IUP-UB analysis: Polarization sensitivity: 3 FoV#s (ACT; 001…110):
FoV#: 001
FoV#: 075
FoV#: 110
Universität Bremen
ife
KNMI
UNIVERSITY OF LEICESTER
SRON
18

XCO_2 errors using industry spectra - VII

Summary & Conclusions:

- SRON used error spectra (for sun-normalized radiance) from industry (straylight & polarization) and computed XCO_2 errors using 4 sets of gains: SRON-NS, SRON-S, IUP, UoL
- IUP-UB did the same analysis and showed:
  - Good agreement between SRON and IUP-UP results for SRON-NS, SRON-S and IUP gains
  - For UoL gains IUP-UB obtained somewhat different errors compared to SRON likely due to a different approach to deal with limitations of the UoL gains when applied to errors given for sun-normalized radiance

Universität Bremen ife KNMI UNIVERSITY OF LEICESTER SRON 19

IUP-UB As to ESA Qs (e-mail BS 9-Jan-2020): STRAY & POL

Straylight:

- BS: 1) As pointed out by Jochen and Hein, the SL errors from full-physics gains are very low for NIR. I'd like to understand this: In absence of aerosol scattering, a less deep O2 absorption feature (filled by straylight) yields a shorter light path (maybe lower pressure or higher elevation) and therefore higher (positive) XCO2. Could it be that a full-physics algorithm absorbs this by estimating a lower aerosol optical depth ? IUP: Yes, this could be possible but it depends not only on AOD but also on scattering profiles and how a retrieval algo deals with scattering (which state vector elements, etc.).

Polarization:

- BS: 1) The polarisation errors are astonishingly low. If this is correct we have over-sized the scrambler and can relax it (with positive effect on spatial co-registration). IUP: Low errors also found in previous studies.
  - For which ACT sample have you done the assessment ? Since the polarisation sensitivity varies over the swath and is usually largest at the edge, you should take the edge samples (FoV #1 and/or #110).
    - SRON (and for comparison therefore also IUP) used FoV # 75.
    - IUP also added results for FoV #1 and #110 -> #110 gives largest bias
    - Note: biases likely even larger for extratropical scenes such as ML and HL, where SZA ≠ 0)

Universität Bremen ife KNMI UNIVERSITY OF LEICESTER SRON 20

7. Acronyms and abbreviations

Acronym	Meaning
ABL	Algorithm Baseline
AOD	Aerosol Optical Depth
ATBD	Algorithm Theoretical Basis Document
BESD	Bremen optimal EStimation DOAS
BESD/C	BESD algorithm used for CarbonSat assessments
BL	Boundary Layer
CA	Continental Average (aerosol scenario)
CarbonSat	Carbon Monitoring Satellite
CC	Continental Clean (aerosol scenario)
CCI	Climate Change Initiative (of ESA)
CL	Close Loop
CNES	Centre national d'études spatiales
CO2M	Anthropogenic CO_2 Monitoring Mission
CO2M-REB	Anthropogenic CO_2 Monitoring Mission Requirements Consolidation and Error Budget study
COD	Cloud Optical Depth
CP	Continental Polluted (aerosol scenario)
CS	CarbonSat
CS-L1L2-II	CarbonSat Earth Explorer 8 Candidate Mission Level-1 Level-2 (L1L2) Performance Assessment Study No. 2
CTH	Cloud Top Height
DE	Desert (aerosol scenario)
DES	Desert (surface albedo)
DOAS	Differential Optical Absorption Spectroscopy
DOF	Degrees of Freedom
E2ES	End-to-end-simulator
EB	Error Budget
EE8	Earth Explorer No. 8 (satellite)
ENVISAT	Environmental Satellite
ESA	European Space Agency
FOV	Field of View
FR	Final Report
FWHM	Full Width at Half Maximum
GHG	Greenhouse Gas
GHG-CCI	Greenhouse Gas project of ESA's Climate Change Initiative (CCI)
GM	Gain Matrix
GMM	Gain Matrix Method
GOSAT	Greenhouse Gases Observing Satellite
GV	Gain vector
HLD	High Latitude Dark (scenario)
ISRF	Instrument Spectral Response Function
IUP-UB	Institute of Environmental Physics (Institut für Umweltphysik), University of Bremen, Germany

L1	Level 1
L2	Level 2
MLB	Mid-latitude dark scenario
MC	Monte Carlo
MLD	Mid-latitude dark scenario
MLS	Mid-latitude summer (profiles)
MODIS	Moderate resolution Imaging Spectrometer
MRD	Mission Requirements Document
NIR	Near Infra Red (band)
OCO	Orbiting Carbon Observatory
OE	Optimal Estimation
OPAC	Optical Properties of Aerosol and Clouds
RfMS	Report for Mission Selection
RMS	Root Mean Square
RMSE	Root Mean Square Error
RSS	Root Sum Square
RTM	Radiative Transfer Model
SCIAMACHY	Scanning Imaging Absorption Spectrometers for Atmospheric Chartography
SCIATRAN	Radiative Transfer Model under development at IUP
SIF	Sun-Induced Fluorescence
SNR	Signal to Noise Ratio
SSD	Spatial Sampling Distance
SSI	Spectral Sampling Interval
SSP	Spectral Sizing Point
SSR	Spectral Sampling Ratio
SW1 or SWIR-1	SWIR 1 band
SW2 or SWIR-2	SWIR 2 band
SWIR	Short Wave Infrared
SZA	Solar Zenith Angle
TCCON	Total Carbon Column Observing Network
TOA	Top of atmosphere
TOF	Temporal Oversampling Factor
TRB	Tropical Bright (scenario)
TRD	Tropical Dark (scenario)
VCF	Vegetation Chlorophyll Fluorescence
VEG	Vegetation (surface albedo)
VIIRS	Visible Infrared Imaging Radiometer Suite
VMR	Volume Mixing Ratio
ZLO	Zero-Level-Offset

8. References and related literature

/Boesch, 2018/ Boesch, H., WP2300: Optimizing Spectral Sizing Concepts, Technical Report ESA „Study on Spectral Sizing for CO_2 Observations“, Issue 1, 15-Mar-2018, Doc ID: UOL-CO2SIZ-TN-2018-WP2300, pp. 17, 2018.

/Bovenmann et al., 2010/ Bovensmann, H., Buchwitz, M., Burrows, J. P., Reuter, M., Krings, T., Gerilowski, K., Schneising, O., Heymann, J., Tretner, A., and Erzinger, J., A remote sensing technique for global monitoring of power plant CO_2 emissions from space and related applications, Atmos. Meas. Tech., 3, 781-811, 2010.

/Bovenmann et al., 2014/ Bovensmann, H., M. Buchwitz, M. Reuter, T. Krings, J. Heymann, H. Boesch, J. Landgraf, CarbonSat Earth Explorer 8 Candidate Mission “Level-2 and Level-1B Requirements Consolidation Study“, Final Report ESA Study CarbonSat Earth Explorer 8 Candidate Mission “Level-2 and Level-1B Requirements Consolidation Study “, ESA Contract No 4000105676/12/NL/AF, Version 2.2, Date: 18. July 2014, Doc.ID: IUP-CS-L1L2-FR-01, 2014.

/Bovenmann et al., 2015/ Bovensmann, H., M. Buchwitz, M. Reuter, T. Krings, J. Heymann, H. Boesch, J. Landgraf, CarbonSat Earth Explorer 8 Candidate Mission “Level-1 Level-2 (L1L2) Performance Assessment Study “, Final Report ESA Study, ESA Contract No 4000109814/13/NL/FF/lf, Version 1.0, Date: 11. December 2015, Doc.ID: IUP-CS-L1L2-II-FR-01, 2015.

/Buchwitz et al., 2013a/ Buchwitz, M., M. Reuter, H. Bovensmann, D. Pillai, J. Heymann, O. Schneising, V. Rozanov, T. Krings, J. P. Burrows, H. Boesch, C. Gerbig, Y. Meijer, and A. Loescher, Carbon Monitoring Satellite (CarbonSat): assessment of atmospheric CO_2 and CH_4 retrieval errors by error parameterization, Atmos. Meas. Tech., 6, 3477-3500, 2013.

/Buchwitz et al., 2013b/ Buchwitz, M., H. Bovensmann, M. Reuter, J. Heymann, O. Schneising, et al., CARBONSAT: ERROR ANALYSIS FOR PRIMARY LEVEL 2 PRODUCTS XCO_2 AND XCH_4 AND SECONDARY PRODUCT VEGETATION CHLOROPHYLL FLUORESCENCE FOR NADIR OBSERVATIONS OVER LAND, ESA Living Planet Symposium, Sept 9-13, 2013, Edinburgh, UK, conference proceedings ESA Special Publication SP-722 (on CD-ROM), link: , 2013.

/Buchwitz et al., 2015/ Buchwitz, M., Bovensmann, T. Krings, M. Reuter, V. V. Rozanov, P. Liebing, J. Landgraf, F. Alkemade, Mission Requirements Analysis and Level 2 Error Characterization for CarbonSat Nadir Observations over Land - WP 1100, 2000 & 4100 Report, ESA Study CarbonSat Earth Explorer 8 Candidate Mission “Level-1 Level-2 (L1L2) Performance Assessment Study“ ESA Contract No 4000109814/13/NL/FF/lf, Version 1.2, 3 Dec 2015, Doc ID: IUP-CS-L1L2-II-TNnadir, 2015.

/Buchwitz et al., 2017/ ESA Climate Change Initiative (CCI) Product Validation and Intercomparison Report (PVIR) for the Essential Climate Variable (ECV) Greenhouse Gases (GHG) for data set Climate Research Data Package No. 4 (CRDP#4), Version 5.0, 9. Feb. 2017, link: , 2017.

/Buchwitz, 2018/ Buchwitz, M., Error analysis for CarbonSat scenarios and different spectral sizing, Technical Report ESA „Study on Spectral Sizing for CO_2 Observations“, Version 4.0, 30-Apr-2018, Doc ID: IUP-CO2SS-TN-5, pp. 93, 2018.

/Buchwitz and Reuter, 2018/ Buchwitz, M., and M. Reuter, Level 2 error files, Technical Report ESA Study of Assessing thresholds for a space borne observation system to monitor fossil CO_2 emissions (PMIF study), Version 2.1, 30-Jan-2018, Doc ID IUP-PMIF_L2e_S7-c, pp. 100, 2018.

/Butz et al., 2017/ Butz, A., K. Graf, J. Landgraf, J. ann den Brugh, D3 – CO_2 errors due to measurement noise and atmospheric scattering for the different spectral sizing concepts of a CO_2 instrument, Technical Report ESA „Study on Spectral Sizing for CO_2 Observations“, Version 1.1, 23-May-2017, pp. 24, 2017.

/Ciais et al., 2015/ Ciais, P., et al.: Towards a European Operational Observing System to Monitor Fossil CO_2 emissions - Final Report from the expert group, http://www.copernicus.eu/main/towards-european-operational-observing-system-monitor-fossil-co2-emissions, pp. 68, October 2015, 2015.

/CO2M MRD v1.0, 2018/ Copernicus CO_2 Monitoring Mission Requirements Document, ESA, v1.0, EOPSM/3088/YM-ym, 2018.

/CO2M MRD v2.0, 2019/ Copernicus CO_2 Monitoring Mission Requirements Document, ESA, v2.0, date of issue: 27/09/2019, EOP-SM/3088/YM-ym, 2019.

/CO2M-REB TN-1000 v1.1, 2019/ Buchwitz, M., M. Reuter, S. Noël, H. Bovensmann, A. Richter, J. Landgraf, P. Vefking, J. de Haan, H. Boesch, Requirements Justification Report for anthropogenic CO2 Monitoring Mission (CO2M), Technical Report ESA Study on Consolidating Requirements and Error Budget for CO_2 Monitoring Mission (CO2M-REB), version 1.1, 25-April-2019, 74 pages, Doc ID: IUP-CO2M-REB-TN-1000, 2019.

/CO2M-REB TN-2000 v1.2, 2019/ Buchwitz, M., M. Reuter, S. Noël, H. Bovensmann, A. Richter, J. Landgraf, P. Vefking, J. de Haan, H. Boesch, Requirements Sensitivity Analysis for anthropogenic CO2 Monitoring Mission (CO2M), Technical Report ESA Study on Consolidating Requirements and Error Budget for CO_2 Monitoring Mission (CO2M-REB), version 1.1, 26-April-2019, 133 pages, Doc ID: IUP-CO2M-REB-TN-2000, 2019.

/CO2M-REB TN-3000 v1.1, 2019/ Buchwitz, M., M. Reuter, S. Noël, H. Bovensmann, A. Richter, J. Landgraf, P. Vefking, J. de Haan, H. Boesch, Error Budgets and Performance for anthropogenic CO2 Monitoring Mission (CO2M), Technical Report ESA Study on Consolidating Requirements and Error Budget for CO_2 Monitoring Mission (CO2M-REB), version 1.1, 25-April-2019, 46 pages, Doc ID: IUP-CO2M-REB-TN-3000, 2019.

/CO2M-REB TN-1000 v2, 2020/ Buchwitz, M., M. Reuter, S. Noël, H. Bovensmann, A. Richter, J. Landgraf, P. Vefking, J. de Haan, H. Boesch, Requirements Justification Report for anthropogenic CO2 Monitoring Mission (CO2M), Technical Report ESA Study on Consolidating Requirements and Error Budget for CO_2 Monitoring Mission (CO2M-REB), version 2.0, Doc ID: IUP-CO2M-REB-TN-1000, 2020.

/CO2M-REB TN-2000 v2, 2020/ Buchwitz, M., M. Reuter, S. Noël, H. Bovensmann, A. Richter, J. Landgraf, P. Vefking, J. de Haan, H. Boesch, Requirements Sensitivity Analysis for anthropogenic CO2 Monitoring Mission (CO2M), Technical Report ESA Study on Consolidating Requirements and Error Budget for CO_2 Monitoring Mission (CO2M-REB), version 2.0, Doc ID: IUP-CO2M-REB-TN-2000, 2020.

/CO2M-REB TN-3000 v2, 2020/ Buchwitz, M., M. Reuter, S. Noël, H. Bovensmann, A. Richter, J. Landgraf, P. Vefking, J. de Haan, H. Boesch, Error Budgets and Performance for anthropogenic CO2 Monitoring Mission (CO2M), Technical Report ESA Study on

Consolidating Requirements and Error Budget for CO_2 Monitoring Mission (CO2M-REB), version 2.0, Doc ID: IUP-CO2M-REB-TN-3000, 2020.

/CO2M-REB TN-1000 v2.1, 2020/ Buchwitz, M., M. Reuter, S. Noël, H. Bovensmann, A. Richter, J. Landgraf, P. Vefking, J. de Haan, H. Boesch, Requirements Justification Report for anthropogenic CO2 Monitoring Mission (CO2M), Technical Report ESA Study on Consolidating Requirements and Error Budget for CO_2 Monitoring Mission (CO2M-REB), version 2.1, Doc ID: IUP-CO2M-REB-TN-1000, 2020.

/CO2M-REB TN-2000 v2.1, 2020/ Buchwitz, M., M. Reuter, S. Noël, H. Bovensmann, A. Richter, J. Landgraf, P. Vefking, J. de Haan, H. Boesch, Requirements Sensitivity Analysis for anthropogenic CO2 Monitoring Mission (CO2M), Technical Report ESA Study on Consolidating Requirements and Error Budget for CO_2 Monitoring Mission (CO2M-REB), version 2.1, Doc ID: IUP-CO2M-REB-TN-2000, 2020.

/CO2M-REB TN-3000 v2.1, 2020/ Buchwitz, M., M. Reuter, S. Noël, H. Bovensmann, A. Richter, J. Landgraf, P. Vefking, J. de Haan, H. Boesch, Error Budgets and Performance for anthropogenic CO2 Monitoring Mission (CO2M), Technical Report ESA Study on Consolidating Requirements and Error Budget for CO_2 Monitoring Mission (CO2M-REB), version 2.1, Doc ID: IUP-CO2M-REB-TN-3000, 2020.

/CO2M SSS FR, 2019/ ESA Spectral Sizing Study Final Report, in preparation, 2019.

/CS L1L2-I study FR, 2014/ Bovensmann, H., M. Buchwitz, M. Reuter, T, Krings, J. Heymann, H. Boesch, J. Landgraf, Final Report ESA study “CarbonSat Earth Explorer 8 Candidate Mission “Level-2 and Level-1B Requirements Consolidation Study“, Technical Report, ESA Contract No. 4000105676/13/NL/AF, Version 2.2, 18-July-2014, Doc ID: IUP-CS-L1L2-FR-01, pp. 188, 2014.

/CS L1L2-II study FR, 2015/ Bovensmann, H., M. Buchwitz, M. Reuter, T, Krings, H. Boesch, J. Landgraf, Final Report ESA study “CarbonSat Earth Explorer 8 Candidate Mission “Level-1 Level-2 (L1L2) Performance Assessment Study“, Technical Report, ESA Contract No. 4000109814/13/NL/FF/lf, Version 1.0, 11-Dec-2015, Doc ID: IUP-CS-L1L2-II-FR-01, pp. 43, 2015.

/CS L1L2-II TN nadir, 2015/ Buchwitz, M., H. Bovensmann, T. Krings, M. Reuter, V. V. Rozanov, P. Liebing, J. Landgraf, F. Alkemade, Mission Requirements Analysis and Level 2 Error Characterization for CarbonSat Nadir Observations over Land, Technical Report ESA study “CarbonSat Earth Explorer 8 Candidate Mission “Level-1 Level-2 (L1L2) Performance Assessment Study“, ESA Contract No. 4000109814/13/NL/FF/lf, Version 1.1, 2-Dec-2015, Doc ID: IUP-CS-L1L2-II-TNnadir, pp. 251, 2015.

/CS MRD v1.0, 2011/ ESA, CarbonSat – Candidate Earth Explorer Opportunity Mission – Mission Requirements Document, Issue 1, Revision 0, 8 July 2011, ESA Mission Science Division, Reference EOP-SMA/2232/PI-pi, 2011.

/CS MRD v1.2, 2013/ ESA, CarbonSat – Candidate Earth Explorer Opportunity Mission – Mission Requirements Document, Issue 1, Revision 2, 23 May 2013, ESA Mission Science Division, Reference EOP-SMA/2232/PI-pi, 2011.

/CS RfMS, 2015/ ESA, Report for Mission Selection: CarbonSat, ESA SP-1330/1 (2 volume series), European Space Agency, Noordwijk, The Netherlands. link: , 2015.

/Eldering et al., 2017/ Eldering, A., O'Dell, C. W., Wennberg, P. O., Crisp, D., Gunson, M. R., Viatte, C., Avis, C., Braverman, A., Castano, R., Chang, A., Chapsky, L., Cheng, C.,

Connor, B., Dang, L., Doran, G., Fisher, B., Frankenberg, C., Fu, D., Granat, R., Hobbs, J., Lee, R. A. M., Mandrake, L., McDuffie, J., Miller, C. E., Myers, V., Natraj, V., O'Brien, D., Osterman, G. B., Oyafuso, F., Payne, V. H., Pollock, H. R., Polonsky, I., Roehl, C. M., Rosenberg, R., Schwandner, F., Smyth, M., Tang, V., Taylor, T. E., To, C., Wunch, D., and Yoshimizu, J.: The Orbiting Carbon Observatory-2: first 18 months of science data products, Atmos. Meas. Tech., 10, 549-563, https://doi.org/10.5194/amt-10-549-2017, 2017.

/Galli et al., 2014/ Galli, A., Guerlet, S., Butz, A., Aben, I., Suto, H., Kuze, A., Deutscher, N. M., Notholt, J., Wunch, D., Wennberg, P. O., Griffith, D. W. T., Hasekamp, O., Landgraf, J., The impact of spectral resolution on satellite retrieval accuracy of CO_2 and CH_4, Atmos. Meas. Tech., Volume 7, Issue 4, pp.1105-1119, 2014.

/Guerlet et al., 2013/ Guerlet, S., Butz, A., Schepers, D., et al., Impact of aerosol and thin cirrus on retrieving and validating XCO_2 from GOSAT shortwave infrared measurements, J. Geophys. Res., VOL. 118, 4887–4905, doi:10.1002/jgrd.50332, 2013.

/Hess et al., 1998/ Hess, M., P. Koepke, and I. Schult, Optical Properties of Aerosols and Clouds: The software package OPAC, Bull. Am. Met. Soc., 79, 831-844, 1998.

/Heymann et al., 2012/ Heymann, J., H. Bovensmann, M. Buchwitz, J. P. Burrows, N. M. Deutscher, J. Notholt, M. Rettinger, M. Reuter, O. Schneising, R. Sussmann, and T. Warneke SCIAMACHY WFM-DOAS XCO_2: reduction of scattering related errors, Atmos. Meas. Tech., 5, 2375-2390, 2012.

/Heymann et al., 2015/ Heymann, J., M. Reuter, M. Hilker, M. Buchwitz, O. Schneising, H. Bovensmann, J. P. Burrows, A. Kuze, H. Suto, N. M. Deutscher, M. K. Dubey, D. W. T. Griffith, F. Hase, S. Kawakami, R. Kivi, I. Morino, C. Petri, C. Roehl, M. Schneider, V. Sherlock, R. Sussmann, V. A. Velazco, T. Warneke, and D. Wunch, Consistent satellite XCO_2 retrievals from SCIAMACHY and GOSAT using the BESD algorithm, Atmos. Meas. Tech., 8, 2961-2980, 2015.

/Landgraf et al., 2017a/ Landgraf, J., J. aan de Brugh, A. Butz, K. Graf, Specification of Instrument Spectral Sizing Concepts, Spectral Errors and Geo-Physical Scenarios, Technical Report ESA „Study on Spectral Sizing for CO_2 Observations“, Doc ID: SRON-CSS-TN-2016-002, 15-Aug-2017, issue 5, pp. 24, 2017.

/Landgraf et al., 2017b/ Landgraf, J., J. aan de Brugh, A. Butz, K. Graf, D2 – Instrument related errors for the different spectral sizing of a CO_2 instrument, Technical Report ESA „Study on Spectral Sizing for CO_2 Observations“, Issue 2, 15-Aug-2018, Doc ID: SRON-CSS-TN-2017-001, pp. 39, 2017.

/Rascher et al., 2009/ Rascher, U., Agati, G., Alonso, L., Cecchi, G., Champagne, S., Colombo, R., Damm, A., Daumard, F., de Miguel, E., Fernandez, G., Franch, B., Franke, J., Gerbig, C., Gioli, B., Gomez, J. A., Goulas, Y., Guanter, L., Gutierrez-de-la-Camara, O´ ., Hamdi, K., Hostert, P., Jimenez, M., Kosvancova, M., Lognoli, D., Meroni, M., Miglietta, F., Moersch, A., Moreno, J., Moya, I., Neininger, B., Okujeni, A., Ounis, A., Palombi, L., Raimondi, V., Schickling, A., Sobrino, J. A., Stellmes, M., Toci, G., Toscano, P., Udelhoven, T., van der Linden, S., and Zaldei, A.: CEFLES2: the remote sensing component to quantify photosynthetic efficiency from the leaf to the region by measuring sun-induced fluorescence in the oxygen absorption bands, Biogeosciences, 6, 1181–1198, doi:10.5194/bg-6-1181-2009, 2009.

/Reuter et al., 2010/ Reuter, M., Buchwitz, M., Schneising, O., Heymann, J., Bovensmann, H., and Burrows, J. P., A method for improved SCIAMACHY CO_2 retrieval in the presence of optically thin clouds, Atmos. Meas. Tech., 3, 209-232, 2010.

/Reuter et al., 2011/ Reuter, M., Bovensmann, H., Buchwitz, M., et al. (2011), Retrieval of atmospheric CO_2 with enhanced accuracy and precision from SCIAMACHY: Validation with FTS measurements and comparison with model results, J. Geophys. Res., 116, D04301, doi:10.1029/2010JD015047.

/Reuter et al., 2017a/ Reuter, M., M. Buchwitz, O. Schneising, S. Noel, V. Rozanov, H. Bovensmann, J. P. Burrows, A Fast Atmospheric Trace Gas Retrieval for Hyperspectral Instruments Approximating Multiple Scattering - Part 1: Radiative Transfer and a Potential OCO-2 XCO_2 Retrieval Setup, Remote Sens., 9, 1159, doi:10.3390/rs9111159, 2017.

/Reuter et al., 2017b/ Reuter, M., M. Buchwitz, O. Schneising, S. Noël, H. Bovensmann, J. P. Burrows, A Fast Atmospheric Trace Gas Retrieval for Hyperspectral Instruments Approximating Multiple Scattering - Part 2: Application to XCO_2 Retrievals from OCO-2, Remote Sens., 9, 1102, doi:10.3390/rs9111102, 2017.

/Reuter et al., 2018/ Reuter, M., H. Bovensmann, S. Noël, K. Bramstedt, H. Bovensmann, Green-House-Gas Total Column Performance Simulations (GHG-TCPS) Validation and Performance Simulation Report, Technical Report Univ. Bremen, version 1.0, 18-June-2018, Doc. ID: IUP-GHG-TCPS-VPSR-01, 2018.

/Rodgers 2000/ Rodgers, C. D.: “Inverse Methods for Atmospheric Sounding: Theory and Practice”, World Scientific, Singapore, 2000.

/Rodgers and Connor, 2003/ Rodgers, C. D. and B. J. Connor, Intercomparison of remote sounding instruments, J. Geophys. Res., Vol. 108, No. D3, 4116, pp. 1-13, 2003.

/Rozanov et al. 2014/ Rozanov, V.V., A.V. Rozanov, A.A. Kokhanovsky, J.P. Burrows: Radiative transfer through terrestrial atmosphere and ocean: Software package SCIATRAN. Journal of Quantitative Spectroscopy and Radiative Transfer, http://dx.doi.org/10.1016/j.jqsrt.2013.07.004, Vol. 133, p. 13–71, 2014.

/Sierk et al. 2018/ Sierk, B., J.-L. Bézy, A. Löscher, Y. Meijer, The European CO_2 Monitoring Mission: Observing anthropogenic greenhouse gas emissions from space, manuscript in preparation, 2018.

/VIIRS Cloud Mask ATBD, 2014/ GSFC JPSS CMO, Joint Polar Satellite System (JPSS) VIIRS Cloud Mask (VCM) Algorithm Theoretical Basis Document (ATBD), Aug. 5, 2014, Revision E, Goddard Space Flight Center, Greenbelt, Maryland, 2014.

***** End of Document *****